# Molecular characterization and identification of genes involved in maize female gametophyte development

DISSERTATION ZUR ERLANGUNG DES DOKTORGRADES DER NATURWISSENSHAFTEN (DR. RER. NAT.) DER NATURWISSENSCHAFTLICHEN FAKULTÄT III – BIOLOGIE UND VORKLINISCHE MEDIZIN DER UNIVERSITÄT REGENSBURG

vorgelegt von

Kanok-orn Srilunchang

geboren in Udonthani, Thailand

im Juli 2009

Promotionsgesuch eingereicht am: 14 Juli 2009.

Die Arbeit wurde angeleitet von: Prof. Dr. Thomas Dresselhaus

Prüfungsausschuss:

Prof. Dr. Reinhard Sterner (Vorsitzender)

Prof. Dr. Thomas Dresselhaus

Prof. Dr. Wolfgang Seufert

Prof. Dr. Herbert Tschochner

Prof. Dr. Gernot Längst

# Contents

page

List of publications…… II

**Chapter 1** Introduction

Female gametophyte development in flowering plants…… .1

The cell cycle of the maize FG…….. 3

DNA imprinting in the maize FG……..……4

The role of post-translational protein modification for FG Development and function

A: Ubiquitination……..5

B: SUMOylation……..7

C: DSULylation……...9

**Chapter 2** The Fertilization-Induced DNA Replication Factor MCM6 of Maize Shuttles between Cytoplasm and Nucleus, and Is Essential for Plant Growth and Development……..10

**Chapter 3** Activation of the imprinted Polycomb Group *Fie1* gene in maize endosperm requires demethylation of the maternal allele…….. 45

**Chapter 4** Asymmetrically inherited maize MATH-BTB proteins are Involved in nuclei positioning and mitotic progression during Megagametogenesis…….. 64

**Chapter 5** DiSUMO-like DSUL is required for nuclei positioning and cell specification during female gametophyte maturation in maize…….98

**Chapter 6** Summary and outlook ……..127

References……...133

Contribution……138

Abbreviations……140

Acknowledgements……..141

Bibliography……..143

Curriculum Vitae……..144

Eidesstattliche Erklärung……145

## List of publications:

1. Dresselhaus, T., **Srilunchang, K-o.,** Leljak-Levanić, D., Schreiber, D N., and Garg, P. (2006). The Fertilization Induced DNA Replication Factor MCM6 of Maize Shuttles between Cytoplasm and Nucleus, and is Essential for Plant Growth and Development. **Plant Phys**., **140**, 512-527.

2. Hermon, P., **Srilunchang, K-o.,** Zou, J., Dresselhaus, T., and Danilevskaya, O N. (2007). Activation of the imprinted Polycomb Group *Fie1* gene in maize endosperm requires demethylation of the maternal allele. Plant Mol. Bio., **64**, 387-395.

3. Leljak-Levanić, D., **Srilunchang, K-o.,** Solijic, L., Juranić, M., Dresselhaus, T., and Sprunck, S.**.** Asymmetrically inherited maize MATH-BTB proteins are involved in nuclei positioning and mitotic progression during megagametogenesis. **Plant Cell**, **in revision.**

4. **Srilunchang, K-o**., and Dresselhaus, T. DiSUMO-like DSUL is required for nuclei positioning and cell specification during female gametophyte maturation in maize. **Development, in revision.**

# CHAPTER 1

## Introduction

### Female gametophyte development in flowering plants

Angiosperms, or flowering plants, are one of the two classes of seed plant including also the gymnosperms. Two kinds of reproductive cells are produced in male (anthers) and female flower organs (ovaries) containing one up to a few hundred ovules (Kiesselbach, 1999). In anthers, four microspores are generated after meioses, which undergo two rounds of mitosis to generate pollen grains and pollen tubes after germination. This process is called microsporogenesis resulting in the formation of the male gametophyte (MG). The MG contains two sperm cells and one vegetative cell (McCormick, 2004). The female gametophyte (FG) develops from the functional megaspore after meiosis during a process called megagametogenesis and takes place inside the ovule (this process is described in more detail below). Sexual reproduction in angiosperm is initiated when pollen released from anthers finally deliver two sperm cells to the FG via the pollen tube. Double fertilization, which the major characteristic of angiosperms then occurs when one sperm fertilizes the egg cell and the other sperm cell fertilizes to the two polar nuclei of the central cell (Drews et al., 1998; Russell, 1992). From a cell biology perspective, megagametogenesis is a very interesting process as it involves many fundamental phenomena such as nuclear migration and fusion, establishment of cell polarity, cell death, asymmetric division and cell fate determination (Drews et al., 1998; Kranz and Lörz, 1994; Yadegari and Drews, 2004). Additionally, FG development has been reported to play a major role during reproduction and is critical for reproductive success involving functions such as pollen tube guidance, maternal control of seed development as well as development of both embryo and endosperm (Chaudhury et al., 1997; Grossniklaus and Schneitz, 1998; Márton et al., 2005; Ohad et al., 1996; Punwani and Drews, 2008; Ray et al., 1997).

FG (embryo sac) development of the model plants Arabidopsis and maize as well as the majority of angiosperms, follows the polygonum type pattern of development. A single megaspore mother cell (megasporocyte) in each ovule forms four megaspores via meiosis. The three spores located at the micropylar end degenerate and the remaining one represents the functional megaspore (Figure 1, FG1). The functional megaspore soon begins to enlarge and its nucleus divides mitotically. At the end of the third mitotic division, an eight-

nucleate embryo sac is formed containing four nuclei at each pole (FG5). Two of these nuclei, one from each pole approach each other and remain in direct contact in the vicinity of the egg apparatus (egg cell and synergids) in maize (FG6-7). While these so called polar nuclei remain unfused in maize, they fuse during FG maturation in other plants such as Arabidopsis (Drews et al., 1998). During FG maturation, the cytoplasm becomes organized around each of three nuclei at the chalazal pole of the FG forming a group of three antipodal cells. In maize, the antipodal cells divide to form a cluster of about 30 cells in the mature FG (FG7). Three cells are also generated at the micropylar pole. One of theses cells enlarges and becomes the egg cell while the others form the adjacent synergids. This group of three cells is often called the egg apparatus (Kiesselbach, 1999).

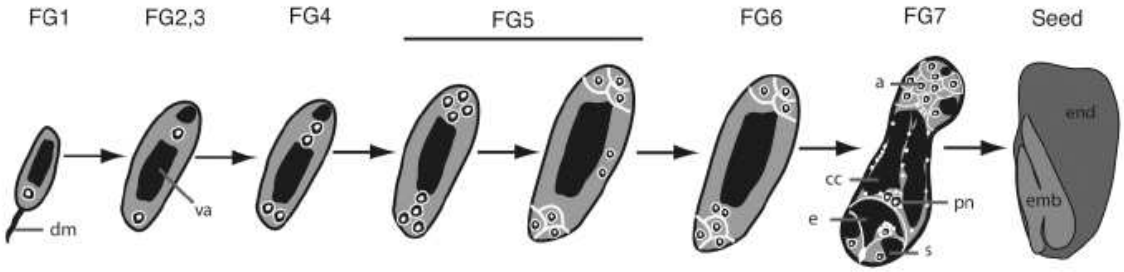


**Figure 1. Maize megagametophyte development**. FG1-FG7=female gametophyte stage 1-7. dm=degenerated megaspores; a=antipodal cells; cc=central cell; pn=polar nuclei; e=egg cell; s=synergid; end=endosperm; emb=embryo; va=vacuole (from Evans and Grossniklaus 2009)

Double fertilization in maize is initiated after silks of the ear are pollinated: the pollen grains germinate and grow toward the base of the individual silks where they leave the transmitting tract to reach the ovule (Figure 2A). Although a number of tubes arrive at the ovule surface, usually only one pollen tube penetrates the micropyle where it grows between the cells of the nucellus until it enters one the recepting synergid, ruptures and releases the two sperm cells (Figure 2Ba). One sperm cell fuses to the egg cell forming the diploid zygote and the embryo (Figure 2Bb), while the other sperm cell nucleus fuses to the two polar nuclei forming the triploid central cell, from which the endosperm develops (Figure 2Bc).

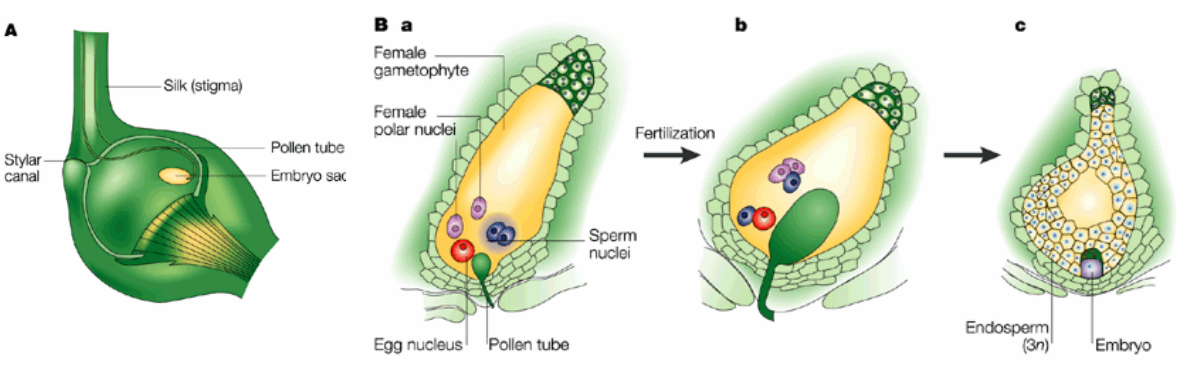

**Figure 2. A**. Pistil (female reproductive organs) of maize. The pistil is shown at the time at which the pollen tube (male gametophyte, MG) enters the embryo sac (female gametophyte, FG). The sperms are still within the cytoplasm from tube. **B.** Double fertilization: double fertilization describes the plant-specific process by which two sperms (blue) from the pollen tube enter the embryo sac **(a)**; one fertilizes the egg (blue and red), which leads to the embryo proper, whereas the other fertilizes one of the two polar nuclei (blue and pink) **(b)**, slightly at the older stage of embryo, and endosperm becomes cellular **(c)**; from Edward, 2001.

In conclusion, the development and function of the FG is crucial for plant reproduction. However, relatively little is known about the genes and molecular mechanisms involved in FG development in general (Drews et al., 1998) and almost nothing is known about these processes in maize (Evans and Grossniklaus, 2009). I was especially interested in the factors controlling pattern formation and identity of the embryo sac cells as well as the establishment of polarity in the whole embryo sac, which are major limiting factors for the reproductive success.

Here I report the functional analysis of different genes which have been reported previously to be expressed in the FG cells of maize and wheat (Danilevskaya et al., 2003; Dresselhaus et al., 1994; 1999; Sprunck et al., 2005) and which might be involved in FG development and the various functions of the FG. The DNA licensing factor gene ***MCM6*** (***m****ini****c****hromosome* ***m****aintenance****6***) for instance has been reported to be involved in regulating the general cell cycle, while the PcG genes ***Fie1*** (***f****ertilization* ***i****ndependent* ***e****ndosperm1*) and ***Fie2*** are candidate genes regulating DNA imprinting during female gametophyte and early seed development. Genes encoding a MATH and BTB domain containing protein **MAB1** and so far undescribed diSUMO-like protein **DSUL** might play key roles in the post-translational regulation of FG development and function.

**The cell cycle of the maize FG**

Cell cycle coordination plays a critical role in regulating growth an development in plants and animals (Tian et al., 2005). Production of haploid gametes is a fundamental requirement for sexual reproduction. In higher plants meiotic products have to undergo a determined number of mitotic divisions before differentiating gametes. This creates a unique meiosis-mitosis interface, traverse of which is absolute requirement for gametophyte development (Ranganath, 2003). Sexual reproduction in flowering plants occurs by a process of double fertilization in which one sperm fuses with an egg cell to form a zygote and a second sperm nucleus fuses with two or more polar nuclei to produce endosperm (reviewed in Kranz et al., 2008; Russell, 1992). In zygotes, the first cell division occurred

about 42 hours after in vitro fertilization (IVF) (Kranz and Lörz, 1993). The initial division of the polarized zygote is generally asymmetrical in angiosperms and leads to two unequal cells (Leduc et al., 1996). While in endosperm, divides mitotically within 3 to 5 hours after fertilization, and repeated divisions continue until a number of free nuclei are formed (Kiesselbach, 1999). To study the cell cycle in the FG of plants, PROLIFERA (PRL) or AtMCM7 was identified to be required during reproduction for megagametophyte and embryo development in Arabidopsis (Springer et al., 1995; 2000). From our study, we found ***MCM6*** which play role in cell cycle of FG development and essential for plant growth and development. The replication of DNA is a fundamental step in the cell cycle, which must be coordinated with cell division to ensure that the daughter cells have the same ploidy as the parent cell. Analysis of budding yeast *mcm* mutants shown that MCM proteins function in the initiation step of DNA replication (Kearsey and Labib, 1998; Schwed et al., 2002). MCM proteins are bound to chromatin around origins of replication during G1 phase, but are subsequently displaced during S phase and remain unbound until the end of mitosis. Some eukaryotic organisms can vary the number of chromosomal replication origins that are active at different stages of the life cycle. For instance, cell proliferation is rapid and S phase is short in early embryos in animals such as frogs and flies, to facilitate rapid development of the embryo. The initiation of DNA replication is highly conserved and found in all eukaryotes studied to date: plants, yeast, flies, worms, fish, frogs, mice and humans (Kearsey and Labib, 1998). The best known essential group of DNA replication proteins comprise the MCM family is MCM2-7 (Bell and Stillman, 1992; Dresselhaus et al., 2006), which assemble at the replication origins during early G1 phase of the cell cycle to form a hexamer. In maize, I have contributed to the functional characterization of the FG expressed and fertilization induced gene *MCM6*. Details are described in **CHAPTER 2**.

**DNA imprinting in the maize FG**

Three epigenetic processes were described as transposition, imprinting and paramutation (Lisch et al., 2002). Imprinting plays a major role for FG development and function and I will further on restrict my remarks on this epigenetic phenomenon. Gene imprinting refers to the regulation of gene expression that is depending on gene inheritance from the maternal or paternal parent, independently evolved in mammals and in flowering plants (Danilevskaya et al., 2003; Grossniklaus et al., 1998; Huh et al., 2008). In maize, many imprinted genes appear to control cell proliferation and found only in the endosperm (Danilevskaya et al., 2003; Huh et al., 2008; Walbot and Evans, 2003) and may also be involved in the cellular differentiation of the two pairs of gametes involved in double fertilization (Gutierrez-Marcos et al., 2006; Huh et al., 2008). Kernel development can also be

affected by parent-of-origin effects that stem from events occurring during FG development (megagametogenesis) (Evans and Grossniklaus, 2009). Several genes have been reported to play an important role in the control of parent-of-origin specific expression in both mammals and plants (Köhler and Grossniklaus, 2005). One example is **FIE** (***F****ertilization* ***I****ndependent* ***E****ndosperm*). The *fie* mutant of Arabidopsis shows a striking phenotype: the diploid central cell can proliferate in the absence of fertilization to form an aberrant endosperm. *FIE* encodes a polycomb group (PcG) protein that acts to repress endosperm development. A second locus, *MEDEA* (*MEA*), which encodes a SET (su(var) 3-9; enhance of zeste; trithorax) domain polycomb protein, is similarly required in the megagametophyte to suppress precocious endosperm development (Kinoshita et al., 1999; Kiyosue et al., 1999). A third gene that might be subject to imprinting is *FERTILIZATION INDEPENDENT SEED 2* (*FIS2*), which encodes a zinc-finger protein and is also involved in the suppression of central cell proliferation before fertilization (Luo et al., 2000). In this study, I have contributed to the detailed examination of *Fie1* and *Fie2* expression in the isolated gametes before fertilization and after fertilization based on previous studies (Danilevskaya et al., 2003; Gutierrez-Marcos et al., 2003; Springer et al., 2002). For further explanation of this study see **CHAPTER 3**.

## The role of post-translational protein modification for FG development and function

### A: Ubiquitination

During the last two decades we have learned that the regulation of many cellular processes involves ubiquitin-dependent degradation of critical proteins (reviewed in Hershko and Ciechanover, 1998). A widely utilized form of posttranslational modification in eukaryotes, but not in prokaryotes, is the covalent addition of a small extremely conserved protein of 76 amino acids, ubiquitin (Ub), to the lysine side chains of target proteins undergoing modification. We know that ubiquitin modification can alter protein location or activity to regulate many biological processes, including DNA repair, endocytosis, transcription and degradation or processing by the proteasome (reviewed in Hershko and Ciechanover, 1998; Hicke and Dunn, 2003; Muratani and Tansey, 2003; Sun and Chen, 2004).

Ubiquitination has also been implicated in a growing number of plant signaling pathways, including those mediating responses to hormones, light, sucrose, developmental cues and pathogens (reviewed in Dreher and Callis, 2007; Ellis et al., 2002; Xu et al., 2009). Moreover, genetic studies in *Caenorhabditis elegans* have identified multiple roles for the ubiquitin system in early development, where ubiquitin-dependent protein degradation

governs such diverse events as a passage through meiosis, mitosis, cytoskeletal regulation and cell fate determination (reviewed in Bowerman and Kurz, 2006; Luke-Glaser et al., 2007).

Regulatory roles for ubiquitin first emerged when cell cycle transitions were found to depend extensively on the rapid, ubiquitin-mediated degradation of the key regulator cyclins, conserved proteins that bind to, activate and provide target specificity for regulatory protein kinases (Glotzer et al., 1991; Hershko et al., 1991). Progression through the cell cycle was found to be regulated by multisubunit E3 ligases that use proteins called cullins as scaffolds (reviewed in Bowerman and Kurz, 2006). Most animal genomes encode five cullin family members (Cul1 to Cul5), with one member of each subfamily present in *C. elegans* (Pintard et al., 2004). BTB domain (Brick-a-brac, Tramtrack, and Broad complex) proteins appear to function as substrate-specific adaptors in Cul3-based E3 ligases of yeast, animals, and plants, as respective BTB domains were found to interact with Cul3, while secondary domains are thought to be responsible for substrate specificity (Figueroa et al., 2005; Geyer et al., 2003; Gingerich et al., 2007; Pintard et al., 2003; Sumara and Peter, 2007; Xu et al., 2003). Over two dozen different domains are found associated with the BTB in proteins, of which five are much more frequent than the others (Perez-Torrado et al., 2006). They are the MATH (Meprin and TRAF homology), Kelch, NPH3, Ion transport and Zinc finger (ZF) domains (Perez-Torrado et al., 2006; Petroski and Deshaies, 2005). Some organism-specific expansions and contraction of the groups have occurred: for instance the BTB-NPH3 proteins are presented only in *Arabidopsis*. Conversely, *Arabidopsis* does not contain BTB-Kelch or BTB-ZF proteins (Perez-Torrado et al., 2006). The MATH domain is a subtype of TRAF-like domain, frequently found in proteins involved in cytoplasmic signal transduction, such as the TRAFs, which interact, for example, with the TNF-alpha receptor (Bradley and Pober, 2001). The illustration of Cul3 and MATH-BTB is shown in Figure 3.

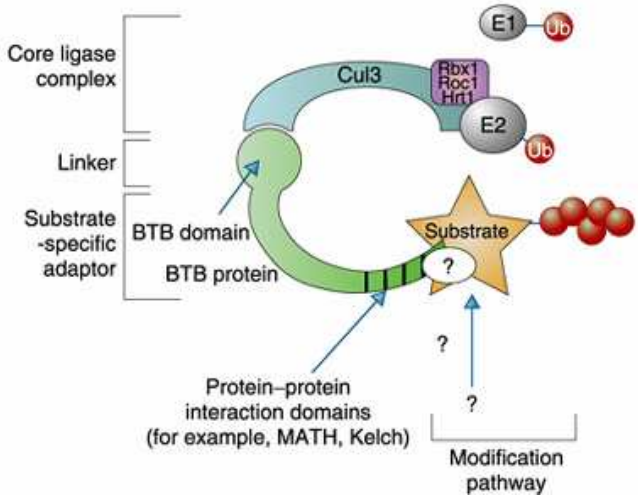


**Figure 3.** Specific classes of substrate-specific adaptors serve cullin-based E3-ligases to recognize target proteins. BTB proteins seem to associate directly with Cul3 through their BTB domain. The use of different substrate adaptors such as MATH domains allows for binding to selected protein substrates, and may underlie the diversity of regulated ubiquitination (Krek, 2003).

In this study we have identified wheat and maize MATH-BTB homologs (*TaMAB1*, *TaMAB2* and *ZmMAB1*) that are specifically expressed in the FG before and after fertilization. We studied the subcellular localization pattern of ZmMAB1-GFP and TaMAB2-GFP fusion proteins as well as those of deletion versions of either the MATH or BTB domain either in the Arabidopsis egg cell or maize suspension cells. Furthermore, the silencing of *ZmMAB1* showed defects in polar migration and further division of nuclei during early FG development. Finally, yeast-2-hybrid experiments indicated that TaMAB2 interacts with Cul3 and thus that MAB protein has important roles as substrate-specific adapters in Cul3-based E3 complexes. Details are described in **CHAPTER 4**.

**B: SUMOylation**

After the discovery of ubiquitin, several related small proteins have been reported displaying structural similarity to ubiquitin (reviewed in Gill, 2004; Herrmann et al., 2007; Kirkin and Dikic, 2007; Zhao, 2007). In higher eukaryotes ubiquitin is joined by about 10 proteins homologs, ubiquitin-like proteins (termed UBLs) with the acronyms **S**mall **U**biquitin-like **Mo**difiers (SUMOs), Related-to-Ub-1 (RUB-1/NEDD-8), Autophagy defective-8 (APG-8) and APG-12, Homologous to Ub-1 (HUB-1/UBL-5), Ubiquitin-Fold-Modifier-1 (UFM-1), Ubiqitin Related Modifier-1 (URM-1) and Fau Ubiquitin-like protein-1 (FUB-1). Moreover, two UBLs have been reported containing two Ub domains: Interferon-Stimulated Gene-15 (ISG-15) and Antigen–F-adjacent Transcript-10 (FAT-10) (reviewed in Jentsch and Pyrowolakis, 2000; Kirkin and Dikic, 2007; Schwartz and Hochstrasser, 2003). The two best studied UBLs are SUMO and Nedd8 (reviewed in Johnson, 2004). SUMO maturation and attachment onto substrates is similar to the ubiquitination process and includes its own set of analogous E1, E2 and E3 enzymes that are involved in activation, conjugation and ligation (Conti et al., 2008). The comparison of the ubiquitination and ubiquitin-like processes such as Neddylation and Sumoylation modified their substrates in subcellular level is shown in Figure 4.

Less complex eukaryotes (yeast, worms and flies) have a single SUMO gene whereas plants and vertebrates generate several SUMO proteins (Meulmeester and Melchior, 2008). Mammals contain at least three SUMO proteins: SUMO1 and the twins SUMO2 and SUMO3 (these two SUMOs display sequence homology of 96%). Plants contain even more SUMO genes: for example, eight *SUMO* genes are present in the *Arabidopsis thaliana* genome (*AtSUM1-8*) (Johnson, 2004; Saracco et al., 2007). Unlike Ub, SUMOs are encoded as precursor proteins. A short peptide extension is proteolytically removed from the C-terminus to generate the mature forms. The most prominent difference between members of the SUMO family and other ubiquitin-related proteins (including Ub) is a very flexible N-terminal extension and the above described extension of amino acids at the C-terminus in

SUMO (Melchior, 2000). Cleavage occurs after a conserved Gly residue at the C-terminus (Kerscher, 2007; Meulmeester and Melchior, 2008; Novatchkova et al., 2004). SUMO is attached to its target proteins by the conserved Gly motif at the C-terminus like Ub but the effect of SUMOylation does not seems to 'tag' these proteins for degradation.

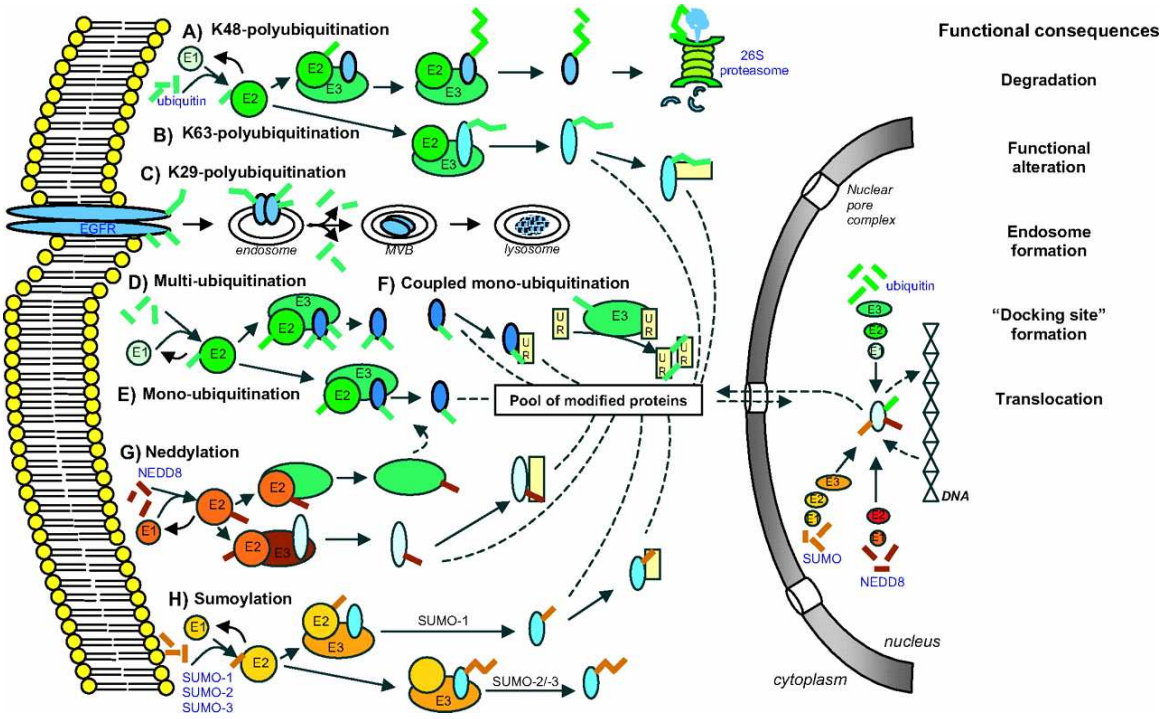


**Figure 4**. Illustration of the consequences of protein modification by ubiquitin and the ubiquitin-like molecules NEDD8, SUMO-1, and SUMO-2/-3. (A) common K48 polyubiquitination leads to degradation of the target protein via the 26S proteasome, whereas K63 and K29 polyubiquitination leads to modification of protein function and lysosomal degradation, respectively (B and C). Similarly, K48 and K63 polyubiquitination, as well as K63 diubiquitination (D), multiubiquitination (E), and monoubiquitination (G), have all been linked to endocytosis and eventually lysosomal degradation of membrane proteins such as growth factor receptors via multivesicular body (MVB) formation. Restricted forms of ubiquitination can lead to diversion from proteasomal degradation, alteration of protein function, and translocation to different cellular compartments. F, Binding to ubiquitin receptor molecules (UR) is another mode of regulation of biological processes, eg, trafficking of endocytotic membranes, which themselves can be monoubiquitinated by a monoubiquitinated HECT-E3 or E2-ubquitin-loaded RING-E3, so-called "coupled monoubiquitination." NEDD8 preferably leads to monomodification (G), as does SUMO-1 (H), whereas SUMO-2 and SUMO-3 can lead to chain formation (Herrmann et al., 2007).

At the molecular level, these highly variable outcomes can occur through one of three mechanisms. First, SUMO can mask a binding site in its target, thereby inhibiting the target protein's interaction with other proteins. Second, SUMO can increase the number of binding sites on its target, thus facilitating the binding of other molecules such as proteins or DNA. Finally, if the SUMOylated protein contains a second, non-covalent binding site for SUMO, a change in its conformation, and thus activity, can be induced (Meulmeester and Melchior, 2008).

The role of SUMOylation in plants is just beginning to emerge. SUMOylation has been shown to play a role in various abiotic stresses (Kurepa et al., 2003; Miura et al., 2005;

2007; Yoo et al., 2006), abscisic acid signaling (Lois et al., 2003), flowering time (Murtas et al., 2003), and pathogen defense (Conti et al., 2008, reviewed in Miura et al., 2007). Moreover, lacking of SUMO-activating enzyme subunit SAE2 and the SUMO-conjugating enzyme SCE1 caused in embryonic lethal, with arrest occurring early in embryo development. Whereas double mutant of missing the single genes encoding the SUMO1 and SUMO2 in *Arabidopsis* are also embryonic lethal (Saracco et al., 2007)

**C: DSULylation**

The major goal of this study was to get a better understanding of the molecular mechanisms of the regulation of FG development in maize. SUMOylation has been shown to play an important role in many genetic and developmental aspects, such as regulating chromosome condensation and segregation via sister chromatid cohesion, kinetochore function as well as mitotic spindle elongation and progression through mitosis (Watts, 2007). In the last part of the PhD project, I have analyzed maize and wheat egg cell EST data (Dresselhaus et al., 1994; Márton et al., 2005; Sprunck et al., 2005) to identify genes expressed in the FG encoding SUMO. In maize, I found three different genes encodeing SUMO which were named *ZmSUMO1, ZmSUMO2* and *ZmSUMO-like*. Expression analysis showed that *ZmSUMO1* and *ZmSUMO2* are expressed in almost all tissues of maize. Therefore, further studies were restricted to *ZmSUMO-like* because it is exclusively expressed in the maize egg apparatus (egg and synergid cell). *ZmSUMO-like* was renamed to *ZmDSUL* (*di-SUMO-like*) because it contains two novel dimeric SUMO-like domains in maize. A homolog was identified to be also expressed in wheat egg cells. In **CHAPTER 5** I could show evidence that ZmDSUL is processed at the di-Gly motif at the C-terminus similar to SUMO. Subcellar localization studies showed different patterns of the N-terminal or C-terminal tagged GFP fusion proteins. Interestingly, the C-terminal cleaved GFP accumulated in an aggresome-like complex located the nuclear surface. Moreover, knock-down of *ZmDSUL* in maize indicated that this gene is indeed required for nuclei segregation and positioning during FG maturation and cell specification after mitosis is completed. Details are described in **CHAPTER 5**.

# CHAPTER 2

# The Fertilization-Induced DNA Replication Factor MCM6 of Maize Shuttles between Cytoplasm and Nucleus, and Is Essential for Plant Growth and Development

**Abstract**

The eukaryotic genome is duplicated exactly once per cell division cycle. A strategy that limits every replication origin to a single initiation event is tightly regulated by a multiprotein complex, which involves at least 20 protein factors. A key player in this regulation is the evolutionary conserved hexameric MCM2-7 complex. From maize (*Zea mays*) zygotes, we have cloned *MCM6* and characterized this essential gene in more detail. Shortly after fertilization, expression of *ZmMCM6* is strongly induced. During progression of zygote and proembryo development, *ZmMCM6* transcript amounts decrease and are low in vegetative tissues, where expression is restricted to tissues containing proliferating cells. The highest protein amounts are detectable about 6 to 20 d after fertilization in developing kernels. Subcellular localization studies revealed that MCM6 protein shuttles between cytoplasm and nucleoplasm in a cell cycle-dependent manner. ZmMCM6 is taken up by the nucleus during G1 phase and the highest protein levels were observed during late G1/S phase. ZmMCM6 is excluded from the nucleus during late S, G2, and mitosis. Transgenic maize was generated to overexpress and down-regulate *ZmMCM6*. Plants displaying minor antisense transcript amounts were reduced in size and did not develop cobs to maturity. Down-regulation of *ZmMCM6* gene activity seems also to affect pollen development because antisense transgenes could not be propagated via pollen to wild-type plants. In summary, the transgenic data indicate that MCM6 is essential for both vegetative as well as reproductive growth and development in plants.

## Introduction

DNA replication of the eukaryotic genome in S phase is accomplished only once during each cell division cycle. This process is precisely regulated and controlled by the prereplicative complex (pre-RC) consisting of origin recognition complex (ORC), Cdt1, Cdc6, as well as minichromosome maintenance (MCM) proteins (Tye, 1999; Bogan et al., 2000; Hyrien et al., 2003; Arias and Walter, 2005; Blow and Dutta, 2005). The initiation of DNA synthesis is thus regulated as a multistep process involving the binding of ORC to replication origins followed by a stepwise recruitment of Cdc6, Cdt1, and MCM proteins to form the pre-RC. Finally, the pre-RC becomes activated by Cdc7/Dbf4 (DDK) and Cdc28 (Cdk2)/cyclin E protein kinases, leading to Cdc45 binding to the pre-RC to initiate DNA unwinding and DNA synthesis (Labib and Diffley, 2001; Lei and Tye, 2001; Hyrien et al., 2003).After the initiation of DNA replication in yeast (*Saccharomyces cerevisiae*) and animal cells, MCM proteins are displaced from chromatin and its reassociation is inhibited until cells pass through mitosis (Blow and Dutta, 2005).

Thus, the dynamic changes in the assembly and disassembly of the MCM subcomplex is critical for the regulation of DNA replication. Originally identified as proteins required for MCM in yeast, the volutionary conserved MCM proteins are now regarded as being essential for both initiation and elongation of DNA replication in eukaryotes and archaebacteria (for review, see Tye, 1999; Forsburg, 2004; Blow and Dutta, 2005). The best known among the MCMs are a family of six structurally related proteins, MCM2 to 7, which assemble at the replication origins during early G1 phase of the cell cycle to form a hexamer. During S phase, MCM proteins bind preferentially to unreplicated DNA rather than to replicating or replicated DNA (Laskey and Madine, 2003) and appear to travel along the chromatin with the replication fork (Claycomb et al., 2002). Based on recent data, the MCM hexamer is currently regarded as the prime candidate for the DNA helicase that unwinds DNA at replication forks (Ishimi, 1997; Labib et al., 2000; Bailis and Forsburg, 2004; Shechter and Gautier, 2004; Blow and Dutta, 2005). Recent experimental data suggest that MCM proteins might also be involved in additional chromosomal processes including transcription, chromatin remodeling, and genome stability (for review, see Forsburg, 2004).

Compared to yeast, animals, and humans, surprisingly little is known about MCM proteins in plants. PROLIFERA (PRL) was the first MCM protein identified in plants and was shown to be required during reproduction for megagametophyte and embryo

development, but is also expressed in dividing sporophytic tissues (Springer et al., 1995). PRL is required maternally and not paternally during the early stages of embryogenesis, suggesting that the female gametophyte provides substantial PRL function during the early stages of embryogenesis in Arabidopsis (*Arabidopsis thaliana*; Springer et al., 2000). A more general role of PRL, which is now called AtMCM7, in cell proliferation and cytokinesis throughout plant development was described by Springer et al. (2000) and Holding and Springer (2002). The maize (*Zea mays*) homolog of PRL (ZmPRL) was recently identified by differential display as *ZmPRL* mRNA accumulates in the apical region of the maize immature embryo (Bastida and Puigdomènech, 2002). Up to now, only one additional member of the plant *MCM* gene family, *ZmMCM3* (also called *Zea mays Replication Origin Activator* [*ZmROA*]) was described in more detail and was shown to be expressed in proliferative tissues to specific subpopulations of cycling cells (Sabelli et al., 1996). The promoters of *ZmROA* and its Arabidopsis homolog, *AtMCM3*, have been cloned (Sabelli et al., 1999; Stevens et al., 2002). The promoter of *AtMCM3* was analyzed in more detail because it contains two consensus binding sites for the cell cycle regulator E2F and was shown to be transcriptionally regulated during late G1/S phase of the cell cycle (Stevens et al., 2002).

Here we report the molecular cloning and functional characterization of *MCM6* from maize (*ZmMCM6*). During our investigations about the onset of zygotic gene activation (ZGA)/embryonic gene activation (EGA), we identified a number of genes that are up-regulated or expressed de novo shortly after fertilization in the maize and wheat (*Triticum aestivum*) zygotes (Dresselhaus et al., 1999; Sprunck et al., 2005). We became especially interested in studying the fertilization-induced gene *ZmMCM6* in more detail because the presence of two *MCM6* homologs has been reported in frog (*Xenopus leavis*). The maternal gene *XlmMCM6* is expressed until the midblastula transition (MBT) stage of embryo development when embryonic transcription begins. After EGA, the cell cycle is remodeled and a zygotic/embryonic MCM6 (XlzMCM6) that differs from maternal MCM6 assembles into MCM complexes (Sible et al., 1998). ZmMCM6 shows a higher homology to XlzMCM6 and has a similar carboxy-terminal extension that is absent in maternal XlmMCM6. In contrast to frog, we found only one *MCM6* gene in databases of other animals and within the genome of Arabidopsis. The other MCM2 to 7 members are encoded by a single-copy gene as well. We have analyzed the gene and protein expression of maize *MCM6* in different reproductive and vegetative tissues. Protein localization was investigated using a ZmMCM6-green fluorescent protein (GFP) fusion

protein in cell cycle-arrested onion (*Allium cepa*) epidermal cells and during the cell cycle in maize Black Mexican Sweet (BMS) suspension cells. In addition, verexpressing and antisense transgenic maize plants were generated to investigate ZmMCM6 function and to modify vegetative and reproductive growth by manipulating the cell cycle.

## RESULTS

### Structural Properties of ZmMCM6 and Other Plant MCM Proteins

We have compared all MCM proteins of Arabidopsis and the known maize MCM proteins with MCM proteins of budding yeast and African clawed frog. Yeast and frog have been selected because all MCM2 to 7 genes from these two species are known and functions of MCM proteins have been most intensely studied in these species, using genetic approaches in the case of budding yeast and biochemistry in the case of frog. As shown in Figure 1, all MCM2 to 7 proteins are encoded by single-copy genes with the exception of a duplicated *MCM6* gene of frog. The expanding tree indicates that MCM proteins of fungi, animals, and plants all evolved from one ancestor molecule. Plant MCMs display a higher homology among each other compared with corresponding MCMs of other organisms. Interestingly, the Arabidopsis genome encodes two non-MCM2 to 7 proteins (MCM8 and MCM9), which show homology to MCM8 of frog and human MCM9, respectively. MCM9 of frog is not known to date.

MCM classes consist of large proteins of 716 to 1,017 amino acid residues (molecular mass between 80 and 113 kD) with the exception of Arabidopsis and human MCM9s, which are 610 and 391 amino acids in length, respectively. Table I shows a summary of characteristic features of MCM proteins. Nuclear localization sequences (NLS) have been predicted by PSORT in MCM2 and MCM3 proteins, but not in maize MCM6 and most other MCMs. We have identified potential zinc-finger motifs that might be involved in protein-protein interactions in the N-terminal regions of all MCM proteins with the exception of the MCM3 class and MCM5 from yeast. The zinc-finger motif $CX_2CX_{18-19}CX_4C$ was found in all MCM6, MCM7, and MCM8 sequences. MCM4 proteins contain either this or the $CX_2CX_{18-19}CX_2C$ motif that was also found in the MCM2 protein sequences. Deviations from these classical motifs were found as $CX_2CX_{20-24}CX_{5-10}C$ in the MCM5 and MCM9 classes. In addition, cyclin/cyclin-dependent kinase (CDK) phosphorylation sites (S/T)Px(K/R), which might function as cell cycle regulation motifs, were identified in some MCM proteins. Interestingly, two of the hexameric MCM2 to 7

proteins of each organism investigated in our studies contain this CDK box. For yeast, these are MCM3 and MCM4, in African clawed frog, these are MCM2 and MCM4, whereas in Arabidopsis and maize, these are MCM3 and MCM6.

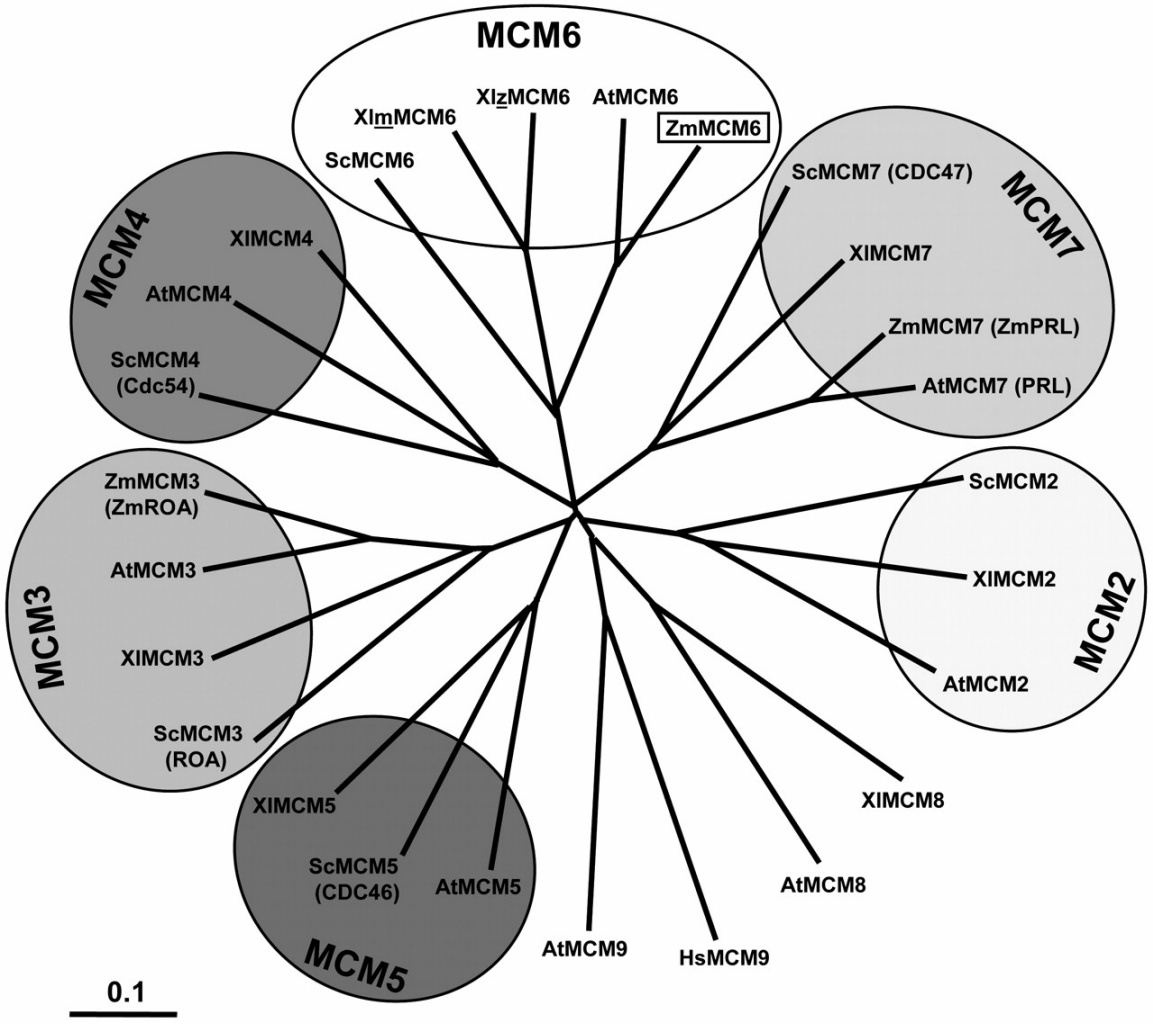


**Figure 1. Phylogenetic tree of MCM2 to 7 protein sequences.** Branch lengths are proportional to phylogenetic distances and scale bar represents 10% substitutions per site. The tree was drawn by Tree-View from a ClustalW alignment using all available MCM protein sequences from Arabidopsis (AtMCM2-9), maize (ZmMCM3, 6, and 7), frog (XlMCM2-8), budding yeast (ScMCM2-7), as well as human MCM9. Due to historical reasons, some proteins were given two names (old names in parentheses). Note that a maternal (m) and a zygotic (z) MCM6 protein have been described in frog. MCM6 of maize is described in this study. For GenBank accession numbers of sequences, see Table I.

**Table I.** *Predicted protein domains and accessions of MCM proteins*

Symbols in parentheses indicate nuclear localization signals (NLS) predicted by PSORT, but deviating from experimental data. Data in the CDK-Box column indicate the number of predicted CDK consensus phosphorylation sites.

| Protein Name | Length (Amino Acids) | NLS | CDK-Box | Zinc Finger | Accession No. |
|---|---|---|---|---|---|
| ScMCM2 | 868 | + | − | + | P29469 |
| XlMCM2 | 886 | + (−) | 2 | + | U44047 |
| AtMCM2 | 928 | + (−) | − | + | NM_103572 |
| ScMCM3 (ROA) | 971 | + | 5 | − | P24279 |
| XlMCM3 | 807 | + | − | − | U26057 |
| AtMCM3 | 776 | + | 1 | − | NM_123997 |
| ZmMCM3 (ZmROA) | 768 | + | 1 | − | AAD48086 |
| ScMCM4 (CDC54) | 933 | − (+) | 2 | + | S56050 |
| XlMCM4 | 858 | − (+) | 2 | + | T47223 |
| AtMCM4 | 743 | − | − | + | NP_179236 |
| ScMCM5 (CDC46) | 775 | − (+) | − | − | P29496 |
| XlMCM5 | 735 | − (+) | − | + | PC4225 |
| AtMCM5 | 727 | − | − | + | NP_178812 |
| ScMCM6 | 1,017 | − (+) | − | + | S64219 |
| XlmMCM6 | 796 | − | − | + | T47222 |
| XlzMCM6 | 824 | − | − | + | AF031139 |
| AtMCM6 | 831 | − | 1 | + | NP_680393 |
| ZmMCM6 | 831 | − | 1 | + | AAW55593 |
| ScMCM7 (CDC47) | 845 | − (+) | − | + | S34027 |
| XlMCM7 | 720 | − (+) | − | + | T47221 |
| AtMCM7 (PRL) | 716 | − | − | + | L39954 |
| ZmMCM7 (ZmPRL) | 720 | − | − | + | CAC44902 |
| AtMCM8 | 777 | − | 2 | + | NM_111800 |
| XlMCM8 | 834 | − | − | + | CAI29793 |
| AtMCM9 | 610 | − | 1 | + | NM_126977 |
| HsMCM9 | 391 | − | 1 | + | NP_694987 |

We have analyzed the structural properties of MCM6 proteins in more detail. With the exception of MCM6 from rat, Figure 2 shows the alignment of all MCM6 protein sequences available in public databases. The largest and most conserved stretch of about 153 amino acids in the central region includes elements of the Walker-type nucleoside triphosphate-binding domain (Walker et al., 1982), which is conserved in a number of ATPases. The putative ATP-binding site of MCM6 proteins is shown by a P-loop that includes the Walker A motif (**G**DPS[C/T][A/S]**KS**) and the Walker B motif. The B motif is part of a highly conserved domain that begins with the acidic amino acid Glu preceding a stretch of hydrophobic residues predicted to form a β-strand and an acidic stretch. Finally, the conserved central domain also contains the R- or SRF (Ser-Arg-Phe)-finger. The Arg residue within the R-finger probably represents the catalytic activity (Davey et al., 2003).

In addition to an N-terminal zinc-finger motif and central catalytic domain, a cyclin/CDK phosphorylation site (S/T)Px(K/R) was found only in the N-terminal region of plant MCM6 proteins at position 107 to 110 (SPnK) in ZmMCM6 and 102 to 105 (TPnK) in AtMCM6, respectively. Finally, a conserved motif of unknown function was found at the very C terminus of most MCM6 proteins (Fig. 2, boxed region). This region of 14 to 16 amino

acids consists of an aliphatic/polar core that is flanked on both sides by acidic amino acids. Although the function of this motif is unknown, it is characteristic for all MCM6 proteins expressed postfertilization in higher eukaryotes, is absent in maternal MCM6 of frog, and is different in fungi.

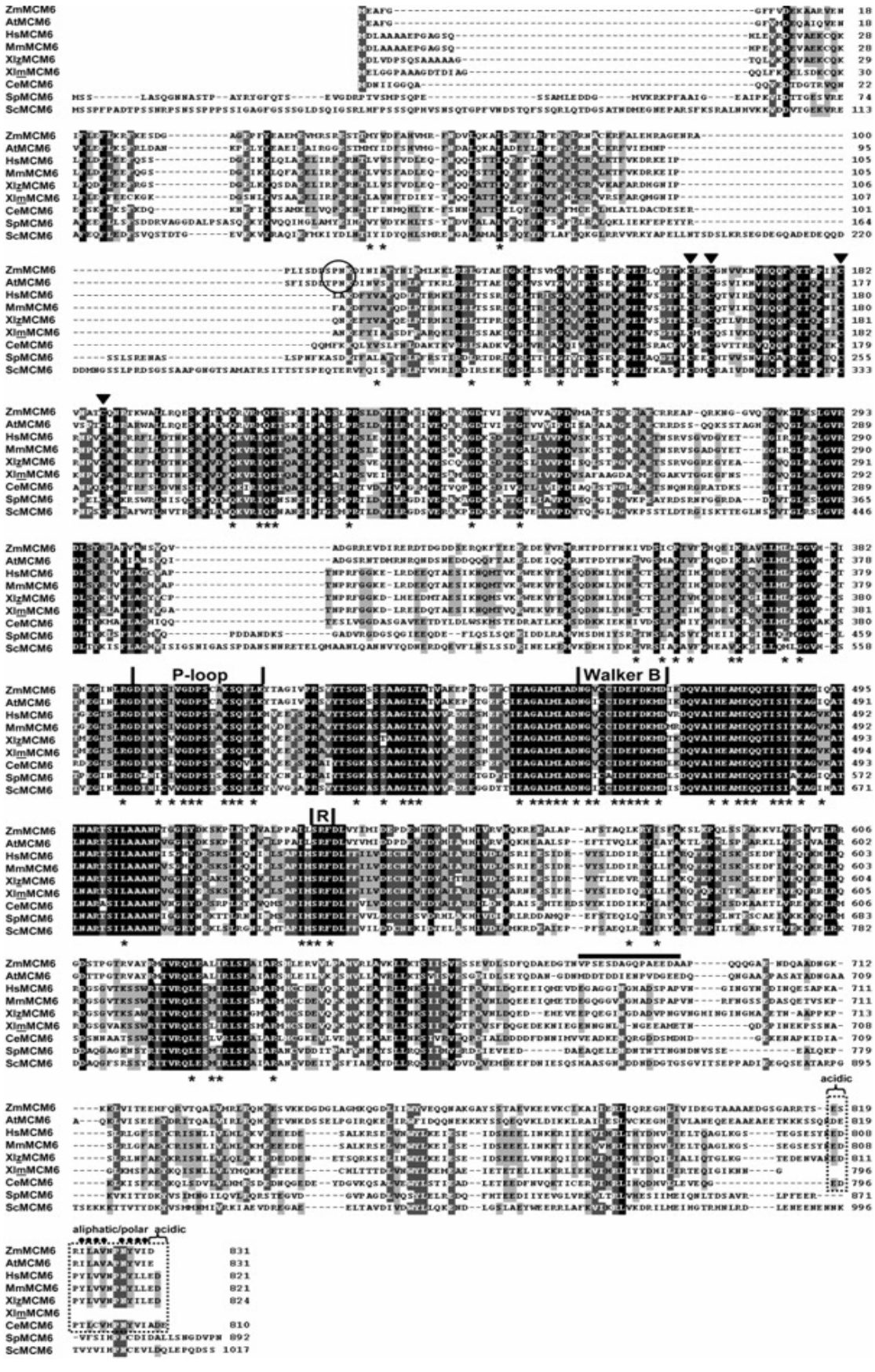
ZmMCM6
AtMCM6
HsMCM6
MmMCM6
XlzMCM6
XlmMCM6
CeMCM6
SpMCM6
ScMCM6
P-loop
Walker B
R
acidic
aliphatic/polar acidic

**Figure 2. ZmMCM6 represents a member of the highly conserved MCM protein family.** Homology searches were performed with BLASTP and protein sequences were aligned with ClustalW and drawn using GeneDoc. Identical residues are shaded in black and similar residues are shaded in gray. The alignment shows deduced amino acid sequences of MCM6 from maize (ZmMCM6) and all other eukaryotes available in public databases with the exception of MCM6 from rat, which is almost identical with MCM6 from humans and mouse. GenBank accession numbers for most MCM6 proteins are given in Table I. The human (HsMCM6), mouse (MmMCM6), *C. elegans* (CeMCM6), and fission yeast (SpMCM6) protein sequence accessions are Q14566, P97311, P34647, and P49731, respectively. Amino acid residues identical/similar in MCM proteins listed in Table I are labeled with asterisks. Highest conserved regions consist of the P-loop, theWalker B motif, and the R- or SRF-finger. The first two motifs are characteristic for ATPases and are essential for NTP binding. The Arg residue within the R-finger probably represents the catalytic activity. The four triangles mark the Cys residues of the zinc-finger-type motif. A predicted cyclin/CDK phosphorylation site that occurs only in plant MCM6 proteins is encircled. A conserved C-terminal region characterized by an aliphatic/polar region of 10 amino acids (dots) flanked on both sides by one to two acidic amino acid residues, which is characteristic for MCM6 of multicellular organisms, but absent in maternal MCM6 of frog and MCM6 proteins of yeast, is boxed with broken lines. The C-terminal region of ZmMCM6 that was used to obtain a peptide antibody is indicated by a horizontal bar.

## ZmMCM6 Is Strongly Up-Regulated in the Female Gametophyte after Fertilization and Expression Is Low in Vegetative Proliferating Tissues

We have analyzed the expression, subcellular localization, and function of the fertilization-induced *MCM6* gene of maize in more detail. Low gene expression levels were detected by single-cell (SC) reverse transcription (RT)-PCR in the unfertilized egg cell (Fig. 3A). Twelve hours after in vitro pollination (IVP; this stage corresponds to about 6 h after fertilization; E. Kranz, personal communication), high transcript amounts have been detected in the zygote. Later, during zygote development (21 h after IVP), *ZmMCM6* transcript levels decrease and remain low 27 to 48 h after IVP. A significant oscillation of gene expression in a cell cycle-dependent manner was not observed. For comparison, another gene, *ZmFEN-1a*, which was also identified in our screen for fertilization-induced genes and which encodes a flap endonuclease required for DNA repair, was used to study cell cycle-dependent gene expression during zygote and proembryo development. ZmFEN-1a is a homolog of RAD27 from yeast showing up-regulation of gene expression during late G1 phase (Vallen and Cross, 1995). Similar to *ZmMCM6*, expression of *ZmFEN-1a* is induced 12 h after IVP, but additional gene expression peaks have been observed 27 to 33 and 48 h after IVP, indicating that G1 phase occurs in the zygote at about 12 h after IVP, in the two-cell proembryo at about 27 to 33 h, and in the four-cell proembryo at about 48 h. To correlate these findings with zygotic cell division, different developmental stages were stained with 4’,6-diamidino-2-phenylindole (DAPI) and fluorescence quantified by ImageJ software. As shown in

Figure 3B, relative DAPI staining of the zygote nucleus 12 h after IVP was about 50% compared with a zygote nucleus 27 h after IVP, indicating that chromatin of the latter cell was in G2 phase, whereas the first cell was in G1 phase. DAPI staining of the egg nucleus was much weaker compared with the zygote nucleus 12 h after IVP (data not shown). Relative DAPI fluorescence measured 33 h after IVP of a two-celled proembryo corresponds to the sum of the zygote nucleus 27 h after IVP, indicating that this proembryo was in G1 phase. A four-celled proembryo was present 48 h after IVP. Please note that the cells used for the expression analysis of *ZmFEN-1a* were collected in early summer when zygote and embryo development are 10% to 20% accelerated, which explains the accelerated gene expression pattern compared with the DAPI measurements. In summary, *ZmMCM6* transcript levels are high about 6 h after fertilization (12 h after IVP) in G1 and continuously decrease throughout zygote and early embryo development (18, 21, 24, 27, 30, 33, and 48 h after IVP; data for stages 18, 24, and 30 h not shown), but significant oscillation of gene expression during early development was not observed. Expression studies of *ZmMCM6* in cells of the female gametophyte revealed relatively high transcript amounts in the central cell (Fig. 3C), but not in the other cells of the unfertilized embryo sac. Only one out of six synergids analyzed showed a weak signal (data not shown). Five sperm cells and antipodal clusters of at least 10 cells were collected and used to study *ZmMCM6* expression. A very weak signal could be detected in one out of three antipodal clusters tested, but never in sperm cells or in leaf mesophyll protoplasts derived from mature leaves.

Compared to zygotes shortly after fertilization, expression of *ZmMCM6* in vegetative and complex reproductive tissues is very low. To display significant *ZmMCM6* transcript signals from a northern blot containing total RNA, hybridization with a radiolabeled probe and exposure of up to 14 d using intensifier screens was necessary (Fig. 4A). A single band slightly smaller than 3.0 kb was detected, indicating that the cloned 2,785 nucleotides of *ZmMCM6* represent the full-length transcript. The strongest signals were obtained from tissues containing proliferating cells such as root tips, nodes, leaf meristem, and developing tassels, but also embryonic and nonembryogenic suspension cultures. In developing tassels, signal intensity correlates with developmental stages, while signals were absent in tassels at maturity. Moreover, signals were detected in whole-seedling tissue 4 d after germination, but were absent in leaf tissues of older seedlings (10 d after germination). Leaf meristem displayed relatively strong signals, whereas signals were absent in mature leaves. A ZmMCM6-specific peptide antibody

against the less conserved C-terminal part of the protein (see also Fig. 2) was used to detect MCM6 in different tissues and developmental stages (Fig. 4B). A single band of about 90 kD was detected in protein blots, which corresponds to the expected size of 92.5 kD. Minor protein amounts could be detected in nodes, immature cobs, and ovaries, whereas significant ZmMCM6 amounts could not be detected in young and mature leaves and whole roots during tassel maturation as well as in mature pollen. The highest protein amounts are present in developing kernels. While ZmMCM6 protein amounts are relatively lowin kernels prior to fertilization (0 days after pollination [DAP]), a strong increase was observed 6 DAP and highest protein levels were detected 10 to 20 DAP.

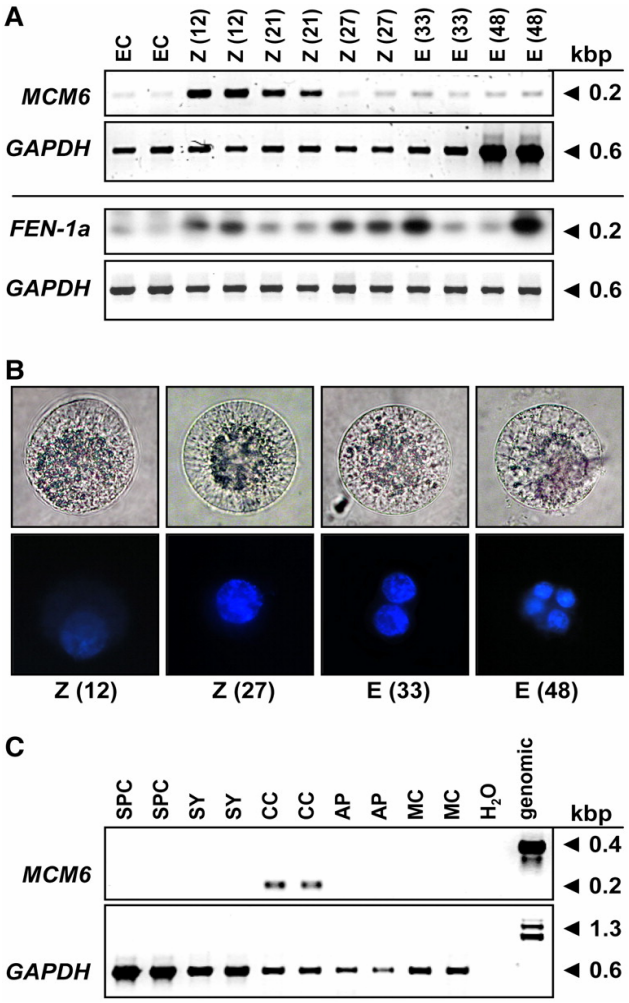


**Figure 3. Expression of *ZmMCM6* in gametic cells before and afterfertilization.** A, SC RT-PCR of *ZmMCM6* and *ZmFEN-1a* in egg cells (EC), zygotes (Z), and proembryos (E) at different time points after IVP. The numbers in parentheses indicate hours after pollination (fertilization occurs about 6 h after IVP; top row). Amplification of GAPDH from the same cells is shown for comparison in the corresponding bottom rows. Note that the cells for *ZmMCM6* and for DAPI staining (B) were collected in winter and for *ZmFEN-1a* in summer. *ZmFEN1a* signals were intensified after blotting and hybridization with a gene-specific radioactive probe. B, Light (top row) and fluorescent images (bottom row) of DAPI-stained zygotes and proembryos. Time points after IVP are indicated. Cell size is about 60 mm. C, SC RT-PCR of *ZmMCM6* in sperm cells (SPC), cells of the female gametophyte, including synergid (SY), central cell (CC), and antipodals (AP), as well as leaf mesophyll cell (MC) and controls (water and genomic). Amplification of *GAPDH* from the same samples is shown in the bottom row.

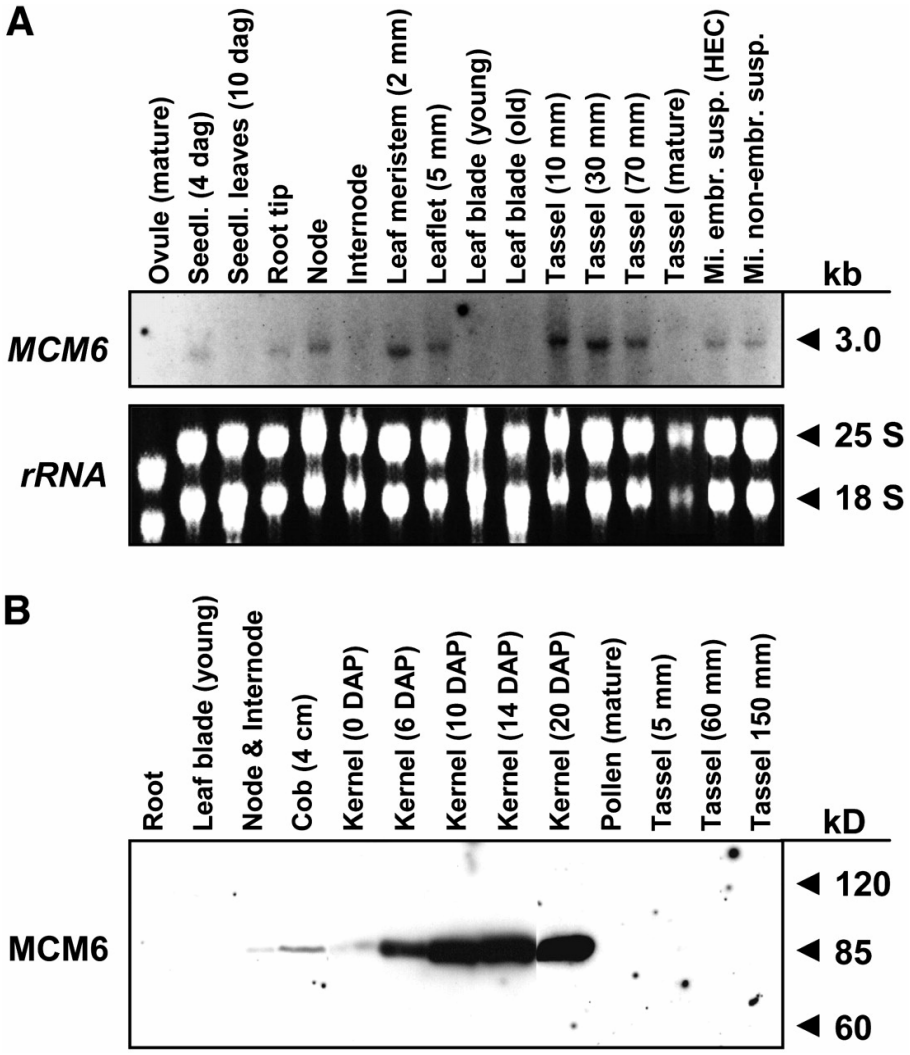


**Figure 4. Expression of *ZmMCM6* gene and protein in vegetative and complex reproductive tissues**. A, RNA gel blot showing expression of *ZmMCM6* in the vegetative and reproductive tissues indicated. Fifteen micrograms of total RNA from each tissue were hybridized to a radioactively labeled probe containing the 3' untranslated region as well as 896 bp encoding the C-terminal region of the gene. The film was exposed for 2 weeks using intensifier screens. B, Protein gel blot incubated with a peptide antibody directed against 15 amino acid residues within a ZmMCM6 C-terminal-specific region (see also Fig. 2). Ten micrograms of protein of the tissues indicated were each separated by 8% SDS-PAGE and blotted onto a polyvinylidene difluoride membrane. A single band was obtained showing the specificity of the antibody.

**ZmMCM6 Shuttles between Cytoplasm and Nucleoplasm in a Cell Cycle-Dependent Manner**

We have used a chimeric ZmMCM6 protein fused to GFP and immunocytochemistry to study the subcellular localization of ZmMCM6. First, onion epidermal cells were bombarded with a construct encoding a ZmMCM6-GFP fusion protein under the control of the strong and constitutively expressing ubiquitin (UBI) promoter of maize. As shown in Figure 5, A and B, relatively strong GFP signals accumulated in cytoplasm around the nucleus and in transvacuolar strands of the cytoplasm surrounding the nucleus. Protein localization in the nucleus was not detectable. Focusing through side views of nuclei displayed more clearly that the fusion protein accumulated in cytoplasm surrounding the nucleus, but was excluded from the nucleoplasm (Fig. 5, C and D). In contrast, the N-terminal 388 amino acids of a maize transcriptional regulator of anthocyanin biosynthesis (Ludwig et al., 1989) that also includes an NLS fused with GFP (Lc-GFP in Fig. 5E) displayed most fluorescence within the nucleus. However, onion epidermal cells are no longer proliferating and might be in G0 phase of the cell cycle. We have therefore used BMS maize suspension cultures to study ZmMCM6-GFP subcellular protein localization during the different stages of the cell cycle. Synchronization of BMS suspension cultures to correlate protein localization with defined cell cycle stages was not successful. We have therefore determined relative DNA amounts of individual BMS cells after DAPI dihydrochloride staining. Strongest DAPI fluorescence was measured from cells in G2 phase. Signals from cells in G1 phase were less than 50%, probably due to higher amounts of heterochromatin and beginning of chromosome condensation in nuclei of cells in G2 in preparation for mitosis. The weakest fluorescence was measured from cells in late G1/S phase, which is likely to result from decondensation of DNA during DNA synthesis. In total, 62 individual cells were analyzed for GFP fluorescence and DAPI staining. As shown in Figure 6, A to C, cells in G1 phase (42% of the cells analyzed) showed localization of the chimeric protein in both cytoplasm and nucleoplasm. A detailed analysis of cells in G1 phase using confocal laser-scanning microscopy (CLSM) displayed a gradient of GFP fluorescence between the cytoplasm and nucleoplasm(Fig. 6,Qand R), indicating precise control of ZmMCM6 import into the nucleus. Highest protein amounts were detected in the nucleus during late G1/S phase (Fig. 6, D–F; 11.5% of the cells studied). At the end of S phase or during early G2 phase, ZmMCM6 became fully excluded from the nucleus, as all cells in G2 phase (45% of the

cells analyzed) lacked GFP fluorescence in the nucleus (Fig. 6, G–L). CLSM studies confirmed this observation (Fig. 6M). One cell was observed in early prophase of mitosis (Fig. 6, N–P) showing condensation of chromosomes (Fig. 6O). Similar to G2 cells, GFP signals were not detectable in the nucleus of this cell. Interestingly, we have never detected GFP fluorescence in the nucleolus (Fig. 6, Q and R). In contrast, BMS suspension cells transiently expressing a *UBI*p:*GFP* construct always showed equal GFP fluorescence in the cytoplasm, nucleoplasm, and nucleolus independently from the stage of cell cycle (Fig. 6S).

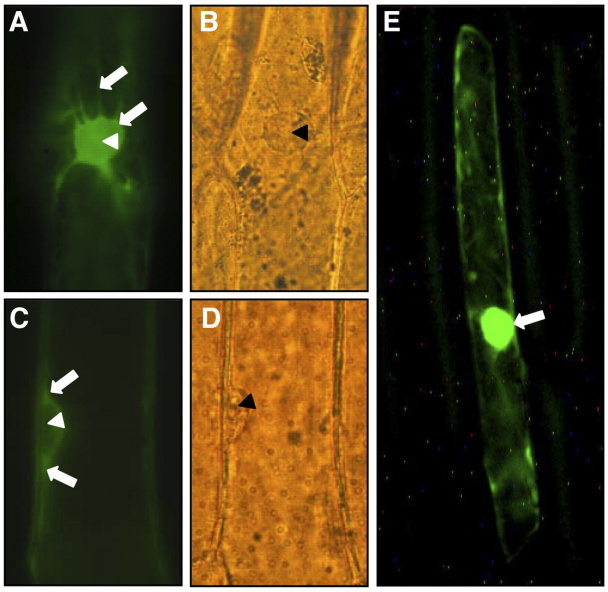


**Figure 5. ZmMCM6 protein is excluded from the nucleus in epidermal onion cells.** Onion cells were transiently transformed with a *UBI*p:*ZmMCM6-GFP* construct and analyzed using epifluorescence (A and C) and light microscopy (B and D). A, Top view of a nucleus showing accumulation of chimeric protein in cytoplasm around the nucleus. The arrows point toward cytoplasm surrounding the nucleus and a transvacuolar cytoplasmic strand. B, Light microscopic image of A. C, Side view of a nucleus showing accumulation of chimeric protein in cytoplasm around the nucleus (arrows), but not inside the nucleus. D, Light microscopic image of C. E, Epifluorescence of an onion epidermal cell bombarded with a *35S*p:*Lc-GFP* construct encoding the N-terminal 388 amino acids (including the NLS) of a maize transcriptional regulator of anthocyanin biosynthesis in maize (GenBank accession no. A41388) fused with GFP. Most of the fluorescence was detected within the nucleus (arrow). Accumulation of the chimeric protein in cytoplasm around the nucleus, as in A and C, was never observed. Arrowheads in A to D point toward nucleoli.

Immunocytochemistry with isolated BMS nuclei was performed to measure the cell cycle dependency of nuclear ZmMCM6 localization more precisely and to prove that the difference of DAPI signal intensity is not originating from problems of dye uptake. DNA and ZmMCM6 content of isolated BMS nuclei were measured after DAPI staining and by

using a fluorescein isthiocyanate (FITC)-coupled secondary antibody against the ZmMCM6-specific peptide antibody described described above. FITC signals of nuclei showing endo-reduplication have not been measured. As shown in Figure 7, A and B, all nuclei displaying strong FITC signals were in G1 or early S phase of the cell cycle. Nuclei in late S or G2 (Fig. 7, C and D) never showed significant signals. Those signals were in the range of background signals that were also obtained after using preimmune serum instead of the serum containing the specific antibody (Fig. 7, E and F). Figure 7G shows a summary of measurements obtained from 44 nuclei. A relative DNA content of 2C (±15%) was considered as G1, a DNA content of 2C (+16% to 25%) as G1/S, and a DNA content of 4C (±15%) as G2. To determine FITC background fluorescence, DNA and FITC signal intensities of 16 randomly chosen nuclei were measured after incubation with preimmune serum (Fig. 7H). In contrast to the control, more than 50% of nuclei in G1 showed significant ZmMCM6 amounts. All nuclei in late G1/early S phase contain high ZmMCM6 levels, which decrease during S phase progression and are no longer measurable at later stages of S phase or in G2. In summary, immunocytochemistry data confirm the above finding that ZmMCM6 is taken up by the nucleus during G1 phase and protein levels are highest during late G1/S phase, while ZmMCM6 is excluded from the nucleus during late S, G2, and mitosis. Attempts to measure ZmMCM6 levels of nuclei from isolated cells of the female gametophyte were not successful, probably because only nuclei of zygotes at defined stages contain sufficient detectable protein amounts and the number of zygote nuclei was not sufficient. Avery high number of nuclei, similar to the approach with the BMS suspension cells, will be necessary to determine relative ZmMCM6 protein amounts in female gametophyte nuclei.

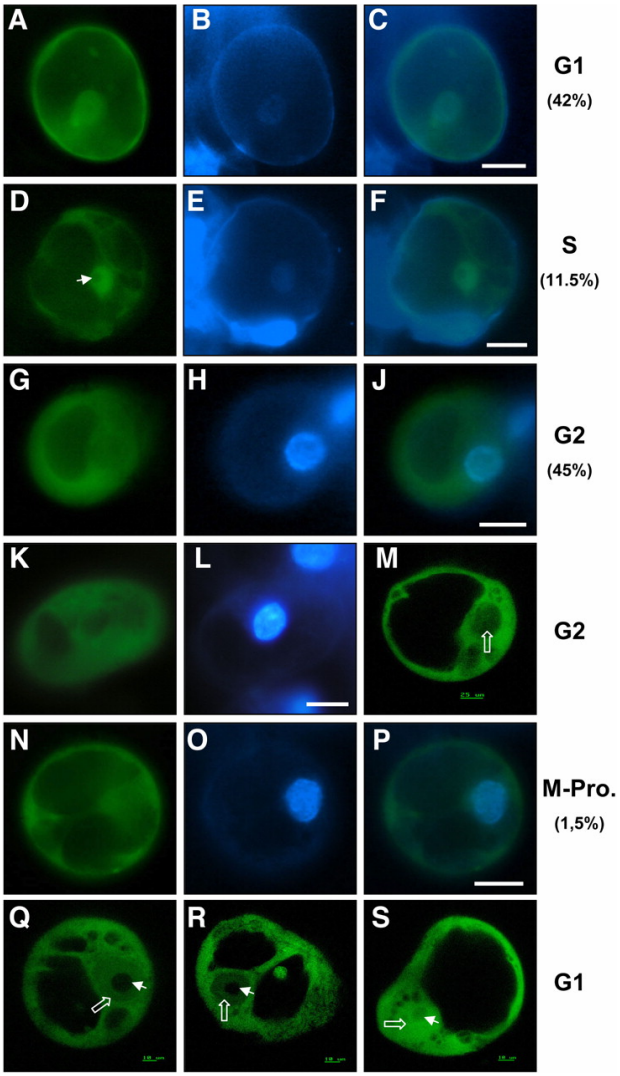


**Figure 6. ZmMCM6 shuttles between nucleus and cytoplasm in maize BMS suspension cells in a cell cycle-dependent manner.** Suspension cells were transiently transformed with a *UBI*p:*ZmMCM6-GFP* construct and analyzed using epifluorescence microscopy (A–L and N–P) as well as CSLM (M, Q–S). Relative DNA content of cells was determined after DAPI staining. A, About 42% cells showed localization of the chimeric protein in both cytoplasm and nucleoplasm. B, DAPI staining of the cell shown in A to display the nucleus. C, Merged image of A and B showing similar DAPI signal in the nucleus compared to GFP fluorescence. These cells were counted for G1 phase. D, About 11.5% of the cells examined accumulated most of the chimeric protein in the nucleoplasm, but not in the nucleolus (arrowhead). E, DAPI staining of the cell shown in D. The image was enhanced to display the weak fluorescence of the nucleus in late G1/S phase. F, Merged image of D and E showing mainly GFP fluorescence in the nucleus. G and K, Majority of cells (about 45%) displayed GFP fluorescence only in the cytoplasm and lacked GFP signals in the nucleus. H and L, Strong DAPI staining of the nuclei of these cells revealed that they were in G2 phase. J, Merged image of G and H showing GFP fluorescence in the cytoplasm and DAPI fluorescence in the nucleus. M, Stack of five CLSM images of a cell in G2 phase confirms lack of GFP fluorescence in the nucleus (open white arrow). N, Cell showing GFP fluorescence exclusively in the cytoplasm displayed condensation of chromosomes (O) during prophase of mitosis. P, Merged image of N and O confirms lack of GFP fluorescence in the nucleus. Q and R, Gradient of the fusion protein between cytoplasm and nucleoplasm was observed in stacks of five images each of two different cells in G1 phase. The weak DAPI staining of these cells is not shown. Note that the chimeric protein is localized in both cytoplasm and nucleoplasm (open white arrows), but never in the nucleolus (arrowhead). S, Control showing a

suspension cell bombarded with a *UBI*p:*GFP* construct showing GFP fluorescence in the nucleolus, nucleoplasm, and cytoplasm. The arrowhead points toward the nucleolus and the open arrow toward the nucleoplasm. Scale bars are 20 mm, unless otherwise indicated.

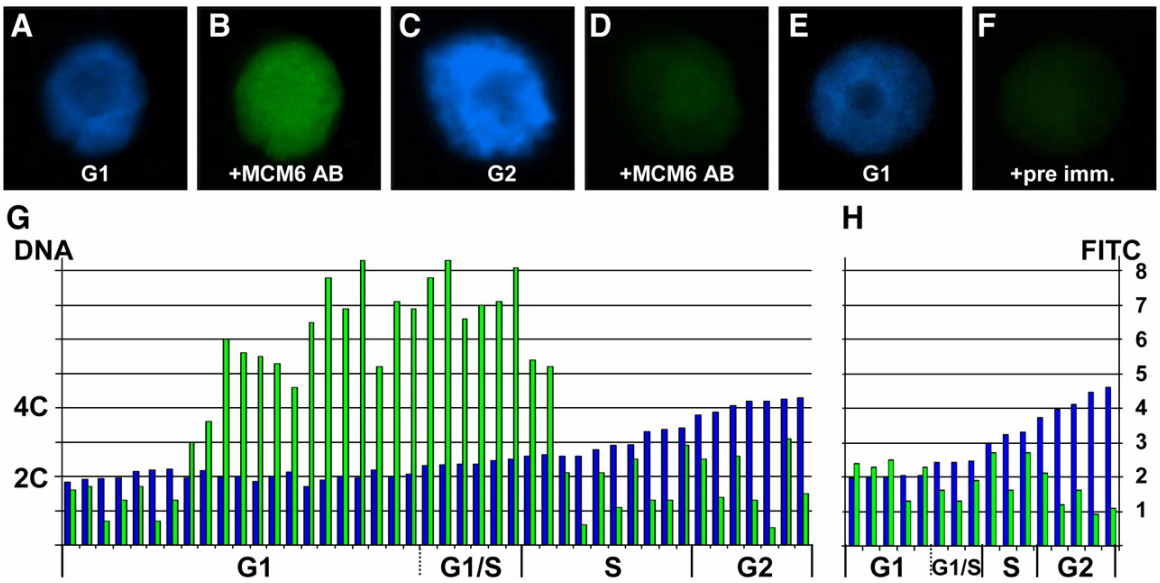


**Figure 7. ZmMCM6 is taken up by the nucleus during G1 phase and highest protein levels are detectable during late G1/early S phase of the cell cycle**. Relative DNA content of isolated BMS nuclei were determined after DAPI staining. ZmMCM6 protein amounts were measured after incubation with an FITC-coupled antibody against a ZmMCM6 peptide antibody. DAPI staining (A) and FITC signals (B) of a nucleus in G1; DAPI staining (C) and FITC signals (D) of a nucleus in G2; DAPI staining of a G1 phase nucleus (E) and the same nucleus after incubation with preimmune serum showing minor background signals (F). G, Summary of measurements of 44 nuclei. After DAPI measurements, nuclei were classified as G1 (2C±15%), G1/S (2C+16%–25%), S (2C+ 26%–84%), and as G2 (4C ± 15%). Histograms show relative DNA (blue bar) and FITC (green bar) levels of individual nuclei. Relative DNA content is indicated at the left and relative FITC signal intensity at the right of image H. H, To show antibody specificity and to determine background signals, nuclei have been incubated with preimmune serum. Classification of nuclei was as described in G.

### Phenotypes of Transgenic Maize after ZmMCM6Up- and Down-Regulation

A transgenic approach was chosen to increase and to down-regulate *ZmMCM6* gene expression in maize. One hundred-fifty immature hybrid embryos have been bombarded with a sense construct (*UBI*p:*ZmMCM6*) to increase *ZmMCM6* transcript amounts by expressing the full-length *ZmMCM6* cDNA under the control of the strong and constitutively expressing maize UBI promoter. Four plants have been regenerated (transformation efficiency of 2.7%), all representing one clonal line as they displayed the

identical transgene integration pattern (plants SE1a–SE1d). The Southern blot in Figure 8A shows that this line contains multiple transgene integrations, including one or more full-length integrations. However, quantification of *ZmMCM6* transcript amounts showed that there was no significant difference between the four transgenic lines compared to wild-type plants (Table II). An obvious phenotype was not observed and plants were both fully male and female fertile. We have therefore bombarded another 400 immature hybrid embryos with a sense construct carrying a GFP conjugate (*UBI*p:*ZmMCM6-GFP*) both to increase *ZmMCM6* transcript amounts and to simultaneously study ZmMCM6 protein localization. Five independent transgenic lines (G1–G5) have been generated (transformation efficiency of 1.2%) containing one to two transgene integrations. Unfortunately, none of these lines contained a full-length and thus functional integration of the construct (Fig. 8A). GFP expression was therefore not detectable in any of the tissues investigated. The observation that these plants were small (Table II) was probably an effect of longer regeneration periods and growth in winter. Reproductive organs were fully developed and seed set was obtained after selfing.

In addition, we have generated transgenic maize with the aim of decreasing *ZmMCM6* transcript levels. Three hundred-eighty immature embryos of the inbred line A188 have been bombarded with an antisense (AS) construct (*UBI*p:*ZmMCM6-AS*). Sixteen plants containing *ZmMCM6* AS integrations were regenerated (transformation efficiency of 4.2%) representing 10 independent lines (Table II, plants AS1–AS10b). The transgene integration pattern of five plants is shown in Figure 8A. The genomic Southern blot shows multiple transgene integrations for each plant. AS4a to AS4c displayed the same pattern, indicating that they represent a clonal line. The other two plants (AS3 and AS5) show a different integration pattern. Full-length integrations could be observed in these two lines as well as in line AS6, while none of the lines AS1, AS2, and AS7 to AS10b, respectively, contained full-copy transgene integrations (Table II). Surprisingly, expression of the AS transcript could not be detected in a single line in northern blots (data not shown). The more sensitive RT-PCR method was therefore applied and showed weak AS expression after 38 PCR cycles in lines AS5 and AS6, respectively (Table II). Quantification of both sense and AS transcript amounts in transgenic AS plants by quantitative real-time RT-PCR were in the range of wild-type background sense signals, indicating that the AS transcript amounts were extremely low and not increased above wild-type sense transcript amounts. Nevertheless, those plants that showed a very weak expression of the AS transgene (AS5 and AS6) and/or contained

functional copies of the transgene (AS3 and AS4a–c) were strongly reduced in size (Fig. 8B) and did either develop only immature cobs (lines AS3, AS4b, S4c, AS5, and AS6) or no cob at all (plant AS4a). As shown in Table II, these plants were additionally male sterile due to the lack of anthers or whole male florets (AS4c and AS5). Three plants produced little pollen (AS4a, AS4b, and AS6). Pollen of the plants AS4a and AS4b was used to pollinate wild-type plants. Forty-two progeny plants (plants AS4a/1–20 and AS4b/1–22) were used to study transgene transmission and expression. Surprisingly, none of these plants contained a transgene (Table II). These findings suggest that even mild *ZmMCM6* down-regulation affects both male and female gametophyte development and thus transgene transmission.

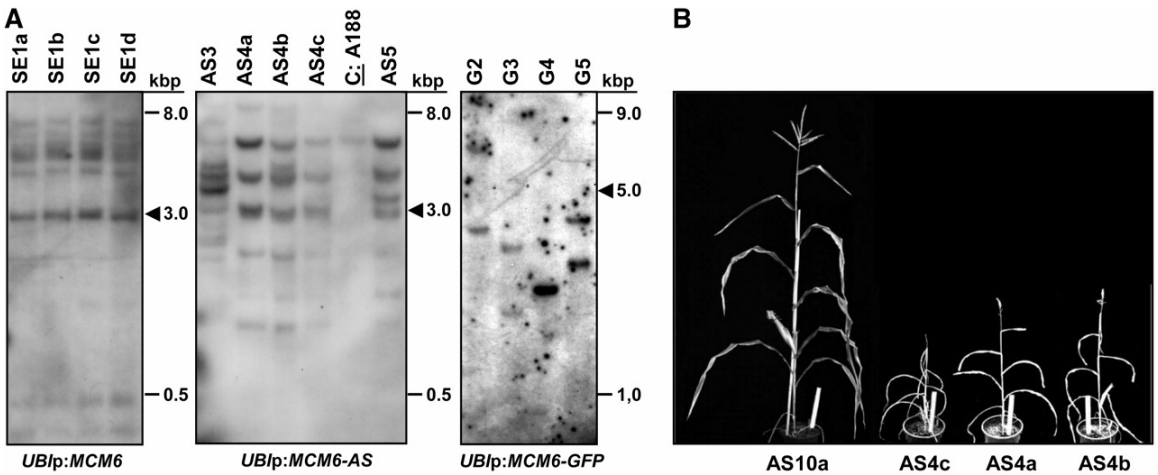


**Figure 8. Molecular and phenotypical analysis of transgenic maize containing the *ZmMCM6* gene under control of the strongand constitutive maize UBI promoter.** A, Examples of Southern blots containing 10 mg genomic DNA of transgenic lines with *ZmMCM6* constructs in sense (SE, left) and antisense (AS, middle) orientation, or fused with GFP (G, right). Genomic DNA was digested with enzyme combinations to display full-copy integrations (arrowheads). Left and middle blots were hybridized with a *ZmMCM6*-specific probe and the right blot with a *GFP*-specific probe. The control (A188) on the blot in the middle shows the endogenous *ZmMCM6* signal. B, Transgenic plants containing a functional *ZmMCM6* AS construct were small in size and did not develop cobs to maturity. Tassels contained little pollen. Here, the clonal line AS4a to AS4c is shown. The line AS10a lacking a functional transgene is shown at the left. Plant height of AS10a was comparable to wild-type plants (A188; 160–190 cm) and both a cob and tassel were fully developed. The white ruler in flower pots is 25 cm.

**Table II.** *Summary of molecular and phenotypical analysis of transgenic maize (T0 and T1 generations, respectively) containing the ZmMCM6 gene under control of the strong and constitutive maize UBI promoter in sense and AS orientation or fused to GFP*

n.d., Not determined.

| Construct | Plant No. | Functional Transgenes[a] | Transgene Quantity[b] | Plant Height[c] | Fertility[d] |
|---|---|---|---|---|---|
| – | Wild type (A188) | – | 100/25/0.68 | 160–190 | + |
| Overexpression | | | | | |
| *UBI*p:*MCM6* (T0) | SE1a | ≥5 (+) | 0.66 | 158 | + |
| *UBI*p:*MCM6* (T0) | SE1b | ≥5 (+) | 0.33 | 185 | + |
| *UBI*p:*MCM6* (T0) | SE1c | ≥5 (+) | 0.27 | 183 | + |
| *UBI*p:*MCM6* (T0) | SE1d | ≥5 (+) | 0.26 | 172 | + |
| UBIp:MCM6-GFP (T0) | G1 | 1 (−) | n.d. | (150) | + |
| UBIp:MCM6-GFP (T0) | G2 | 2 (−) | n.d. | (100) | + |
| UBIp:MCM6-GFP (T0) | G3 | 2 (−) | n.d. | (60) | + |
| UBIp:MCM6-GFP (T0) | G4 | 1 (−) | n.d. | (60) | + |
| UBIp:MCM6-GFP (T0) | G5 | 2 (−) | n.d. | (96) | + |
| Down-regulation | | | | | |
| UBIp:MCM6-AS (T0) | AS1 | ≥3 (−) | 0.63 | 175 | + |
| UBIp:MCM6-AS (T0) | AS2 | ≥4 (−) | 0.96 | 182 | + |
| UBIp:MCM6-AS (T0) | AS3 | ≥7 (+) | 0.39 | 130 | FS |
| UBIp:MCM6-AS (T0) | AS4a | ≥5 (+) | 0.73 | 83 | FS/(MS) |
| UBIp:MCM6-AS (T0) | AS4b | ≥5 (+) | 0.48 | 86 | FS/(MS) |
| UBIp:MCM6-AS (T0) | AS4c | ≥5 (+) | 0.36 | 58 | FS/MS |
| UBIp:MCM6-AS (T0) | AS5 | ≥6 (+) | 1.10 | 66 | FS/MS |
| UBIp:MCM6-AS (T0) | AS6 | ≥5 (+) | 0.42 | 68 | FS/(MS) |
| UBIp:MCM6-AS (T0) | AS7 | ≥4 (−) | 0.90 | 182 | + |
| UBIp:MCM6-AS (T0) | AS8a | ≥4 (−) | 0.55 | 161 | + |
| UBIp:MCM6-AS (T0) | AS8b | ≥4 (−) | 0.78 | 159 | + |
| UBIp:MCM6-AS (T0) | AS8c | ≥4 (−) | 0.96 | 175 | + |
| UBIp:MCM6-AS (T0) | AS9a | ≥4 (−) | 0.08 | 174 | + |
| UBIp:MCM6-AS (T0) | AS9b | ≥4 (−) | 1.10 | 158 | + |
| UBIp:MCM6-AS (T0) | AS10a | ≥6 (−) | 0.42 | 187 | + |
| UBIp:MCM6-AS (T0) | AS10b | ≥6 (−) | 0.49 | 169 | + |
| [*UBI*p:*MCM6-AS*] (T1)[e] | AS4a/1–20 | – | n.d. | 155–185 | + |
| [*UBI*p:*MCM6-AS*] (T1)[e] | AS4b/1–22 | – | n.d. | 155–185 | + |
| [*UBI*p:*MCM6-AS*] (T1)[e] | AS6/1 | – | n.d. | 150 | + |

[a]Number of transgene integration events, functional transgene integrations (+), and lack of functional transgene (−), respectively. [b]Quantification of relative sense and AS transcript amounts. Expression in immature wild-type tassels (10 mm; see also Fig. 4A) was set as 100%. Relative expression in wild-type roots was 25% and 0.68% in mature leaves. No distinction between sense and AS transcript levels. [c]Plant height in centimeters. G1 to 5 plants were generated in winter after a long tissue culture stage. [d]Fully developed and fertile cobs as well as tassels (+). FS, Female sterility; MS, male sterility; parentheses, tassels mostly sterile, development of little pollen. [e]Pollen of transgenic lines were back crossed to wild-type (A188) plants to generate T1 progeny. One selfed kernel was obtained from a tassel flower of plant AS6, which developed into a female spikelet.

## DISCUSSION

Structure and Domains of Plant MCM Proteins Similar to fungi and animals, plants seem to possess a single gene for each subunit of the MCM hexamer complex. In addition to the classical MCM2 to 7 genes, Arabidopsis contains two additional *MCM* genes (*AtMCM8* and *AtMCM9*). Homologs of these genes are not present in the yeast genome (Forsburg, 2004), but MCM8 homologs have recently been reported in humans (Gozuacik et al. 2003; Johnson et al., 2003) as well as in frog (Maiorano et al., 2005). While HsMCM8 is involved in the assembly of the pre-RC (Volkening and Hoffmann, 2005), XlMCM8 was shown to function as a DNA helicase during replication elongation, but not during initiation of DNA replication. A function of MCM9 has not been elucidated to date (Yoshida, 2005).

All MCM proteins are likely to have evolved from a single gene, as the archeon *Methanobacterium thermoautotrophicum* contains a single MCM gene that is able to form a homohexamer complex and that possesses both a DNA-dependent ATPase and a 3' to 5' helicase activity to unwind 500 bp of DNA (Kelman et al., 1999). It is thus not surprising that the central domains of MCM proteins for this activity are most highly conserved. Interestingly, only the trimeric complex of MCM4, MCM6, and MCM7 has been shown to possess in vitro helicase activity (Ishimi, 1997; Lee and Hurwitz, 2001). In mouse, it was recently reported that it is the ATP-binding activity of MCM6 that is critical for DNA helicase activity (You et al., 1999). As in plant MCM6 proteins, the putative catalytic Arg residue is embedded in a conserved SRF motif (Davey et al., 2003), suggesting a similar protein activity.

The other domains of MCM proteins are less conserved. Although the known MCM functions are within the nucleus, only a few MCM proteins were predicted to contain NLS. Experimentally, nuclear import of MCM monomers has been functionally demonstrated only for MCM2 of fission yeast (*Schizosaccharomyces pombe*), budding yeast, and mice, as well as for MCM3 of yeast and humans (for review, see Forsburg, 2004). However, probably all MCM proteins contain domains to interact with other proteins. The zinc-finger motif that was found in almost all MCMs (with the exception of the MCM3 class) is likely to be involved in protein- protein interactions, which are necessary to form the hexamer, but may also be required to bind either to MCM2 and/or MCM3 for cotranslocation into the nucleus. Reconstitution experiments have demonstrated recently that yeast MCM6 physically interacts with MCM2 (Davey et al., 2003). Thus a major function of MCM2 might be to shuttle the enzymatically active MCM6 and other MCM proteins into the nucleus. Finally, a motif for cell cycle regulation (Cdk-box) was identified in some MCM proteins, indicating that the periodic association of the MCM complex with chromatin, nuclear import-export, and/or protein-protein interactions might be regulated via phosphorylation by CDKs. In yeast, nuclear export of MCM4 was shown to be regulated by CDK activity (Labib et al., 1999; Nguyen et al., 2000). Whether a similar mechanism exists for MCM6 as well as MCM8 and MCM9 of plants that contain such motifs remains to be shown. MCM3 from Arabidopsis, which also contains a putative Cdk-box, was shown to localize nuclear throughout interphase and prophase (Sabelli et al., 1999), indicating a role of this motif not involved in nuclear import and export.

**Expression of Plant MCM Genes and Cell Cycle-Dependent Nuclear Localization**

Little is known about the expression and subcellular protein localization of plant *MCM* genes. Abundance in the expression of *ZmMCM3, ZmMCM7,* and *AtMCM7* genes has been correlated with cell proliferation throughout vegetative plant development (Sabelli et al., 1996; Springer et al., 2000; Bastida and Puigdome`nech, 2002; Holding and Springer, 2002). *MCM7* from Arabidopsis and maize was shown to be strongly expressed in developing embryo and endosperm, respectively (Springer et al., 2000; Bastida and Puigdomènech, 2002). Expression of *ZmMCM6* was found to be similar and only detectable in tissues containing proliferating cells. The highest protein amounts were detected in the developing embryo and endosperm. Expression of *AtMCM7* in the female gametophyte was indirectly demonstrated by Springer et al. (1995), as gene function is required for female gametophyte development. We have shown that the *MCM6* from maize is only expressed in those cells of the mature female gametophyte, which are the precursor cells of both embryo and endosperm (egg and central cell), but not in mature synergids and antipodals or mature male gametes (sperm cells). The high supply of maternal *ZmMCM6* transcript amounts in the central cell correlates well with the observation that mitosis after fertilization is initiated much faster during endosperm development compared with embryogenesis (Kranz et al., 1998; Faure et al., 2002).

Compared with frog, where distinct maternal and zygotic genes encode MCM6 (Sible et al., 1998), a single gene seems to exist in maize and Arabidopsis, which is expressed at a low level in maize egg cells, but strongly induced shortly after fertilization. A cell cycle-dependent expression of *ZmMCM6* after fertilization was not observed. We have therefore used *ZmFEN-1a*, the maize homolog of rice (*Oryza sativa*) *OsFEN-1a* (Kimura et al., 2001), as a cell cycle marker. The yeast homolog RAD27 (a flap endonuclease required for DNA repair) was previously shown to be up-regulated during late G1 phase (Vallen and Cross, 1995). In contrast to *ZmFEN-1a*, a significant cell cycle-dependent gene expression pattern after fertilization was not observed for *ZmMCM6*, suggesting that either the strong induction of gene expression after fertilization generated enough protein for the next cell cycles or the low level of gene expression is sufficient to generate enough protein for the first cell division cycles and regulation of ZmMCM6 activity is mainly posttranscriptional. The finding that MCM protein amounts in the nucleus during G1/S phase have been estimated to be approximately 10- to 100-fold higher than the number of replication origins and replication forks (MCM paradox; Walter and Newport, 1997; Blow and Dutta, 2005) favors the latter hypothesis and suggests

that regulation at the level of gene expression is less important. However, the strong induction after fertilization might also be correlated with the highly heterochromatic sperm chromatin, which becomes decondensed 2 to 3 h after fertilization in maize (Scholten et al., 2002). Thus, without a larger maternal supply, a bulk of MCM proteins will be required to saturate the numerous replication origins of the sperm genome for initiation of DNA synthesis during zygote development. Additionally, ZmMCM6 might also be required for chromatin remodeling and transcription of the sperm chromatin, which might explain this strong increase of gene activity. The lack of *ZmMCM6* expression and probably of MCM6 protein in sperm cells supports this hypothesis.

In yeast, it was shown that MCM proteins shuttle in and out of the nucleus during a single cell cycle. In contrast, MCM proteins in metazoans remain in the nucleus throughout the cell cycle (Blow and Dutta, 2005). In yeast, MCM proteins are taken up by the nucleus during G1 phase of the cell cycle and the bulk of protein is present in the nucleus shortly before S phase begins. During S phase, MCM proteins are exported to the cytoplasm rather than degraded and excluded from the nucleus by G2 and M phase (Yan et al., 1993; Dalton and Whitbread, 1995; Nguyen et al., 2000). We have used a gene fusion of *MCM6* with GFP and immunocytochemistry to study subcellular protein localization. Our data show a cell cycle-dependent nuclear localization of ZmMCM6 similar to observations in yeast, but completely different for metazoans. A similar result was described for MCM7 from Arabidopsis, as it localizes transiently to the nucleus (Springer et al., 2000).

ZmMCM6-GFP was evenly distributed in the nucleoplasmand we never found accumulation at certain spots that might represent pre-RC sites. It is thus likely that ZmMCM6 not only binds pre-RC sites, but is also capable of binding chromatin from all parts of the genome, excluding genomic regions containing rDNA genes, as we never observed ZmMCM6 protein in the nucleolus. Perhaps MCM6 is replaced in this chromosomal region by another MCM protein, for example, MCM8 or MCM9. Binding of human and frog MCM proteins to genomic DNA outside of ORCs, and not specifically to many sites of the chromatin, has been reported recently (Edwards et al., 2002; Schaarschmidt et al., 2002).

**ZmMCM6 Is Essential for Plant Growth and Development**

In fungi and animals, loss of MCM function causes severe effects, including DNA damage and genome instability. In *Caenorhabditis elegans*, for example, reduction of

MCM5 and MCM6 function using RNAi resulted in failure of nuclear reassembly following mitosis (Gönczy et al., 2000). An essential role for MCM proteins during meiosis was shown for fission yeast, as *mcm4* mutants were unable to carry out premeiotic DNA replication (Lindner et al., 2002). Mutations in the Drosophila *MCM2* and *MCM4* genes resulted in DNA replication and developmental defects in late embryo and larval stages. These studies also indicated that a maternal supply of MCM proteins is sufficient for early embryo development (Treisman et al., 1995; Su et al., 1997). Large quantities of maternal MCM proteins are also present in frog egg extracts (Kubota et al., 1997) and members of this family have been shown to be involved in restricting DNA replication to a single cell cycle throughout embryo development until the MBT stage (Leno et al., 1992; Sible et al., 1998). However, this mechanism seems to be different in higher plants. In maize and wheat, ZGA occurs shortly after fertilization (Sauter et al., 1998; Dresselhaus et al., 1999; Scholten et al., 2002; Sprunck et al., 2005; this study) and the strong induction of *ZmMCM6* expression after fertilization suggests that MCM6 function is required already shortly after fertilization in the zygote, as gene expression in the egg cell is low and the existence of a large maternal MCM6 supply is unlikely.

We have chosen an AS approach to decrease, but not to eliminate, *ZmMCM6* transcript levels. Under control of the strong maize UBI promoter, transgenic maize lines usually display a broad level of transgene expression, sometimes exceeding endogenous transcript levels up to 20 times (Dresselhaus et al., 2005). Surprisingly, this was completely different for *ZmMCM6* because we have not been able to generate plants displaying significant AS transcript levels. The few transgenic plants containing functional transgene integrations were strongly reduced in growth of vegetative tissues and reproductive organs, respectively. In addition, attempts to increase *ZmMCM6* transcript levels have been unsuccessful as well. Taken together, these data indicate that expression of the *MCM6* gene in maize is strictly regulated and every deregulation is likely to cause severe effects because ZmMCM6 function is important throughout the plant life cycle. In yeast, MCM2 and MCM6 are the main factors limiting the initiation of replication (Lei et al., 1996). This might explain the strong phenotypes obtained for the *ZmMCM6* AS plants.

A correlation of cell cycle control and plant growth as well as morphogenesis has already been reported for a number of plant cell cycle regulators including CDKs and cyclins (for review, see Hemerly et al., 1999). However, these proteins are encoded by multigene families and knockouts of individual cell cycle regulators rarely resulted in lethality. Gene

functions probably have been compensated by other members of the corresponding gene family. This is obviously different for *MCM* genes. Each member might be required to form a functional hexamer. In addition, each member might have evolved specific functions, and thus is not capable of fully complementing another member of the hexamer. For future analyses of *MCM* genes and proteins in plants, we suggest using their own or inducible promoters to avoid lethality. Yeast two-hybrid screens, for example, might be useful to identify interacting partners of MCM proteins. Developing seeds, especially where MCM proteins amount to high levels, seem to be the right source for such screens. T-DNA and transposon insertion in C-terminal regions of plant MCM genes, as was the case for *AtMCM7*, might elucidate specific functions of domains in this region. N-terminal or central insertions in the catalytic domain are likely to be lethal.

## MATERIALS AND METHODS

### Plant Material, Isolation of Cells from the Female Gametophyte, and In Vitro Cultures

Maize (*Zea mays*) inbred lines A188 (Green and Phillips, 1975) and H99 (D'Halluin et al., 1992) as well as transgenic lines were grown under standard greenhouse conditions at 26ºC with 16 h light and a relative air humidity of about 60%. Cells of the maize embryo sac were isolated according to Kranz et al. (1991) and zygotes according to Cordts et al. (2001). Microspore-derived suspension cultures were obtained from B. Krautwig (described in Krautwig and Lörz, 1995). The BMS maize cells were cultivated as a suspension culture in Murashige and Skoog medium in the dark with centrifugation at 60 to 70 rpm at 26ºC according to Kirihara (1994). Onion (*Allium cepa*) bulbs were obtained from the supermarket.

### Differential Plaque Screening, 5'-RACE, DNA Sequencing, and Bioinformatic Analysis

A cDNA library of maize in vitro zygotes (Dresselhaus et al., 1996) was screened by differential plaque screening against a cDNA library of unfertilized egg cells (Dresselhaus et al., 1994) to identify fertilization-induced genes. Double plaque lifts were prepared from 15-cm plates of the zygote library at a density of 500 plaque-forming units (pfu). The filters were hybridized with PCR-amplified [$^{32}$P] cDNA from the egg cell and

[$^{32}$P] cDNA of in vitro zygotes. Candidate cDNA clones were further analyzed by reverse northern hybridization (Dresselhaus et al., 1999). Among the putative fertilization-induced genes, 1,123 bp of a cDNA encoding the 3' end of the *ZmMCM6* transcript and 273 bp of the *ZmFEN-1a* transcript (GenBank accession no. DQ138311) were identified. The 5' region of the *ZmMCM6* transcript was isolated from zygote cDNA as follows: 2.5 µg Eco-Adaptor was ligated to PCR-amplified cDNA from in vitro zygotes (Dresselhaus et al., 1996), ligated products purified using a low-melting agarose gel, cloned into calf intestine alkaline phosphatasetreated *EcoR*I restriction sites of the λ-vector UniZAP II, and packed using the Gigapack-Gold II extract (Stratagene) to generate a cDNA library from zygotes containing full-length cDNAs. The 5' region (2 kb) of *ZmMCM6* was amplified from this library using the T3 vector primer and the gene-specific primer 19A (5'-CATGATGTAGACCAGATCAA-3') in a standard PCR reaction with *Taq* DNA polymerase. PCR products were blunted, purified, and cloned into the pPCR-Script vector (Stratagene), according to the manufacturer's specifications. The full-length cDNA of *ZmMCM6* was amplified from 1 µg poly(A)$^+$ RNA extracted from root tips. Twenty nanograms of the primer 19U2 (5'-GTCAGACTACAGATGCTAATT-3') derived from the 3' end of the *ZmMCM6* transcript was incubated with poly(A)$^+$ RNA and SuperScript reverse transcriptase according to the protocol of the 5'-RACE system (Life Technologies). PCR was performed with proofreading *pfu* DNA polymerase (Stratagene) as well as primers 19U2 and GB19A (5'-TGCCAATCTCCAACTCATACCC-3'), the latter derived from the 5' region of the *ZmMCM6* transcript. The PCR product was cloned into the pPCR-script vector (see above) generating the plasmid pK19U2 and fully sequenced. The full-length *ZmMCM6* nucleotide sequence data reported in this article is available in the EMBL, GenBank, and DNA Data Bank of Japan (DDJB) nucleotide sequence databases under accession number AY862320 (*ZmMCM6* cDNA). The protein sequence is available under accession number AAW55593.

Sequence data were compiled and compared online with EMBL, GenBank, DDBJ, Swiss-Prot, Protein Information Resource, and Protein Research Foundation databases with FASTA and BLAST algorithms (Pearson, 1990). MCM protein sequences were obtained from GenBank and aligned online by ClustalW (Higgins et al., 1994; http://www.ebi.ac.uk/clustalw). The alignment data obtained were used to generate a phylogram (Fig. 1) with Treeview, version 1.6.6 (Page, 1996). Protein alignments were drawn by GeneDoc, version 2.6.02 (Nicholas et al., 1997), using protein alignments generated by ClustalW. Prediction of protein localization sites was performed online

using PSORT (http://psort.nibb.ac.jp), iPSORT (http://www.HypothesisCreator.net/iPSORT), and SignalP version 2.0 (http://www.cbs.dtu.dk/services/SignalP-2.0). Protein motifs such as putative CDK phosphorylation sites and zinc-finger motifs were searched online using Prosite (http://www.expasy.org/tools/scanprosite).

**DNA and RNA Extraction, Northern and Southern Blots, SC RT-PCR, and Quantitative RT-PCR**

Extraction of genomic DNA from plant tissues was performed according to Dellaporta et al. (1983). Plant material for northern-blot analyses was either collected in the greenhouse from different tissues and organs of the maize inbred line A188 or from in vitro cultures. Total RNA was extracted from all samples with TRIzol (Life Technologies) and poly(A)$^+$ RNA from total RNA using the PolyATtract mRNA isolation system (Promega), according to the manufacturer's specifications.

Capillary Southern and northern blots, as well as labeling, hybridization, washing, and autoradiographic exposures, were performed as described in Dresselhaus et al. (2005). The 1,123 bp representing the 3' region of *ZmMCM6* was labeled as a probe for northern blots. Probes to detect sense and AS transgene integrations were isolated from plasmids that have been used for maize transformations. DNA fragments were purified using the Gel Band isolation kit (Pharmacia Biotech) and radioactively labeled as described (Dresselhaus et al., 2005), after digestion with enzyme combinations that were also used to restrict genomic DNA. Genomic DNA of transgenic sense and AS lines was restricted using *Bam*HI/*Sal*I and *Bam*HI/*Sst*I, respectively. These enzyme combinations cut out the full-length *ZmMCM6* cDNA. A GFP specific probe was prepared as follows. The GFP sequence was amplified in a standard PCR using the primers GFP1for (5'-GAGGAACTGTTCACTGGCGT-3') and GFP3rev (5'-TTCATCCATGCCATGCGTG-3'). After amplification, the PCR product was purified and labeled as described above. Genomic DNA of putative transgenic *ZmMCM6-GFP* maize plants was restricted with DraI, which cuts out the complete construct except for the first 135 bp of the UBI promoter.

SC RT-PCR analysis was performed as described by Cordts et al. (2001) using the primers MCM6rev (5'-GAACACCACCCAAAAGCATAAGAA-3') or FENrev (5'-GGACTCCCTTACTTTTGGG-3') in addition to Gap2 (5'-GTAGCCCCACTCGTTGTCGTA-3') for cDNA synthesis. After RT, reactions were split

into two reaction tubes and 38 PCR cycles were conducted in separate reactions with *ZmMCM6*-specific primers MCM6for (5'-GCAGGTCGCAGATGGTAGGAGAG-3') and MCM6rev, *ZmFEN-1a*-specific primers FENfor (5'-CCAAGATGCTTTCTATGGAC-3') and FENrev, as well as *GAPDH*-specific primers Gap1 (5'-AGGGTGGTGCCAAGAAGGTTG-3') and Gap2. Twenty-five microliters of the *ZmMCM6* and *ZmFEN-1a*, as well as 15 µL *GAPDH* PCR products, were each separated in agarose gels. The size of the amplified *ZmMCM6* transcript was 219 bp (genomic approximately 550 bp), 241 bp for *ZmFEN-1a* (genomic approximately 450 bp), and 622 bp for GAPDH (genomic approximately 1.2–1.3 kb). Quantitative RT-PCR analyses were performed as described by Dresselhaus et al. (2005) using 1 µg total RNA extracted from leaf material. The *ZmMCM6*-specific primers MCM6for and MCM6rev (400 nM each primer) or *GAPDH*-specific primers Gap1 and Gap2 (400 nM each primer; Richert et al., 1996) were used in an iCycler iQ machine with iQ SYBR Green Supermix (Bio-Rad), according to the manufacturer's recommendations. PCR results were controlled by agarose gel electrophoresis. Samples showing both *ZmMCM6*- and *GAPDH*-specific amplifications were further processed with the iCycler iQ real-time detection system software, version 3.0 (Bio-Rad). *GAPDH*-specific PCR products were used to normalize *ZmMCM6* transcript amounts.

**Protein Extraction, Western Blots, and Immunodetection**

Plant tissuewas ground in liquid nitrogen. One volume of extraction buffer (250 mM KCl, 20 mM Tris-HCl, pH 6.8, 50% v/v glycerol, 2.5% w/v polyvinylpyrrolidone, 5 mM dithiothreitol, and one mini protease inhibitor tablet [Roche] in 10 mL extraction buffer) was added and mixed until material thawed. Samples were centrifuged at 13,000 rpm for 30 min at 4ºC. This step was repeated twice with the supernatant. Protein concentrations were measured after adding 100 µL Bradford reagent (Bradford, 1976; Bio-Rad), according to the manufacturer's recommendations.

SDS-PAGE in a discontinuous Tris-Gly buffer system was performed according to Sambrook et al. (1989) using mini gels (5% stacking gel and 8% resolving gel). Protein samples (each 10 µg) were mixed 1:1 in 23 Laemmli sample buffer and denatured at 96ºC for 12 min before loading on the gel. Gels were blotted onto Immobilon-P polyvinylidene difluoride membranes from Millipore with transfer buffer (25mM Tris, 192mM Gly, 10% v/v methanol) in a semidry method according to Frey (2002) using the Transblot synthetic dextrose system (Bio-Rad) followed by a Ponceau-S staining.

For immunodetection, a rabbit peptide antibody (anti-MCM6-Ab) was generated by BioTrend against a ZmMCM6 C-terminal-specific region (VPSESDAGQPAEEDA) between position 680 and 694 (Fig. 2) and tested for specificity by ELISA. Protein blots were blocked overnight in 5% phosphate-buffered saline (PBS)-Blotto at 4ºC or for 1 h at room temperature. Blots were incubated with a 1:500 dilution of anti-MCM6-Ab in 5% PBS-Blotto for 2 h at room temperature, rinsed twice with PBS for 5 min each, followed by a 1-h treatment at room temperature with a 1:5,000 dilution of the secondary antibody, a mouse monoclonal anti-rabbit IgG (γ-chain-specific) horseradish peroxidase conjugate clone RG-96 (Sigma). Blots were rinsed twice with PBS for 5 min, incubated for 5 min in 1:1 luminol:peroxide solution from Pierce in the dark, followed by exposure to autoradiographic films, according to the manufacturer's instructions.

Immunocytochemistry to determine ZmMCM6 levels during the cell cycle were performed as follows. Each 2-mL BMS cell was collected by centrifugation at 1,000 rpm for 4 min. Supernatants were removed and cell pellets immediately fixed in 1 mL 4% paraformaldehyde and 0.25% glutaraldehyde in PBS, and incubated for 1 h at room temperature. Fixed cells were centrifuged at 1,000 rpm, supernatant discarded, and pellets rinsed four times with PBS (containing 1% Triton) and each time centrifuged for 10 min at 1,000 rpm to collect cells. Cell walls were degraded for 30 min at room temperature after adding 500 µL of enzyme mixture, which contained 1.5% pectinase, 0.5% pectolyase, 1.0% hemicellulase, and 1.0% cellulase in mannitol solution (570 milliosmolar; pH 4.9–5.0). Digested cells were resuspended with a pipette, nuclei collected after centrifugation at 1,000 rpm, and supernatants removed. Nuclei were washed four times in 1 mL PBS containing 0.1% Triton for 10 min during centrifugation at 1,000 rpm at 4ºC. The pellets were resuspended in 500 mL PBS containing the 1:250 diluted anti-MCM6-Ab and incubated at 4ºC overnight. Nuclei were washed three times in 1 mL PBS and centrifuged at 1,000 rpm for 10 min. After a final wash, pellets containing nuclei were resuspended in 500 µL PBS containing an FITC-coupled anti-rabbit antibody (1:500) and incubated for 4 h at 4ºC. Nuclei were collected after centrifugation at 1,000 rpm for 10 min and washed five times each in 1 mL PBS as described above. Finally, nuclei were resuspended in 500 µL PBS and centrifuged at 500 rpm for 1 min. Twenty-microliter fractions containing nuclei were collected from the bottom of the tubes and transferred to microscopic slides after adding 0.25 µL DAPI solution.

**Generation of Constructs, Biolistic Transformation, and Regeneration of Transgenic Plants**

To generate an AS construct (*UBI*p:*MCM6-AS*) of *ZmMCM6*, the full-length cDNA of *ZmMCM6* was excised from pK19U2 (see above) using the enzymes *Sst*I and *Bam*HI and cloned into the corresponding restriction sites of the vector pUbi.Cas (Christensen and Quail, 1996). The open reading frame of *ZmMCM6* was amplified from pK19U2 using the primers MCM6 (5'-GTCGACCCTGATTCTTCCAC-3') and MCMB (5'-GGATCCATGTTAAGATGCCGTTGC-3') containing *Sal*I and *Bam*HI restriction sites, respectively, to generate the sense construct (*UBI*p:*MCM6*). After PCR amplification using *pfu* DNA polymerase, the PCR product was restricted with *Sal*I and *Bam*HI, cloned in the corresponding restriction sites of the vector pUbi.Cas, and fully sequenced. A construct encoding a MCM6-GFP fusion protein (*UBI*p:*MCM6-GFP*) was prepared as follows. The full-length *ZmMCM6* sequence was amplified from the plasmid pK19U2 using the primers M6F-Spe (5'-CGACACTAGTTGTCGGTGATG-3') and M6R-Bam (5'-CGTGGATCCAATCAATAACATAGTTCG-3') containing *Spe*I and *Bam*HI restriction sites, respectively, which were then used for cloning the fragment between the *Spe*I and *Bam*HI sites of the vector pLNU-GFP (*UBI*p:*GFP:NOS*t; unpublished data). This vector contains a multicloning site between the maize UBI promoter and the GFP gene, the latter containing the ST-LS1 intron (derived from pMon30049; Pang et al., 1996), followed by the nopaline synthase terminator. The vector pLNU-GFP was also used as a positive control for transient biolistic transformation experiments.

Epidermal onion cell layers were bombarded with 2 to 5 µg plasmid DNA, according to the procedure described by Scott et al. (1999), except that inner onion peels (2 x 2.5 cm) were placed with the concave side up on 0.5% agar plates. The condition of bombardment was 1,100-psi rupture discs under a vacuum of 28 mm Hg with 6-cm target distance using the particle gun model PDS100/He (Bio-Rad). Bombarded peel halves were placed after transformation with the concave side down and the cut surface in sterile 0.6% agar (Fluka) petri dishes for about 17 to 22 h in the dark before removing the epidermis for observation using a fluorescence microscope. For bombardment of maize BMS cells, a uniform layer was spread on solid Murashige and Skoog medium and incubated at 26ºC for 1 to 2 h before biolistic transformation. After transformation, plates were incubated overnight in the dark at 26ºC. Cells were transferred to fresh liquid medium in 35-mm petri dishes and cultivated in darkness using a shaker (60 rpm) for at least 4 h before microscopic observations. Photos were taken immediately after a

transfer of 100 µL of medium containing individual cells or cell clusters showing GFP fluorescence onto glass slides followed by an addition of 1 µL DAPI staining solution.

Embryos of the maize inbred line A188 were used 12 to 14 DAP for stable transformation using the construct *UBI*p:*MCM6-AS*. Hybrid embryos from both lines A188 and H99 were used for stable transformation experiments with the constructs *UBI*p:*MCM6* and *UBI*p:*MCM6-GFP*. Constructs were cotransformed with the plasmid construct *35S*p:*PAT* carrying the selectable marker PAT for glufosinate ammonium resistance. Particle bombardment, tissue culture, and selection of transgenic maize plants were performed according to Brettschneider et al. (1997).

**Microscopy**

Axiovert 35 M or Axiovert 200 fluorescence microscopes (Zeiss) with the filter set 01 (FITC filter with excitation at 450–490 nm; emission at >515 nm) or filter set 38 (GFP filter with excitation at 470–495 nm; emission at 525 nm) were used to observe GFP fluorescence in onion epidermal and maize BMS cells, as well as FITC fluorescence of isolated BMS nuclei after immunostaining. A DAPI filter (Zeiss, excitation at 359–371 nm and emission >397 nm) was used to visualize DNA and cell wall material. Samples were excited with UV light produced by a HBO 50/Ac lamp and images taken with a Nikon DS-5Mc camera. Nikon software EclipseNet plug in MCF was used to obtain and merge fluorescence images. ImageJ software was used to measure DAPI, GFP, and FITC fluorescence. CLSM was performed using the Leica TCS 4D CLSM (Leica-Laser-Technologie). Samples were excited by 488 nm with an Argon laser as described in Knebel et al. (1990).

Sequence data from this article can be found in the GenBank/EMBL data libraries under accession numbers AY862320 (ZmMCM6 cDNA), AAW55593 (ZmMCM6 protein), and DQ138311 (ZmFEN-1a cDNA).

## Acknowledgments

We are grateful to Stefanie Sprunck for critical comments on the manuscript and to Gislind Bräcker for excellent technical support. We thank Natascha Techen for the *35S*p:*Lc-GFP* construct and Hartmut Quader for help with the CLSM studies.

## References

**Arias EE, Walter JC.** (2005). Replication-dependent destruction of Cdt1 limits DNA replication to a single round per cell cycle in *Xenopus* egg extracts. Genes Dev **19**: 114–126

**Bailis JM, Forsburg SL.** (2004). MCM proteins: DNA damage, mutagenesis and repair. Curr Opin Genet Dev **14**: 17–21

**Bastida M, Puigdomènech P.** (2002). Specific expression of ZmPRL, the maize homolog of MCM7, during early embryogenesis. Plant Sci **162**:97–106

**Blow JJ, Dutta A.** (2005). Preventing re-replication of chromosomal DNA. Nat Rev Mol Cell Biol **6**: 476–486

**Bogan JA, Natale DA, Depamphilis ML.** (2000). Initiation of eukaryotic DNA replication: conservative or liberal? J Cell Physiol **184**:139–150

**Bradford MM.** (1976). A rapid and sensitive method for the quantification of microgram quantities utilising the principle of protein dye binding. Anal Biochem **72**: 248–254

**Brettschneider R, Becker D, Lörz H.** (1997). Efficient transformation of scutellar tissue of immature maize embryos. Theor Appl Genet **94**:737–748

**Christensen AH, Quail PH.** (1996). Ubiquitin promoter-based vectors for high-level expression of selectable and/or screenable marker genes in monocotyledonous plants. Transgenic Res **5**: 213–218

**Claycomb JM, MacAlpine DM, Evans JG, Bell SP, Orr-Weaver TL.** (2002). Visualization of replication initiation and elongation in *Drosophila*. J Cell Biol **159**: 225–236

**Cordts S, Bantin J, Wittich PE, Kranz E, Lörz H, Dresselhaus T.** (2001). *ZmES* genes encode peptides with structural homology to defensins and are specifically expressed in the female gametophyte of maize. Plant J **25**: 103–114

**Dalton S, Whitbread L.** (1995). Cell cycle-regulated nuclear import and export of CDC47, a protein essential for initiation of DNA replication in budding yeast. Proc Natl Acad Sci USA **92**: 2514–2518

**Davey MJ, Indiani C, O'Donnell M.** (2003). Reconstitution of the Mcm2-7p heterohexamer, subunit arrangement, and ATP site architecture. J Biol Chem **278**: 4491–4499

**Dellaporta SL, Wood J, Hicks JB.** (1983). A plant DNA minipreparation: version II. Plant Mol Biol Report 4: 19–21 D'Halluin K, Bonne E, Bossut M, De Beuckeleer M, Leemans J (1992) Transgenic maize plants by tissue electroporation. Plant Cell **4**: 1495–1505

**Dresselhaus T, Amien S, Márton ML, Strecke A, Brettschneider R, Cordts S.** (2005). *TRANSPARENT LEAF AREA1* encodes a secreted proteolipid required for anther maturation, morphogenesis, and differentiation during leaf development in maize. Plant Cell **17**: 730–745

**Dresselhaus T, Cordts S, Heuer S, Sauter M, Lörz H, Kranz E.** (1999). Novel ribosomal genes from maize are differentially expressed in the zygotic and somatic cell cycles. Mol Gen Genet **261**: 416–427

**Dresselhaus T, Hagel C, Lörz H, Kranz E.** (1996). Isolation of a full-length cDNA encoding calreticulin from a PCR-library of in vitro zygotes of maize. Plant Mol Biol **31**: 23–34

**Dresselhaus T, Lörz H, Kranz E.** (1994). Representative cDNA libraries from few plant cells. Plant J **5**: 605–610

**Edwards MC, Tutter AV, Cvetic C, Gilbet CH, Prokhorova TA, Walter JC.** (2002). MCM2-7 complexes bind chromatin in a distributed pattern surrounding the origin recognition complex in Xenopus egg extracts. J Biol Chem **277**: 33049–33057

**Faure JE, Rotman N, Fortuné P, Dumas C.** (2002). Fertilization in Arabidopsis thaliana wild type: developmental stages and time course. Plant J **30**: 481–488

**Forsburg SL.** (2004). Eukaryotic MCM proteins: beyond replication initiation. Microbiol Mol Biol Rev **68**: 109–131

**Frey A.** (2002). Protein-Blotting und Nachweis membrangebundener Proteine. *In* G Schrimpf, ed, Gentechnische Methoden: eine Sammlung von Arbeitsanleitungen fu¨ r das molekularbiologische Labor, Ed 3. Spektrum Akademischer Verlag, Heidelberg, pp 343–368

**Gönczy P, Echeverri C, Oegema K, Coulson A, Jones SJ, Copley RR, Duperon J, Oegema J, Brehm M, Cassin E, et al.** (2000). Functional genomic analysis of cell division in *C. elegans* using RNAi of genes on chromosome III. Nature **408**: 331–336

**Gozuacik D, Chami M, Lagorce D, Faivre J, Murakami Y, Poch O, Biermann E, Knippers R, Brechot C, Paterlini-Brechot P.** (2003). Identification and functional characterization of a new member of the human Mcm protein family: hMcm8. Nucleic Acids Res **31**: 570–579

**Green CE, Phillips RL.** (1975). Plant regeneration from tissue cultures of maize. Crop Sci **15**: 417–421

**Hemerly AS, Ferreira PCG, Van Montagu M, Inzé D.** (1999). Cell cycle control and plant morphogenesis: is there an essential link? Bioessays **21**: 29–37

**Higgins D, Thompson J, Gibson T, Thompson JD, Higgins DG, Gibson TJ.** (1994). ClustalW: improving the sensitivity of progressive multiple sequence alignment through sequence weighting, position-specific gap penalties and weight matrix choice. Nucleic Acids Res **22**: 4673–4680

**Holding DR, Springer PS.** (2002). The Arabidopsis gene *PROLIFERA* is required for proper cytokinesis during seed development. Planta **214**: 373–382

**Hyrien O, Marheineke K, Goldar A.** (2003). Paradoxes of eukaryotic DNA replication: MCM proteins and the random completion problem. Bioessays 25: 116–125 Ishimi Y (1997) A DNA helicase activity is associated with an MCM4, -6, and -7 protein complex. J Biol Chem **272**: 24508–24513

**Johnson EM, Kinoshita Y, Daniel DC.** (2003). A new member of the MCM protein family encoded by the human MCM8 gene, located contrapodal to GCD10 at chromosome band 20p12.3-13. Nucleic Acids Res **31**:2915–2925

**Kelman Z, Lee J-K, Hurwitz J.** (1999). The single minichromosome maintenance protein of *Methanobacterium thermoautotrophicum* H contains DNA helicase activity. Proc Natl Acad Sci USA **96**: 14783–14788

**Kimura S, Suzuki T, Yanagawa Y, Yamamoto T, Nakagawa H, Tanaka I,**
**Hashimoto J, Sakaguchi K.** (2001). Characterization of plant proliferating cell nuclear antigen (PCNA) and flap endonuclease-1 (FEN-1), and their distribution in mitotic and meiotic cell cycles. Plant J **28**: 643–653

**Kirihara JA.** (1994). Selection of stable transformants from Black Mexican Sweet maize suspension cultures. In M Freeling and V Walbot, eds, The Maize Handbook. Springer, New York, pp 690–694

**KnebelW, Quader H, Schnepf E.** (1990). Mobile and immobile endoplasmic reticulum in onion bulb epidermis cells: short- and long-term observations with a confocal laser scanning microscope. Eur J Cell Biol **52**: 328–340

**Kranz E, Bautor J, Lörz H.** (1991). In vitro fertilization of single, isolated gametes of maize mediated by electrofusion. Sex Plant Reprod **4**: 12–16

**Kranz E, vonWiegen P, Quader H, Lörz H.** (1998). Endosperm development after fusion of isolated, single maize sperm and central cells in vitro. Plant Cell **10**: 511–524

**Krautwig B, Lörz H.** (1995). Single androgenic structures of maize (*Zea mays* L.) for the initiation of homogeneous cell suspension and protoplast cultures. Plant Cell Rep **14**: 477–481

**Kubota Y, Mimura S, Nishimoto S, Masuda T, Nojima H, Takisawa H.** (1997). Licensing of DNA replication by a multi-protein complex of MCM/P1 proteins in Xenopus eggs. EMBO J **16**: 3320–3331

**Labib K, Diffley JF.** (2001). Is the MCM2-7 complex the eukaryotic DNA replication fork helicase? Curr Opin Genet Dev **11**: 64–70

**Labib K, Diffley JFX, Kearsey SE.** (1999). G1-phase and B-type cyclins exclude the DNA-replication factor Mcm4 from the nucleus. Nat Cell Biol **1**: 415–422

**Labib K, Tercero JA, Diffley JFX.** (2000). Uninterrupted MCM2-7 function required for DNA replication fork progression. Science **288**: 1643–1647

**Laskey RA, Madine MA.** (2003). A rotary pumping model for helicase function of MCM proteins at a distance from replication forks. EMBO Rep **4**: 26–30

**Lee J-K, Hurwitz J.** (2001). Processive DNA helicase activity of the minichromosome maintenance proteins 4, 6, 7 complex requires forked DNA structures. Proc Natl Acad Sci USA **98**: 54–59

**Lei M, Kawasaki Y, Tye BK.** (1996). Physical interactions among MCM proteins and effects of MCM dosage on DNA replication in *Saccharomyces cerevisiae*. Mol Cell Biol **16**: 5081–5090

**Lei M, Tye BK.** (2001). Initiating DNA synthesis: from recruiting to activating the MCM complex. J Cell Sci **114**: 1447–1454

**Leno GH, Downes CS, Laskey RA.** (1992). The nuclear membrane prevents replication of human G2 nuclei but not G1 nuclei in *Xenopus* egg extract. Cell **69**: 151–158

**Lindner K, Gregan J, Montgomery S, Kearsey S.** (2002). Essential role of MCM proteins in pre-meiotic DNA replication.Mol Biol Cell **13**: 435–444

**Ludwig SR, Habera LF, Dellaporta SL,Wessler SR.** (1989). Lc, a member of the maize R gene family responsible for tissue-specific anthocyanin production, encodes a protein similar to transcriptional activators and contains the myc-homology region. Proc Natl Acad Sci USA **86**: 7092–7096

**Maiorano D, Cuvier O, Danis E, Mechali M.** (2005). MCM8 is an MCM2-7-related protein that functions as a DNA helicase during replication elongation and not initiation. Cell **120**: 315–328

**Nguyen VQ, Co C, Irie K, Li JJ.** (2000). Clb/Cdc28 kinases promote nuclear export of the replication initiator proteinsMcm2-7. Curr Biol **10**: 195–205

**Nicholas KB, Nicholas HB Jr, Deerfield DW II.** (1997). GeneDoc: analysis and visualization of genetic variation. Embnew News **4**: 14

**Page RDM.** (1996). TREEVIEW: an application to display phylogenetic trees on personal computers. Comput Appl Biosci **12**: 357–358

**Pang S, DeBoer DL, Wan Y, Ye G, Layton JG, Neher MK, Armstrong CL, Fry JE, Hinchee M, Fromm ME.** (1996). An improved green fluorescent protein gene as a vital marker in plants. Plant Physiol **112**: 893–900

**Pearson WR.** (1990). Rapid and sensitive sequence comparison with FASTP and FASTA. Methods Enzymol **183**: 63–98

**Richert J, Kranz E, Lörz H, Dresselhaus T.** (1996). A reverse transcriptase polymerase chain reaction assay for gene expression studies at the single cell level. Plant Sci **114**: 93–99

**Sabelli P, Parker J, Barlow P.** (1999). cDNA and promoter sequences for *MCM3* homologues from maize, and protein localization in cycling cells. J Exp Bot **50**: 1315–1322

**Sabelli PA, Burgess SR, Kush AK, Young MR, Shewry PR.** (1996). cDNA cloning and characterisation of a maize homologue of the MCM proteins required for the initiation of DNA replication. Mol Gen Genet **252**: 125–136

**Sambrook J, Fritsch EF, Maniatis T.** (1989). Molecular Cloning: A Laboratory Manual, Ed 2. Cold Spring Harbor Laboratory Press, Cold Spring Harbor, NY

**Sauter M, von Wiegen P, Lörz H, Kranz E.** (1998). Cell cycle regulatory genes from maize are differentially controlled during fertilization and first embryonic cell division. Sex Plant Reprod **11**: 41–48

**Schaarschmidt D, Ladenburger EM, Keller C, Knippers R.** (2002). Human Mcm proteins at a replication origin during the G1 to S phase transition. Nucleic Acids Res **30**: 4176–4185

**Scholten S, Lörz H, Kranz E.** (2002). Paternal mRNA and protein synthesis coincides with male chromatin decondensation in maize zygotes. Plant J **32**: 221–231

**Scott A, Wyatt S, Tsou P-L, Robertson D, Allen NS.** (1999). Model system for plant cell biology: GFP imaging in living onion epidermal cells. Biotechniques **26**: 1125–1132

**Shechter D, Gautier J.** (2004). MCM proteins and checkpoint kinases get together at the fork. Proc Natl Acad Sci USA **101**: 10845–10846

**Sible JC, Erikson E, Hendrickson M, Maller JL, Gautier J.** (1998). Developmental regulation of MCM replication factors in *Xenopus laevis*. Curr Biol **8**: 347–350

**Springer PS, Holding DR, Groover A, Yordan C, Martienssen RA.** (2000). The essential Mcm7 protein PROLIFERA is localized to the nucleus of dividing cells during the G1

phase and is required maternally for early *Arabidopsis* development. Development **127**: 1815–1822

**Springer PS, McCombie WR, Sundaresan V, Martienssen RA.** (1995). Gene trap tagging of *PROLIFERA*, and essential *MCM2-3-5* like gene in Arabidopsis. Science **268**: 877–880

**Sprunck S, Baumann U, Edwards K, Langridge P, Dresselhaus T.** (2005). The transcript composition of egg cells changes significantly following fertilization in wheat (*Triticum aestivum* L.). Plant J **41**: 660–672

**Stevens R, Mariconti L, Rossignol P, Perennes C, Cella R, Bergounioux C.** (2002). Two E2F sites in the Arabidopsis MCM3 promoter have different roles in cell cycle activation and meristematic expression. J Biol Chem **277**: 32978–32984

**Su TT, Yakubovich N, O'Farrell PH.** (1997). Cloning of *Drosophila MCM* homologs and analysis of their requirement during embryogenesis. Gene **192**: 283–289

**Treisman JE, Follette PJ, O'Farrell PH, Rubin GM.** (1995). Cell proliferation and DNA replication defects in a *Drosophila MCM2* mutant. Genes Dev **9**: 1709–1715

**Tye BK.** (1999). MCM proteins in DNA replication. Annu Rev Biochem **68**:649–686

**Vallen EA, Cross FR.** (1995). Mutations in RAD27 define a potential link between G1 cyclins and DNA replication. Mol Cell Biol **15**: 4291–4302

**Volkening M, Hoffmann I.** (2005). Involvement of human MCM8 in prereplication complex assembly by recruiting hcdc6 to chromatin. Mol Cell Biol **25**: 1560–1568

**Walker JE, Saraste M, Runswick MJ, Gay NJ.** (1982). Distantly related sequences in the alpha- and beta-subunits of ATP synthase, myosin, kinases and other ATP-requiring enzymes and a common nucleotide binding fold. EMBO J **1**: 945–951

**Walter J, Newport JW.** (1997). Regulation of replicon size in *Xenopus* egg extracts. Science **275**: 993–995

**Yan H, Merchant AM, Tye BK.** (1993). Cell cycle-regulated nuclear localization of *MCM2* and *MCM3*, which are required for the initiation of DNA synthesis at chromosomal replication origins in yeast. Genes Dev **7**: 2149–2160

**Yoshida K.** (2005). Identification of a novel cell-cycle-induced MCM family protein MCM9. Biochem Biophys Res Commun **331**: 669–674

**You Z, Komamura Y, Ishimi Y.** (1999). Biochemical analysis of the intrinsic Mcm4-Mcm6-Mcm7 DNA helicase activity. Mol Cell Biol **19**: 8003–8015

# CHAPTER 3

## Activation of the imprinted Polycomb Group *Fie1* gene in maize endosperm requires demethylation of the maternal allele

**Abstract**

Imprinting refers to the epigenetic regulation of gene expression that is dependent upon gene inheritance from the maternal or paternal parent. Previously, we have identified two maize homologs of the single *Arabidopsis* Polycomb Group gene *FIE*. Here, we report on the expression pattern of these genes in individual gametes before and after fertilization, and on the role of DNA methylation in determining the maternal expression of the *Fie1* gene. We found that *Fie1* is neither expressed in the sperm, egg cell nor central cell before fertilization. Activation of the Fie1 maternal allele occurs around two days after pollination (DAP) in the primary endosperm and peaks at 10–11 DAP coinciding with endosperm transition from mitotic division to endoreduplication. In contrast, *Fie2* is expressed in the egg cell and more intensively in the central cell similar to Arabidopsis *FIE*, which strongly supports the hypothesis that it functions as a repressor of endosperm development before fertilization. Using MSREPCR and bisulfite sequencing, we could show that the methylated inactive state is the default status of *Fie1* in most tissues. In the endosperm the paternal *Fie1* allele remains methylated and silent, but the maternal allele appears hypomethylated and active, explaining monoallelic expression of *Fie1* in the endosperm. Taking together, these data demonstrate that the regulation of *Fie1* imprinting in maize is different from Arabidopsis and that *Fie1* is likely to have acquired important novel functions for endosperm development.

**Keywords**: Imprinting · DNA methylation · Fertilization · Endosperm · Gametes · PcG

## Introduction

A subset of animal and plant genes is expressed in a parentof-origin-specific manner either from the aternal or maternal allele. This phenomenon, called imprinting, was first discovered in maize as a maternal control of the kernel aleurone color (Kermicle 1970). Later, imprinting was described in mice through pronuclear transplantation experiments (Surani and Barton 1983; Reik and Walter 2001). To date, more than 80 imprinted genes have been described in mammals (Morison et al. 2005). In plants imprinting has been found so far only in the endosperm, a terminal nutritive tissue that develops after double fertilization from the fertilized central cell. The endosperm provides nutrients for developing embryos in dicots and for germinating seedlings in monocots (Kranz et al. 1998; Walbot and Evans 2003). A dozen or so imprinted genes have been discovered in plants, of which the majority are maternally expressed and paternally silenced in the endosperm (Alleman and Doctor 2000; Baroux et al. 2002; Gehring et al. 2004a, b). So far, only the *Arabidopsis* MADS-box gene *PHERES1* was shown to be expressed paternally due to the epressing activity of the Polycomb Group (PcG) protein, MEDEA (Köhler et al. 2003a, b, 2005). Plant PcG proteins are important components of parentof-origin control of gene expression and have been reported recently to be involved also in the self-regulation of imprinting (Baroux et al. 2006; Gehring et al. 2006; Jullien and Katz et al. 2006; Jullien and Kinoshita et al. 2006). PcG proteins form complexes that are able to silence genes and maintain their silencing over many cell divisions by a mechanism that relies mainly on histone modifications at the repressed locus (Delaval and Feil 2004). The *Drosophila* Enhancer of Zeste-Extra Sex Combs [E(Z)-ESC] PcG complex, for example, functions as a repressor of a number of homeotic genes (Sathe and Harte 1995). The E(Z)-ESC PcG complex appears to be conserved, but more complex in plants (Grossniklaus and Schneitz 1998; Grossniklaus et al. 1998; Luo et al. 1999; Ohad et al. 1999; Springer et al. 2002; Jullien and Katz et al. 2006; Jullien and Kinoshita et al. 2006). In *Arabidopsis* the Fertilization-independent seed (FIS) complex that controls seed development is composed of Medea (MEA), Fertilization-independent endosperm (FIE), Fertilization-independent seed2 (FIS2) and Multicopysupressor of IRA 1 (MSI1), which are homologs of the Drosophila E(Z), ESC, Suppressor of Zeste12 and CAF1/P55 PcG proteins, respectively (Grossniklaus and Schneitz 1998; Grossniklaus et al. 1998; Luo et al. 1999; Ohad et al. 1999; Köhler et al. 2003a, b). *MEA* and *FIS2* are imprinted

genes and are expressed maternally in the endosperm (Grossniklaus and Schneitz 1998; Kinoshita et al. 1999; Jullien and Katz et al. 2006; Jullien and Kinoshita et al. 2006). These two genes as well as the imprinted gene *FWA*, which displays an endosperm-specific expression, have been studied intensively to elucidate the mechanism of imprinting in *Arabidopsis* (Kinoshita et al. 2004; Baroux et al. 2006; Gehring et al. 2006; Jullien and Katz et al. 2006; Jullien and Kinoshita et al. 2006). It was shown that the maintenance of *FWA* and *FIS2* imprinting depends on DNA methylation (Kinoshita et al. 2004; Jullien and Katz et al. 2006; Jullien and Kinoshita et al. 2006). In contrast, the *MEA* paternal allele is silenced by the MEA-FIE PcG complex due to histone methylation and thus is independent of DNA methylation (Baroux et al. 2006; Gehring et al. 2006; Jullien and Katz et al. 2006; Jullien and Kinoshita et al. 2006). However, *MEA*, *FWA* and *FIS2* imprinting share a common feature such as the activation of maternal alleles in the central cell due to demethylation by Demeter (DME) DNA glycosylase before fertilization (Choi et al. 2002; Kinoshita et al. 2004; Gehring et al. 2006; Jullien and Katz et al. 2006; Jullien and Kinoshita et al. 2006). After fertilization, the maternal allele remains transcriptionally active in the endosperm, whereas the paternal allele remains silent as it was in the sperm. Because the endosperm is a terminal tissue and is not transmitted to the next generation, the epigenetic state of the imprinted genes does not require re-setting of the imprinting marks and a model for the one way control of imprinting in *Arabidopsis* was proposed (Kinoshita et al.2004).

Despite the original discovery of imprinting in maize, the paucity of information about the molecular mechanisms of imprinting is available in this species. Maternal demethylation of certain alleles of zein and α-tubulin genes have been reported in the maize endosperm (Lund and Ciceri et al. 1995; Lund and Messing et al. 1995; Alleman and Doctor 2000). Extensive maternal hypomethylation was detected in the maize endosperm by a PCR-based genomic scan (Lauria et al. 2004). However, DNA methylation of locus-specific imprinted genes has not been reported in maize until recently (Gutierrez-Marcos et al. 2006). Previously, we identified two *FIE* homologs in maize, *Fie1* and *Fie2*, that show distinct expression patterns and imprinting during kernel development (Springer et al. 2002; Danilevskaya et al. 2003). *Fie1* expression is restricted to the endosperm and shows mono-allelic expression from the maternal allele, whereas, *Fie2* is broadly expressed in many tissues and shows bi-allelic expression in the embryo and the endosperm at later stages (Danilevskaya et al. 2003; Gutierrez-Marcos et al. 2003). Based on the pattern of expression we proposed that *Fie1* and *Fie2*

may have evolved divergent functions in maize. In this study, we examined *Fie1* and *Fie2* expression in the isolated gametes before fertilization, and in zygotes and developing kernels at the early stages after fertilization. We also investigated DNA methylation of *Fie1* and *Fie2* and report the demethylation of the maternal *Fie1* allele, but not of the paternal allele after fertilization and the silencing by DNA metylation of *Fie1* in other tissues including the embryo and endosperm.

## Materials and methods

### Plant material

Reciprocal crosses were performed between maize inbred lines B73 and Mo17. Embryo and endosperm tissues were dissected from kernels at 14 days after pollination (DAP). Pericarp was removed from the kernels and was not included in DNA extraction. Tissues were frozen in liquid nitrogen and stored at -80ºC. Pollen and leaf tissue were obtained from mature B73 or Mo17 plants. Inbred line A188 was used for isolation of individual gametes.

### DNA isolation and MSRE-PCR

Genomic DNA was isolated from 10 mg to 20 mg of frozen embryo and endosperm tissues using PuregeneTM DNA isolation components (Gentra Systems, Minneapolis, MN). About 0.5 µg of genomic DNA was digested at 37ºC overnight in a 50 µl reaction with 25 U of either *Hpa*II or *Msp*I (New England Biolabs, Beverly, MA) for MSREPCR (Liang et al. 2004). After an overnight incubation, 25 additional units of the appropriate restriction enzyme were added and the reaction was incubated for 2 h at 37ºC. PCR amplification was performed using Expand Long Template DNA polymerase (Roche, Germany). About 2 µl of the restriction enzyme reaction was used for PCR amplification in a 50 µl volume. The PCR conditions were 95ºC for 5 min followed by 35 cycles at 95ºC for 45 s, 60ºC for 45 s, 72ºC for 1 min and a final extension of 72ºC for 10 min.

### Bisulfite sequencing

Bisulfite treatment (Engemann et al. 2001) was performed with the EZ DNA Methylation Kit™ (Zymo Research, Orange, CA). In a 50 µl reaction, 1 µg of genomic DNA was treated according to the manufacturer's recommendations. After bisulfite treatment, PCR

was performed using gene specific primers for the bisulfite converted DNA sequence (Details in Suppl. Materials). The PCR conditions used were the same as outlined for MSRE-PCR. PCR products were subcloned into pCR®4-TOPO vector (Invitrogen, Carlsbad, CA) and sequenced with M13F and M13R primers.

**Single Cell RT-PCR (SC RT-PCR)**

Cells of the female gametophyte before and after fertilization as well as sperm cells were isolated from the maize inbred line A188 as described by Cordts et al. (2001). SC RT-PCR was performed according to Richert et al. (1996) with one modification. A multiplex reverse transcription reaction was conducted on each cell either with reverse R-fie1 and R-fie2 primers for *Fie1* and *Fie2*, respectively, in addition to the reverse *GAPDH* (glyceraldehyde-3-phosphate dehydrogenase) primer Gap2. Generated cDNA was split into two equal amounts to amplify Fie and *GAPDH* transcripts separately during 40 PCR cycles using primers described in Table S1. Gels were blotted and hybridized as described (Dresselhaus et al. 1999) with radio-labeled *Fie1* and *Fie2*-specific probes.

**Real-time quantitative RT-PCR (qRT-PCR)**

Developing kernels were collected every 24 h from the ear base harvested from the B73 inbred pollinated by the Mo17 inbred in the field. Total RNA was isolated from whole kernels using TRIzol® Reagent with Phase Lock Gel-Heavy (Eppendorf North America, Inc., Molecular Research Center, Inc.). Total RNA was treated with DNase I (Invitrogen, Carlsbad, CA) and reverse-transcribed by using the Taqman Reverse Transcription kit (Applied Biosystems, Foster City, CA) according to the manufacturer's instructions. The final RNA concentration in the cDNA synthesis reaction was 30 ng/*µ*l. The absence of genomic DNA contamination was confirmed by the PCR without the reverse transcriptase. To ensure gene-specific amplification, primers and 5' FAM labeled LNA probes (Tab. 2) were designed against 3' UTR of *Fie1* and *Fie2* using Universal ProbeLibrary (Roche Diagnostics, Indianapolis, IN). Primers and the 5' VIC labeled MGB probe (Table S2) for *β-Actin* were designed using Primer Express 2.0 software (Applied Biosystems, Foster City, CA). The expression of each gene was assayed in triplicate in a total volume of 20 *µ*l containing 1x Taqman master mix, 300 nM forward and reverses primers, 100 nM probes and 3µl of the 1:4 diluted cDNA. The PCR thermal cycling parameters were 50ºC for 2 min, 95ºC for 10 min followed by 40 cycles of 95ºC for 15 s and 60ºC for 1 min. All assays were run on an ABI 7500 Real Time PCR System

(Applied Biosystems, Foster City, CA). Transcript levels of *Fie1* and *Fie2* were measured relatively to the endogenous reference *β*-Actin with the Ct method as described by the manufacturer. The PCR amplification efficiency was determined by measuring a series of input cDNA concentrations. The PCR efficiency for *Fie1, Fie2* and *β-Actin* was 1.01, 1.03 and 1.02, respectively.

## Results

### The maternal *Fie1* allele is activated in the endosperm after fertilization whereas Fie2 is expressed in both gametes and zygotes.

As shown previously, *Fie1* transcript was detected exclusively in the endosperm where it is expressed from the maternal allele. *Fie2* is expressed in a broad set of tissues including ovules before fertilization (Danilevskaya et al. 2003; Gutierrez-Marcos et al. 2003). However, *Fie1* and *Fie2* expression was never analyzed in gametes. To address this issue, transcription of *Fie1* and *Fie2* was examined in manually isolated gametes and zygotes by single cell RT-PCR (SC RT-PCR) (Richert et al. 1996; Cordts et al. 2001). *Fie1* mRNA was neither detected in the individual gametes nor in zygotes 12 h after in vitro pollination, which is around 6 h after fertilization (Fig. 1A). In contrast, *Fie2* transcript is present in all gametic cells with the highest transcript level in the central cell (Fig. 1B). To detect the onset of *Fie1* activation in the endosperm, developing kernels were collected every 24 h after pollination and analyzed by quantitative real-time RT-PCR (qRT-PCR) for *Fie1* and *Fie2* expression. *Fie1* transcript was at background level in the ovules and in developing kernels at 1 DAP. *Fie1* mRNA was first detected around 2 DAP (Fig. 1C and Tab. 1 and 2). Because fertilization occurs around 16–24 h after in vivo pollination (Kiesselbach 1999), we conclude that *Fie1* activation takes place approximately 24–32 h after fertilization. The highest Fie1 mRNA level was detected in kernels at 10–11 DAP and gradually decreased at later stages (Fig. 1C). In contrast, *Fie2* transcript was present in mature ovules and its level slightly increased at 1–4 DAP, but decreased at later stages. Overall, *Fie2* mRNA level was significantly lower than *Fie1*. At 10 DAP, expression of Fie1 is about 80 times higher than that of *Fie2*.

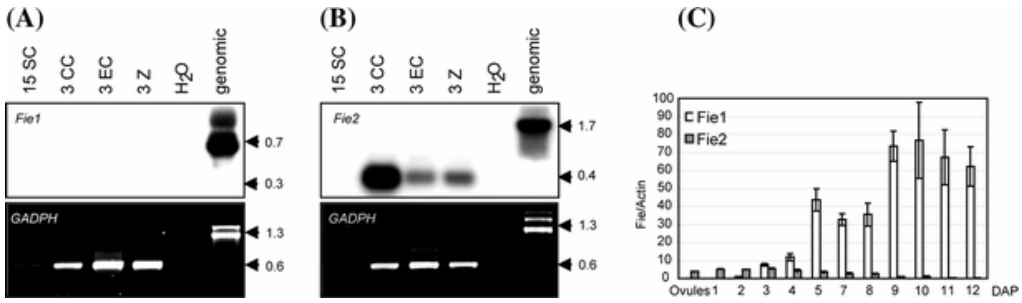


**Figure. 1 *Fie1* and *Fie2* expression in gametes and developing kernels**
(**A**) RT-PCR analysis of *Fie1* and (**B**) *Fie2* expression in 15 sperm cells (SC), 3 central cells (CC), 3 egg cells (EC), and 3 zygotes (Z) collected 12 h after in vitro pollination (around 6 h after fertilization). *Fie* PCR products were blotted and hybridized with a gene-specific probe. DNA fragment sizes (kb) are indicated by arrows. This experiment was repeated twice to confirm the obtained result. (**C**) Quantification of the *Fie1* and *Fie2* mRNAs in developing kernels by qRT-PCR. Relative amounts were calculated and normalized with respect to *actin* transcript levels (=100%). Data shown represent mean values obtained from three independent amplification reactions, and the error bars indicate the standard error of the mean. The original numbers are shown in Table 1.

**Table 1.** qRT-PCR ratio *Fie*/ actin.

| | Fie1/actin | | | Fie2/actin | | |
|---|---|---|---|---|---|---|
| Samples | Fie1 | STDEV | SE | Fie2 | STDEV | SE |
| Ovules | 0.11 | 0.04 | 0.02 | 3.95 | 0.28 | 0.16 |
| 1DAP | 0.02 | 0.02 | 0.01 | 5.25 | 0.55 | 0.32 |
| 2DAP | 1.02 | 0.25 | 0.15 | 4.96 | 0.53 | 0.30 |
| 3DAP | 7.56 | 1.22 | 0.70 | 5.30 | 0.59 | 0.34 |
| 4DAP | 11.94 | 3.50 | 2.02 | 4.41 | 1.15 | 0.66 |
| 5DAP | 43.54 | 10.64 | 6.14 | 3.58 | 0.98 | 0.57 |
| 7DAP | 32.70 | 5.45 | 3.14 | 2.70 | 0.74 | 0.43 |
| 8DAP | 35.50 | 11.18 | 6.46 | 2.45 | 0.84 | 0.49 |
| 9DAP | 73.46 | 14.32 | 8.27 | 0.99 | 0.08 | 0.05 |
| 10DAP | 76.72 | 36.78 | 21.23 | 0.95 | 0.65 | 0.38 |
| 11DAP | 67.14 | 26.52 | 15.31 | 0.39 | 0.09 | 0.05 |
| 12DAP | 62.23 | 18.67 | 10.78 | 0.17 | 0.04 | 0.02 |

STDEV –standard deviation, SE –standard error

**Table 2:** A list of oligonucleotides for real-time RT-PCR.

| Oligonucleotide | Sequence (5' to 3') |
|---|---|
| Fie1_F | TTGGTTCAGAGTCGCCAGAT |
| Fie1_R | ACAGCAGCATCCTAACATTCAA |
| Fie1_probe | CAGCCACA |
| Fie2_F | GGGTTGCGATGGTTGAAT |
| Fie2_R | AACACCAACCATTTTGACTAGAAA |
| Fie2_probe | TTCCACCA |
| β-Actin_F | CTTCGAATGCCCAGCAATGT |
| β-Actin_R | GTTCGCCCACTAGCGTACAAC |
| β-Actin_probe | TCGAGGCTGTTCTTT |

### *Fie1* is methylated in most tissues whereas *Fie2* is not methylated

To examine the role of DNA methylation in determining the expression pattern of the *Fie1* (GenBank Accession #AY150645) and *Fie2* (GenBank Accession #AY150646) genes, we analyzed their methylation status in different tissues. Methylation sensitive restriction enzyme digestion PCR (MSRE-PCR) analysis with the isoschizomers *Hpa*II and *Msp*I was performed to assess the methylation pattern across the two genes (Liang et al. 2004). Both enzymes recognize CCGG sites but *Hpa*II does not cut DNA if either cytosine is methylated. *Msp*I does not cut DNA if the external cytosine is methylated. *Fie1* contains seven CCGG sites distributed throughout the gene and *Fie2* contains ten CCGG sites clustered in upstream and at exon 1 (Fig. 2A and Tab. 3). Using both enzymes for MSRE-PCR analysis, we found that CCGG sites at exon 1 and exon 7 were methylated in the embryo, endosperm and leaf DNA (Fig. 2B). CCGG sites at exons 11–13 showed a low level of methylation. DNA methylation was not detected in Fie2 (Fig. 2B).

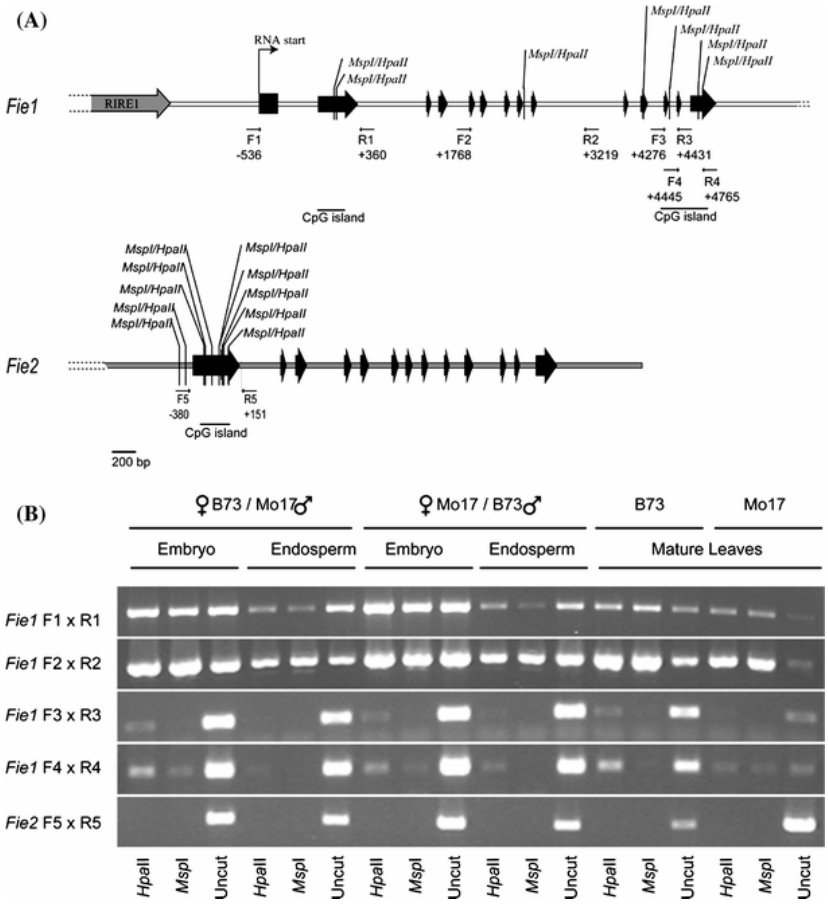


**Figure 2. Methyl-sensitive restriction-enzyme-dependent (MSRE) PCR of *Fie1* and *Fie2***
(**A**) Genomic maps of Fie1(GenBank accession #AY150645) and *Fie2* (GenBank accession #AY150646) are shown with *Msp*I/*Hpa*II restriction sites. Exons are depicted by black arrows. Introns are shown with lines. Retrotransposon *RIRE* is depicted by the shaded arrow. Gene specific primers, shown with small arrows, were used to amplify four regions of *Fie1* and one region of *Fie2* containing *Msp*I/*Hpa*II sites. Primers are marked with location relative to the ATG start codon. (**B**) Agarose gel with PCR products of the five analyzed regions of the *Fie* genes. Genomic DNA was isolated from embryo and endosperm tissue from reciprocal crosses of inbred lines B73 and Mo17 (female shown first). DNA was treated with *Msp*I or *Hpa*II restriction enzyme prior to amplification. The presence of PCR products indicates methylation of *Msp*I/*Hpa*II sites within the region. Undigested DNA was used as a positive control.

**Table 3:** A list of primers for RT-PCR, MSRE-PCR and Bisulfate sequencing

| Primers | Sequence in 5' to 3' direction. |
|---|---|
| **SC RT-PCR** | |
| F-fie1 | GGAACCAAAACCAGACAAGCGTAGGC |
| R-fie1 | CCTTATCGGCGACTTGCATTCCTGGTT |
| F-fie2 | ATGGACTGACCTTCCATCAAAGTTTCCAAC |
| R-fie2 | CAATGAGGACAGGAGGGC |
| Gap1 | AGGGTGGTGCCAAGAAGGTTG |
| Gap2 | GTAGCCCCACTCGTTGTCGTA |
| **SC MSRE-PCR** | |
| F1-fie1 | CGCCGCCACCATATAGAACCACTTATC |
| R1-fie1 | ATTGCAACTGGCGATGGC |
| **Tissue MSRE-PCR** | |
| Fie1, F1 | GCCGCCACCATATAGAACCACTTATC |
| Fie1, R1 | TTGCAACTGGCGATGGC |
| Fie1, F2 | ATGAGATAAGGACTCATGCCTCGAAGCCA |
| Fie1, R2 | CCCACTCACGTGCAGGTAGAAAG |
| Fie1, F3 | AGGCGAGATCTATGTCTGGGAAGTGCAGTC |
| Fie1, R3 | ATCGGCGACTTGCATTCC |
| Fie1, F4 | AATGCAAGTCGCCGATAAGGCAGACCGCAG |
| Fie1, R4 | CAACCAGCACGGAGTACGATCGATGTGAA |
| Fie2, F5 | GCGACACTAGTAACGGTCTACACCA |
| Fie2, R5 | CGCGTCCATGAAGTTGAACCCGATAG |
| **Bisulfite Sequencing** | |
| Fie1, -1202 | TAGTGGGAGGTGGATGTTTTATT |
| Fie1, -1098 | TCACTTACATACCTTAACTTAATTCCTTAC |
| Fie1, -815 | ATGGTATGGTTGTATAGGTGTTTTTAATTA |
| Fie1, -604 | AAAAAAATTATTTCCCCCTAATCCT |
| Fie1, +22 | GAAAGAGGTTATTTTGTGATATTATTGTT |
| Fie1, +217 | CTACTTCACATCCTAATCCTTATCATAAA |
| Fie1, +2245 | GGTTTGGGAATTATTTTAAATTAGTTTT |
| Fie1, +2575 | CACCAAACCATCTTAATACAATCAACAT |
| Fie2, -84 | GGGAAAGTAGTAGAGGAGGGGGTAGTAAT |
| Fie2, +280 | TAATTTTACCTTACCATTAATCAACAAA |

Bisulfite sequencing (Engemann et al. 2001) was applied to quantify *Fie1* and *Fie2* DNA methylation at CpG and CpNpG sites in the embryo, endosperm, pollen and leaf tissues. The promoter region was of particular interest because it lacks *Hpa*II/*Msp*I sites. The promoter, exon 1 and the region including exons 6–8 of *Fie1* are shown in Fig. 3A. Endosperm DNA revealed a low level of methylation ranging from 20% to 40% at CG sites and from 14% to 16% at CNG sites (Fig. 3A and Tab. 4) in all segments analyzed including the promoter. In contrast, *Fie1* DNA from embryo, pollen and leaves

was methylated up to 58–97% at CG-sites and 50–75% at CNG sites (Fig. 3A and Tab. 4). Combining MSREPCR and bisulfite sequencing allowed the conclusion that the *Fie1* gene is methylated across the promoter region and approximately half of the coding region up to exon 8. Significant cytosine methylation was not detected at the *Fie2* gene (Fig. 3B).

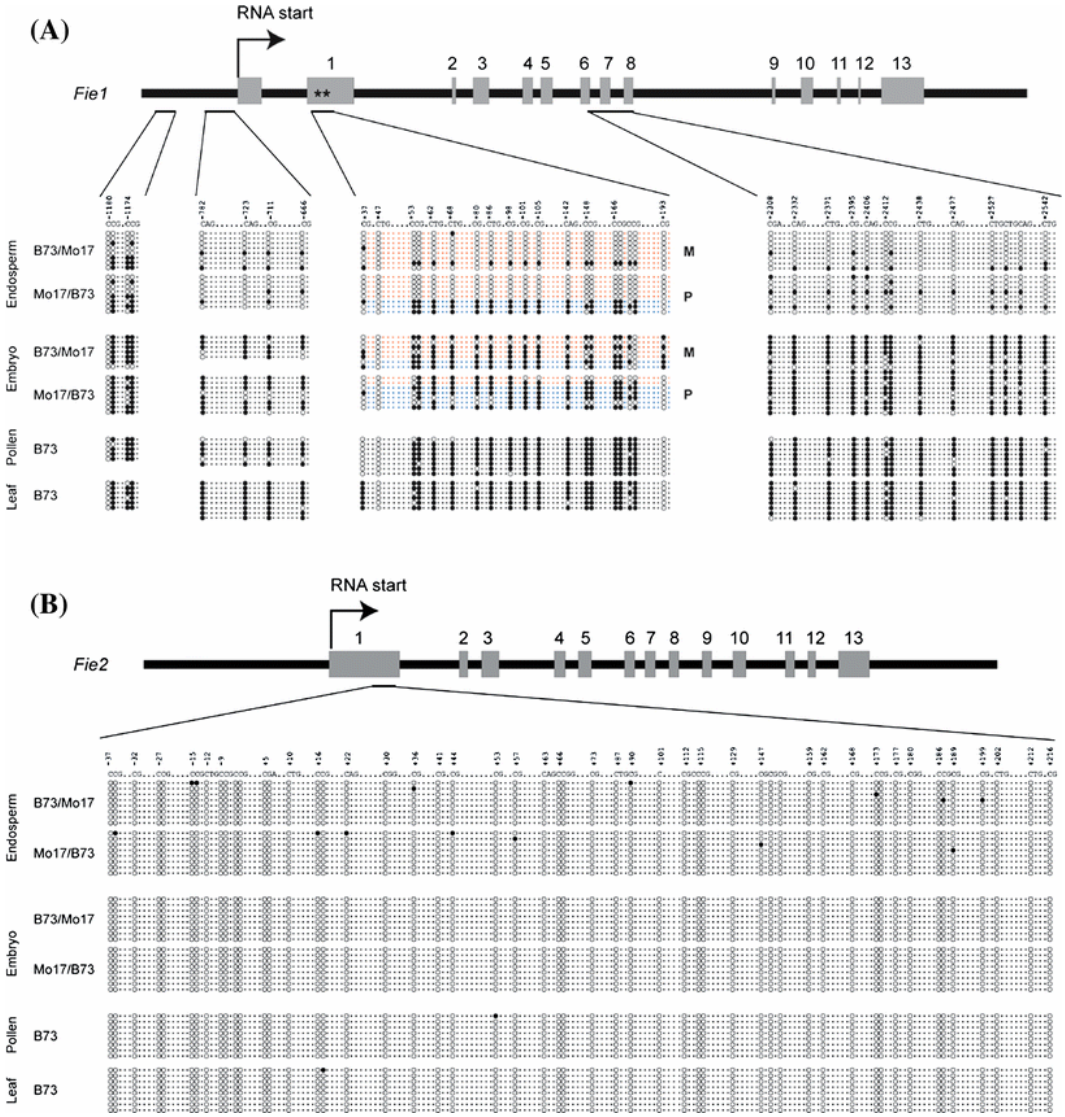


**Fig. 3 Bisulfite DNA methylation pattern of *Fie1* and *Fie2* in different maize tissues.**
(**A**) Genomic structure of *Fie1* is shown above methylation profiles. Exons are depicted with shaded boxes. Introns are shown by solid black lines. The transcription start point is marked with an arrowhead and two SNPs in exon 1 between parental inbred lines B73 and Mo17 are marked with asterisks. Regions used for bisulfite sequencing are underlined. Percent methylation at CG, CNG and asymmetric sites in endosperm, embryo, pollen and leaf is indicated. (**B**) Genomic structure and methylation profile of *Fie2*. Description as in (A). Detailed information about numbers and clones analyzed and primers used are provided in Tables 3 and 4.

**Table 4.** Number of methylated cytosines across four *Fie1* regions in different tissues.

| Promoter region 1 | Number of molecules | CG (2 sites) | CNG (2 sites) | Asymmetric (14 sites) |
|---|---|---|---|---|
| Pollen | 5 | 9/10 (90%) | 5/10 (50.00%) | 0/70 (0%) |
| Leaf | 12 | 24/24 (100%) | 8/24 (33.33%) | 0/168 (0%) |
| Embryo | 15 | 27/30 (90%) | 9/30 (30.00%) | 3/210 (1.43%) |
| Endosperm | 16 | 18/32 (56.25%) | 4/32 (13.33%) | 0/224 (0%) |

| Promoter region 2 | Number of molecules | CG (1 sites) | CNG (2) | Asymmetric (39) |
|---|---|---|---|---|
| Pollen | 6 | 4/6 (66.67%) | 8/12 (66.67%) | 6/234 (2.56%) |
| Leaf | 16 | 12/16 (75.00%) | 24/32 ( 75.00%) | 15/624 (2.40%) |
| Embryo | 13 | 9/13 (69.23%) | 21/26 (80.77%) | 9/507 (1.78%) |
| Endosperm | 15 | 2/15 (13.33%) | 5/30 (16.67%) | 3/585 (0.51%) |

| Exon 1 | Number of molecules | CG (10) | CNG (9) | Asymmetric (30) |
|---|---|---|---|---|
| Pollen | 8 | 62/80 (77.50%) | 72/54 (75.00%) | 17/240 (7.08%) |
| Leaf | 14 | 82/140 (58.57%) | 60/126 (47.62%) | 15/420 (3.57%) |
| Embryo | 14 | 92/140 (65.71%) | 62/126 (49.21%) | 18/420 (4.29%) |
| Endosperm | 16 | 35/160 (21.88%) | 21/144 (16.67%) | 9/480 (1.88%) |

| Exons/introns 6-7-8 | Number of molecules | CG (3) | CNG (11) | Asymmetric (45) |
|---|---|---|---|---|
| Pollen | 8 | 23/24 (95.83%) | 75/88 (85.23%) | 8/360 (2.22%) |
| Leaf | 16 | 47/48 (97.92%) | 147/176 (83.52%) | 24/720 (3.33%) |
| Embryo | 16 | 43/48 (89.58%) | 126/176 (71.59%) | 8/720 (1.11%) |
| Endosperm | 16 | 14/48 (29.17%) | 29/176 (16.48%) | 3/720 (0.42%) |

CGG sites are counted as CG sites not as CNG. Asymmetric is defined by cytosines in the context CHH, where H=A, T, or C. Each fraction represents the number of cytosines methylated out of the total number of sites analyzed.

**Maternal *Fie1* allele is hypomethylated in the endosperm**

To discriminate maternal and paternal alleles in bisulfite treated DNA molecules, we took advantage of two SNPs in exon 1 in inbred lines B73 and Mo17 (Fig. 4A). Due to the preferential amplification of the maternal molecules from the endosperm DNA (Fig. 3A) we have sequenced 116 clones amplified from exon 1 using endosperm DNA from reciprocal B73 x Mo17 crosses. 102 clones were of maternal and 14 of paternal origin. We found that maternal endosperm molecules were hypomethylated (2.8% methylated cytosines at CG sites and 3.3% at CNG) compared to corresponding paternal endosperm molecules (65.7% at CG and 49.2% at CNG). Maternal DNA isolated from embryos displayed a high methylation content (64.0% at CG and 56.7% at CNG) similar

to corresponding paternal DNA regions (70.0% at CG, 63.9% at CNG) (Fig. 4B and Tab 5). Because the maternal endosperm alleles have been preferentially amplified, we designed an additional experiment to confirm methylation at the paternal allele. Embryo and endosperm DNA from reciprocal crosses of B73 and Mo17 were digested to completion with *Hpa*II and amplified across *Hpa*II sites and SNPs in exon 1 with gene-specific primers extended with T3 and T7 adapters (Fig. 4A). PCR fragments obtained were directly sequenced with T3 and T7. Sequencing chromatograms of PCR products from digested and undigested embryo DNA showed the presence of SNPs from both parents, B73 and Mo17 (Fig. 4C), indicating that both parental alleles are methylated in the embryo. Conversely, the chromatograms of PCR products generated from digested endosperm DNA showed the presence of paternal SNPs but a complete absence of maternal SNPs (Fig. 4D). Undigested endosperm DNA showed a mixture of traces from both parents. These results confirm that the paternal *Fie1* allele is methylated in the endosperm and therefore protected from digestion by *Hpa*II. The maternal alleles are unmethylated and can be digested by *Hpa*II. In summary, the maternal Fie1 allele is hypomethylated in the endosperm but methylated in the embryo. The expression of *Fie1* is thus strongly correlated with a loss of DNA methylation of the maternal allele in the endosperm. The paternal allele is methylated in the endosperm and all other tissues investigated.

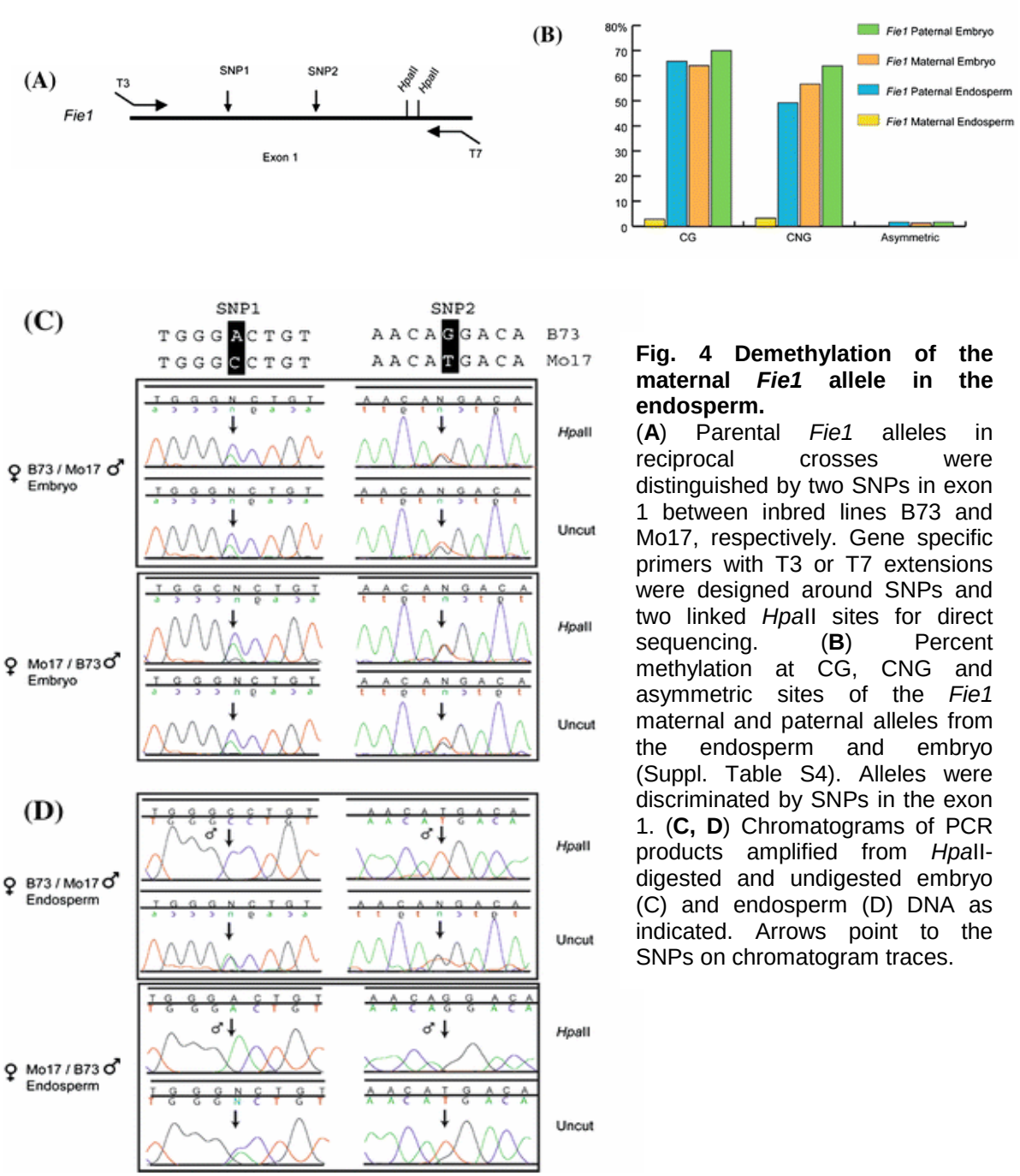


**Fig. 4 Demethylation of the maternal *Fie1* allele in the endosperm.**
(**A**) Parental *Fie1* alleles in reciprocal crosses were distinguished by two SNPs in exon 1 between inbred lines B73 and Mo17, respectively. Gene specific primers with T3 or T7 extensions were designed around SNPs and two linked *Hpa*II sites for direct sequencing. (**B**) Percent methylation at CG, CNG and asymmetric sites of the *Fie1* maternal and paternal alleles from the endosperm and embryo (Suppl. Table S4). Alleles were discriminated by SNPs in the exon 1. (**C, D**) Chromatograms of PCR products amplified from *Hpa*II-digested and undigested embryo (C) and endosperm (D) DNA as indicated. Arrows point to the SNPs on chromatogram traces.

**Table 5.** Number of methylated cytosines at *Fie1* maternal and paternal alleles of exon 1.

| | Genotype | Number of Molecules | CG (10) | CNG (9) | Asymmetric (30) |
|---|---|---|---|---|---|
| Endosperm | Fie1 Maternal | 102 | 29/1020 (2.84%) | 30/918 (3.27%) | 6/3060 (0.19%) |
| | Fie1 Paternal | 14 | 92/140 (65.71%) | 62/126 (49.21%) | 7/420 (1.66%) |
| Embryo | Fie1 Maternal | 10 | 64/100 (64.00%) | 51/90 (56.66%) | 4/300 (1.33%) |
| | Fie1 Paternal | 4 | 28/40 (70.00%) | 23/36 (63.88%) | 2/120 (1.66%) |

## Discussion

The maize genome contains two homologous *Fie* genes which have distinct expression pattern (Danilevskaya et al. 2003). *Fie1* is a highly regulated gene, expressed exclusively in the endosperm, where its expression is controlled by imprinting, resulting in mono-allelic expression of the maternal but not the paternal allele. In contrast, *Fie2* shows bi-allelic expression in many tissues including embryo and endosperm at later stages of development. The Arabidopsis *FIE* gene functions as a repressor of endosperm development in the central cell prior to fertilization (Ohad et al. 1999) and seems to be involved in the regulation of the ontogenic sequence of endosperm development after fertilization (Ingouff et al. 2005). To elucidate functions of maize *Fie* genes prior to fertilization, we examined their expression pattern in manually isolated gametes from maize. Neither gene is expressed in the sperm. Out of both *Fie* genes, only *Fie2* transcript was detected in the central cell supporting its putative function as a repressor of endosperm development before fertilization. At a lower level, *Fie2* transcription was also detected in the egg cell and after fertilization in the zygote and developing endosperm. This expression pattern might be attributed to additional functions of *Fie2* during kernel development similar to that of Arabidopsis *FIE*. Knock-out mutants should now be analyzed to study *Fie2* functions. However, such mutants are not available yet.

The absence of *Fie1* transcript in the central cell and the egg cell indicates that this gene does not play a role in the regulation of pre-fertilization events in the embryo sac. Rather it might have very specific function(s) during endosperm development. Endosperm development in maize and other cereals is characterized by distinct changes of the cell

cycle pattern. The primary endosperm nucleus, resulting from fusion of a sperm with the two polar nuclei of the central cell, divides mitotically within 3–5 h after fertilization without cytokinesis forming a multinucleate syncytium (Kiesselbach 1999). Cell wall deposition is activated around 3 DAP and is completed at 4–5 DAP. Mitotic proliferation continues up to 10–15 DAP until the cell cycle switches to endoreduplication (Kowles and Phillips 1988). The transition from mitotic divisions to endoreduplication is thought to be controlled by parental imprinting (Dilkes et al. 2002; Leblanc et al. 2002). Expression of *Fie1* begins approximately 24–32 h after fertilization reaching the highest level at 10–11 DAP coinciding with the described switch of the cell cycle from mitotic divisions to endoreduplication. As a PcG protein, *Fie1* might regulate imprinting of other genes and it is therefore tempting to speculate that *Fie1* might have a function in the maternal control of the transition to endoreduplication in the maize endosperm. Rice and sorghum genomes also contain two *FIE* homologues (Lai et al. 2004), suggesting that *Fie* genes in cereals might have evolved distinct functions compared to the single Arabidopsis *FIE* gene. It is interesting now to study whether rice and sorghum *Fie1*-like genes are also regulated by imprinting as is the case for the maize *Fie1* gene. This would indicate conserved functions in the grasses.

The distinct feature of the *Fie1* gene is its mono-allelic expression from the maternal allele in the endosperm at all stages of development (Danilevskaya et al. 2003). *Fie2* shows bi-allelic expression in the embryo and in the endosperm at later stages. However, in the early endosperm at 6 DAP, *Fie2* has been shown to be expressed maternally (Danilevskaya et al. 2003; Gutierrez-Marcos et al. 2003). To understand the role of DNA methylation in tissue-specific expression and imprinting, we have examined the methylation status of both *Fie* genes. *Fie1* was found to be methylated in all tissues tested, which is consistent with its restricted expression pattern and indicates that the methylated silent state is the default for *Fie1*. DNA methylation was not detected in the *Fie2* gene, which is consistent with its broad expression in many tissues. However, recently *Fie2* methylation of the paternal allele was observed in 6 DAP endosperm indicating that the transient methylation of this gene takes place only during early stages of endosperm development (Gutierrez-Marcos et al. 2006), as the gene is no longer methylated at 14 DAP (this report).

Using bisulfite sequencing, we found a high level of *Fie1* methylation at the promoter region, exon 1 and exons 6–8 in DNA samples isolated from embryos, pollen and leaves. A lower level of DNA methylation was detected in the endosperm, where only the

maternal *Fie1* alleles are expressed. Our results further showed that the maternal *Fie1* allele is hypomethylated in the endosperm, but the paternal allele is hypermethylated. In DNA extracted from embryos, both maternal and paternal alleles are methylated at the same level.

This methylation pattern strongly correlates with *Fie1* expression. *Fie1* is methylated and silent in most tissues except the endosperm where the maternal allele is demethylated and transcribed.

Because *Fie1* transcript was not detected in the central cell, it was unclear when demethylation of the *Fie1* gene actually occurs. According to a recent study by Gutierrez-Marcos et al. (2006), Fie1 is methylated in the sperm and the egg cell, but hypomethylated in the central cell. Thus the demethylation of the *Fie1* gene occurs before fertilization in the central cell. Despite its demethylation in the central cell, *Fie1* becomes transcriptional active only in the primary endosperm after fertilization suggesting that demethylation is necessary but not sufficient for its activity. Endosperm-specific factors are apparently required to activate transcription of the maternal *Fie1* gene in the endosperm. Demethylation and transcriptional activation of the maternal alleles of *MEA* (Xiao et al. 2003; Kinoshita et al. 2004), *FWA* (Kinoshita et al. 2004) and *FIS2* (Jullien and Katz et al. 2006; Jullien and Kinoshita et al. 2006) occur during female gametogenesis in the central cell by the antagonistic activity of MET1 methyltransferase and DME, a DNA glycosylase with a 5-methylcytosine excising activity (Choi et al. 2002; Gehring et al. 2006). *DME* is specifically expressed in the central cell preceding fertilization, erasing methylation marks set up by *MET1* on *MEA*, *FWA* and *FIS2* (Xiao et al. 2003; Kinoshita et al. 2004; Jullien and Katz et al. 2006; Jullien and Kinoshita et al. 2006). The DME-like genes might play similar roles by erasing methylation marks on imprinted genes in maize as well.

Until recently, the molecular mechanisms of imprinting in plants have most extensively been studied in *Arabidopsis*. These studies revealed two types of imprinted genes. *MEA*, for example, shows bi-allelic expression in many tissues except the endosperm, where the gene is maternally expressed. Other genes, like *FWA* and *FIS*, are silent and methylated in all tissues except the endosperm, suggesting that methylation is the default state. The *Fie1* default state is also methylated and the maternal allele is activated due to its demethylation in the central cell prior to fertilization. We found that *Fie1* is methylated across the extended ~4 kb segment including the promoter and

coding region up to exon 7. This is significantly deviating from imprinted genes in *Arabidopsis*, where methylation is directed to specific segments, for example, the tandem repeats in the promoter of *FWA* (Kinoshita et al. 2004, 2007) and a 200-bp upstream segment in *FIS2*, respectively (Jullien and Katz et al. 2006; Jullien and Kinoshita et al. 2006). There are no direct or inverted repeats, which could act as cis-acting methylation elements in the *Fie1* gene. Recently a DMR (Differentially Methylated Region) was identified in *Fie1* at the 5' promoter region and in exon 1. However, in the central cell and the 6 DAP endosperm, DNA methylation was detected only in the promoter segment of the DMR but not in exon 1 and other downstream sequences (Gutierrez-Marcos et al. 2006). In contrast, we have detected that the paternal *Fie1* allele is methylated over the same extended region including the promoter, exon 1 and exons 6–8 in the 14 DAP endosperm as it was in the pollen. The different methylation pattern of *Fie1* at 6DAP (Gutierrez-Marcos et al. 2006) and 14 DAP endosperm (this report) may reflect the complex dynamics of demethylation and de novo methylation of the paternal *Fie1* allele that occurs during endosperm development in maize. Our study of the imprinted *Fie1* gene in maize provides new evidence for diversity and adds further complexity of imprinting mechanisms in plants.

**Acknowledgements**

We thank Evgueni Ananiev and Mike Muszynski for numerous critical comments, Dan Spielbauer and Laura Gottschalk for help with a real-time PCR experiment as well as Kejian Li and Anna Lyznik for technical assistance. This work was supported by a post-graduate scholarship in accordance with Hamburg's Young Academics Funding Law to K.S.

## References

**Alleman M, Doctor J.** (2000). Genomic imprinting in plants: observations and evolutionary implications. Plant Mol Biol **43**(2–3):147–161

**Baroux C, Gagliardini V et al.** (2006). Dynamic regulatory interactions of Polycomb group genes: MEDEA autoregulation is required for imprinted gene expression in Arabidopsis. Genes Dev **20**(9):1081–1086

**Baroux C, Spillane C et al.** (2002). Genomic imprinting during seed development. Adv Genet **46**:165–214

**Choi Y, Gehring M et al.** (2002). DEMETER, a DNA glycosylase domain protein, is required for endosperm gene imprinting and seed viability in arabidopsis. Cell **110**(1):33–42

**Cordts S, Bantin J et al.** (2001). ZmES genes encode peptides with structural homology to defensins and are specifically expressed in the female gametophyte of maize. Plant J **25**(1):103–114

**Danilevskaya ON, Hermon P et al.** (2003). Duplicated fie genes in maize: expression pattern and imprinting suggest distinct functions. Plant Cell **15**(2):425–438

**Delaval K, Feil R.** (2004). Epigenetic regulation of mammalian genomic imprinting. Curr Opin Genet Dev **14**(2):188–195

**Dilkes BP, Dante RA et al.** (2002). Genetic analyses of endoreduplication in Zea mays endosperm: evidence of sporophytic and zygotic maternal control. Genetics **160**(3):1163–1177

**Dresselhaus T, Cordts S et al.** (1999). Novel ribosomal genes from maize are differentially expressed in the zygotic and somatic cell cycles. Mol Gen Genet **261**(2):416–427

**Engemann S, El-Maarri O et al.** (2001). Bisulfite-based methylation analysis of imprinted genes. Methods Mol Biol **181**:217–228

**Gehring M, Choi Y et al.** (2004a). Imprinting and seed development. Plant Cell **16**:S203–S213

**Gehring M, Choi Y et al.** (2004b). Imprinting and seed development. Plant Cell **16**(Suppl):S203–S213

**Gehring M, Huh JH et al.** (2006). DEMETER DNA glycosylase establishes MEDEA polycomb gene self-imprinting by allelespecific demethylation. Cell **124**(3):495–506

**Grossniklaus U, Schneitz K.** (1998). The molecular and genetic basis of ovule and megagametophyte development. Semin Cell Dev Biol **9**(2):227–238

**Grossniklaus U, Vielle-Calzada JP et al.** (1998). Maternal control of embryogenesis by MEDEA, a polycomb group gene in Arabidopsis. Science **280**(5362):446–450

**Gutierrez-Marcos JF, Costa LM et al.** (2006). Epigenetic asymmetry of imprinted genes in plant gametes. Nat Genet **38**(8):876–878

**Gutierrez-Marcos JF, Pennington PD et al.** (2003). Imprinting in the endosperm: a possible role in preventing wide hybridization. Philos Trans R Soc Lond B Biol Sci **358**(1434):1105–1111

**Ingouff M, Haseloff J et al.** (2005). Polycomb group genes control developmental timing of endosperm. Plant J **42**(5):663–674

**Jullien PE, Katz A et al.** (2006). Polycomb group complexes selfregulate imprinting of the Polycomb group gene MEDEA in Arabidopsis. Curr Biol **16**(5):486–492

**Jullien PE, Kinoshita T et al.** (2006). Maintenance of DNA Methylation during the Arabidopsis life cycle is essential for parental imprinting. Plant Cell **18**(6):1360–1372

**Kermicle JL.** (1970). Dependence of the R Mottled Aleurone phenotype in maize-M on mode of sexual transmission. Genetics **66**(1):69–85

**Kiesselbach TA.** (1999). The structure and reproduction of corn. 50$^{th}$ aniversary edition. Cold Spring Harbor Laboratory Press, Cold Spring Harbor, New York

**Kinoshita T, Miura A et al.** (2004). One-way control of FWA imprinting in *Arabidopsis* endosperm by DNA methylation. Science **303**(5657):521–523

**Kinoshita T, Yadegari R et al.** (1999). Imprinting of the MEDEA polycomb gene in the Arabidopsis endosperm. Plant Cell **11**(10):1945–1952

**Kinoshita Y, Saze H et al.** (2007). Control of FWA gene silencing in *Arabidopsis thaliana* by SINE-related direct repeats. Plant J **49**(1):38–45

**Köhler C, Hennig L et al.** (2003a). Arabidopsis MSI1 is a component of the MEA/FIE Polycomb group complex and required for seed development. Embo J **22**(18):4804–4814

**Köhler C, Hennig L et al.** (2003b). The Polycomb-group protein MEDEA regulates seed development by controlling expression of the MADS-box gene PHERES1. Genes Dev **17**(12):1540–1553

**Köhler C, Page DR et al.** (2005). The *Arabidopsis thaliana* MEDEA Polycomb group protein controls expression of PHERES1 by parental imprinting. Nat Genet **37**(1):28–30

**Kowles RV, Phillips RL.** (1988). Endosperm development in maize. Int Rev Cytol **112**:97–136

**Kranz E, von Wiegen P et al.** (1998). Endosperm development after fusion of isolated, single maize sperm and central cells in vitro. Plant Cell **10**(4):511–524

**Lai J, Ma J et al.** (2004). Gene loss and movement in the maize genome. Genome Res **14**(10A):1924–1931

**Lauria M, Rupe M et al.** (2004). Extensive maternal DNA hypomethylation in the endosperm of Zea mays. Plant Cell **16**(2):510–522

**Leblanc O, Pointe C et al.** (2002). Cell cycle progression during endosperm development in Zea mays depends on parental dosage effects. Plant J **32**(6):1057–1066

**Liang HE, Hsu LY et al.** (2004). Variegated transcriptional activation of the immunoglobulin kappa locus in pre-b cells contributes to the allelic exclusion of light-chain expression. Cell **118**(1):19–29

**Luo M, Bilodeau P et al.** (1999). Genes controlling fertilization-independent seed development in Arabidopsis thaliana. Proc Natl Acad Sci USA **96**(1):296–301

**Morison IM, Ramsay JP et al.** (2005). A census of mammalian imprinting. Trends Genet **21**(8):457–465

**Ohad N, Yadegari R et al.** (1999). Mutations in FIE, a WD polycomb group gene, allow endosperm development without fertilization. Plant Cell **11**(3):407–416

**Reik W, Walter J.** (2001). Genomic imprinting: parental influence on the genome. Nat Rev Genet **2**(1):21–32

**Richert J, Kranz E, Lörz H, Dresselhaus T.** (1996). Plant Sci **114**:93–99

**Sathe SS, Harte PJ.** (1995). The Drosophila extra sex combs protein contains WD motifs essential for its function as a repressor of homeotic genes. Mech Dev **52**(1):77–87

**Springer NM, Danilevskaya ON et al.** (2002). Sequence relationships, conserved domains, and expression patterns for maize homologs of the polycomb group genes E(z), esc, and E(Pc). Plant Physiol **128**(4):1332–1345

**Surani MA, Barton SC.** (1983). Development of gynogenetic eggs in the mouse: implications for parthenogenetic embryos. Science **222**(4627):1034–1036

**Walbot V, Evans MM.** (2003). Unique features of the plant life cycle and their consequences. Nat Rev Genet **4**(5):369–379

**Xiao W, Gehring M et al.** (2003). Imprinting of the MEA Polycomb gene is controlled by antagonism between MET1 methyltransferase and DME glycosylase. Dev Cell **5**(6):891–901

# CHAPTER 4

# Asymmetrically inherited maize MATH-BTB proteins are involved in nuclei positioning and mitotic progression during megagametogenesis

**SUMMARY**

Female gametophyte (FG) and early embryo development constitute ideal model systems to study the establishment of polarity and asymmetric cell division in plants. We describe here three conserved MATH-BTB domain proteins (TaMAB1, TaMAB2, and ZmMAB1) which are specifically expressed during FG development and early embryogenesis of wheat and maize. ZmMAB1 is shown to be necessary for the correct positioning of daughter nuclei and the mitotic progression during the early coenocytic phase of megagametogenesis in maize. The asymmetric co-localisation of MABs with microtubuli around the nuclear envelope, their asymmetric inheritance during zygotic division as well as the interaction with Cullin 3 suggests a functional role for MABs in organizing the assembly and proper position of microtubular spindles during asymmetric cell divisions in plants via ubiquitin-dependent degradation of target proteins.

## INTRODUCTION

During the development of a multicellular organism, cell and tissue polarity as well as asymmetric cell division (ACD) play decisive roles in cell specialization, differentiation and fate determination, and rely on the asymmetric organization of cellular components and structures. In the flowering plant life cycle, polarity and ACD become apparent in processes such as female and male gametophyte development (megagametogenesis and microgametogenesis), and patterning during early embryogenesis (Scheres and Benfey, 1999; Souter and Lindsey, 2000; Ranganath, 2005). The apparent polarity of the mature female gametophyte (embryo sac) along its micropylar-chalazal axis arises during megagametogenesis. In the most common monosporic *Polygonum*-type embryo sac a linear tetrad of four megaspores is formed after meiosis. While the three micropylar-most megaspores generally degenerate, the chalazal-most megaspore continues to develop, forming the functional megaspore. During subsequent megagametogenesis the functional megaspore conducts three cycles of free-nuclear mitosis resulting in an eight nucleate coenocyte with four nuclei at each pole, which are separated by a large central vacuole. One nucleus from each pole migrates toward each other, forming the polar nuclei of the central cell, located in the micropylar half of the embryo sac. During following cellularization, four different cell types become specified: the egg cell, flanked by two synergids is located at the micropylar pole of the embryo sac, three antipodal cells are positioned at the chalazal pole, and the large central cell fills the center of the embryo sac. While almost nothing is known about the molecular mechanisms generating cellular asymmetries and cell specification within the developing female gametophyte, the polar positioning of nuclei and associated cell fate determination appears to be achieved by the precise control of mitotic divisions, alignment and elongation of mitotic spindles, vacuolization, nuclear migration, as well as by nuclear fusion (Christensen et al., 1997; Huang and Sheridan, 1994). Polarity is also evident within the differentiated cell types of the embryo sac and during embryogenesis: in mature egg cells, the nucleus and major parts of the cytoplasm are located towards the chalazal end, while the large vacuole occupies the micropylar end of the cell. In contrast, the synergids and the central cell display opposite polarity (Christensen et al., 1997). Upon fertilization, the zygote elongates rapidly followed by a first asymmetric cell division producing two cells of a different size and fate (Laux et al., 2004; Willemsen and Scheres, 2004).

Cytoskeletal elements (F-actin and microtubules) provide the structural basis for cell polarization in animals, yeast, and plants (Li and Gundersen, 2008; Mathur and Hülskamp, 2002). In animals and fungi, radial arrays of microtubules (MTs) emanate from a discrete microtubular organizing centre (MTOC), the centrosome and the spindle pole body,

respectively. The centrosome consists of a pair of centrioles surrounded by proteinaceous pericentriolar material (PCM). The nucleation of cytoplasmic and spindle microtubules occurs from the PCM, where γ-tubulin ring complexes (γTuRCs) act as nucleation cores (Lüders and Stearns, 2007). During mitosis, the centrosomes define spindle poles, and the formation of the bipolar spindle is essential for faithful chromosome segregation. Proper spindle positioning and orientation is necessary for ACD as it determines not only the asymmetry of cell division but also the relative location of daughter cells and thus cell fate decisions, and MTOCs are involved via interaction with defined cortical capture sites (McCarthy and Goldstein, 2006; Morris, 2003; Yamashita and Fuller, 2008). In contrast, little is known about the molecular mechanisms involved in asymmetric spindle positioning and nuclear migration during ACD in plants. Certainly one of the major reasons is that higher plants lack discrete MTOCs (Erhardt, 2007; Wasteneys, 2002). Nevertheless, plants have highly organized MT arrays such as the interphase cortical MTs, a cortical ring of MTs contributing to prophase spindle bipolarity and division plane determination (preprophase band), the mitotic spindle, and the phragmoplast which appears in between the separated daughter nuclei during cytokinesis (Canaday et al., 2000; Ambrose and Cyr, 2008). All these MT arrays are nucleated from flexible and dispersed sites of unknown composition, which are located at the nuclear surface and the cell cortex (Erhardt and Shaw, 2006). However, it is not understood how the assembly of an acentrosomal spindle could be regulated. Also in plants γ-tubulin is recognized to be one key element for MT nucleation, and a number of proteins with homology to animal MTOC components have meanwhile been identified (reviewed by Erhardt and Shaw, 2006; Lloyd and Chan, 2004).

In animals and yeast, there is increasing evidence that the temporally and spatially controlled targeting of key regulators to the ubiquitin/26S proteasome pathway is not only required for cell cycle transition and progression, but also for cytoskeletal regulation and cell fate determination. Recent studies in mammalian cells and in *C. elegans* show that multisubunit Cullin 3 (CUL3)-based E3 ligases are involved regulating mitotic progression, cytokinesis, and the proper regulation of microtubule dynamics and spindle assembly during meiosis-to-mitosis transition (Bowerman and Kurz, 2006; Sawin and Tran, 2006; Sumara et al., 2008). BTB domain (Brick-a-brac/tramtrack/broad complex) proteins appear to function as substrate-specific adaptors in CUL3-based E3 ligases of yeast, animals, and plants. BTB domains were reported to interact with CUL3, while secondary domains are thought to be responsible for substrate specificity (Figueroa et al., 2005; Geyer et al., 2003; Gingerich et al., 2005; Pintard et al., 2003; Sumara et al., 2007; Xu et al., 2003). The best characterized CUL3 substrate adaptor is Maternal Effect Lethal 26 (MEL-26) of *C. elegans*, which is responsible for the spatial and temporal targeting of the microtubule severing katanin

(defective in meiosis 1; MEI-1) and the microtubule-interacting fidgetin-like 1 AAA-ATPase (FIGL-1) for degradation (Luke-Glaser et al., 2007; Pintard et al., 2003). MEL-26 has a MATH (Meprin and TRAF homology)-BTB domain configuration which is conserved among proteins of multicellular eukaryotes (Stogios et al., 2005). In the genome of *Arabidopsis thaliana*, a small family of six MATH-BTB encoding genes is present (Weber et al., 2005; Gingerich et al., 2005) while the MATH-BTB gene family has greatly expanded in the genome of rice (Gingerich et al., 2007). At this time, however, neither a substrate nor a function has been assigned for any of the plant MATH-BTB proteins.

We report here about three MATH-BTB protein (MAB) encoding genes from wheat and maize (*TaMAB1*, *TaMAB2*, and *ZmMAB1*) that are specifically expressed in the FG before and early after fertilization. Subcellular localization of ZmMAB1- and TaMAB2-GFP fusion proteins show a strong and polar accumulation near the nuclear envelope, and some small fluorescent spots inside the nucleus and at the cell cortex. The observed co-localization of TaMAB2-GFP with microtubules adjacent to the nuclear envelope is lost after oryzalin treatment. Deletion experiments indicate that the MATH domain targets the protein to the nuclear envelope, while the BTB domain reallocates in scattered protein complexes, which remain in the larger mother cell after asymmetric division. Tracking TaMAB2-GFP provided by the *Arabidopsis* egg cell during fertilization and early embryogenesis reveals its invariable inheritance to the larger basal cell after the asymmetric division of the zygote. Transient over-expression of TaMAB2- or ZmMAB1-GFP prevents mitotic divisions of maize suspension cells, while silencing of *ZmMAB1* leads to severe defects in the polar positioning of nuclei during the early megagametogenesis, suggesting a functional role in organizing microtubular spindles during mitosis. This, together with the observed interaction of TaMAB2 with Cullin 3, indicates an important role for MAB proteins as substrate-specific adapters in CUL3-based E3 ligase complexes, thereby regulating mitotic spindle assembly and positioning during female gametophyte development and early embryogenesis.

## RESULTS

### Conserved MATH-BTB proteins TaMAB1, TaMAB2, and ZmMAB1 are specifically expressed in the female gametophyte of wheat and maize

We have used a transcriptomics based approach to identify cell-type specific transcripts present in cDNA libraries generated from isolated egg cells and 2-celled pro-embryos of wheat (Sprunck et al., 2005) as well as maize egg cells (Dresselhaus et al., 1994). Amongst others, we identified novel transcripts encoding proteins containing each, a MATH (Meprin and TRAF homology) and a BTB (Brick-a-brac/tramtrack/broad complex) domain. The

corresponding wheat genes were designated as *TaMAB1* and *TaMAB2*, and the maize gene was named *ZmMAB1*, in which MAB denotes the two domains MATH and BTB. To verify the specific expression of *MAB*s in zygotes and early embryos, we adapted the isolation protocol for wheat egg cells (Sprunck et al., 2005) and collected isolated zygotes, 2-celled embryos, and later embryonic stages (Fig. 1) for expression analysis by RT-PCR. The isolated *in vivo* wheat zygotes and pro-embryos exhibit a much more pronounced polarity than *in vitro* cultivated wheat and maize zygotes (Sprunck et al., 2005; Dresselhaus et al., 2006). The DAPI stained nucleus of *in vivo* wheat zygotes is positioned in the apical cytoplasm-rich region (Fig. 1B), and the first cell division results in a 2-celled stage with a small apical and a larger basal cell (Fig. 1C). The occurrence of three nuclei in 24 to 28 hap wheat pro-embryos indicates a delay of the larger basal cell in cell cycle progression (Fig. 1D).

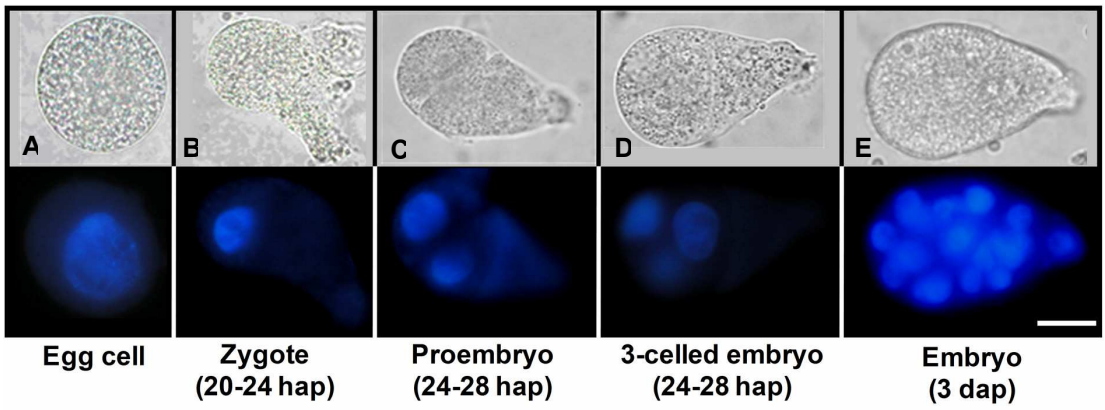


**Figure 1. *In vivo* isolated egg cell, zygote and early embryos of wheat**
Bright field (upper row) and corresponding fluorescent images after DAPI-staining (bottom row). (**A**) isolated egg cell, (**B**) zygote, (**C**) 2-celled pro-embryo, (**D**) 3-celled pro-embryo, and (**E**) embryo 3 days after pollination (dap). hap; hours after pollination. Scale bar: 25 µm.

Expression analysis of *TaMAB1* and *TaMAB2* by RT-PCR revealed that *TaMAB1* can not be detected in any vegetative tissue or anthers of wheat, but seems exclusively expressed in egg cells, being immediately down-regulated after fertilization (Fig. 2, A and B). In contrast, the expression of *TaMAB2* can be detected in zygotes and 2-celled embryos, it is down regulated in later embryo stages and is, like *TaMAB1*, not detectable in any other tissue (Fig. 2, A and B). Similar to wheat *MAB*s, *ZmMAB1* from maize is expressed neither in any of the vegetative tissues tested nor in anthers (Fig. 2, C). In contrast to *TaMAB1* and *TaMAB2*, *ZmMAB1* is expressed in both, the unfertilized egg cell and zygote (Fig. 2, D). A faint signal of *ZmMAB1* in one out of three synergids (Sy) indicates also a weak expression in synergids, which was confirmed by Southern blot analysis (not shown).

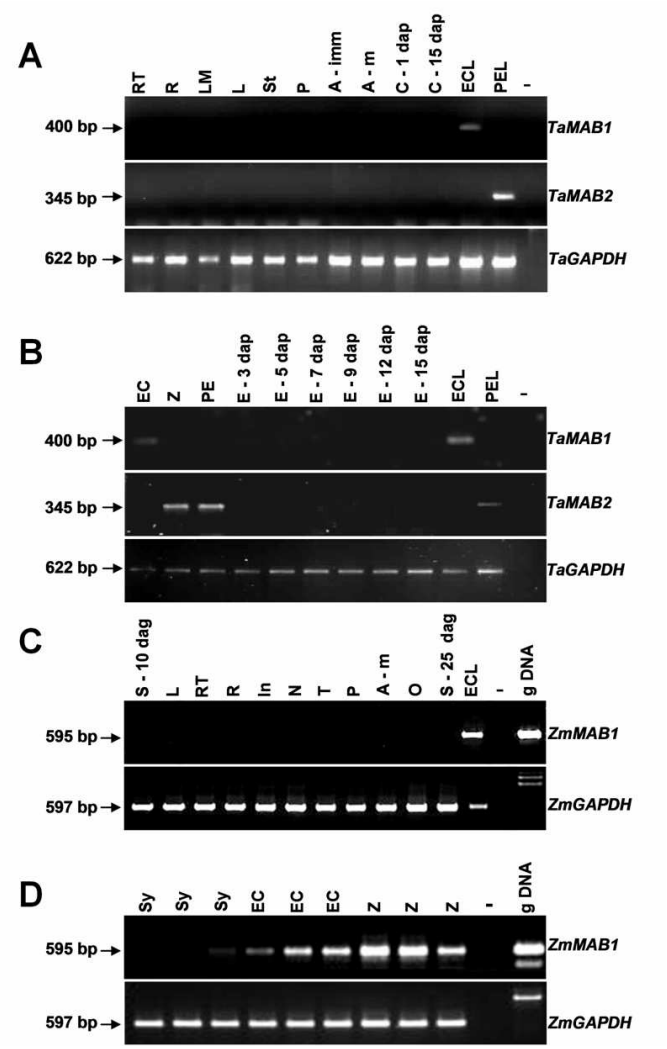


**Figure 2. Expression pattern of *TaMAB1, TaMAB2* and *ZmMAB1* within the female gametophyte as well as in various tissues and plant organs.**
The expression pattern of the individual wheat and maize *MAB*s was analyzed by RT-PCR using gene-specific primers. RNA samples were DNase treated as genes do not contain introns. *GAPDH* of wheat (*TaGAPDH*) and maize (*ZmGAPDH*) were used as controls. (**A**) Expression of *TaMAB1, TaMAB2* and *TaGAPDH* in different tissues of wheat. For tissue explanations see below. (**B**) Expression of *TaMAB1*, *TaMAB2*, and *TaGAPDH* in isolated egg cell, zygotes, 2-celled proembryos and different embryo stages of wheat. (**C**) Expression of Zm*MAB1* and *ZmGAPDH* in different tissues of maize. (**D**) Expression of Zm*MAB1*and *ZmGAPDH* in isolated egg cell, zygotes, and synergids of maize. The sizes of the respective amplification products are indicated (arrows). Abbreviations: A-m: mature anther, A-imm: immature anther, E: embryo, EC: egg cell, ECL: egg cell cDNA library, C: caryopsis, dag: days after germination, dap: days after pollination, In: internode, L: leaf, LM: leaf meristem, PE: proembryo, PEL: proembryo cDNA library, GAPDH: glyceraldehyde 3-phosphate dehydrogenase, gDNA: genomic DNA, N: node, O: ovary, P: pistil, R: root, RT: root tip, S: seedling, Sy: synergid, St: stem, T: tassel, Z: zygote, : water control.

The corresponding *MAB* genes encode predicted proteins of 347 to 362 amino acids, with a molecular mass between 38 to 40 kDa. We compared the predicted amino acid sequences and domain architecture of TaMAB1, TaMAB2, and ZmMAB1 by multiple sequence alignment and found that they possess a similar structure with a low conserved MATH domain in the N-terminal half, while a more conserved BTB domain is located in the C-terminal region (Fig. 3). Sequence similarity searches revealed that *MABs* are conserved throughout the eukaryotic kingdom. In plants, they display significant similarities to MATH-BTB protein encoding genes in the genome of rice and maize, to MATH-BTB proteins of *Arabidopsis* (Fig. 3 and 4), as well as predicted protein sequences from other plant species including barley, tomato, soybean, sorghum, sugarcane, and the moss *Physcomitrella patens* (not shown). We have performed multiple sequence alignments to compare TaMAB1, TaMAB2, and ZmMAB1 with selected plant MATH-BTB proteins from *Arabidopsis*, maize and rice, with mammalian MATH-BTB proteins, and with *C. elegans* MEL26. According to the classification of Gingerich et al. (2007) the three female gametophyte-specific MABs group into subclades formed by members of monocot-specific MATH-BTB proteins and not into the

subclade of the core group of plant MATH-BTBs (Fig. 4). Animal MATH-BTB proteins form a distant subclade to plant MATH-BTB proteins.

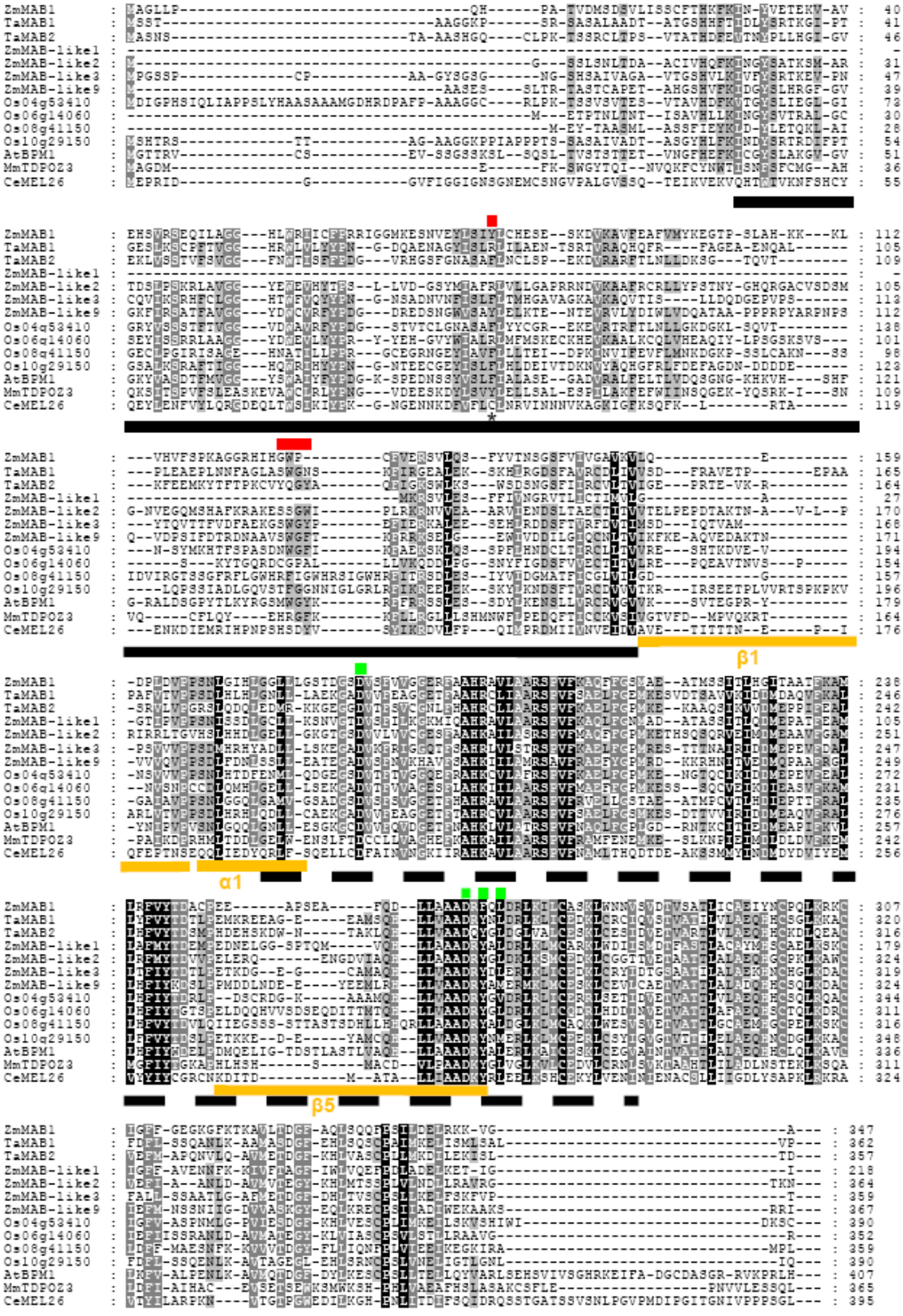

**Figure 3. Alignment of selected plant and animal MATH-BTB domain proteins.**
Protein sequences were aligned using M-Coffee and processed with GeneDoc. Similar amino acid residues are shaded in black and conserved amino acid residues are highlighted in grey. The position of MATH domain is marked by a continuous black line, the BTB/POZ domain is underlined with a dashed black line. Conserved amino acid residues probably involved in Cullin3 interaction or substrate targeting are marked by green squares above respective amino acids. Yellow underlined regions are predicted to be responsible for dimerization. The substrate binding residues within the MATH domain (marked by red squares above sequences) are predicted according to the substrate-binding site of human TRAF and HAUSP proteins. The substrate binding pocket might have the same location in other MATH domains, but the specific substrates are likely very different. Please note that residue C94 (labeled by an asterisk) in CeMEL-26 is shown as required for interaction of CeMEL-26 with katanin. For GenBank Accessions see Figure S3.

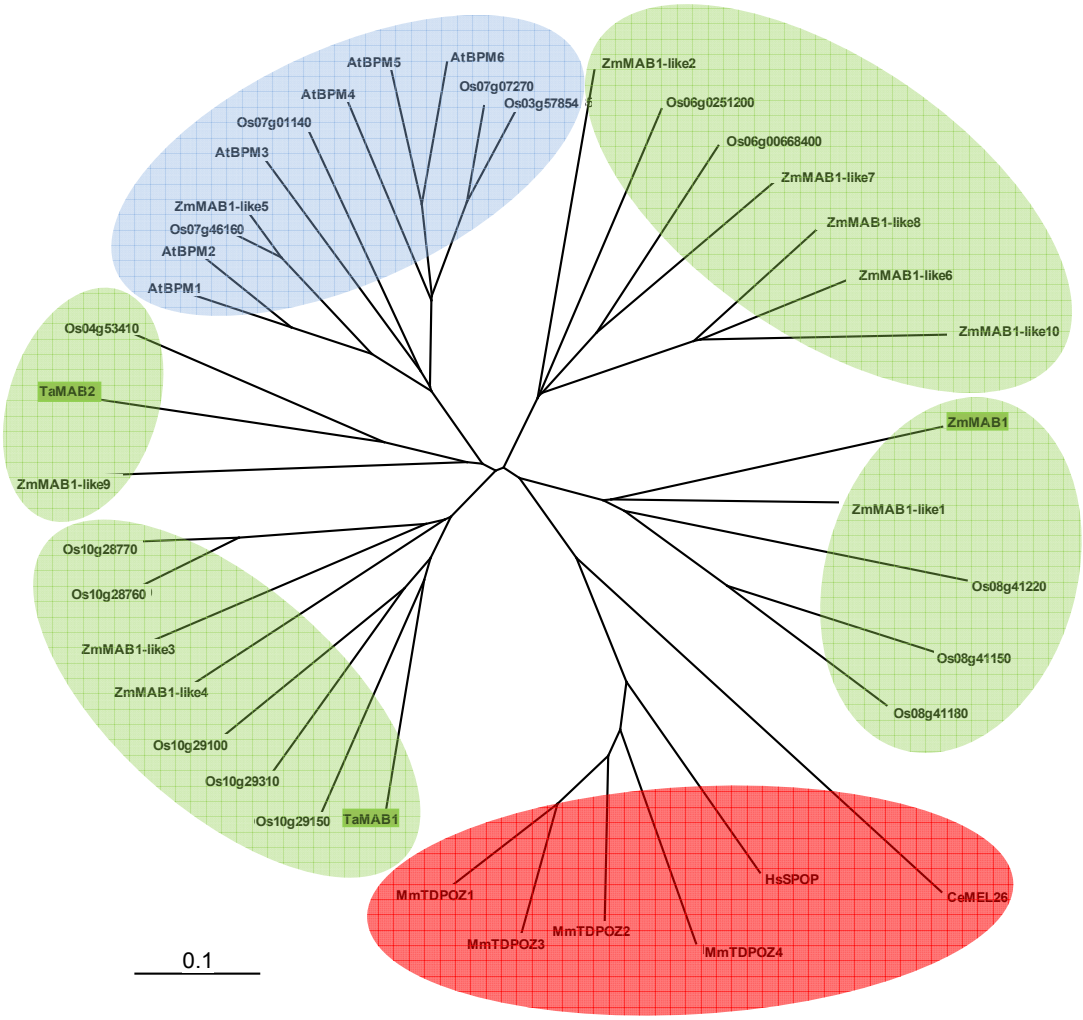


**Figure 4. Phylogenetic relationship of selected plant and animal MATH-BTB domain proteins.**
ZmMAB1 (GenBank acc. no. EU344973), TaMAB1 (GenBank acc. no. FJ515275), and TaMAB2 (GenBank acc. no. EU360467) (all boxed in green) described in this study were aligned with proteins from *Z. mays* (ZmMAB1-like1 to 11; GenBank acc. no. EU974550, BT037633, BT035122, EU974172, EU966879, EU965363, EU965105, BT037672, EU951851, BT038660, BT041703), from *O. sativa* (MSU rice locus identifiers at http://rice.plantbiology.msu.edu/: Os08g41220, Os08g41150, Os08g41180, Os04g53410, Os10g28760, Os10g28770, Os10g29150, Os10g29310, Os10g29100, Os03g57854, Os07g07270, Os07g46160, Os07g01140, Os06g14060, Os06g45730), from *A. thaliana* (AtBPM1 to 6; *Arabidopsis* Genome Initiative identifiers At5g19000, At3g06190, At2g39760, At3g03740, At5g21010, At3g43700), from *C. elegans* (CeMEL-26; GenBank acc. no. NP_492449), *H. sapiens* (HsSPOP; GenBank acc. no. NP_003554), and *M. musculus* (MmTDPOZ1 to 4; GenBank acc. no. NP_683751, NP_001007223, NP_997154, and NP_997155). Protein sequences were aligned by ClustalW and the tree was drawn by Tree-View. Branch lengths are proportional to phylogenetic distances and the scale bar represents 10% substitutions per site. The clade formed by human and animal MAB proteins is highlighted in red and the clade of conserved core plant MABs in light blue. Only four rice and one maize MAB belong to the core group. Monocotyledonous-specific MABs are divergent and grouped into four subclades (highlighted in light green).

**ZmMAB1- and TaMAB2-GFP fusion proteins accumulate in a polar manner around the nucleus and show partial co-localization with α-tubulin**

In order to analyze the subcellular localization of ZmMAB1 and TaMAB2, we have expressed GFP-fusion proteins under control of the strong and constitutive *ubiquitin* (*UBI*) promoter from maize (*ZmMAB1-GFP; TaMAB2-GFP*) in "Black Mexican Sweet" (BMS) maize suspension cells. In the majority of cells we detected the signals of both, TaMAB2-GFP (Fig. 5A to F) and ZmMAB1-GFP (Fig. 5G to I) accumulating unilateral around the nucleus. Staining of DNA with DAPI revealed that the fluorescent signals were positioned in the cytoplasm around the nuclear envelope but not inside the nucleus (Fig. 5C). We found this localization invariably present in over 100 transiently transformed cells analyzed by fluorescent microscopy or CLSM. The presence of additional small fluorescent spots located in some areas near the cell cortex was observed in around 50% of cells expressing ZmMAB1-GFP (Fig. 5H and I), and TaMAB2-GFP (Fig. 5J to L). CLSM analysis revealed the presence of a few small fluorescent spots in the nucleoplasm (Inset in Fig. 5L). Interestingly, we never observed any cytokinesis in *ZmMAB1-GFP* or *TaMAB2-GFP* expressing cells.

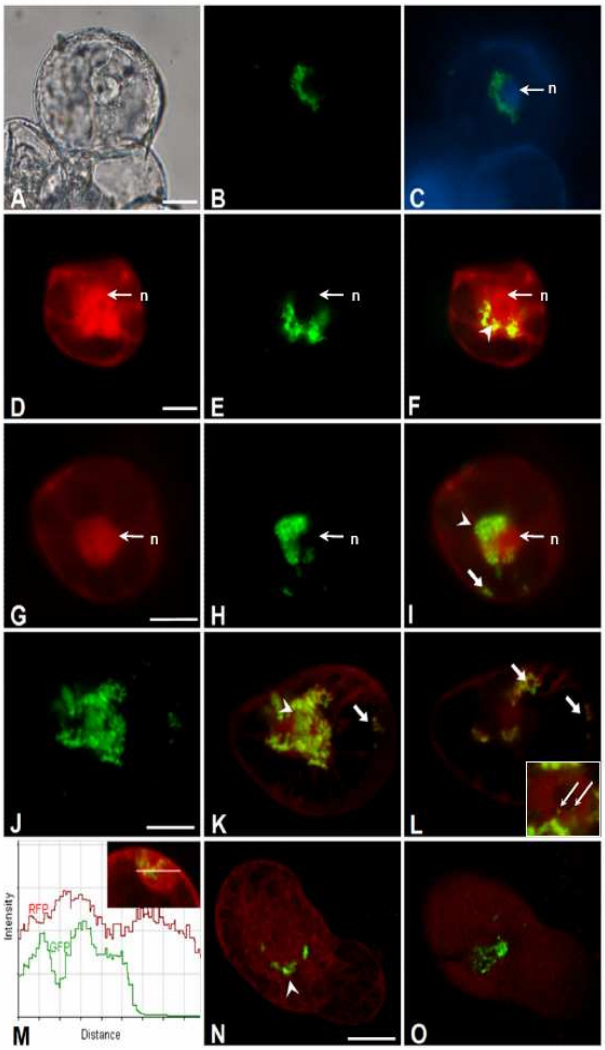


**Figure 5. Subcellular localisation of wheat and maize MAB-GFP fusion proteins in transiently transformed maize suspension cells**
(**A-C**) Bright field (A) and epifluorescence pictures (B, C) of a suspension cell transiently expressing *TaMAB2-GFP*. TaMAB2-GFP (green signal) accumulates asymmetrically around the nucleus (n), stained by DAPI (blue signal in C). (**D-F**) Epifluorescence microscopy of a cell co-expressing TUA6-mRFP1 (red signal in D) and TaMAB2-GFP (green signal in E). The overlay (F) shows partial co-localization of TaMAB2-GFP and TUA6-mRFP1 asymmetrically distributed around the nucleus (n) (yellow signal; arrowhead). (**G-I**) Epifluorescence images of a cell co-expressing TUA6-mRFP1 (red signal in G) and ZmMAB1-GFP (green signal in H). ZmMAB1-GFP accumulates at one side around the nucleus (n), where it co-localizes with TUA6-mRFP1 (arrowhead in I). ZmMAB1-GFP also appears at few sites near the cell cortex (arrow in I). (**J-L**) CLSM of a cell co-expressing TaMAB2-GFP (J) and TUA6-mRFP1 (red signal in K). The overlay of two individual optical sections (K, L) shows that TaMAB2-GFP partially co-localizes with tubulin around the nucleus (arrowhead) and near the plasma membrane (arrows). The inset in (L) shows a magnification of the nucleus, with two signals of TaMAB2-GFP visible in the nucleoplasm (arrows). (**M**) Intensity plots of red and green fluorescence at the nucleus (indicated by white line in inset) indicate partial co-localization of TaMAB2-GFP and TUA6-RFP near the nucleus. (**N-O**) Suspension cell before (N) and 90 min after (O) oryzalin treatment. Oryzalin-treated cell reveals a destroyed tubulin cytoskeleton, visible as weak and scattered signal of TUA6-RFP (O). The accumulation of TaMAB2-GFP around the nucleus (arrowhead in N) becomes more dispersed after oryzalin treatment (O). Scale bars: 40 µm.

Dual-color fluorescent imaging after co-transforming *TaMAB2-GFP* or *ZmMAB1-GFP* each with a construct for mRFP1-labelled α-Tubulin6 (*35Sp::TUA6-mRFP1*) revealed that signals of both TaMAB2-GFP and ZmMAB1-GFP partially co-localize with TUA6-mRFP1 in the region around the nucleus (arrowheads in Fig. 5F, I and K), and near the cell cortex (arrows in Fig. 5I, K and L). Transformation with *TUA6-mRFP1* alone revealed a strong red fluorescence of nuclei excluding nucleoli as well as red signals throughout the cytoplasm (Fig. 6A to C). However, accumulation of mRFP-labeled tubulin at the nuclear periphery was not as prominent as in cells co-transformed with *TaMAB2-GFP* or *ZmMAB1-GFP* (Fig. 6D to F). Intensity plots of co-localization experiments confirmed that fluorescent peaks of TUA6-mRFP1 and TaMAB2-GFP partially overlap (Fig. 5M). We treated co-transformed cells with the microtubule-depolymerizing herbicide oryzalin, to investigate the subcellular distribution of TaMAB2-GFP after disrupting the cytoskeleton. The complete depolymerization of TUA6-mRFP1 labeled microtubules was monitored in the course of a 90 min drug treatment (Fig. 5N and O). Concurrently, we observed a more dispersed fluorescence of the afore polar accumulating TaMAB2-GFP, together with the appearance of small spots distributed in the cytoplasm (Fig. 5N).

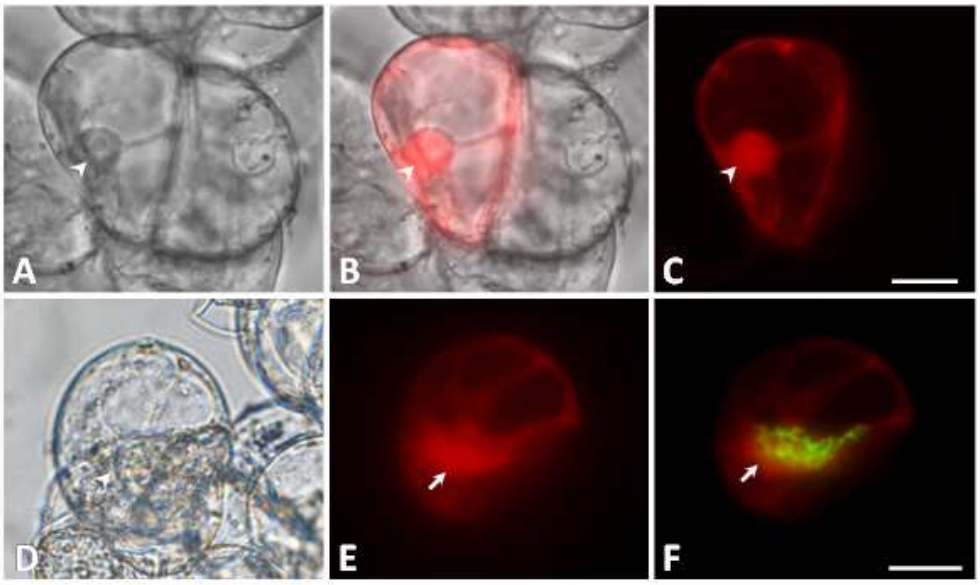


**Figure 6. Epifluorescence microscopy of transient transformed maize suspension cells expressing either TUA6-mRFP1 alone or co-expressing *TUA6-mRFP1* and *TaMAB2-GFP*.**
(**A-C**) Subcellular localization of TUA6-mRFP1 (red signal) in the nucleus (arrowhead), in transvacuolar cytoplasmic strands and in peripheral cytoplasm of a suspension cell expressing *TUA6-mRFP1*. (**D-F**) Subcellular localization of TUA6-mRFP1 (red signal) and TaMAB2-GFP in a maize suspension cell coexpressing *TUA6-mRFP1* and *TaMAB2-GFP*. Red fluorescence of TUA6-mRFP1 (E) is enriched at the nuclear surface (arrow), where it co-localizes with green fluorescence derived from TaMAB2-GFP (green signal in F). A, D: bright-field images; C, E: red fluorescence, only; B: overlay of bright-field image and image from red channel shown in (A) and (C), respectively; F: overlay of images from red channel (E) and green channel. Scale bars are 40 µm.

**The MATH domain of TaMAB2 mediates its polar accumulation around the nuclear envelope**

We analyzed the role of each the MATH and the BTB domain on the subcellular distribution of TaMAB2-GFP in transiently transformed maize cells by creating deletions of either the BTB domain (TaMAB2ΔBTB) or the MATH domain (TaMAB2ΔMATH). Removing the BTB domain did not provoke any significant change on subcellular protein localization (Fig. 7A). In 96% of analyzed cells (n = 50) we observed, similar to the full length TaMAB2-GFP, a strong signal of TaMAB2ΔBTB accumulating asymmetrically around the nucleus (Fig. 7A). A more evenly distributed and speckled fluorescence of TaMAB2ΔBTB was noticed in only 4% of the cells, which might resemble cells in which a cell-cycle related breakdown of the nuclear envelope (NE) took place (Fig. 8A, B). However, like in cells expressing the intact TaMAB2-GFP fusion protein, we never observed any cells completing mitotic cell division within a period of three days observation. In contrast, deletion of the MATH domain resulted in a completely different subcellular localization. In 82% of cells expressing TaMAB2ΔMATH (n = 47) we observed fluorescent patches of varying size, distributed throughout the cytoplasm (Fig. 7B, C). The remaining 18% of cells showed similar fluorescent patches of varying size throughout the cytoplasm but a significant amount of TaMAB2ΔMATH was located close to the nucleus (arrowheads in Fig. 7D and Fig. 8C, D). When we monitored the progress of the cell cycle within three days in either TaMAB2ΔBTB or TaMAB2ΔMATH expressing cells embedded in agarose, we found cell division only in cells expressing TaMAB2ΔMATH. A cell co-expressing TaMAB2ΔMATH and TUA6-mRFP1 at the beginning of a time series (t = 0h) is shown in Fig. 7D. Besides several fluorescent spots of TaMAB2ΔMATH in the cytoplasm, both fusion proteins co-localize close to the nucleus (arrowhead in Fig. 7D). Sixty five hours later (t = 65h) mitosis was completed and cytokinesis was observed (Fig. 7E). TUA6-mRFP1 was found in both, mother and daughter cell, being enriched in the region of phragmoplast/cell plate formation (arrow in Fig. 7E). In contrast, TaMAB2ΔMATH was exclusively present in the larger mother cell after asymmetric division (Fig. 7E; green channel and merged image), showing co-localization with TUA6-mRFP at the phragmoplast/new cell plate (arrows in Fig. 7E).

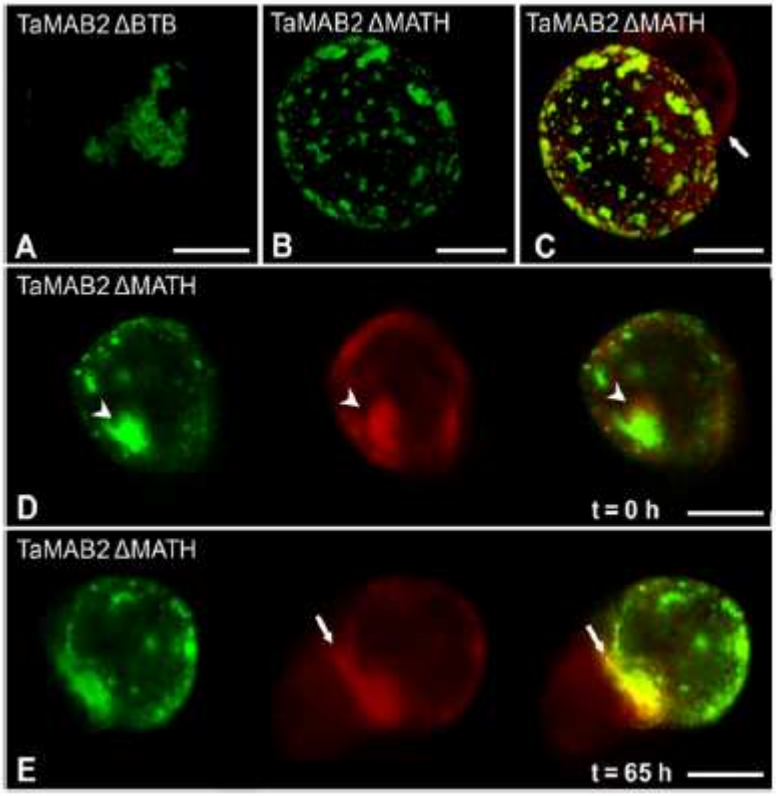


**Figure 7. Impact of MATH and BTB domain on the subcellular protein localization**.

Deletions of either the BTB domain (TaMAB2ΔBTB) or the MATH domain (TaMAB2ΔMATH) were transiently expressed in maize BMS cells. (**A**) TaMAB2ΔBTB expressing cell (CLSM). The truncated fusion protein still accumulates around the nucleus. **(B-C**) TaMAB2ΔMATH appears as green fluorescent patches of varying size present throughout the cytoplasm in one of the two daughter cells (B), while co-transformed TUA6-mRFP1 (red signal in C) can be detected in both cells (arrow points at smaller cell). (**D, E**) Monitoring of TaMAB2ΔMATH (green signal) and TUA6-mRFP1 (red signal) during cell division (epifluorescence microscopy). TaMAB2ΔMATH is distributed throughout the cytoplasm and accumulates to some extend together with TUA6-mRFP1 near the nucleus (arrowhead in D) by the time monitoring started (t=0). Sixty five hours later (t=65) the cell plate is formed (arrow in E). TaMAB2ΔMATH is inherited to the “old” daughter cell, while TUA6-RFP can be detected in both daughter cells. The yellow signal in the overlay shown in (E) indicates a co-localization of TaMAB2ΔMATH and TUA6-mRFP1 at the cell plate. Scale bars: 40 µm.

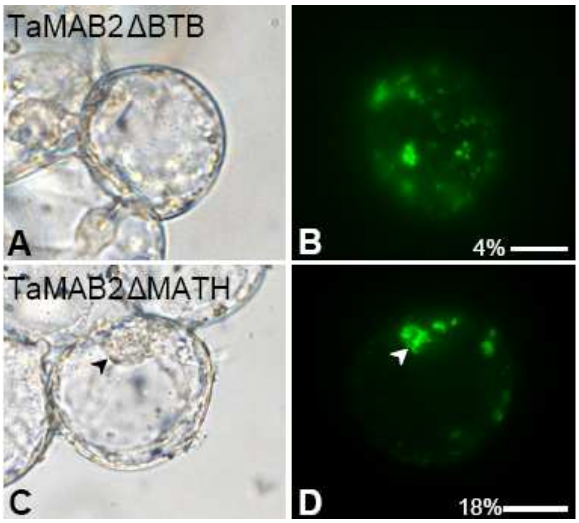


**Figure 8. Infrequent subcellular localization of TaMAB2ΔBTB and TaMAB2ΔMATH in transiently transformed maize BMS cells, analyzed by epifluorescence microscopy.**
(**A-B**) Subcellular localization of TaMAB2ΔBTB appears in 4% of all analyzed BMS cells as fluorescent speckles of varying size (B; green signals) which are distributed throughout the cytoplasm. Note that no nucleus was visible in this cell. The bulk (96%) of analyzed cells displayed a localization like shown in Figure 3 A.
(**C-D**) Subcellular localization of TaMAB2ΔMATH appears in 18% of all analyzed BMS cells as fluorescent speckles of varying size (D; green signals) which appear to be enriched near the nucleus (arrowhead). A fraction of 82% of the analyzed cells displayed a localization like shown in Figure 3 B. A, C: bright-field images; B, D: green fluorescence, only. Scale bars are 40 µm.

**TaMAB2-GFP is invariably inherited to the large basal cell after the first asymmetric division of Arabidopsis zygotes**

To monitor the subcellular distribution of a MAB protein in egg cells and to follow its localization in zygotes and during the first zygotic cell division, we have deposited heterologous TaMAB2-GFP in *Arabidopsis* egg cells by utilizing the egg cell specific *Arabidopsis* promoter *EC1.1* (Ingouff et al., 2008). As this promoter is switched off immediately after fertilization (S. Sprunck, unpublished), it allows tracking of egg cell deposited TaMAB2 in *Arabidopsis* embryo sacs before and after fertilization (Fig. 9). Isolated *Arabidopsis* ovules were counterstained with propidium iodide (PI; red fluorescence) to better visualize nuclei and cell boundaries of embryo sac cells and embryos. Similar to our data reported for transient over-expression analyses in maize BMS cells, the strongest fluorescent signal of TaMAB2-GFP appeared unilateral near the nucleus of the *Arabidopsis* egg cell (Fig. 9A and B). In addition, some smaller fluorescent spots were detected inside the egg cell nucleus and at the micropylar egg cell cortex (arrows in Fig. 9A). A magnification of the egg cell nucleus shown in Figure 4A reveals that the discrete spot of TaMAB2-GFP is located in the nucleoplasm (arrow in Fig. 9B).

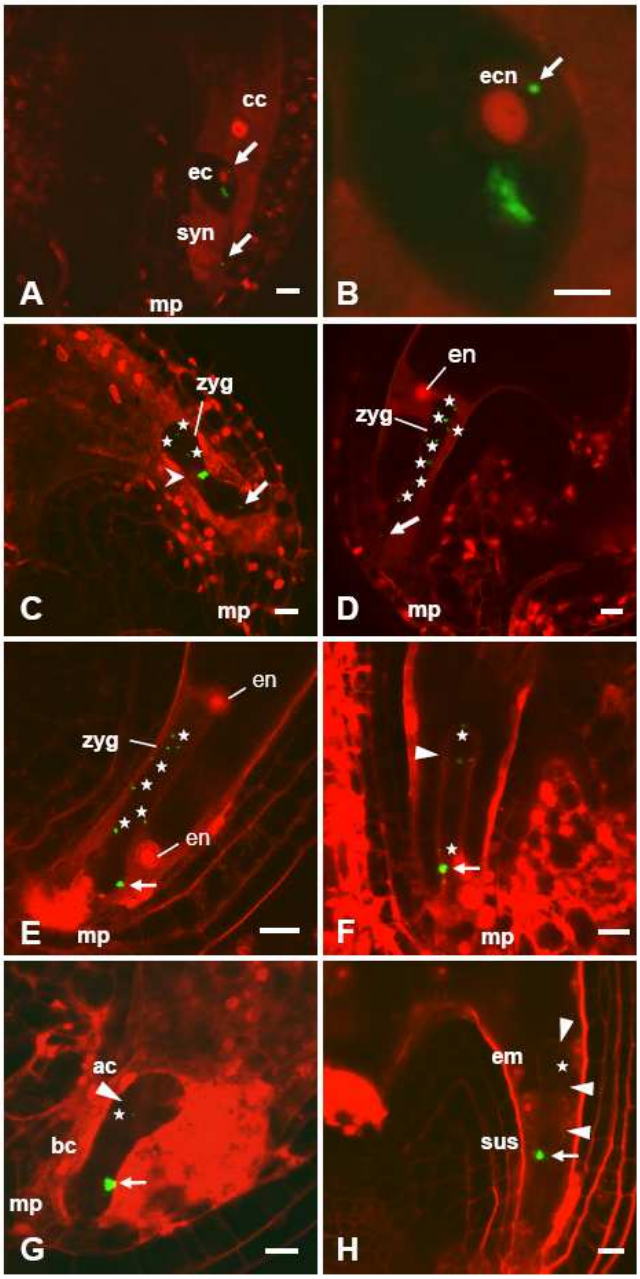


**Figure 9. Localization and inheritance of egg cell deposited TaMAB2-GFP during early embryogenesis of *Arabidopsis thaliana***

CLSM analysis of ovules from *EC1p::TaMAB2* expressing plants before and after fertilization, counterstained with propidium iodide. (**A, B**) In unfertilized ovules, a major fraction of TaMAB2-GFP (green signal) is attached to one side of the egg cell nucleus (ecn). Two small fluorescent spots (arrows in A) are located at the micropylar egg cell boundary and in the nucleoplasm, respectively. (B) is a magnification of the nucleus shown in (A). (**C**) In early zygotes (zyg), TaMAB2-GFP keeps its position near the nucleus (arrowhead) which moves towards the center.

Some small fluorescent spots appear in the upper part (asterisks) and one signal is visible at the micropylar pole of the zygote (arrow). (**D, E**) Before first zygotic division, a larger number of tiny fluorescent spots are visible throughout the zygote (asterisks). Some accumulation of TaMAB2-GFP becomes visible at the micropylar pole of the zygote (arrow in E). (**F**) Shortly before first zygotic division the micropylar fraction of TaMAB2-GFP (arrow) increased and several small fluorescent spots appear to locate at the future cell division plane (triangle). (**G**) In the 2-celled stage the bulk of TaMAB2-GFP becomes apparent in the basal cell (bc) but not in the small apical cell (ac). One small fluorescent spots (asterisk) is visible near the cell division plane (triangle). (**H**) In the 4-celled stage TaMAB2-GFP is mainly visible in the large basal cell of the suspensor (sus). One very small fluorescent spots (asterisk) can be found in the embryo (em). Triangles in (H) indicate cell division planes. ac: apical cell; bc: basal cell; cc: central cell; ec: egg cell; em: embryo; en: endosperm nucleus; mp: micropylar pole; sus: suspensor; syn: synergid. Each picture shows a stack of up to five optical sections of 0.38 to 0.53 µm each. Scale bars: 10 µm (A, C, D to F) or 5 µm (B).

In early zygotes the nucleus typically moves from the chalazal position towards the center of the cell (arrowhead in Fig. 9C), together with the polar attached signal of TaMAB2-GFP. At this time a couple of additional small fluorescent spots become visible in the apical (chalazal) moiety of the zygote (asterisks in Fig. 9C) while the micropylar signal of TaMAB2-GFP remains unchanged (arrow in Fig. 9C). Strikingly, the afore nucleus-attached accumulation of TaMAB2-GFP disappears at the beginning of mitosis, when the nuclear envelope disintegrates. Instead, multiple small fluorescent spots were visible throughout the zygote (asterisks in Fig. 9D) and the micropylar-most signal appeared to become stronger in later zygotes (arrow in Fig. 9E). The bulk of TaMAB1-GFP was detectable at the micropylar pole of the zygote during cytokinesis (Fig. 9F). Moreover, the small fluorescent spots appeared to arrange in a region corresponding to the later cell division plane (arrowhead in Fig. 9F, G). After first zygotic division, we found the bulk of TaMAB2-GFP in the large basal cell, where it accumulates at the micropylar pole (Fig. 9G). Only some tiny green spots were eventually present in the small apical cell (not visible in Fig. 9G). This pattern of inheritance was invariably present in all 2-celled stages analyzed. Also in subsequent divisions the bulk of TaMAB2-GFP was inherited to the basal cell of the suspensor (Fig. 9H).

**TaMAB2 is able to form homodimers and to interact with Arabidopsis AtCUL3a**

It was previously shown that members of the *Arabidopsis* and rice MATH-BTB protein family can interact with CUL3 proteins (Gingerich et al., 2005, 2007) and thus likely act as substrate-specific adapters in CUL3-based E3 ligases. Moreover, the BTB domain is known to mediate the assembly of homo- and heterodimers of several BTB domain containing proteins (Perez-Torrado et al., 2006; Weber et al., 2005). To investigate the interaction of TaMAB2 with a CUL3 protein and to study the possible formation of homodimers, we performed directed yeast two-hybrid (Y2H) assays with full length protein sequences of TaMAB2 and *Arabidopsis* Cullin 3a. As shown in Figure 10, MAB2 from wheat was not only

able to form homodimers, but is also able to interact with *Arabidopsis* CUL3a. The latter interaction was relatively weak when co-transformed yeast was grown on selective medium without histidine. However, the positive β-galactosidase assay verified the interaction between TaMAB2 and AtCUL3a.

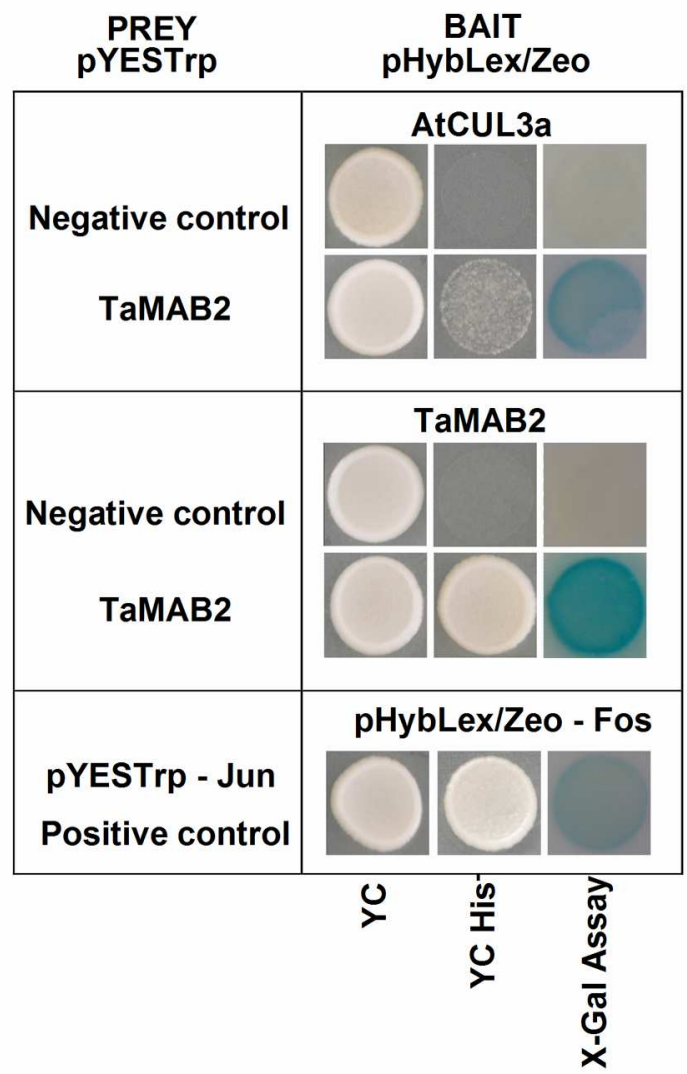


**Figure 10. TaMAB2 can form homodimers and interacts with AtCUL3a.**
Yeast two-hybrid interaction studies using TaMAB2 as a prey and either AtCUL3a or TaMAB2 as a bait show that TaMAB2 can both interact with AtCUL3a (top panel) or assemble as homodimer (middle panel). *pYESTrp* and *pHybLex/Zeo* were used as prey and bait vectors in a lexA-based yeast two hybrid system, together with the yeast reporter strain L40. pYESTrp-Jun and pHybLex/Zeo-Fos were used as a positive controls for bait and prey, respectively (bottom panel). Non-specific activation of the bait plasmid was tested by co-transforming each TaMAB2 or AtCUL3a as bait with empty pYESTrp (negative control). YC: minimal medium w/o tryptophane, supplemented with Zeocin™; YCHis-: YC w/o Tryp and His; X-Gal- Assay: β-galactosidase filter assay.

**RNAi silencing of ZmMAB1 impairs positioning and further division of nuclei during early megagametogenesis in maize**

To analyze the function of the *MAB*s we used RNA interference (RNAi) to down-regulate *TaMAB2* and *ZmMAB1* in transgenic wheat and maize plants, respectively. While we did not obtain any transgenic wheat plant, we were able to generate 13 transgenic maize lines for which integration pattern and transgene expression was confirmed. Based on the strength of transgene expression we selected two independent *ZmMAB1*-RNAi lines (lines No. 1149 and 143) containing four transgene integrations for detailed functional analysis. Cobs of self-pollinated T0 plants and following T1 generations showed a significantly reduced seed set,

compared to self-pollinated wild-type cobs (Fig. 11). Closer examination (arrowheads in Fig. 11) revealed that the observed developmental arrest was caused before or during fertilization.

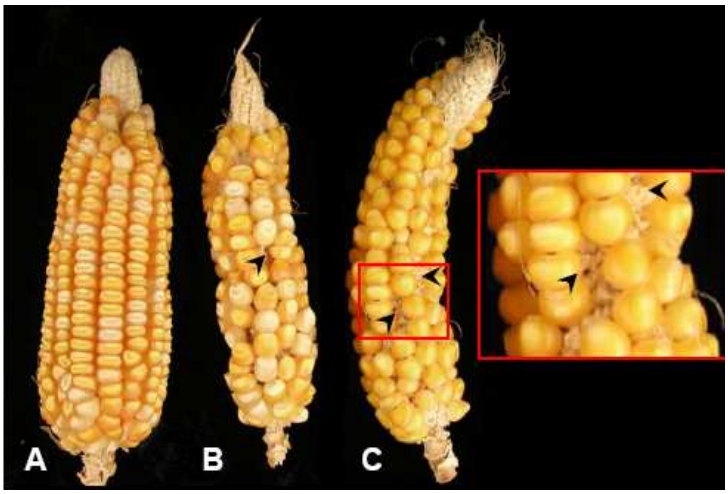


**Figure 11. Seed set of a mature wild type maize cob compared with seed set of cobs from two independent *ZmMAB1*-RNAi mutant lines.**
(**A**) Cob of a wild type maize plant 6 weeks after self-pollination. (**B** and **C**) Cobs of two independent *ZmMAB1*-RNAi mutant lines (line 1149 and line 143, respectively) 6 weeks after self-pollination. Arrowheads point towards sterile and non-developed kernels, which constituted approximately 40% of all kernels. The inset shows an enlargement of the red box indicated in (C) to visualize that kernel development was not initiated (arrowheads), suggesting a developmental arrest before or during fertilization but not at later stages during seed development.

To investigate the effect of *ZmMAB1* RNAi silencing on the maize female gametophyte development in more detail, we analyzed ovules from both transgenic offspring and wild type plants by Confocal Laser Scanning Microscopy (CLSM). According to Huang and Sheridan (1994), the silk length of immature maize cobs was used as external morphological feature to determine the corresponding stages of the developing maize embryo sacs. In wild type (wt) ovules, a single enlarged hypodermal cell develops into an archeosporial cell, which differentiates into an asymmetric, cup-shaped megaspore mother cell (MMC) (Fig. 12). During megasporogenesis the MMC undergoes meiotic divisions (Fig. 12B to D) and forms a linear tetrad of haploid megaspores (Fig. 12E). While the three micropylar-most megaspores degenerate, the chalazal-most megaspore develops into the functional megaspore (Fig. 12F), corresponding to the female gametophyte stage FG1 of *Arabidopsis* (Christensen et al., 1997). The functional megaspore undergoes three rounds of free-nuclear mitosis. After first division both daughter nuclei appear at opposite poles of the elongated embryo sac, separated by a central vacuole (FG2/3; Fig. 12G). The second and third division occurs synchronously resulting in an eight-nucleated embryo sac (FG4/5; Fig. 12H, I). Before cellularization, one nucleus from each pole migrates toward the center of the embryo sac to

become the polar nuclei of the central cell (FG6, Fig. 12J). After cellularization and cell specification, the egg apparatus is visible at the micropylar end of the embryo sac, comprising the egg cell flanked by two synergids (Fig. 12K). The polar nuclei remain unfused, while the three antipodals at the chalazal pole of the embryo sac proliferate and form a cluster of about 20–40 cells (Fig. 12K). In ovules of *ZmMAB1*-RNAi plants we found a total of 37% (line 143) to 41% (line 1149) of the analyzed embryo sacs to be either arrested during early FG stages, or to be collapsed (Fig. 12L to P; Tab. 1). In contrast to wild type, where 96% of all analyzed embryo sacs were fully developed, a ratio of about 48% affected embryo sacs would be expected in case of a full knock-out in heterozygous offspring of *ZmMAB1*-RNAi lines. However, RNAi approaches are rarely 100% effective in plants (Smith et al., 2000). A minor percentage of the arrested ovules revealed a block of mitotic progression at stage FG1 (Fig. 12L and 12M; Tab. 1). For another 6% (line 1149) to 22% (line 143) of ovules the developmental arrest could not be assessed, as the embryo sac was collapsed (Fig. 12P). However, the major fraction of ovules (11% for line 143; 25% for line 1149) offered embryo sacs arrested during or after the first nuclear division. Strikingly, either the formation of two distinct daughter nuclei was disturbed (Fig. 12O), or two distinct nuclei were formed but were located in close vicinity to each other (Fig. 12N), indicating a failure in proper assembly and positioning of the first mitotic spindle.

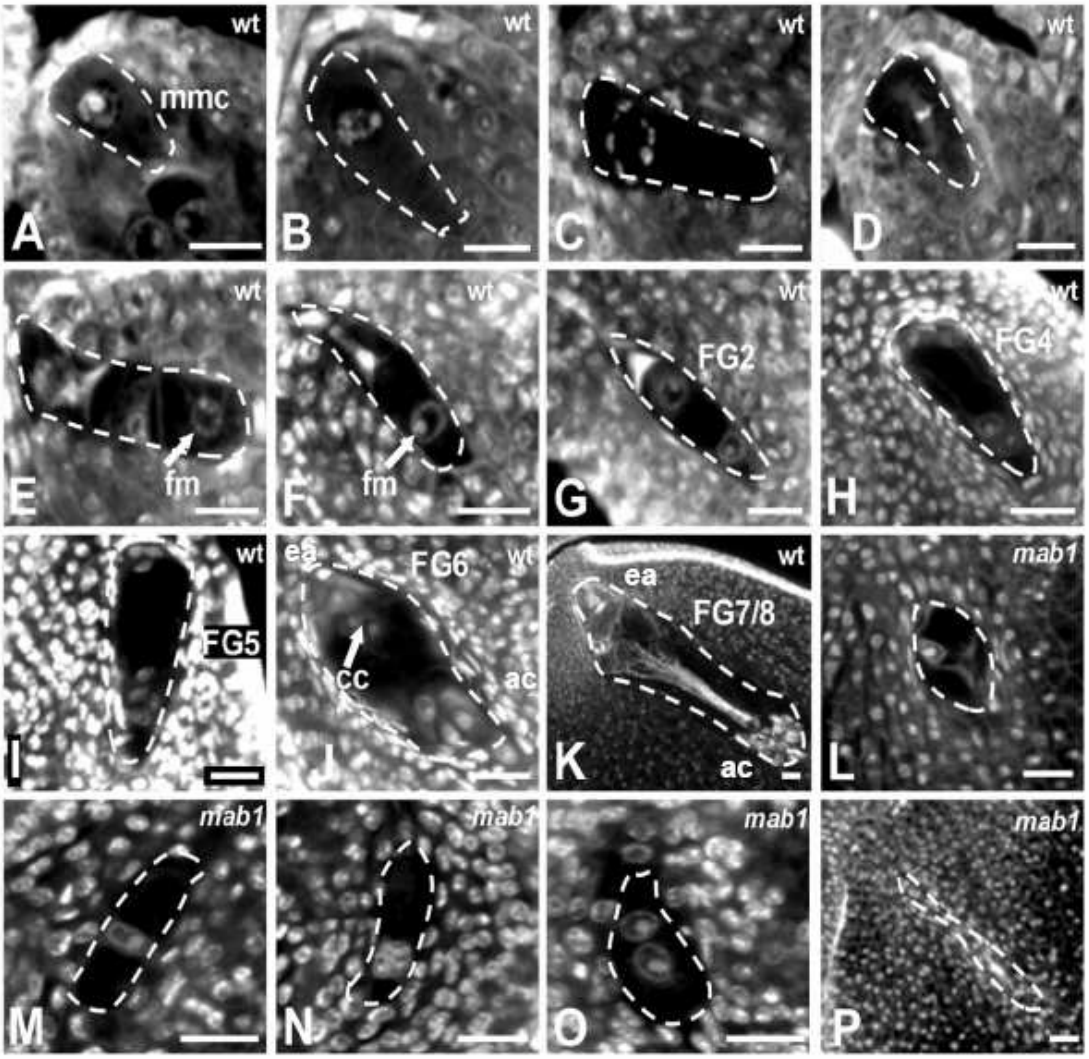


**Figure 12. CLSM analysis of megasporogenesis and megagametogenesis in wild type and *ZmMAB1*-RNAi lines.**

(**A-D**) First meiotic division of wild type (wt) megaspore mother cell (mmc) (A) Megaspore mother cell; (B) Zygotene; (C) Diakinesis; (D) Metaphase. (**E**, **F**) Linear tetrad of four megaspores. Arrows mark large nucleus of the functional megaspore (fm), the three micropylar-most megaspores start to degenerate (F). (**G**) Two-nucleate stage (FG2) of megagametogenesis. (**H**) Four-nucleate embryo sac (FG4). (**I**) Eight-nucleate stage (FG5), before the two polar nuclei migrate towards each other. (**J**) Eight-nucleate stage after cellularization (FG6). Antipodal cells (ac) are positioned at the chalazal end, egg and synergids form the egg apparatus (ea) at the micropylar end. The two polar nuclei of the central cell (cc) are near the egg apparatus. (**K**) Mature embryo sac (FG7/8). Egg cell and synergids are fully differentiated. Polar nuclei are not in focus. Antipodal cells (ac) form a cluster of cells. (**L**, **M**) Arrested embryo sac development of *ZmMAB1*-RNAi line (*mab1*) at FG1, arrested immediately after meiosis. (**N**; **O**) *ZmMAB1*-RNAi embryo sacs, arrested after first round of free–nuclear mitosis. Nuclei were either closely attached to each other (N) or in close vicinity (O; compare with G). (**P**) Collapsed *ZmMAB1*-RNAi embryo sac. Scale bars: 20 µm.

**Table 1. Mutant female gametophyte (FG) phenotypes of heterozygous *ZmMAB1*-RNAi silencing lines**. Ovules were examined by CLSM after periodic acid-Schiff staining. Development of maternal tissues was normal in all cases studied. Wild type (wt) FGs were analyzed as controls.

| **Position of nuclei during FG development arrest (in%)** | | | | | | |
|---|---|---|---|---|---|---|
| | | one nucleus | two nuclei attached | uncompleted nuclear migration | collapsed embryo sac | Fully developed FG |
| **Genotype of mother plant** | **n[1]** | 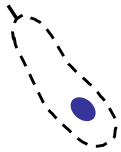 | 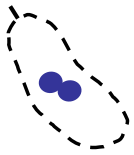 | 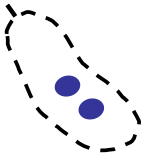 | | 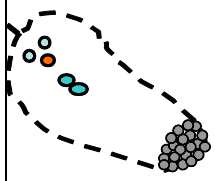 |
| Line 1149 | 80 | 10 | 8 | 17 | 6 | 59 |
| Line 143 | 55 | 4 | 4 | 7 | 22 | 63 |
| wt | 63 | - | - | - | 4 | 96 |

n[1]: total number of ovules analyzed by CLSM.

## DISCUSSION

Proteins with MATH-BTB domain architecture have been identified in a number of eukaryotes, except yeast (Gingerich et al., 2007; Huang et al., 2004; Perez-Torrado et al., 2006; Stogios et al., 2005). While only one MATH-BTB protein is present in the *Drosophila melanogaster* genome (Stogios et al., 2005), a large and divergent group of 47 MATH-BTB proteins was found in *C. elegans* (Thomas, 2006). Dicotyledonous plant species such as *Arabidopsis thaliana* possess only a small, ancient core group of MATH-BTB proteins, while an expanded and highly divergent group of MATH-BTB proteins was recently reported in rice, which appears to have evolved in addition to a core group of four more conserved MATH-BTB proteins (Gingerich et al., 2007). Unlike the more or less ubiquitously expressed core group loci of *Arabidopsis* (Weber et al., 2005) and rice, the expanded rice *MATH-BTB*s are less well represented in rice expression databases suggesting that they are either expressed at lower levels, or in highly temporal or tissue specific manners (Gingerich et al., 2007). This is consistent with our finding that the three female gametophyte-specific MATH-BTB proteins from wheat and maize (TaMAB1, TaMAB2, and ZmMAB1) cluster into clades formed by the expanded rice group, but not into the core group of plant MATH-BTBs. It has been suggested that the large expansion and diversification of MATH-BTB proteins in the

genomes of *Caenorhabditis elegans* and rice has evolved as part of an innate pathogen defence system (Thomas, 2006; Gingerich et al., 2007). However, the high abundance of the *MAB* transcripts in egg cells and zygotes of wheat and maize imply an important role for the corresponding proteins in female gametophyte development, fertilization, and/or early embryogenesis. Interestingly, also one mouse MATH-BTB gene (*Tdpoz1*) was found to be temporary transcribed in unfertilized eggs and early embryos while others (*Tdpoz3 to -5*) are strongly upregulated in 2-celled pro-embryos (Choo et al., 2001; Huang et al., 2004). However, a function has not been assigned to any of these genes.

Several studies have confirmed that yeast, animal, and plant BTB-domain containing proteins can interact with Cullin 3-based E3 ligases via their BTB domain (reviewed by Pintard et al., 2004), and we approved that also TaMAB2 is able to interact with CUL3 in direct yeast two-hybrid interaction assays. This interaction is likely to be mediated by the BTB domain, as we found all essential amino acid residues, shown to be important for BTB-CUL3 interaction (Zheng et al., 2002; Geyer et al., 2003; Xu et al., 2003; Weber et al., 2005), to be conserved in wheat and maize MABs. Additional protein motifs present in BTB proteins, such as the MATH domain, are thought to serve as substrate binding domains, responsible for targeting specific proteins to the CUL3 ligase complex and thus towards the ubiquitin-dependent degradation by the 26S proteasome (Perez-Torrado et al., 2006). Substrate specificity is therefore likely to be reflected by the much lower conservation of the individual MATH domains compared to the BTB domains (our results; Thomas, 2006; Gingerich et al., 2007).

Maternal Effect Lethal (MEL-26), a well-characterized substrate-specific MATH-BTB adapter of a CUL3-based E3 ligase in *C. elegans* is known to act as a regulator of microtubule dynamics, spindle assembly, and cytokinesis via interactions with at least three different proteins: During meiosis-to-mitosis-transition of the nematode germline the microtubule-severing AAA-ATPase katanin or MEI-1 (defective in meiosis 1), required for the short acentrosomal meiotic spindle assembly, has to be specifically degraded to guarantee correct mitotic spindle formation (Pintard et al., 2003; Xu et al., 2003). The AAA-ATPase FIGL-1 (fidgetin-like 1) controls mitotic progression and must be targeted to degradation during the meiotic stages in the gonad (Luke-Glaser et al., 2007). The third interaction partner of MEL-26 is POD-1 (Polarity and osmotic sensitivity defective 1), a cortically localized F-actin binding protein locating MEL-26 to the cell cortex where it promotes cytokinesis in an CUL3-independent but yet unknown mechanism (Luke-Glaser et al., 2005). However, other MATH-BTB proteins target nuclear localized proteins such as transcription regulators, a histone variant, and a Polycomb-group protein for CUL3 based degradation (Furukawa et al., 2003; Hernández-Muñoz et al., 2005; Kwon et al., 2006; Zhang et al., 2006). Although we do not

yet know the substrate(s) for TaMAB1, TaMAB2, and ZmMAB1, the described phenotypes of *mab1* in maize female gametophytes and of TaMAB2 or ZmMAB1 over-expressing cells strongly point towards factors regulating the microtubular organization during mitosis. It is known that a dynamic microtubular organization is essential for both the nuclear division and nuclear positioning during female gametophyte development in plants (Huang and Sheridan, 1994; 1996; Pastuglia et al., 2006). Moreover, a recent study on the *Regulatory Particle 5a* (*RPT5a*) of *Arabidopsis* points towards the importance of the ubiquitin/26S proteasome for mitotic divisions during male and female gametogenesis (Gallois et al., 2009). The discovery of female-gametophyte specific MATH-BTB proteins as substrate adaptors for the CUL3 ligase complex together with the observed phenotype of aberrant nuclear positioning and lack of mitotic progression in *mab1* female gametophytes indicates a connection between the 26S proteasome and the regulation of microtubule organization. The slightly different expression pattern of the FG/zygote expressed *ZmMAB1*, the egg cell specific *TaMAB1*, and the zygotic-induced *TaMAB2* makes it likely that the encoded proteins target different or multiple substrates involved in mitotic progression. Moreover, the observed nuclear localization of MAB-GFPs points towards the possibility that nuclear protein(s) are additional targets. The major goal of our future studies will therefore be the identification of MAB substrate(s), to elucidate the regulation of microtubule organization during asymmetric gametic and zygotic mitosis by targeted ubiquitin-mediated degradation.

Higher plants and vertebrates undergo, in contrast to yeast, open mitosis during which the nuclear envelope completely dissolves and reassembles. However, contrary to the animal centrosomes, in plants the nuclear envelope acts as an MTOC during G2 phase of mitosis, and a prospindle is formed before nuclear envelope breakdown (Canaday et al., 2000). In human cells the dynamic association of the proteasome with the centrosome has been described (Wigley et al., 1999; Wójcik and DeMartino, 2003), and the accumulation of MAB-GFP fusion proteins around the nuclear envelope and at some areas of the cell cortex strongly resembles described microtubule nucleation sites in plants (Erhardt and Shaw, 2006). Still, under conditions of impaired proteolysis and in case of increased levels of damaged or misfolded proteins the “proteolytic centers” around centrosomes have been reported to even enlarge by recruiting cytosolic pools of the proteasome and associated regulatory proteins (Wójcik and DeMartino, 2003). Therefore, the polar localization of MAB-GFPs around the nuclei of over-expressing suspension cells might reflect the accumulation of detrimental fusion protein targeted for degradation, which in consequence might interfere with mitosis. However, a deletion of the MATH domain enabled the over-expressing cells to divide, pointing to the possibility that the MATH domain of TaMAB2 targets a substrate necessary for mitotic progression to the plant MTOC-associated proteasome for degradation.

*Arabidopsis* egg cells ectopically expressing TaMAB2-GFP did not show any negative effect on cell division after fertilization, suggesting a lack of TaMAB2-specific substrates in dicotyledonous plant species or in their female gametes.

However, the observed location of plant MABs reflects the close vicinity of the ubiquitination machinery with both the 26S proteasome and the plant MTOCs. This close vicinity might play an important role in the rapid on-site degradation of proteins, e.g. involved in the organization of microtubules. Moreover, recent experiments with dividing mammalian cells and *Drosophila* embryos indicate that proteins specifically targeted for proteasomal degradation are inherited preferentially by one mitotic daughter cell (Fuentealba et al., 2008). The unequal distribution of polyubiquitinated proteins appears to be achieved by the asymmetric inheritance of peripheral centrosomal proteins, when centrioles separate and migrate to opposite poles of the cell (Fuentealba et al., 2008; Macara and Mili, 2008). Analogous to these findings we found egg cell deposited TaMAB2-GFP to be always inherited to the large basal cell after first asymmetric zygotic division in *Arabidopsis thaliana*, but never to the small apical cell. Although little is known about the unequal inheritance of centrosomes/MTOCs, pericentrosomal material/proteasomes, and of proteins specifically targeted for degradation it is tempting to speculate that our findings represent a general mechanism used by both animal and plant cells not only to cleanse themselves of proteins destined for degradation at cell division, but to regulate, for example, the cellular status, cell cycle progression, establishment of asymmetry and thus cell specification.

## EXPERIMENTAL PROCEDURES

### Plant material and isolation of cells from maize and wheat female gametophytes

Commercial bread wheat cultivar Florida (*Triticum aestivum* L.) served as a donor for egg cell, zygote, and embryo isolation. Plants were cultivated in the greenhouse with a supplementary 16 h of artificial light (24,000 lx) per day, and day/night temperatures of 18/14°C. Maize plants of hybrid line A188 x H99 and transgenic plants were grown under standard greenhouse conditions at 26°C with a 16 h supplementary light and a relative air humidity of about 60%.

Single embryo sac cells of maize were isolated according to Kranz et al. (1991). Maize zygotes were isolated according to Cordts et al. (2001), except that the maize ears were placed on wet filter paper. Egg cells, zygotes and pro-embryos of wheat were isolated mechanically like described previously (Sprunck et al., 2005), except that the wheat zygotes and 2-celled pro-embryos were isolated *in vivo*, either 20 to 24 hours or 24 to 28 hours after hand-pollination of emasculated spikes. The “Black Mexican Sweet” (BMS) maize cell

suspension was subcultured according to Kirihara (1994) every 3 to 4 days in liquid MS2D medium (Murashige and Skoog medium containing 2 mg/l 2,4-D), and kept in the dark with shaking at 60-70 rpm and 26°C.

**DNA and RNA Extraction, RT-PCR, and Southern blot analysis**

Total RNA isolation from different tissues of wheat or maize with TRIzol® (Invitrogen), as well as the mRNA isolation procedure from single egg cell, synergid, three zygotes or three pro-embryos using the Dynabeads® mRNA DIRECT™ Micro kit (Invitrogen), was performed as described previously (Sprunck et al., 2005). Details of RT-PCR, standard PCR, DNA and RNA extraction, and Southern analysis are given in Supplemental Material and Methods, online.

**Transient transformation of maize BMS cells**

“Black mexican sweet” (BMS) maize cells were transiently transformed by particle bombardment using plasmids encoding GFP- and/or mRFP1-fusion proteins under the control of constitutive active promoters (detailed description of constructs is given in Supplemental Experimental Procedures). For preparation of plasmid-coated gold particles 5-10 µg of plasmid solution (1µg/µl) was added to 50 µl aliquots of a 60mg/ml gold suspension (0.4-1.2 µm, Heraeus) and prepared as described previously (Dresselhaus et al., 2006). One to two hours before bombardment the cells were filtered through a sterile 100µm nylon mesh to remove larger cell clusters. Cells were collected by filtering through a 50µm nylon mesh, and spread as a thin layer onto 35 mm petri dishes with solid MS2D medium (Kirihara et al, 1994). Cells were bombarded with 7 µl aliquots of plasmid-coated gold particles, using the particle delivery system PDS1000/He (BioRad), 1,100-psi rupture discs, a partial vacuum of 28 inch Hg, and a 6 cm target distance. After transformation, plates were incubated overnight in the dark at 26°C. At least 4 hours before microscopic observation, the cells were rinsed from the plates into 35 mm petri dishes using liquid MS2D medium and placed in the dark with shaking (60 rpm, 26°C). For microscopy, 100 µl of suspension culture was transferred onto cover slips fixed to metal slides provided with an opening (∅ 20 mm) in the center. DNA was stained by adding DAPI (4′,6-Diamidino-2-phenylindol) at a final concentration of 0.2-0.3 µg/ml. Oryzalin was added at a final concentration of 10 µM, a concentration shown to be sufficient to depolymerize microtubule arrays in BY-2 cells (Van Damme et al., 2004). BMS cells expressing fluorescent fusion proteins were monitored before and 60 to 90 minutes after the addition of oryzalin. To monitor subcellular protein localization during the cell cycle, individual cells or cell clusters were transferred carefully into a liquid drop of 0.7% low-melting agarose placed in a small petri dish. After solidification, the droplets were covered

with 7 ml of BMS cell suspension, for growth conditioning. Pictures were captured in 12 hours intervals to avoid overexposure of cells to UV light.

**Generation of transgenic plants**

*Arabidopsis* plants (ecotype Col-0) were transformed by the “floral dip” method (Clough and Bent, 1998), using the *Agrobacterium* strain GV3101 (pMP90RK). Seeds of transformed plants were sown on soil, stratified at 4°C for 2 days, and germinated at 20°C at 8 h light/16 h dark intervals. Immediately after germination BASTA® resistant seedlings were selected by spraying three times with 200 mg/l glufosinate ammonium (BASTA®; Bayer Crop Science) supplemented with 0.1 % Tween 20. After 3 weeks, plantlets were transferred into a growth chamber with 20°C and long day conditions (16 h light, 8 h dark).

Immature embryos of the maize hybrid line (A188xH99) were isolated under sterile conditions, 11-13 days after pollination (DAP). Culture, osmotic pre-treatment and particle bombardment of explants was performed according to Brettschneider et al. (1997) with the exception that 0.6% phytagel (Sigma, Germany) was used instead of agarose. For co-transformation with the selection marker phosphinothricin acetyltransferase (PAT), a plasmid mixture of 3 µg Zm*MAB1-RNAi* and 2 µg *35Sp::PAT* (for generation of constructs see Supplemental Experimental Procedures, online) was precipitated onto gold particles (1 µm; BioRad), like described (Becker et al., 1994). Subsequent culture and selection of PAT-resistant maize explants was performed like described (Brettschneider et al., 1997). One week after transferring into soil the regenerants were sprayed two times within one week with an aqueous solution of 250mg/l BASTA®, added with 0.1% Tween 20.

**Preparation of *Arabidopsis* and maize ovules for microscopic analyses**

For CLSM analysis of *Arabidopsis* ovules, mature pistils from emasculated flowers or young siliques were prepared on a glass slide in a drop of freshly prepared aqueous propidium-iodide solution (100 µg/ml) using fine hypodermic needles. Carpels were cut lengthwise on both sides of the septum and removed, leaving ovules attached to the septum, which was then additionally split into two strings. After carefully placing the cover slip, unfertilized ovules were analyzed immediately, while preparations of siliques were left in a humid chamber for 10-30 min before examination.

Defined stages of immature and mature maize embryo sacs were identified according to the silk length of the ear, which can be used as a morphological feature with respect to the corresponding stage of FG development (Huang and Sheridan, 1994). At a silk length of 0 - 0.5 mm we found the corresponding ovules to contain either megaspore mother cell in meiosis or four megaspores. The functional megaspore during the first mitotic division

(female gametophyte stage 1; FG1) corresponded to a silk length in the range of 0.5 - 1 mm. Two-nucleate (FG2) and four-nucleate (FG4) embryo sacs were found in ovules with a silk length of 1 - 2.5 mm. In the later stages (silk length ranging from 2.5 - 7 mm), most ovules contained eight-nucleate or mature embryo sacs. For phenotypical analysis of maize embryo sacs, immature and mature cobs were harvested and treated by fixing/clearing followed by a Kasten's fluorescent periodic acid-Schiff staining, according Vollbrecht and Hake (1995), with the exceptions that each hydration and dehydration step was increased to 30 min, and that the ears were dissected after clearing with methyl salicylate (Young, et al, 1979). Samples were mounted in methyl salicylate on glass slides under a cover slip and analyzed by CLSM.

**Microscopy**

For bright field and fluorescent microscopy a Zeiss Axioskop FL equipped with an epifluorescence UV-filter set and differential interference contrast (DIC) was used. Filter set 02 (365 nm excitation, LP 420 nm) was used for DAPI staining and filter set 09 (450-490 nm excitation, LP 515 nm) for GFP fluorescence. Filter set 14 (510-560 nm excitation, 590 nm emission) was used for mRFP1. A Nikon DS-5Mc camera and the software EclipseNet (Nikon) was used to capture, measure, and merge fluorescence images. Confocal laser scanning microscopy (CLSM) was performed using inverted microscopes either equipped with the confocal laser scanning module TCS 4D (Leica), or a Zeiss LSM510 META (Zeiss). For GFP, specimen were excited using an Argon 488 nm laser in combination with BP 505-550 filter, and for mRFP1 and propidium iodide fluorescence, a Helium Neon laser (543 nm) was used for excitation in combination with a LP 560 filter. Fluorescence of periodic acid-Schiff stained nuclei of maize embryo sacs was detected using an Argon 488 nm laser and the LP 505 filter. For capture and processing of confocal images the LSM 510 META software and the LSM image browser version 3.5.0.359 (Zeiss) was used.

**Yeast two-hybrid assays**

A lexA-based two hybrid system (Hybrid Hunter™, Invitrogen) was used according to the manufacturer′s recommendations. A detailed description of cloning and performing the assays is available in Supplemental Material and Methods, online.

**ACCESSION NUMBERS**

Sequence data from this article can be found in the GenBank/EMBL databases under the following accession numbers/*Arabidopsis* Genome Initiative identifiers: FJ515275 (TaMAB1),

EU360467 (TaMAB2), and EU344973 (ZmMAB1), ZmMAB1-like1 (EU974550), ZmMAB1-like2 (BT037633), ZmMAB1-like3 (BT035122), ZmMAB1-like4 (EU974172), ZmMAB1-like5 (EU966879), ZmMAB1-like6 (EU965363), ZmMAB1-like7 (EU965105), ZmMAB1-like8 (BT037672), ZmMAB1-like9 (EU951851), ZmMAB1-like10 (BT038660), ZmMAB1-like11 (BT041703), CeMEL26 (NP_492449), HsSPOP (NP_003554), MmTDPOZ1 (NP_683751), MmTDPOZ2 (NP_001007223), MmTDPOZ3 (NP_997154), MmTDPOZ4 (NP_997155), AtBPM1 (At5G19000), AtBPM2 (At3G06190), AtBPM3 (At2G39760), AtBPM4 (At3G03740), AtBPM5 (At5G21010), AtBPM6 (At3G43700), AtCUL3a (At1G26830). MSU rice locus identifiers at Rice Genome Annotation Project Database (http://rice.plantbiology.msu.edu/) are: Os08g41220, Os08g41150, Os08g41180, Os04g53410, Os10g28760, Os10g28770, Os10g29150, Os10g29310, Os10g29100, Os03g57854, Os07g07270, Os07g46160, Os07g01140, Os06g14060, Os06g45730.

**DNA and protein sequence analysis**

The analysis of putative novel expressed sequence tags (ESTs) found among ESTs generated from maize and wheat egg cell and proembryo cDNA libraries (Dresselhaus et al., 1994; Sprunck et al., 2005) revealed the presence of MATH and BTB domain encoding transcripts in the maize egg cell (Acc. no. DW531123), in the wheat egg cell (Acc. no. AL831180), and in the wheat 2-celled proembryo (Acc. no. CV973336). After generating full length sequences of the corresponding cDNA clones, putative open reading frames (ORFs) were identified and translated into proteins using the programs ORF finder (http://www.ncbi.nlm.nih.gov/gorf/gorf.html) and EditSeq 4.05 (Lasergene© 1989-2000 DNAStar Inc). The cDNAs and the corresponding ORFs of ZmMAB1 (GenBank acc. no. EU344973), TaMAB1 (GenBank acc. no. FJ515275) and TaMAB2 (GenBank acc. no. EU360467) were used as queries to run BLASTX and TBLASTN searches in the nucleotide collection (nr/nt) and dbEST databases at NCBI (http://www.ncbi.nlm.nih.gov) and Rice Genome Annotation Project Database (http://rice.plantbiology.msu.edu/). Corresponding protein sequences were downloaded and applied to protein alignments performed using MCoffee (Moretti et al., 2007) and GeneDoc 2.7.000 (Nicholas and Nicholas, 1997) for processing. The phylogeny of ClustalW alignments was visualized with Treeview, version 1.6.6 (Page, 1996). The Conserved Domain search service (http://www.ncbi.nlm.nih.gov/Structure/cdd/wrpsb.cgi) and the Pfam 22.0 data base (http://pfam.sanger.ac.uk) were used to identify domain architecture and substrate recognition residues.

**Reverse transcriptase PCR (RT-PCR)**

To study the expression of *TaMAB1*, *TaMAB2*, and *ZmMAB1* genes, total RNA was extracted from different tissues and whole seedlings of maize and wheat plants using TRIzol® reagent (Invitrogen) according to the manufacturer's recommendations. The quality of RNA preparations was analysed by denaturating agarose gel electrophoresis. Prior to first strand cDNA synthesis, RNA samples were treated with 1 U RNAse free DNAse I (MBI Fermentas) according to the manufacturer's instructions. mRNA was isolated from manually isolated single egg cells, synergids, zygotes, proembryos or embryos using the Dynabeads® mRNA DIRECTTM Micro kit (Dynal) and a magnetic particle transfer device (PickPenTM, BioNobile), like described previously (Sprunck et al., 2005). First strand cDNA synthesis was performed by using 0.5 µg Oligo (dT)18 primer and 1 µg of DNAse treated total RNA or isolated poly(A)+ mRNA and RevertAidTM H Minus M-MuLV Reverse Transcriptase (MBI Fermentas) following the manufacturer's protocol with addition of 40 U RNAseOUT (RNaseOutTM Recombinant Ribonuclease Inhibitor; Invitrogen). After the RT reaction, quality and quantity of the individual cDNA populations was tested by control PCRs using specific primer pairs for *GAPDH* from maize and wheat, respectively. Afterwards, 2-3 µl of each individual cDNA population was applied for a PCR (38 cycles) using gene-specific primers pairs for the respective MABs from wheat or maize. Primer sequences used for RTPCR were as follows:

TaMAB1-fw: 5'-TCTACTCGCGCACCAAGGGCATCC-3'
TaMAB1-rev: 5'-GCGGCAGGCTCAGGCGTCTCC-3'
TaMAB2-fw: 5'-CGGCGGCTTTAACTGGACGAT-3'
TaMAB2-rev: 5'-CGCCCCGGCACAAGAACA-3'
TaMAB3-fw: 5'-CTGAGCGAAGCAATTGATGTGGA-3'
TaMAB3-rev: 5'-GCGGGCAGCTAGCTACGAGATG-3'
ZmMAB1-fw: 5'-GCAGGAGGACCCTCTCGACGTG-3'
ZmMAB1-rev: 5'-GCCATTATTGGCTAGCTGCCGCTG-3'.
ZmGAP-fw: 5'-AGGGTGGTGCCAAGAAGGTTG-3'
ZmGAP-rev: 5'-GTAGCCCCACTCGTTGTCGTA-3'
TaGAP-fw: 5'-AAGGGTGGTGCCAAGAAGGTC-3'
TaGAP-rev: 5'-GGATCCCCACTCGTTGTCGTA-3'.

**Southern hybridization**

Extraction of genomic DNA from maize leaves was performed according to Palotta et al. (2000). 10 µg of genomic DNA sample from each *ZmMAB1*-RNAi transgenic (see below) and wt maize plants was restricted over night with *Not*I and *Bsp*TI, and separated in 0.8%

agarose gels. DNA was transferred onto HybondTM NX nylon membranes (Amersham) by capillary transfer (20x SSC) and fixed to membranes with 120 mJ using the StratalinkerTM 1800UV crosslinker (Stratagene) or were transferred by alkaline capillary transfer (0.4 M NaOH) without fixation.

Radioactive-labeled probes were generated by standard PCR reactions with *Ubiquitin* promoter primer pair UbiC-fw (5´-GTAGATAATGCCAGCCTGTTA-3´) and UbiR1-rev (5´-GAGCATCGACAAAAGAAACAG-3´). After purification of the respective PCR fragments, incorporation of (α-32P)-dCTP (6.000 Ci mmol-1) was achieved by using the Prime-it II Random Primer labeling Kit (Stratagene). Prehybridization and hybridization with radioactive probe was conducted overnight using Church buffer (0.5 M NaH2PO4, pH7.2; 1mM EDTA, 7%SDS) containing 100 µg/ml denaturated salmon sperm DNA. Membranes were washed under stringent (65 °C) conditions as follows: 10 min in 2x SSC/0.1% SDS, 10 min in 1xSSC/0.1% SDS, 10 min in 0.5x SSC/0.1% SDS and 10 min in 0.2x SSC/0.1% SDS. Hybridization signals were detected by exposing HyperfilmTM MP X-ray films (Amersham) to membranes from one day up to two weeks at -70 °C.

**Generation of constructs for transient and stable transformation experiments**

*ZmMAB1*-RNAi: A 249 bp fragment of the *ZmMAB1* coding sequence (amplified from nucleotide position 1922 in the *ZmMAB1* genomic sequence; Genbank acc. no. EU344973) containing 135 bp of the ORF and 114 bp of the 3' UTR was cloned in sense and anti-sense orientation, separated by the *FAD2* omega-6 desaturase intron 1 from *Arabidopsis* (Genbank Acc. no. AJ271841), under control of the maize *Ubiquitin* promoter and the *A. tumefaciens* OCS terminator (*Ubip::ZmMAB1(AS)::iF2::ZmMAB1(S)::OCSt*). Therefore, the *ZmMAB1* fragment was amplified from a cDNA library of maize egg cells (Dresselhaus et al., 1994) by using the primers *ZmMAB1RNAi-Eco* (5'-CGCTGAATTCGAAAAGGAAGTGCATT-3') and *ZmMAB1RNAi-Bam* (5'-CAGTGGATCCAGAGAACTCAAGCA-3'), and cloned into the *Eco*RI/*Bam*HI digested vector pUbi-IF2 (DNA Cloning Service), generating the intermediary vector *Ubip::ZmMAB1(AS)::iF2::OCSt*. In the second step, the identical *ZmMAB1* fragment was amplified using the primer pair *ZmMAB1RNAi-Mlu* (5'-CAGTACGCGTCAGAGAGAACTCAAGCA-3') and *ZmMAB1RNAi-Bsr* (5'-CGCGTGTACAGAAAAGGAAGTGCATT-3') and ligated into *Mlu*I/*BsrG*I digested intermediary vector *Ubip::ZmMAB1(AS)::iF2::OCSt*, resulting in the *ZmMAB1*-RNAi construct. *ZmMAB2-GFP*: the open reading frame of *ZmMAB1* (1041bp without STOP codon) was amplified from genomic DNA of maize cultivar B73 by using the primer pair *ZmMAB1F-Spe* (5´-ATCGACTAGTATGGCCGGCCTCCTG-3') and Zm*MAB1R-Bgl* (5'-GGCCAGATCTTTGCTCCAACCTTC-3') containing *Spe*I and *Bgl* II restriction sites,

respectively. The PCR product was cloned into ZeroBlunt TOPO vector (Invitrogen) and subsequently cloned into *Spe* I and *Bam* HI restriction sites of pLNU-GFP (DNA Cloning Service), containing an improved GFP for expression in plants (Pang et al., 1996), thereby generating the vector *Ubip::TmMAB1-GFP::NOSt*.

*TaMAB2-GFP*: The TaMAB2-GFP fusion protein construct was generated by fusing the open reading frame of TaMAB2 N-terminal to GFP under the control of the maize *Ubiquitin* promoter as follows: the 1071 bp open reading frame of *TaMAB2* (without STOP codon) was amplified from a proembryo-specific cDNA library (Sprunck et al. 2005) by using the primer pair *TaMAB2F-Spe* (5'-GCGCACTAGTTCCTCTTTCGCTTTC-3') and *TaMAB2R-Bam* (5'-CCGGGATCCAGTCAGTAAGAGAAATTTTT-3') containing *Spe*I and *Bam*HI restriction sites, respectively. After restriction digest, the *TaMAB2* ORF containing cDNA fragment was ligated into the *Spe*I and *Bam*HI digested vector pLNU-GFP (DNA Cloning Service) thereby generating the construct *Ubip::TaMAB2-GFP::NOSt*. The vector pLNU-GFP was used as a positive control for transient transformation experiments. *TaMAB2ΔMATH-GFP* and *TaMAB2ΔBTB-GFP*: The construct *Ubip::TaMAB2-GFP::NOSt* (see above) was used for generating deletion constructs of either the MATH domain (*TaMAB2ΔMATH-GFP*) or the BTB domain (*TaMAB2ΔBTB-GFP*). The deletions were generated by PCR amplification from *Ubip::TaMAB2-GFP::NOSt* using *Pfu* DNA polymerase (MBI Fermentas) and primers located 5´ upstream and 3´ downstream of the corresponding domains (MATHdel-fw: 5'-TCTGACAGCAATGGGAGCTTCATTATA-3';MATHdel-rev:5'-TCTCGACGAGGTCTTGGGCAGGC-3'; BTBdel-fw: 5'-TTTGTGAAAGCAAGCTCTGTGAGAG-3'; BTBdel-rev: 5'–TGTCTTCCAGCTGGTCTTGCAGACT-3'). The blunt ends of resulting PCR fragments were phosphorylated at 37 °C for 30 min by using T4 DNA kinase (MBI Fermentas) and religated at 16 °C for 10 hours with T4 DNA ligase (MBI Fermentas).

*AtEC1p::TaMAB2-GFP*: The binary vector for expression of TaMAB2-GFP under control of the *Arabidopsis* egg cell specific promoter *EC1.1* was generated by replacing the maize *Ubiquitin* promoter in *Ubip::TaMAB2-GFP::NOSt* (see above) by the *EC1.1* promoter. After the promoter fragment was amplified from the plasmid *EC1.1p::GUS* (Ingouff et al., 2008) by using the primer pair EC1-Not (5´-CTCTCGGCCGCCTTATGATTTCTTC-3´) and EC1-SpeI (5´-CTCTACTAGTTTCTCAACAGATTGATAA-3´), it was digested with NotI and SpeI and ligated into the NotI and SpeI sites of the digested vector *Ubip::TaMAB2-GFP::NOSt*. Afterwards, the cassette containing *EC1p::TaMAB2-GFP::NOSt* was recovered by SfiI digestion and ligated into the SfiI digested binary vector p7N (DNA Cloning Service).

**Yeast two-hybrid assays**

A lexA-based yeast two hybrid system (Hybrid Hunter™ ; Invitrogen) containing *pYESTrp* as prey and *pHybLex/Zeo* as bait vectors were used together with the yeast reporter strain L40 [MATα *his3Δ200 trp1-901 leu2-3112 ade2 LYS2*::(4*lex*Aop-*HIS*3) *URA3*::(8*lex*Aop-*lac*Z) *GAL4*] according to the manufacturer's recommendations. The open reading frame of *TaMAB2* was amplified from *Ubip::TaMAB2-GFP::NOSt* (see above) using primers containing restriction sites appropriate for cloning into pYESTrp as a prey vector (MAB2-YT-fw: 5'-CCGGAATTCCGATGGCCAGCAACTCCACC-3'; MAB2-YT-rev: 5'-CCGCTCGAGCGGCTAGTCAGTAAGAGAAATTTT-3'). Here, TaMAB2 was in frame with the B42 activation domain. TaMAB2 was also amplified using another set of specific primers with restriction sites suitable for cloning into the bait vector pHybLex/Zeo MAB2-Hy-fw: 5'-CCGGAATTCCGGATGGCCAGCAACTCCACC-3'; MAB2-Hy-rev: 5'-CCGCTCGAGCGGCTAGTCAGTAAGAGAAATTTT-3'), in frame with the *LexA* DNA binding domain. The open reading frame of *AtCUL3a* (AT1G26830) was amplified by RT-PCR from mRNA extracted from *Arabidopsis* (Col-O) leaves using the primer pair CUL3-Hy-fw (5'-CTGCAGAAGAGCTCATGAGTAATCAGAAGAAGAG-3') and CUL3-Hy-rev (5'-AAGGAAAAAAGCGGCCGCTTAGGCTAGATAGCGGTAAA -3'). The PCR product was cloned into the pCR_BLUNT II-TOPO (Zero Blunt® TOPO® PCR Cloning Kit, Invitrogen), regained by *Sac*I and *Not*I digest and subsequently ligated into the BAIT vector pHybLex/Zeo (Invitrogen), in frame with the *LexA* DNA binding domain. Successful cloning of ORF containing fragments fused with the B42 activation or LexA DNA binding domains was verified by sequencing the fusion products with primers pYESTrp-fw and pYESTrp-rev, or pHybLex/Zeo-fw and pHybLex/Zeo-rev, provided with the Hybrid Hunter Kit. L40 yeast cells were grown and transformed with both bait and prey constructs using a standard lithium acetate technique described in the manufacturer's protocol. To assay for histidine prototrophy, individual colonies of transformants were diluted 1:500 in autoclaved distilled water before 25 µl was spotted on a selective YC-WH Z300 medium lacking tryptophane and histidine. For testing additional β-galactosidase activity, another 25 µl of the diluted transformants were spotted in a grid pattern on YC-W Z300 plates. All plates were incubated at 30°C for 2 to 4 days until colonies appeared. Strong interaction yielded detectable color in less than 30 minutes. Longer incubations for up to 4 hours were required for weaker interactions. The controls pHybLex/Zeo-Fos and pYESTrp-Jun included in the Hybrid Hunter™ kit were used as a positive control for bait and prey plasmids, respectively, to test for an interaction with known protein partners. To test for non-specific activation of the bait plasmid, TaMAB2 and AtCUL3a cloned into pHybLex/Zeo were co-transformed together with pYESTrp without insertion into yeast reporter strain L40.

**ACKNOWLEDGEMENTS**

We thank Daniel Van Damme for providing the construct pH7WGR2-TUA6-mRFP1. We are grateful to Adam Vivian-Smith and Matthew M.S. Evans for their helpful suggestions on FG analyses. This work was supported by grants from the Alexander von Humboldt-Foundation, and by the Croatian Ministry of Science, Education and Sport to DLL (Project No. 119-1191196-1225).

## REFERENCES

**Ambrose, C.J., and Cyr, R.** (2008). Mitotic Spindle Organization by the Preprophase Band. Mol. Plant **1**, 950-960.

**Becker, D., Brettschneider, R., and Lörz H.** (1994). Fertile transgenic wheat plants from microprojectile bombardment of scutellar tissue. Plant J. **5**, 299-307.

**Bowerman, B., and Kurz, T.** (2006). Degrade to create: developmental requirements for ubiquitin-mediated proteolysis during early C. elegans embryogenesis. Development **133**, 773-784.

**Brettschneider, R., Becker, D., and Lorz, H**. (1997). Efficient transformation of scutellar tissue of immature maize embryos. Theor. Appl. Genet. **94**, 737-748.

**Canaday, J., Stoppin-Mellet, V., Mutterer, J., Lambert, A.M., and Schmit, A.C.** (2000). Higher plant cells: Gamma-tubulin and microtubule nucleation in the absence of centrosomes. Microsc. Res. Tech. **49**, 487-495.

**Choo, K.-B., Chen, H.-H., Cheng, W.T.K., Chang, H.-S., and Wang, M.** (2001). In silico mining of EST databases for novel pre-implantation embryo-specific zinc finger protein genes. Mol. Reprod. Dev. **59**, 249–255.

**Christensen, C.A., King, E.J., Jordan, J.R., and Drews, G.N.** (1997). Megagametogenesis in Arabidopsis wild type and the Gf mutant. Sex. Plant Rep. **10**, 49-64.

**Clough, S. J., and Bent, A. F.** (1998). Floral dip: a simplified method for Agrobacterium-mediated transformation of *Arabidopsis thaliana*. Plant J. **16**, 735-43.

**Cordts, S., Bantin, J., Wittich, P.E., Kranz, E., Lörz, H., and Dresselhaus, T.** (2001). ZmES genes encode peptides with structural homology to defensins and are specifically expressed in the female gametophyte of maize. Plant J. **25**, 103-114.

**Dresselhaus, T., Lörz, H., and Kranz, E.** (1994). Representative cDNA libraries from few plant cells. Plant J. **5**, 605-610.

**Dresselhaus, T., Srilunchang, K.-o., Leljak-Levanic, D., Schreiber, D.N., and Garg, P.** (2006) The fertilization-induced DNA replication factor MCM6 of maize shuttles between cytoplasm and nucleus, and is essential for plant growth and development. Plant Physiol. **140**, 512-527.

**Erhardt, D.W.** (2007). Straighten up and fly right – microtubule dynamics and organization of non-centrosomal arrays in higher plants. Curr Op Cell Biol. **20**: 107-116.

**Erhardt, D.W., and Shaw, S.L.** (2006). Microtubule dynamics and organization in the plant cortical array. Annu. Rev. Plant Biol. **57**, 859-875.

**Figueroa, P., Gusmaroli, G., Serino, G., Habashi, J., Ma, L.G., Shen, Y.P., Feng, S.H., Bostick, M., Callis, J., Hellmann, H., et al.** (2005). Arabidopsis has two redundant Cullin3 proteins that are essential for embryo development and that interact with RBX1 and BTB proteins to form multisubunit E3 ubiquitin ligase complexes in vivo. Plant Cell **17**, 1180-1195.

**Fuentealba, L.C., Eivers, E., Geissert, D., Taelman, V., and De Robertis, E.M.** (2008). Asymmetric mitosis: Unequal segregation of proteins destined for degradation. Proc. Natl. Acad. Sci. USA **105**, 7732-7737.

**Furukawa, M., He, Y. J., Borchers, C., and Xiong, Y.** (2003). Targeting of protein ubiquitination by BTB−Cullin 3−Roc1 ubiquitin ligases. Nat. Cell Biol. **5**, 1001 - 1007.

**Gallois, J.-L., Guyon-Debast, A., Lécureuil, A., Vezon, D. Carpentier, V., Bonhomme, S., and Guerche, P.** (2009). The *Arabidopsis* Proteasome RPT5 Subunits Are Essential for Gametophyte Development and Show Accession-Dependent Redundancy. Plant Cell Advance Online Publication 10.1105/tpc.108.062372.

**Geyer, R., Wee, S., Anderson, S., Yates, J., and Wolf, D.A.** (2003). BTB/POZ domain proteins are putative substrate adaptors for cullin 3 ubiquitin ligases. Mol. Cell **12**, 783-790.

**Gingerich, D.J., Gagne, J.M., Salter, D.W., Hellmann, H., Estelle, M., Ma, L.G., and Vierstra, R.D.** (2005). Cullins 3a and 3b assemble with members of the broad complex/tramtrack/bric-a-brac (BTB) protein family to form essential ubiquitin-protein ligases (E3s) in Arabidopsis. J. Biol. Chem. **280**, 18810-18821.

**Gingerich, D.J., Hanada, K., Shiu, S.H., and Vierstra, R.D.** (2007). Large-scale, lineage-specific expansion of a bric-a-brac/tramtrack/broad complex ubiquitin-ligase gene family in rice. Plant Cell **19**, 2329-2348.

**Hernández-Muñoz, I., Taghavi, P., Kuijl, C., Neefjes, J., and van Lohuizen, M**. (2005). Association of BMI1 with polycomb bodies is dynamic and requires PRC2/EZH2 and the maintenance DNA methyltransferase DNMT1. Mol. Cell. Biol. **25**, 11047-11058.

**Huang, B.Q., and Sheridan, W.F.** (1994). Female Gametophyte Development in Maize - Microtubular Organization and Embryo Sac Polarity. Plant Cell **6**, 845-861.

**Huang, C.J., Chen, C.Y., Chen, H.H., Tsai, S.F., and Choo, K.B.** (2004). TDPOZ, a family of bipartite animal and plant proteins that contain the TRAF (TD) and POZ/BTB domains. Gene **324**, 117-127.

**Ingouff, M., Sakata, T., Li, J., Sprunck, S., Dresselhaus, and T., Berger, F**. (2009). Functional equivalence of both male gametes for the egg cell in *Arabidopsis*. Curr. Biol. **19**, R19-R20.

**Kirihara, J.A.** (1994). Selection of stable transformants from Black Mexican Sweet maize suspension cultures. In The Maize Handbook, M. Freeling and V. Walbot, eds. (New York: Springer Verlag), pp. 690–694.

**Kranz, E., Bautor, J., and Lörz, H.** (1991). Invitro Fertilization of Single, Isolated Gametes of Maize Mediated by Electrofusion. Sex. Plant Rep. **4**, 12-16.

**Kwon, J.E., La, M., Oh, K.H., Oh, Y.M., Kim, G.R., Seol, J.H., Baek, S.H., Chiba, T., Tanaka, K., Bang, O.S., Joe, C.O., and Chung, C.H.** (2006). BTB domain-containing speckle-type POZ protein (SPOP) serves as an adaptor of Daxx for ubiquitination by CUL3-based ubiquitin ligase. J. Biol. Chem. **281**, 12664–12672.

**Laux, T., Wurschum, T., and Breuninger, H.** (2004). Genetic regulation of embryonic pattern formation. Plant Cell **16**, 190-202.

**Li, R., and Gundersen, G.G.** (2008). Beyond polymer polarity: how the cytoskeleton builds a polarized cell. Nature Rev. Mol. Cell Biol. **9**, 860-873.

**Lloyd, C., and Chan, J.** (2004). Microtubules and the shape of plants to come. Nature Rev. Mol. Cell Biol. **5**, 13-22.

**Lüders, J., and Stearns, T.** (2007). Microtubule-organizing centres: a re-evaluation. Nature Rev. Mol. Cell Biol. **8**, 161-167.

**Luke-Glaser, S., Pintard, L., Lu, C.G., Mains, P.E., and Peter, M.** (2005). The BTB protein MEL-26 promotes cytokinesis in C-elegans by a CUL-3-independent mechanism. Curr. Biol. **15**, 1605-1615.

**Luke-Glaser, S., Pintard, L., Tyers, M., and Peter, M.** (2007). The AAA-ATPase FIGL-1 controls mitotic progression, and its levels are regulated by the CUL-3(MEL-26) E3 ligase in the C-elegans germ line. J. Cell Sci. **120**, 3179-3187.

**Macara, I.G., and Mili, S.** (2008). Polarity and Differential Inheritance-Universal Attributes of Life? Cell **135**, 801-812.

**Mathur, J., and Hulskamp, M.** (2002). Microtubules and microfilaments in cell morphogenesis in higher plants. Curr. Biol. **12**, R669-R676.

**McCarthy, E.K., and Goldstein, B.** (2006). Asymmetric spindle positioning. Curr. Opin. Cell Biol. **18**, 79-85.

**Moretti, S., Armougom, F., Wallace, I.M., Higgins, D.G., Jongeneel, C.V., and Notredame, C.** (2007). The M-Coffee web server: a meta-method for computing multiple sequence alignments by combining alternative alignment methods. Nucleic Acids Res. *35*, 645-648.

**Morris, N.R.** (2003). Nuclear positioning: the means is at the ends. Curr. Opin. Cell Biol. **15**, 54-59.

**Nicholas, K.B., Nicholas H.B. Jr., and Deerfield, D.W. II.** (1997). GeneDoc: analysis and visualization of genetic variation. Embnew. News *4*, 14.

**Palotta, M.A., Graham, R.D., Langridge, P., Sparrow, D.H.B., and Barker, S.J.** (2000) RFLP mapping of manganese efficiency in barley. Theor. Appl. Genet. *101*, 1100–1108.

**Page, R. D. M.** (1996). TREEVIEW: An application to display phylogenetic trees on personal computers. Comp. Appl. Biosci. *12*, 357-358.

**Pang, S., DeBoer, D.L., Wan, Y., Ye, G., Layton, J.G., Neher, M.K., Armstrong, C.L., Fry, J.E., Hinchee, M., and Fromm, M.E.** (1996). An improved green fluorescent protein gene as a vital marker in plants. Plant. Physiol. *112*, 893–900.

**Pastuglia, M., Azimzadeh, J., Goussot, M., Camilleri, C., Belcram, K., Evrard, J.L., Schmit, A.C., Guerche, P., and Bouchez, D.** (2006). Gamma-tubulin is essential for microtubule organization and development in Arabidopsis. Plant Cell **18**, 1412-1425.

**Perez-Torrado, R., Yamada, D., and Defossez, P.A.** (2006). Born to bind: the BTB protein-protein interaction domain. BioEssays **28**, 1194-1202.

**Pintard, L., Willems, A., and Peter, M.** (2004). Cullin-based ubiquitin ligases: CUL3-BTB complexes join the family. EMBO J. **23**, 1681-1687.

**Pintard, L., Willis, J.H., Willems, A., Johnson, J.L.F., Srayko, M., Kurz, T., Glaser, S., Mains, P.E., Tyers, M., Bowerman, B., and Peter, M.** (2003). The BTB protein MEL-26 is a substrate-specific adaptor of the CUL-3 ubiquitin-ligase. Nature **425**, 311-316.

**Ranganath, R.M.** (2005). Asymmetric cell divisions in flowering plants - one mother, "two-many" daughters. Plant Biol **7**, 425-448.

**Sawin, K.E., and Tran, P.T.** (2006). Cytoplasmic microtubule organization in fission yeast. Yeast **23**, 1001-1014.

**Scheres, B., and Benfey, P.N.** (1999). Asymmetric cell division in plants. Annu. Plant Physiol. Plant Mol. Biol. **50**, 505-537.

**Smith N.A., Singh S.P., Wang M.B., Stoutjesdijk P.A., Green A.G., and Waterhouse P.M.** (2000). Total silencing by intron-spliced hairpin RNAs. Nature **407**, 319-320.

**Souter, M., and Lindsey, K.** (2000). Polarity and signalling in plant embryogenesis. J. Exp. Bot. **51**, 971-983.

**Sprunck, S., Baumann, U., Edwards, K., Langridge, P., and Dresselhaus, T.** (2005). The transcript composition of the egg cell changes significantly following fertilization in wheat (*Triticum aestivum* L.). Plant J. **41**, 660-672.

**Stogios, P.J., Downs, G.S., Jauhal, J.J.S., Nandra, S.K., Prive, G.G.** (2005). Sequence and structural analysis of BTB domain proteins. Genome Biol. **6**, R82.

**Sumara, I., Maerki, S., and Peter, M.** (2008). E3 ubiquitin ligases and mitosis: embracing the complexity. Trends Cell Biol. **18**, 84-94.

**Sumara, I., Quadroni, M., Frei, C., Olma, M.H., Sumara, G., Ricci, R., and Peter, M.** (2007). A CUL3-based E3 ligase removes aurora B from mitotic chromosomes, regulating mitotic progression and completion of cytokinesis in human cells. Dev. Cell **12**, 887-900.

**Thomas, J.H.** (2006). Adaptive evolution in two large families of ubiquitin-ligase adapters in nematodes and plants. Genome Res. **16**, 1017-1030.

**Thompson, J. D., Higgins, D. G. and Gibson, T. J.** (1994). Clustal-W - Improving the Sensitivity of Progressive Multiple Sequence Alignment through Sequence Weighting, Position-Specific Gap Penalties and Weight Matrix Choice. Nucl. Acids Res. *22*, 4673-4680.

**Van Damme, D., Van Poucke, K., Boutant, E., Ritzenthaler, C., Inze, D., and Geelen, D.** (2004). In vivo dynamics and differential microtubule-binding activities of MAP65 proteins. Plant Physiol. **136**, 3956-3967.

**Vollbrecht, E., and Hake, S.** (1995). Deficiency analysis of female gametogenesis in maize. Developmental Genetics **16**, 44-63.

**Wasteneys, G.O.** (2002). Microtubule organization in the green kingdom: chaos or self-order? J. Cell Sci. **115**, 1345–1354.

**Weber, H., Bernhardt, A., Dieterle, M., Han, P., Hano, P., Mutlu, A., Estelle, M., Genschik, P., and Hellmann, H.** (2005). Arabidopsis AtCUL3a and AtCUL3b form complexes with members of the BTB/POZ-MATH protein family. Plant Physiol. **137**, 83-93.

**Wigley, W.C., Fabunmi, R.P., Lee, M.G., Marino, C.R., Muallem, S., DeMartino, G.N., and Thomas, P.J.** (1999). Dynamic association of proteasomal machinery with the centrosome. J. Cell Biol. **145**, 481-490.

**Willemsen V., and Scheres, B.** (2004) Mechanisms of pattern formation in plant embryogenesis. Annu. Rev. Genet. **38**, 587-614.

**Wójcik, C., and DeMartino, G.N.** (2003). Intracellular localization of proteasomes. Int. J. Biochem. Cell Biol. **35**, 579-589.

**Xu, L., Wei, Y., Reboul, J., Vaglio, P., Shin, T.H., Vidal, M., Elledge, S.J., and Harper, J.W.** (2003). BTB proteins are substrate-specific adaptors in an SCF-like modular ubiquitin ligase containing CUL-3. Nature **425**, 316-321.

**Yamashita, Y.M., and Fuller, M.T.** (2008). Asymmetric centrosome behavior and the mechanisms of stem cell division. J. Cell Biol. **180**, 261-266.

**Young, B.A., Sherwood, R.T., and Bashaw, E.C.** (1979). Cleared-pistil and thick-sectioning techniques for detecting aposporous apomixis in grasses. Can. J. Bot. **57**, 1668-1672.

**Zhang, Q., Zhang, L., Wang, B., Ou, C.Y., Chien, C.T., and Jiang, J.** (2006). A hedgehog-induced BTB protein modulates hedgehog signaling by degrading Ci/Gli transcription factor. Dev. Cell **10**, 719-729.

**Zheng, N., Schulman, B. A., Song, L., Miller, J.J., Jeffrey, P.D., Wang, P., Chu, C., Koepp, D.M., Elledge, S.J., Pagano, M., et al.** (2002). Structure of the Cul1-Rbx1-Skp1-F box Skp2 SCF ubiquitin ligase complex. Nature **416**, 703−709.

# CHAPTER 5

# DiSUMO-like DSUL is required for nuclei positioning and cell specification during female gametophyte maturation in maize

**SUMMARY**

The reversible post-translational modification of numerous proteins by small ubiquitin-related modifiers (SUMO) represents a major regulatory process in various eukaryotic cellular and developmental processes. With the aim to study the role of SUMOylation during female gametophyte (FG) development in maize, we identified three *Zea mays* genes encoding SUMO (ZmSUMO1a and ZmSUMO1b) and a diSUMO-like protein called ZmDSUL that contains two head-to-tail SUMO-like domains. While *ZmSUMO1a* and *ZmSUMO1b* are almost ubiquitously expressed, *ZmDSUL* transcripts were detected exclusively in the egg apparatus and zygote of maize. The latter gene was selected for detailed studies. ZmDSUL is processed close to the C-terminus generating a dimeric protein similar to animal FAT10 and ISG15 that contain two ubiquitin-like domains. While GFP fused to the ZmDSUL N-terminus was located in the cytoplasm and predominately in the nucleoplasm of some cells, C-terminal GFP fusions accumulated at the nuclear surface. ZmDSUL-GFP under control of its endogenous promoter displayed earliest GFP signals in the micropylar region of the FG at stage 5/6 before migration of polar nuclei and cellularization occurs. Mature FGs displayed GFP signals exclusively in the egg apparatus. RNAi silencing of *ZmDSUL* showed that it is required for female gametophyte viability. Moreover, nuclei segregation and positioning defects occurred at FG stage 5 after mitotic nuclei division was completed. In summary, we report a diSUMO-like protein that appears to be essential for nuclei segregation and positioning, the prerequisite for cell specification during FG maturation.

**Key words**: SUMOylation, female gametophyte, polarity, aggresome, *Zea mays*

## INTRODUCTION

Reversible posttranslational modifications are widely used to dynamically regulate protein activity and degradation. Proteins can be modified by small chemical groups, sugars, lipids, and even by covalent attachment of other polypeptides. The highly conserved ubiquitin consisting of 76 amino acids is the best-known and studied example of a polypeptide modifier (for review Herrmann et al., 2007). It was shown that conjugation of polyubiquitin chains (polyubiquitination) involving lysine residue K48 has a well-established role in marking proteins for degradation by a multi-enzyme complex called the 26S proteasome (Müller et al., 2001). K29 and K63 polyubiquitination leads to endosome formation and modification of protein function. Monoubiquitination and multiubiquitination can also direct target proteins toward the endosome-lysosome pathway (Haglund and Stenmark, 2006).

After the discovery of ubiquitin, several related small proteins displaying structural similarity to ubiquitin have been reported (for review Gill, 2004; Herrmann et al., 2007; Kirkin and Dikic, 2007). These small ubiquitin-like proteins (called UBLs) include small ubiquitin-like modifiers (SUMOs), related-to-ubiquitin-1 (RUB-1/NEDD-8), autophagy defective-8 (APG-8) and APG-12, homologous to ubiquitin-1 (HUB-1/UBL-5), ubiquitin-fold-modifier-1 (UFM-1), ubiqitin related modifier-1 (URM-1) and Fau ubiquitin-like protein-1 (FUB-1). Moreover, two UBLs containing two head-to-tail ubiquitin-like domains have been reported: interferon-stimulated gene-15 (ISG-15) and antigen–F-adjacent transcript-10 (FAT-10). Human SUMO-1-3 (corresponding to yeast SMT3C, B and A, respectively) have been studied most intensively (Kirkin and Dikic, 2007).

SUMOs, which were first described in 1996, constitute a highly conserved protein family found in all eukaryotes (Johnson, 2004). Although SUMO shares only about 18% sequence identity to ubiquitin, the protein structure is quite similar (Gill, 2004). SUMO and ubiquitin share the overall mechanistic principles of substrate selection and attachment, including a flexible carboxy (C) terminus, which is generally a glycine residue that forms an isopeptide linkage to a lysine side chain within the target protein (Schwartz and Hochstrasser, 2003). The most prominent difference between members of the SUMO family and other ubiquitin-related proteins (including ubiquitin) is a very flexible N-terminal extension and an extension of amino acids at the C-terminus in SUMO (Melchior, 2000). The C-terminus is processed by limited proteolysis to expose a C-terminal glycine residue for target linkage (Kerscher, 2007). While yeast and invertebrates studied to date contain a single *SUMO* gene, vertebrates contain four genes (*SUMO-1-4*) and plants even more. For example, eight *SUMO* genes are found in the *Arabidopsis thaliana* genome (Saracco et al., 2007). Human SUMO-2 and

SUMO-3 polypeptides are ~96% identical to each other (and are referred to collectively as SUMO-2/-3), whereas they share only ~45% identity with SUMO-1 (Zhang et al., 2008). Interestingly, while human SUMO-1 is apparently unable of self-conjugation, SUMO-2/-3 can lead to chain formation (Tatham et al., 2001; Ulrich, 2008)

The reversible attachment of SUMO to their target proteins (SUMOylation) proceeds in analogy to ubiquitin. In an initial ATP-dependent process, SUMO forms a thioester bond with the heterodimeric SUMO-activating enzyme (SAE) (Desterro et al., 1999). The activated SUMO moiety is subsequently passed to SUMO-conjugating enzyme (SCE), which acts in concert with E3 ligases to attach SUMO to its targets through an isopeptide bond. In contrast to ubiquitin, the SUMO system utilizes only a single E2 enzyme, UBC-9 (ubiquitin-conjugating Enzyme 9), and probably fewer E3 ligases (Anckar and Sistonen, 2007). Moreover, Ubc-9 can recognize the substrate itself and directly transfers activated SUMO by the formation of an isopeptide bond between the C-terminal carboxyl group of SUMO and the ε-amino group of lysine in substrate proteins (Welchman et al., 2005). DeSUMOylation is catalyzed by cysteine proteases, called ubiquitin-like-protein-specific protease-1 and -2 (Ulp-1 and Ulp-2) in yeast as well as sentrin/SUMO-specific proteases (SENP) in human. While SENP-1 and -2 are able to process all three SUMOylating isoforms without distinction, SENP-3 and SENP-5 display a preference for SUMO-2/-3. Interestingly, all of these proteases are located at distinct subcellular localizations matching the function of their substrates: SENP-1 localizes to the nucleus, SENP-3 and SENP-5 to the nucleolus and SENP-2 to the cytoplasm, nuclear pore or nuclear body (for review Herrmann et al., 2007).

Compared to ubiquitin, SUMO has much fewer cellular substrates but, intriguingly, several indentified targets turned out to be important cellular and especially transcriptional regulators (Geiss-Friedlander and Melchior, 2007; Gill, 2004; Müller et al., 2001; Vertegaal et al., 2006). Lately, it has become clear that SUMOylation is involved in surprisingly diverse biological pathways, such as genome integrity, chromosome packing and dynamics, transcriptional regulation, nucleocytoplasmic translocalization and various aspects of signal transduction acting *via* modulation of protein–protein interactions as well as protein–DNA binding (Hay, 2005). Through biochemical and proteomic approaches over 200 proteins have been identified as SUMO substrates (Vertegaal et al., 2006; Zhang et al., 2008), implicating SUMOylation as a post-translational modification mechanism of a wide range of cellular and developmental functions, predominately associated with the nucleus (Seeler and Dejean, 2003). Genetic studies identified roles for SUMOylation in regulating chromosome condensation and segregation via sister chromatid cohesion, kinetochore function as well as mitotic spindle elongation and progression through mitosis (Watts, 2007).

The proper function of these processes is a major prerequisite for cell specification and fate determination during development of higher eukaryotes. In order to understand the underlying molecular mechanisms of cell polarity establishment and cell identity in flowering plants (angiosperms), we are studying the development of the haploid female gametophyte, or embryo sac, as a model. After meiosis, development of the angiosperm embryo sac begins with a phase of free nuclear division to produce an eight-nuclei coecytium during a process called megagametogenesis. During this process, embryo sac nuclei undergo a stereotypical number of mitotic divisions. Migration and asymmetric positioning of nuclei is highly regular. The embryo sac then cellularizes and differentiates to produce four cell types: an egg cell, usually two synergids, a homodiploid central cell and, depending on the plant species, up to around 40 antipodals (Brukhin et al., 2005; Drews and Yadegari, 2002). Embryo sac development thus provides an ideal system to study fundamental cellular processes such as asymmetric nuclei position and migration as well as position dependent cell fate determination. As SUMOylation plays a prevalent role in functions associated with the mitotic nucleus, we searched maize and wheat egg cell EST data (Márton et al., 2005; Sprunck et al., 2005) for transcripts encoding SUMO and SUMO related proteins for further functional studies during female gametophyte development. Here, we report the identification of ubiquitously expressed *SUMO* genes and of a diSUMO-like (DSUL) protein gene displaying a highly specific expression pattern during embryo sac development and early embryogenesis in maize. Unlike FAT10 and ISG15 that contain two UBL domains, DSUL contains two head-to-tail SUMO-like domains thus represents the first protein displaying such a protein structure. We further analysed DSUL processing, subcellular localization as well as its role during female gametophyte development.

## MATERIALS AND METHODS

### EST sequencing and bioinformatic analyses

988 EST sequences derived from a cDNA library of maize egg cells (Dresselhaus et al., 1994) were clustered and analyzed for the presence of transcripts encoding SUMO/SMT3 proteins. ZmSUMO1a (GenBank accession # FJ515939), ZmSUMO1b (GenBank accession # FJ515940) and ZmDSUL (GenBank accession # FJ515941) sequences were compared online and aligned by ClustalW (Thompson et al., 1994). Alignment data were used to generate a phylogram (Supplemental Figure 1) with Treeview (version 1.6.6; Page, 1996). Protein alignments were drawn by GeneDoc, version 2.6.02 (Nicholas et al., 1997), using ClustalW alignment data. Prediction of 3-dimensional protein structures was performed using

HHpred (http://toolkit.tuebingen.mpg.de/hhpred) based on PDB 1Z2M structural data. Based on hits to known protein structures from HsISG15, the structure of ZmDSUL was modeled by using Accelrys discovery studio 1.7.

**Plant growth, isolation of cells from the female gametophyte and *in vitro* suspension culture**

Maize (*Zea mays*) inbred lines A188 (Green and Phillips, 1975) and H99 (D'Halluin et al., 1992) and transgenic lines were grown under standard greenhouse conditions at 26ºC with 16 h light and a relative air humidity of about 60%. Cells of the maize embryo sac before fertilization were isolated according to Kranz et al. (1991) and after fertilization according to Cordts et al. (2001) with the exception that ears were kept on wet paper instead of MS medium. Tobacco (*Nicotiana benthamiana*) plants were grown at 22ºC with 16 h light and at 18ºC in the dark with a relative air humidity of about 70%. Black Mexican Sweet (BMS) maize cells were cultivated in MS (Murashige and Skoog, 1962) medium containing 2 mg/l 2,4D. Stock cultures on solid and suspension cultures in liquid MS medium were maintained in the dark at 26ºC on a shaker at 60-70 rpm and sub-cultured into fresh medium every 3 weeks and 4 days, respectively.

**DNA and RNA extraction, Southern blots and SC RT-PCR**

Extraction of genomic DNA from plant tissues was performed according to Pallotta et al. (2000). Total RNA was extracted from all samples with TRIzol® reagent (Invitrogen) according to the manufacturer's specifications. Before RT-PCR, 1 µg of total RNA was digested with DNaseI (DNaseI amp grade, Invitrogen) and used for first-strand cDNA synthesis using Oligo $(dT)_{18}$ (MBI Fermentas) and reverse transcriptase (RevertAid™ M-MuLV Reverse Transcriptase, MBI Fermentas) following the manufacturer's protocol. Quality and amount of generated cDNAs was analyzed by PCR using maize *GAPDH* (*Glyceraldehyde 3-phosphate dehydrogenase*)-specific primers ZmGap1 (5'-AGGGTGGTGCCAAGAAGGTTG-3') and ZmGap2 (5'-GTAGCCCCACTCGTTGTCGTA-3'). For detection of transgenic plants, mRNA from plant leaves was isolated using Dynabead® oligo $(dT)_{25}$ (Invitrogen) following the manufacturer's guidelines. cDNA was generated as described above.

For Southern blot analysis, genomic DNA (gDNA) was digested with *Bsp*TI and *Not*I. This enzyme combination cuts out the full-length *ZmDSUL* cDNA from the pZmDSUL-RNAi vector described below. Restricted DNA was separated in 1% agarose gels and transferred with 20xSSC onto Hybond-XL membranes (GE Healthcare). DNA was cross-linked to membranes with 300 mJ radiation in a UV Stratalinker 1800 (Stratagene). Hybridization,

washing and exposure were performed according to the procedure described for DNA gel blots according to the specifications of the manufacturer (Roche). Single cell RT-PCR analysis (SC RT-PCR) was performed as described by Cordts et al. (2001) with minor modifications: SC reverse transcription (RT) was performed using the primers ZmDSULRev (5'-GCTGCCATCAATGATGGAGCAG-3'), ZmSUMO1aRev (5'-GTCCCTCAGCAATGGCACAAG-3') or ZmSUMO1bRev (5'-CAAGGAGCCAGAGCATCACAAG-3') in addition to ZmGap2 (5'-GTAGCCCCACTCGTTGTCGTA-3') for cDNA synthesis. After RT, each reaction was split into two reaction tubes and 38 PCR cycles were conducted with each reaction using *ZmDSUL*-specific primers ZmDSULFor (5'- CGATCAGGCTTCAGGCATGGC-3') and ZmDSULRev, *ZmSUMO1a*-specific primers ZmSUMO1aFor (5'-CGCCCGGAAACTGACCTCTACC-3') and ZmSUMO1aRev, *ZmSUMO1b*-specific primers ZmSUMO1bfor (5'-ATCGATCGCCGGAAAACTAACC-3') and ZmSUMO1bRev as well as *GAPDH*-specific primers ZmGap1 (5'-AGGGTGGTGCCAAGAAGGTTG-3') and ZmGap2. Twenty-five micro liters of the *ZmDSUL, ZmSUMO1a* and *ZmSUMO1b* as well as 15 µl of the *GAPDH* PCR products were each separated in 1% agarose gels. The size of the amplified *ZmDSUL* transcript was 753 bp, 440 bp for the *ZmSUMO1a* transcript, 415 for *ZmSUMO1b* and 622 bp for *GAPDH*. While maize *SUMO* and *DSUL* genes do not contain introns, *GAPDH* derived genomic amplificates are approximately 1.2–1.3 kbp in size and were used as a control to visualize genomic DNA contaminations.

**Generation of constructs, biolistic transformation and regeneration of transgenic maize plants**

pZmDSUL-RNAi construct (*UBI*p::*ZmDSUL-AS*::*iF2intron*::*ZmDSUL::OCSt*): for this construct, the *ZmDSUL* cDNA was PCR amplified from vector pUbi-IF2-15 (DNA Cloning Service) using primers F15Eco (5'-CGCGGAATTCACGATCAGGCTTCA) and R15Bam (5'-CAGTGGATCCGGTTCTCAATCGATGT) and cloned in anti-sense orientation into the *Bam*HI and *Eco*RI restriction sites of the vector pUbi-ZmDSUL (DNA Cloning Service). In a second cloning step, *ZmDSUL* cDNA was PCR amplified using the primers F15Bsr (5'-GCGGCCTGTACACGATCAGGCTTCA) and R15Bss (5'-CAGTGCGCGCGGTTCTCAATCGATGT) from vector pUbi-IF2-15, and cloned in sense-orientation into the *Bsr*GI and *Bss*HII restriction sites of the vector pUbi-ZmDSUL, generating the pZmDSUL-RNAi construct.

pZmDSUL:ZmDSUL-GFP vector (*ZmDSUL*p::*ZmDSUL-GFP*::*NOSt)*: for this construct, the open reading frame (ORF) of *ZmDSUL* together with 1566 bp upstream of the ORF were

PCR-amplified from genomic DNA with primers 15Fgen (5'-CTCTGCGGCCGCTTTGCTCACAG-3') and 15Rgen (5'CCGGATCCAATAAAAATTATTAGCTGCC) containing *Not*I and *Bam*HI restriction sites, respectively, which were then used for cloning the fragment between the *Not*I and *Bam*HI restriction sites of the vector pLNU-GFP-Neu (DNA Cloning Service) to generate the pZmDSUL:ZmDSUL-GFP construct.

pN-DSUL-GFP and pC-DSUL-GFP constructs (*35S*p:*GFP::ZmDSUL::35S*t and *35S*p*::ZmDSUL::GFP::35St*): for these constructs, the ORF of *ZmDSUL* DNA was PCR-amplified from the plasmid pZmDSUL-ZmDSUL-GFP (see above) with modified primers ZmDSULgateFor (5'-CACCATGGCGTCCCCTGGCCGG-3') and ZmDSULgateRev (5'-GGATCCATAAAAATTATTAG-3') generating CACC and *Bam*HI restriction sites, respectively. PCR products were cloned using the pENTR™ Directional TOPO® cloning kit (Invitrogen). Entry clones were generated using the Gateway system (Gateway® LR Clonase™ II Enzyme Mix, Invitrogen) and the destination vectors pB7FWG2.0 for C-terminal GFP fusion to ZmDSUL and pB7WGF2.0 for N-terminal GFP fusion to ZmDSUL, respectively (Karimi et al., 2002). Plasmids were generally isolated with a plasmid mini prep kit (Avegene) and fully sequenced. 0.1µg was generally used for transformation of *E. coli* cells or cells of *Agrobacterium tumefaciens* strain GV3101 (Holsters et al., 1980) according to standard procedures.

Biolistic transformation of BMS suspension cells was performed as follows: cells were grown at 26ºC in a dark chamber with 60-70 rpm shaking. Before transformation cells were sterile filtrated through a 500 µm metal net and then passed through a 100 µm pore sized nylon mesh to spread a uniform cell layer on solid MS medium. Before biolistic transformation, cells were incubated at 26ºC for 1 to 2 h. After transformation, plates were incubated overnight in the dark at 26ºC. Cells were transferred to fresh liquid medium and cultivated in darkness using a shaker (60-70 rpm) for at least 4 h before microscopic observations. Photos were taken immediately after a transfer of 100 µl of medium containing individual cells or cell clusters showing GFP fluorescence onto glass slides.

Transformation of immature maize embryos using biolistic particle bombardement was performed as follows: immature hybrid embryos of the maize inbred lines A188 and H99 were isolated 11 to 13 days after pollination (DAP). The constructs pZmDSUL-RNAi and pZmDSUL-ZmDSUL-GFP were each co-transformed with the vector *35S*p:*PAT* carrying the selectable marker PAT for glufosinate ammonium resistance (Becker et al., 1994). Particle bombardment, tissue culture, and selection of transgenic maize plants were performed according to Brettschneider et al. (1997).

**Recombinant protein expression in *Nicotiana benthamiana***

To express recombinant ZmDSUL fusion proteins in *Nicotiana benthamiana, Agrobacterium tumefaciens* strain GV3101 was grown at 28ºC in LB medium with 40 µg $ml^{-1}$ gentamycin and 50 µg $ml^{-1}$ spectomycin to the stationary phase. Bacteria were sedimented by centrifugation at 3500 xg for 15 min at room temperature and resuspended in infiltration buffer (10 mM $MgCl_2$, 10 mM MES-KOH pH 5.7 and 100 µM Acetosyringone). Cells were left in this medium for 2 h and then infiltrated into the abaxial air spaces of 2-4 week old *Nicotiana benthamiana* plants. The Agrobacterium cultures carrying ZmDSUL-fusion protein (N- and C-terminal GFP versions) and a p19 construct to suppress post-transcriptional gene silencing (PTGS) of the host silencing response and thus to increase transient gene expression (Voinnet et al., 2000; 2003). These two constructs were brought to an optical density ($OD_{600}$) of a maximum of 1.0 to avoid toxicity.

For total protein extraction, 1 gram of *N. benthamiana* leaves was each collected after 2 days infiltration. Leaf samples were grinded to powder by a Retsch homogenizer MM200 for 2 min at 30 Hz speed. 300-500 µl of protein extraction buffer [20 mM Tris-Cl pH7.5, 150 mM NaCl, 1 mM EDTA, 10 mM DTT and 1 cocktail protease inhibitor tablet (per 10 mL of extraction buffer)] were added to the grinded sample. Samples were centrifuged at 48,000 xg for 1 hour at 4ºC. Protein concentrations were determined by a standard Bradford assay (Bio-Rad). Thirty micrograms of the supernatant was then loaded onto a 12% SDS gel or stored at -20ºC for later analyses. Proteins were separated and transferred onto PVDF membranes (Millipore) by wet electro-blotting. For detection of GFP, a mouse IgG κ monoclonal GFP antibody (Roche) and an anti-mouse IgG-POD antibody conjugated to peroxidase (Roche) were used at 1:5000 dilutions for both antibodies. Signals were detected using an ECL detection kit (GE Healthcare).

**Histological studies and GFP imaging**

For phenotypical analysis of wild-type and *ZmDSUL*-RNAi embryo sacs, immature and mature cobs were harvested from green-house grown maize plants. Whole cobs were treated according to a fixing/clearing method using Kasten's fluorescent periodic acid-Schiff's reagent decscribed by Vollbrecht and Hake (1995). The phases for hydration and dehydration of ears was prolonged from 20 to 30 minutes in each step and ears were dissected after they were cleared with methyl salicylate (Young et al., 1979). Samples were mounted in methyl salicylate on glass slides under a cover slip and analysed with a LSM 510-META confocal laser scanning microscopy (CLSM, Zeiss) with 488 nm excitation and a LP 505 filter.

GFP fluorescence from BMS suspension cells and embryo sacs of maize were monitored by CLSM with 488 nm excitation and a BP 505-550 filter for selective GFP visualization. Image capture and processing were done using the AxioCam HRc camera, the Zeiss LSM 510 META software, and the Zeiss LSM image browser version 3.5.0.359.

## RESULTS

### DSUL encodes a diSUMO-like protein localized to nucleoplasm and cytoplasm

Previous studies from our and other labs indicated that post-translational protein modification by ubiquitination and SUMOylation might play a major role in gametophyte development in plants (for example Sprunck et al., 2005; Borges et al., 2008; Kim et al. 2008; Liu et al., 2008). To study the role of SUMO during female gametophyte development, we searched for transcripts encoding SUMO in an EST collection from maize egg cells (Dresselhaus et al., 1994; Márton et al., 2005). Among the 30 largest EST clusters, we identified three genes encoding proteins with homology to SUMO (Tab. 1). A more detailed analysis (see also Fig. 1A and Fig. 2) comparing these proteins with highly conserved ubiquitin and SUMOs from man (HsUbi, 76 amino acids, and HsSUMO1-4 consisting of 95-103 amino acids) as well as *Arabidopsis* AtSUMO1-6 (100-117 amino acids) revealed two highly homologous proteins, called *Zea mays* SUMO1a/b (ZmSUMO1a and ZmSUMO1b; precursor lengths of 99 and 109 amino acids, respectively). Interestingly, the third protein contained two head-to-tail SUMO-like domains and was named *Zea mays* diSUMO-like (ZmDSUL). For alignments and phylogenetic investigations, the ZmDSUL sequence, consisting of 250 amino acids (aa), was split into two domains [ZmDSUL-N (126 aa) and ZmDSUL-C (124 aa)] after a putative di-glycine (GG) cleavage site typically found at the C-terminal end of all SUMO proteins. The GG motif for SUMOylation is boxed in red in Figure 1A. Until now, dimeric SUMO-like proteins have not been described. However, FAT10 and ISG15 (each 165 amino acids) contain two ubiquitin-like domains. As shown in Tab. 1, the sequence homology of both domains in FAT10 and ISG15 is higher compared with ubiquitin (27/34% and 28/36%, respectively) than to SUMO (15/11% and 12/18%, respectively), while ZmDSUL shows a higher sequence homology to SUMO (25/22%) compared with ubiquitin (17/15%).

**Table1. DSUL proteins are more closely related to SUMO than to ubiquitin proteins.**
Comparison of maize SUMO and DSUL with related ubiquitin and SUMO proteins. Homology of N-terminal (1st number) and C-terminal (2nd number) domains of ZmDSUL, HsISG15 and HsFAT10 are shown separately.

| Protein | Ubiquitin sequence homology (%) | SUMO sequence homology (%) |
|---|---|---|
| ZmSUMO1a | 15[1] | 42[4] |
| ZmSUMO1b | 14[1] | 41[4] |
| ZmDSUL | 17, 15[1] | 25, 22[3] |
| HsISG15 | 28, 36[2] | 12, 18[4] |
| HsFAT10 | 27, 34[2] | 15, 11[4] |

$n^1$, $n^2$, $n^3$ and $n^4$ indicate protein sequence homology by using ZmUbi, HsUbi, ZmSUMO1a and HsSUMO-1 proteins as references, respectively.

Thus ZmDSUL represents the first dimeric SUMO-like protein. Another transcript for a diSUMO-like protein consisting of 204 aa was identified in a wheat egg cell EST collection (*Triticum aestivum* diSUMO-like: TaDSUL; Fig. 1A) (Sprunck et al., 2005). DSUL homologs were not found in the Arabidopsis genome. This indicates that SUMOL might represent a Gramineae or monocot specific gene. Phylogenetic analyses showed that DSUL proteins form an own clade, while dimeric FAT10 and ISG15 form a clade with ubiquitin (Fig. 2). ZmSUMO1a and ZmSUMO1b cluster into the same group with Arabidopsis AtSUM1 and AtSUM2.

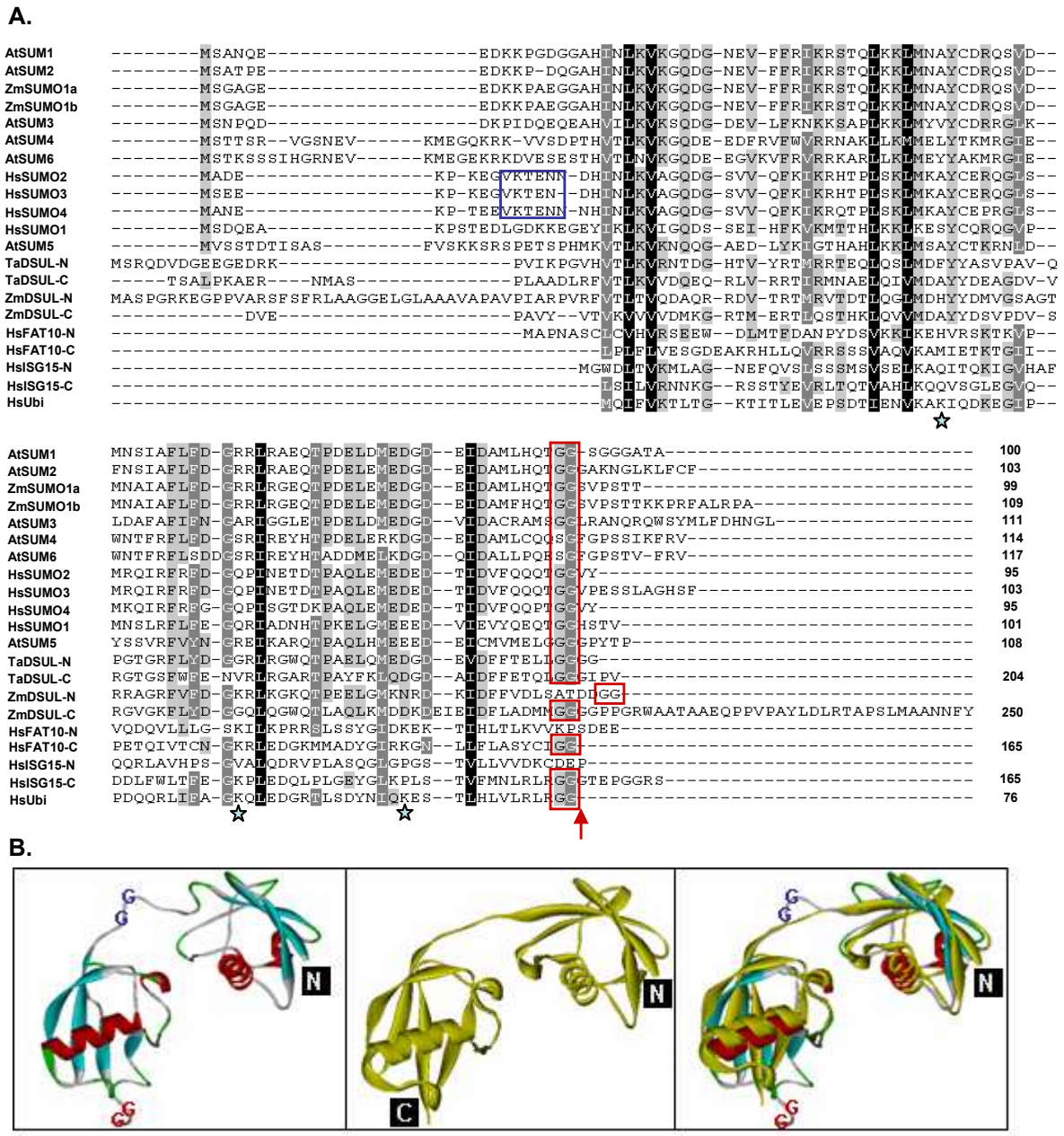


**Figure 1. Primary structure alignment of ubiquitin, diubiquitin-like, SUMO and DSUL proteins, and predicted 3-D structure of ZmDSUL**.

(**A**) Protein sequences encoded by human (Hs), Arabidopsis (At), wheat (Ta) and maize (Zm) *Ubi (ubiquitin)*, *SUMO* and *DSUL* genes were aligned using ClustalW and processed with GeneDoc. See Supplementary Figure 1 for protein accession numbers. Letters in black blocks indicate identical amino acid residues/conserved substitutions, amino acid residues with more than 80% conservation are highlighted in dark grey, and those with more than 60% conservation are shown as light grey boxes. The dimeric SUMO-like proteins DSUL from maize and wheat as well as dimeric human ubiquitin-like FAT10 and ISG15 were split into an N-terminal and a C-terminal domain for alignment. Stars label Lys 29, Lys 48 and Lys 63 in HsUbi, which serve as common sites for ubiquitin polymerization. The predicted cleavage sites (arrow) exposing C-terminal glycine-glycine (GG in red boxes) residues to generate mature SUMO and DSUL proteins are indicated and the length of precursor proteins is given. The N-terminal polySUMOylation motif of HsSUMO-2/3 and HsSUMO-4 is boxed in blue. (**B**) Predicted 3-D structure of ZmDSUL (left) based on the NMR-structure of HsISG15 (middle; PDB IZ2M). N- and C-terminal ends of proteins are indicated. ZmDSUL (left) forms two globular domains that are connected by a linker containing a putative SUMO-cleavage site (blue GGs). Each domain consists of a β-sheet (light-blue) and two α-helices (red). Loops/turns are indicated in green. GGs at the C-terminus are in red. An overlay of ZmDSUL and HsISG15 3-D projections is shown at the right.

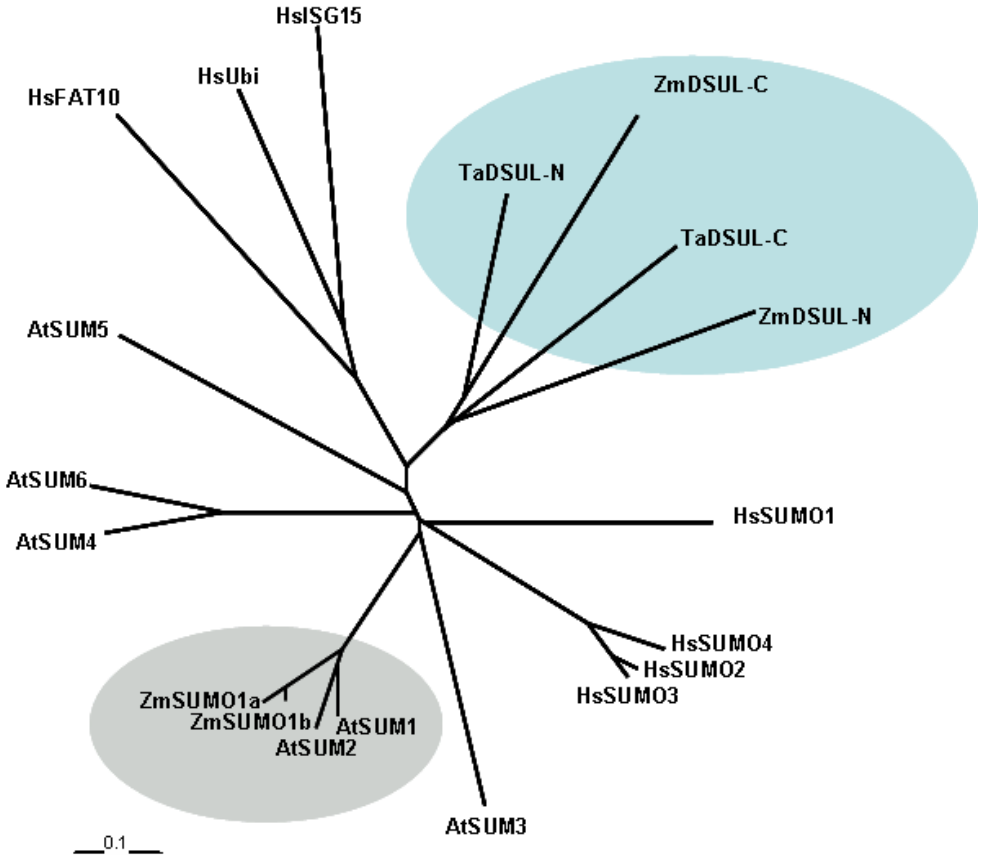


**Figure 2**. **Phylogenetic relationship of selected members of the ubiquitin (Ubi), diubiquitin-like, SUMO and DSUL protein families.**
Protein sequences were aligned by ClustalW and the unrooted tree was drawn by Tree-View. Branch lengths are proportional to phylogenetic distances and the scale bar represents 10% substitutions per site. Protein accession numbers at GenBank are as follows: *Zea mays* ZmSUMO1a (FJ515939), ZmSUMO1b (FJ515940), ZmDSUL (FJ515941), *Triticum aestivum* TaDSUL (FJ515942), *Arabidopsis thaliana* AtSUM1-6 (NP_194414, NP_200327, NP_200328, NP_199682, NP_565752, and NP_199681) and *Homo sapiens* HsSUMO1-4 (AAC50996, AAH71645, NP_008867 and NP_001002255), HsFAT10 (NP_006389), HsISG15 (NP_005092) as well as HsUbi (P62988). The dimeric DSUL proteins were split in N- and C-terminal domains, which together form an own clade (colored in light blue). Maize SUMO proteins (ZmSUMO1a and ZmSUMO1b) form a highly homologous clade with Arabidopsis SUM1 and SUM2 proteins (grey circle). HsFAT10 and HsISG15 are most closely related to HsUbi.

The common sites for ubiquitin polymerization at Lys 29 and Lys 63 are missing in SUMO and DSUL sequences, indicating that polymerization does not occur. The conserved Lys 48 residue found in ZmDSUL is not present in TaDSUL. This indicates that also this site might not be involved in polymerization, although biochemical proof is missing. As mentioned above, both DSUL proteins contain two conserved predicted di-glycine (GG) processing

sites, one in the middle and the second at the C-terminal region of the protein. SUMO-specific proteases cleave after the GG site to expose these residues for activation and SUMOylation (Herrmann et al., 2007). 3D structure modeling of ZmDSUL (Fig. 1B, left) based on the X-ray crystal structure of HsISG15 (1Z2M; Narasimhan et al., 2005; Fig. 1B, middle) not only showed that the structure of ZmDSUL is highly conserved and strongly overlapping with HsISG16 (Fig. 1B, right), but also consists of two globular domains linked by a long stretch containing the predicted GG processing site in the middle of the protein as well as an exposed second GG site at the very C-terminus. In order to determine whether ZmDSUL is processed at either or both predicted cleavage sites, we fused GFP N- or C-terminally to ZmDSUL and transiently expressed the fusion proteins in tobacco leaves (*Nicotiana benthamiana*). Two days after infection, crude protein extracts were separated by SDS-PAGE and analyzed by immunoblotting using an anti-GFP antibody (Fig. 3A). Lack of processing should generate 54 kDa bands. Processing behind the central GG-site between both SUMO-like domains should give a 42 kDa band, and cleavage after the C-terminal GG-site should generate a 52 kDa band for the N-terminal and a 32 kDa band for the C-terminal GFP-fusions. A 31 kDa ER-GFP was used as a positive control for comparison. The N-terminal fusion showed a 52 kDa band and the C-terminal fusion a weak band at 32 kDa (Fig. 3A). Additionally, 34 kDa bands and a 31 kDa band for the N-terminal fusion were visible probably derived from degradation products. A 42 kDa band was never detected. We thus conclude that ZmDSUL is only processed at the C-terminus, but not in the middle of the protein thus generating a naturally occurring diSUMO-like protein with an exposed di-glycine at the very C-terminus. The GFP degradation products always observed with both chimeric proteins suggests that ZmDSUL might not possess a very long half-life itself.

We used the same constructs in order to study the sub-cellular localization of ZmDSUL in maize BMS (Black Mexican Sweet) suspension cells. As shown in Figure 2B-E, GFP signals from the N-terminal fusion protein were evenly distributed in the cytoplasm and nucleoplasm excluding the nucleolus. About one third of the cells showed a stronger accumulation inside the nucleus (Fig. 3B). Interestingly, when GFP was fused to the C-terminus of ZmDSUL, from where it is cut (Fig. 3A), fluorescence signals were exclusively detected polar at one cytoplasmic site of the nuclear surface, but neither in the nucleoplasm nor in the remainder of the cytoplasm (Fig. 3F-I). Similar protein localization and aggregation has been described previously for animal cells that accumulate unfolded or misfolded proteins at the pericentriolar region in immediate vicinity to the cell nucleus. This region was also shown to contain many proteasome complexes and was called aggresome in animal cells (Hatakeyama and Nakayama, 2003). Similar protein localization was neither observed when

GFP was fused to the N-terminus of ZmDSUL nor in cells expressing very high amounts of free GFP. Free GFP always showed equal fluorescence in the cytoplasm and nucleus excluding the nucleolus (Fig. 3 J and K).

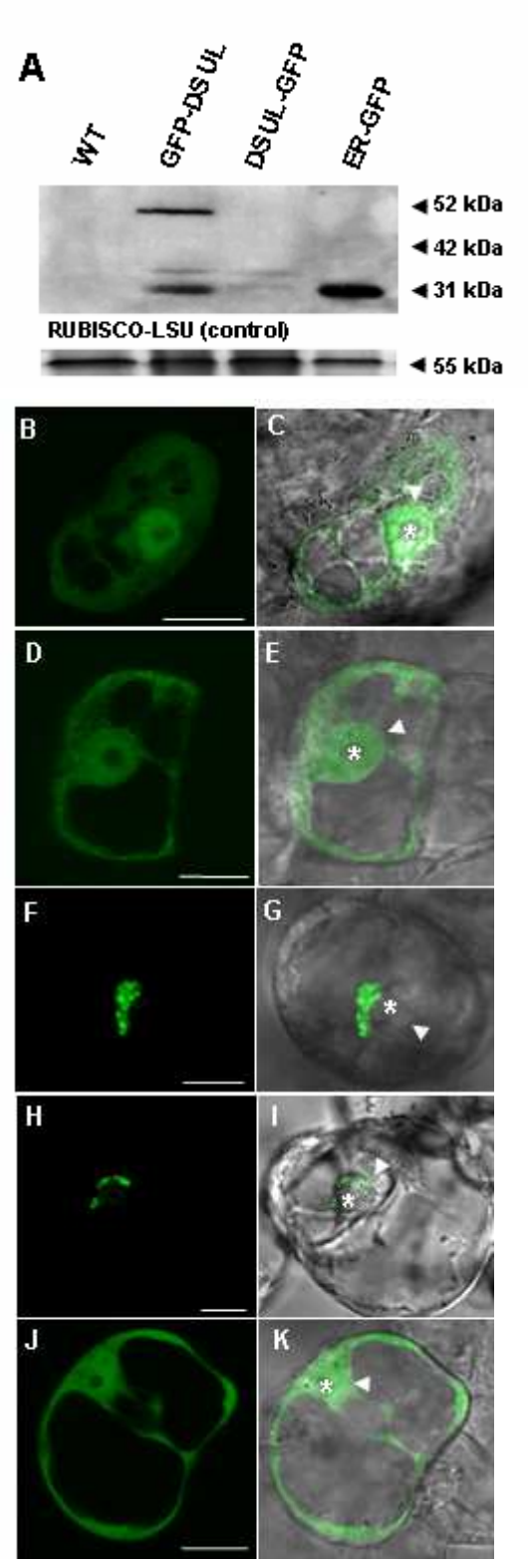


**Figure 3. Processing and subcellular localization of ZmDSUL in *Nicotiana benthamiana* leaves two days after infection.**
(**A**) Dimeric ZmDSUL is processed at the C-terminus, but is not cleaved to generate monomeric DSUL protein domains. Two days after infiltration (infection) with constructs described below, tobacco leaf protein extracts were blotted and the length of GFP-fusion proteins detected with an anti-GFP antibody. The full length fusion protein (52 kD) was only detectable when GFP was fused to the N-terminus. GFP cleaved from the predicted C-terminal diglycine motif generates a band at 32 kDa. A fusion protein containing a monomeric ZmDSUL domain containing GFP either attached to the N- or C-terminus (42 kD) was never detectable. ER-GFP (31 kDa) was loaded as a positive control. (**B-E**) BMS suspension cells bombarded with gold particles carrying a construct *p35S:GFP-ZmDSUL* encoding GFP fused to the N-terminus of ZmDSUL. (**B** and **C**) In some cells GFP signals were predominantly visible in the nucleus (arrow head), but not in the nucleolus (asterisk). Strong GFP-ZmDSUL fluorescence was also visible in the cytoplasm, while the majority of cells showed an even distribution between nucleus and cytoplasm (**D** and **E**). (**F-I**) BMS suspension cells bombarded with gold particles harboring a *p35S:ZmDSUL-GFP* construct. Signals were exclusively detected in the cytoplasm polar at the nuclear surface (**F** and **H**). (**J** and **K**) BMS suspension cells bombarded with gold particles carrying a *pUbi:GFP* construct . GFP signals are visible at equal intensities in the nucleus and cytoplasm excluding the nucleolus. Nuclei in the images are indicated by arrowheads and nucleoli by asterisks. B, D, F, H and J: UV microscopy images and C, E, G, I and K UV images merged with respective bright field microscopy images. Scale bars are 20µm.

### *ZmDSUL* is exclusively expressed in the micropylar region of the female gametophyte and up-regulated after fertilization

We analyzed the expression pattern of *ZmSUMO1a*, *ZmSUMO1b* and *ZmDSUL* in various maize tissues and cells of the female gametophyte (FG) by RT-PCR. As shown in Fig. 4A, *ZmSUMO1b* is ubiquitously expressed in all tissues analyzed, while *ZmSUMO1a* is particularly expressed in vegetative and male reproductive tissues. In contrast, expression of *ZmDSUL* could not be detected in any of the vegetative and reproductive tissues analyzed. A more detailed expression analysis of these genes in isolated cells of the FG before and after fertilization (Fig. 4B) indicated relatively low transcript amounts of *ZmSUMO1a* and *ZmSUMO1b* in both egg cells and zygotes (24 hours after pollination). Transcripts derived from synergids were detected after Southern blotting (data not shown). In contrast, *ZmDSUL* is highly expressed in egg cells and even stronger in zygotes confirming the egg cell EST cluster data, where *ZmDSUL* was identified as one of the most abundant ESTs present in the maize egg cell. Significant expression was also detected in synergids, while expression in central cells and sperm cells was not detectable. Due to its specific expression pattern in the female gametophyte, we have restricted further analyses to *ZmDSUL.*

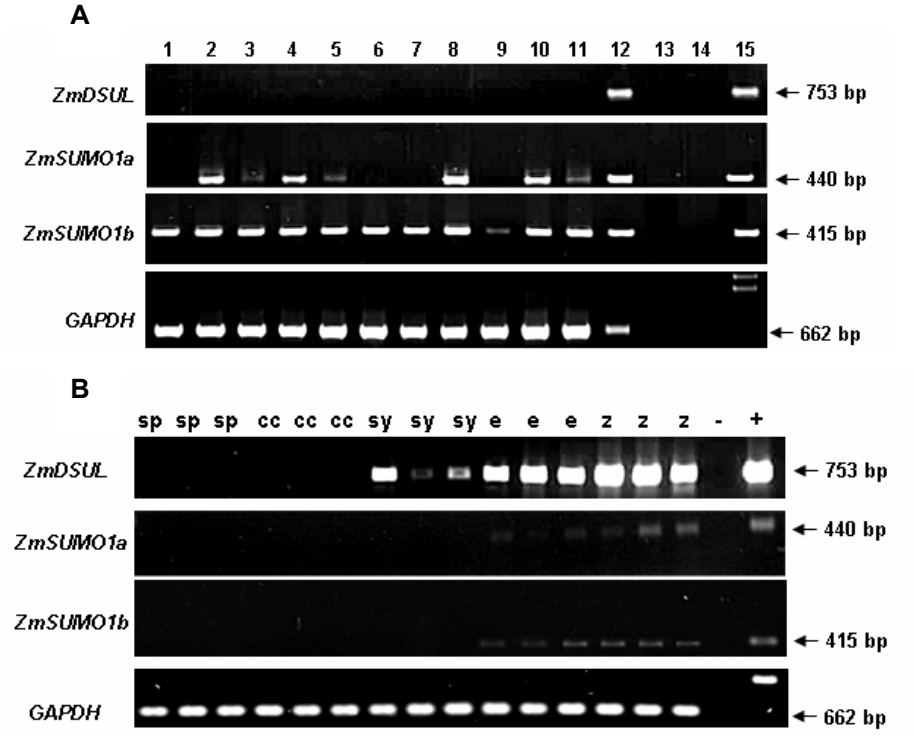


**Figure 4. Expression of *ZmDSUL, ZmSUMO1a* and *ZmSUMO1b* in various tissues and microdissected cells of the female gametophyte of maize before and after fertilization.**
(**A**) RT-PCR was performed from various maize tissues by using *ZmDSUL, ZmSUMO1a, ZmSUMO1b* and *GAPDH* specific primers. Tissues are as follows: 1: embryo 10 days after pollination; 2: mature leaf; 3: root tips; 4: roots; 5: internodes; 6: nodes; 7: mature tassels; 8: mature pollen; 9: mature ovules; 10: mature anthers; 11: embryo 25 days after pollination; 12, egg cell (positive control); 13: water (negative control); 14: blank lane and 15: PCR from genomic DNA. (**B**) RT-PCR was performed on mRNA from individual cells of the female gametophyte by using same primers as A (cc: central cell; e: egg cell; sp: sperm cells; sy: synergid; z: zygote, isolated 24 hours after pollination; -: blank line; +: PCR from genomic DNA). The length of the PCR products is indicated.

In order to study the onset of *ZmDSUL* expression during FG development, we cloned 1567 base pairs upstream of the open reading frame (ORF) as the *ZmDSUL* promoter (*ZmDSULp*). This promoter region was then used to drive expression of GFP fused C-terminally to ZmDSUL in transgenic maize in order to identify both, the earliest promoter activity in the female gametophyte and the sub-cellular localization pattern of the GFP signal perhaps enhanced due to aggregate formation as shown in Fig. 3F-I. A major drawback of these studies was that the FG in maize is deeply embedded in the maternal tissues of the ovary. A large number of unfertilized maize ears at various stages of development were therefore collected from transgenic and control plants, and ovule pieces containing the FG had to be dissected in each case before microscopy. As shown in Fig. 5A and B, earliest GFP signals were detectable at FG stage 5 in the micropylar spindle pole region containing undifferentiated egg and synergid nuclei. At this FG developmental stage (see Fig. 6 for stages), the FG contains already eight nuclei, four at each pole, but polar nuclei not yet approached to each other (not visible in this image) and cellularization did not yet occur. Three examples of mature FGs (FG stage 7/8) are shown in Fig. 5C-H. These examples display GFP signals exclusively in the micropylar region of the FG containing the egg apparatus (egg cell and two synergids). GFP accumulation sites could be observed in some FGs (Fig. 5E and F), but the resolution was not good enough to conclude whether these represent the vicinity of egg and synergid nuclei, respectively.

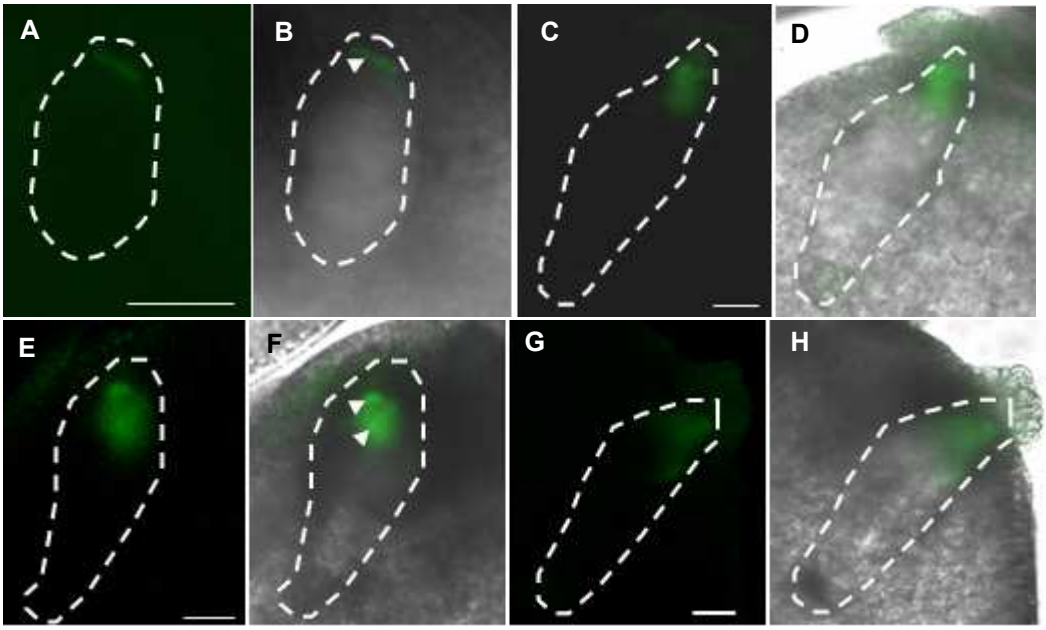

**Figure 5. *ZmDSUL* promoter activity is exclusively detectable in the maize female gametophyte from FG stage 5 onward depositing a C-terminal GFP fusion protein at the micropylar pole.**
Ovules of transgenic *pZmDSUL:ZmDSUL-GFP* lines were sectioned and scanned by CLSM. (A, C, E and G) show UV microscopy images, while (B, D, F and H) display the particular UV image merged with its corresponding bright field microscopy image to visualize the deeply in maternal tissues embedded FG (outlined with an interrupted white line). (**A** and **B**) GFP signals (arrowhead) were first detectable at FG stage 5/6 in the micropylar spindle pole region containing undifferentiated egg and synergid nuclei. (**C**-**H**) Three examples of mature FGs (FG stage 7/8) displaying GFP signals in the egg apparatus. The arrowheads in (F) point towards GFP accumulation sites.

## ZmDSUL is required for polar nuclei positioning and cell specification during female gametophyte maturation

In order to investigate the role of ZmDSUL during FG and zygote/early embryo development, we first established a method to visualize megasporogenesis and megagametogenesis in maize. The size of the female inflorescence and silk length was measured and correlated with developmental stages as described by Huang and Sheridan (1994). We adapted a method originally described by Young et al. (1979) with modifications by Vollbrecht and Hake (1995). In order to understand whole FG structures, cleared ovules were sectioned and pieces containing FGs scanned by CLSM. Only sections with a cut face longitudinally to the mature FG could be fully scanned and taken into consideration to quantify phenotypes (see below).

Meiotic stages could be observed at a silk/female inflorescence length of 0-0.5 mm. Fig. 6A shows an enlarged sub-epidermal megaspore mother cell (archesporial cell). During progression of differentiation and enlargement, the nucleus is positioned towards the micropylar pole and the chromatin becomes condensed (pachytene stage in Fig. 6B). The nucleolus is still visible at the diplotene stage (Fig. 6C). Figure 5D shows the ten homologous chromosome pairs aligned at the equatorial plate and the spindle apparatus is visible. Female meiosis finally results in a linear tetrad of four megaspores. The three megaspores orientated towards the micropyle degenerate (Fig. 6E and F). The functional megaspore (FG stage 1) forms the mature FG after three mitotic nuclear divisions. At FG stage 1 silk length of 0.5-1 mm was measured. After the first mitotic nucleus division (FG stage 2), both nuclei are separated from each other by a large vacuole (Fig. 6G). The micropylar and chalazal poles are occupied by additional vacuoles. Further mitotic nuclei divisions occur at both poles first generating a four nucleate (FG stage 3-4, silk length 1-4 mm, in Fig. 6H) and later eight nucleate immature FG (stage FG 5, silk length 4-5 mm, in Fig. 6J). Between stage FG 5 and 6, one nucleus from each pole moved towards the center of the FG (Fig. 6J) to approach each other and to stay in direct contact. An eight-nucleate immature FG at stage 6 (silk length 5-7 mm) is shown in Fig. 6K. Polar nuclei have approached each other, egg and two

synergid nuclei are visible in the micropylar region and antipodal cells are beginning to form at the chalazal pole. Finally, a fully mature and differentiated FG (at stage FG 7/8, silk length 7 mm onwards) is shown in Fig. 6L. Egg cell and two synergids have been specified, polar nuclei of the central cell are positioned close to the egg cell, large vacuoles have formed inside the central cell and antipodals have divided to form a cluster of at least 20 cells.

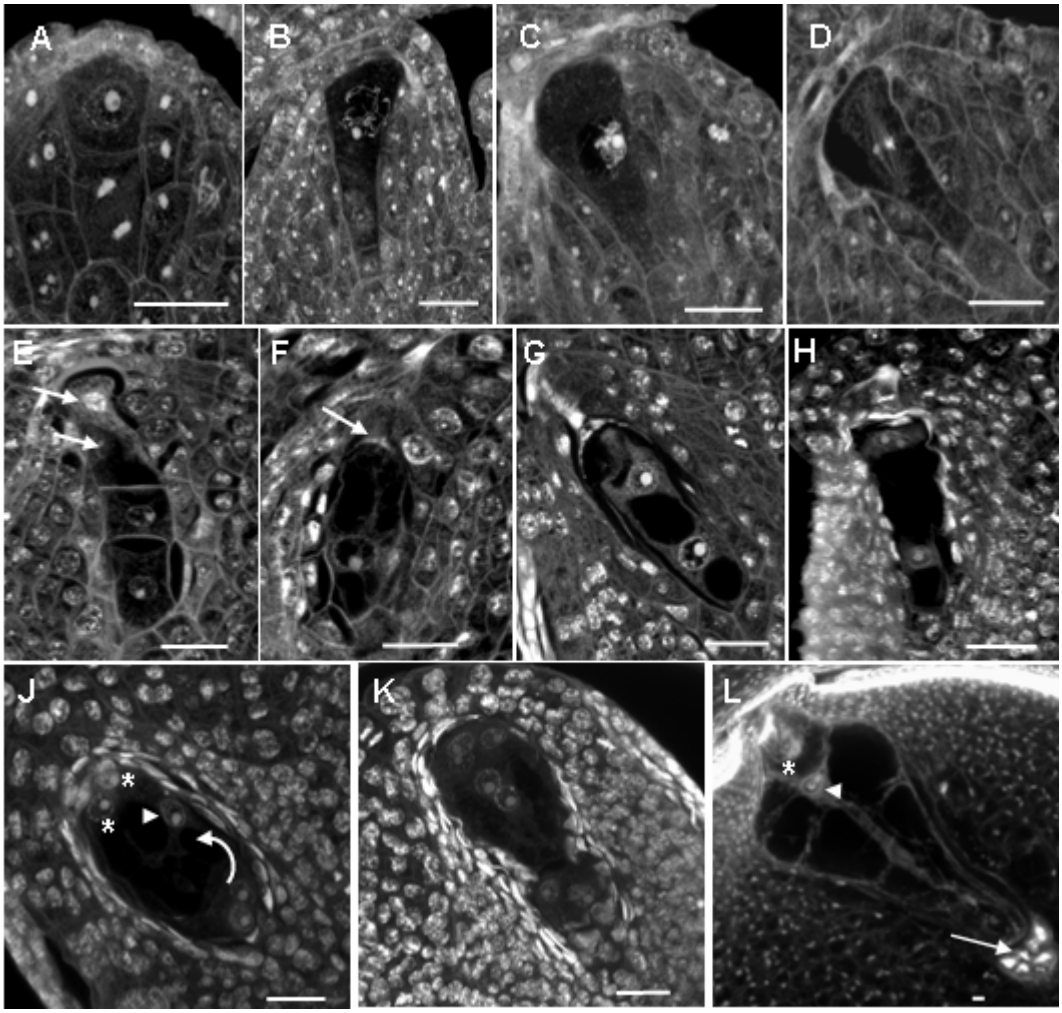


**Figure 6. Longitudinal CLSM sections of maize ovules to visualize nuclei division and migration during megasporogenesis and megagametogenesis.**
(**A**) Sub-epidermal megaspore mother cell (MMC) before the first meiotic division. MMC at pachytene stage (**B**), at diplotene stage (**C**) and at metaphase I (**D**). (**E**) Quartet megaspore stage formed after meiosis. The two micropylar megaspores have started to degenerate (arrows). (**F**) The three micropylar megaspores are degenerated (arrow). The remaining large nucleus represents the functional megaspore (stage FG 1). (**G**) Two-nucleate female gametophyte (FG) stage (stage FG 2). Nuclei are separated by a large vacuole. (**H**) Four-nucleate FG (stage FG 3/4). (**J**) Eight-nucleate immature FG (stage FG 5/6) shortly before the polar nuclei approached each other. A nucleus from the micropylar region moved towards the center of the FG (arrowhead) to meet the second polar nucleus migrating at a longer distance (arrow) from the chalazal region of the immature FG. Egg and one synergid nuclei (asterisks) are visible in the micropylar region of the FG. (**K**) Eight-nucleate immature FG (stage FG 6). Polar nuclei have approached each other, egg and two synergid nuclei are visible in the micropylar region and antipodal cells are beginning to form at the chalazal pole. (**L**) Mature FG (stage FG 7/8). Egg cell (asterisk) and synergids are fully differentiated, polar nuclei (arrowhead) are positioned close to the egg cell and antipodals have divided to form a cluster of cells (arrow). Large vacuoles have formed in the cytoplasm of the central cell. Scale bars are 20 µm.

An RNAi silencing approach was conducted to down-regulate *ZmDSUL* gene activity and to study its role during FG development, maturation and function. In contrast to WT plants (Fig. 7A), seed set was impaired in a number of independent transgenic *ZmDSUL*-RNAi lines. The RNAi lines # 1 (accession #1513) and RNA line # 2 (accession # 1515) showed the most severe effect with about 35 to 44% undeveloped seeds in the T1 generation (Fig. 7B). Ears from these two independent heterozygous *ZmDSUL*-RNAi lines of the T2 generation (Tab. 2) were collected at maturity (silk length of about 5 cm onwards) and subjected to a cytological analysis using the fixing/clearing method described above. Maternal sporophytic tissues of all ovaries were fully developed to maturity and we could not observe morphological differences between WT and *ZmDSUL*-RNAi ovaries. WT control plants contained about 96% fully differentiated FGs (Fig. 6L; Tab. 2). In contrast, heterozygous *ZmDSUL*-RNAi ovaries only contained about 62-79% differentiated FGs (Tab. 2). A more detailed analysis revealed a variation of phenotypes, but meiotic and mitotic nuclei division seemed to be completed as all FGs contained eight nuclei (Fig. 7C-G) or a degenerated FG at a later stage of maturation (Fig. 7H-K). A number of ovules contained eight nuclei in the center of the FG (Fig. 7C-F) that were positioned at opposite poles in WT ovules (Fig. 6J). Additionally the large central vacuole was missing. Moreover, nuclei were not separated from each other, a prerequisite for cell specification occurring at this stage of FG maturation. We also observed a number of FGs displaying a more polar distribution of four nuclei towards each pole at a slightly later developmental stage (Fig. 7G), but also in these FGs polar localization was not completed, nuclei directly attached to each other and nuclei in the micropylar region of unequal size, either due the initiation of egg apparatus specification or the beginning of disintegration processes. When very mature ovaries at FG stage 8 were analyzed, a relative large number of ovaries showed disintegration of FG nuclei and cytoplasm, were collapsed or appeared empty (Fig. 7H-K). The frequency of phenotype occurrence is shown in Tab. 2. The RNAi lines #1 and #2 were analyzed while silks from the ears had a maximum length of about 6 cm corresponding to FG maturation stage FG7/8. Mutant ovaries displayed a developmental arrest at FG stage 5/6. Very mature mutant ovaries (RNAi line # 2 with a silk length >6cm) analyzed at FG stage 8 showed one/third collapsed or empty FGs. Due to the thickness of very mature FG samples, scanning was difficult and a reduced number of FGs were analyzed. In summary, we conclude that megagametogenesis is not affected by *ZmDSUL* down-regulation until FG stage 5, which correlates with the onset of *ZmDSUL* promoter activity. All mitotic divisions were completed, but nuclei neither properly positioned at FG poles nor sufficiently separated from each other. As a consequence, egg cell-, synergid-,

central cell- and antipodal cell-specification could not take place and the FG instead disintegrated without affecting maturation of surrounding maternal tissues.

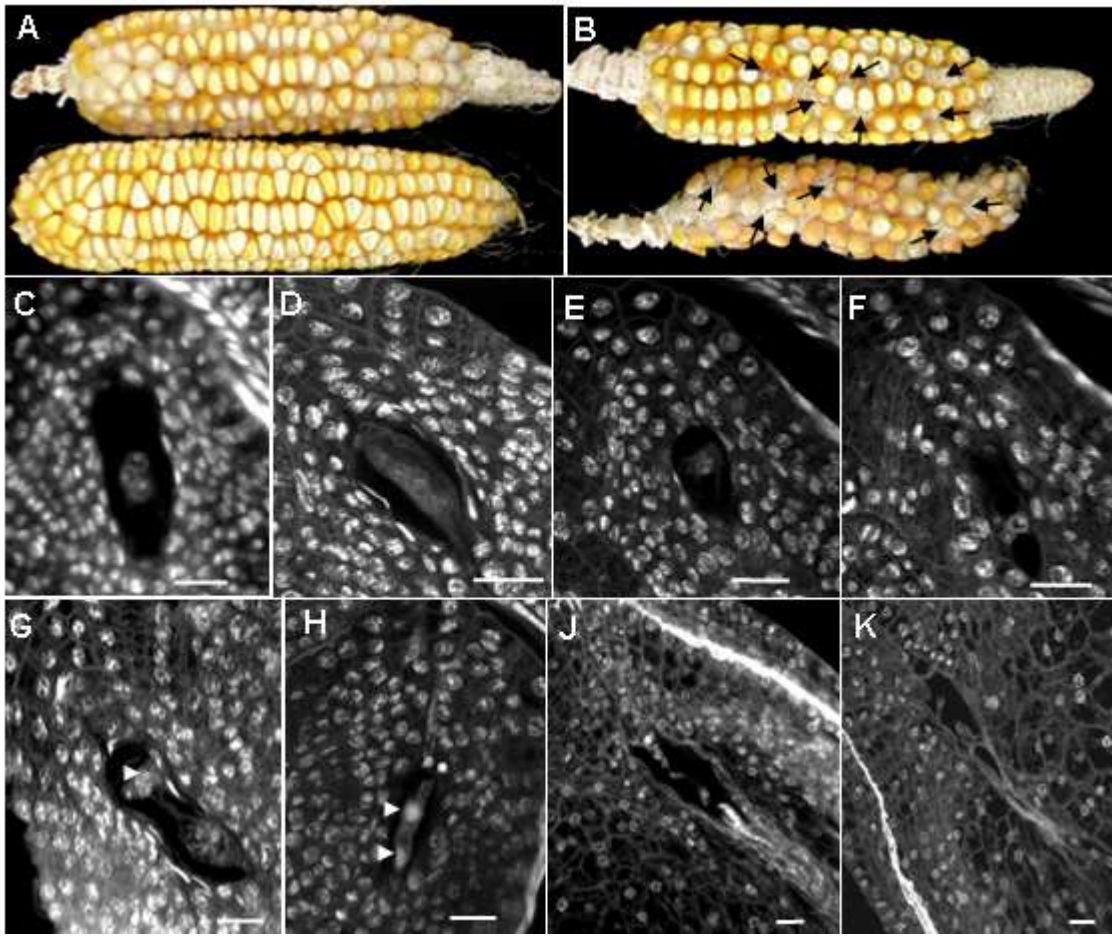


**Figure 7. Longitudinal CLSM sections of *ZmDSUL*-RNAi ovules display lack of polar nuclei positions and abnormal nuclei size during female gametophyte maturation.**
(**A**) Ears from an A188 wild-type plants. (**B**) Ears from *ZmDSUL*-RNAi mutant plants line #1 (accession 1513, top) and line #2 (accession 1515, bottom), respectively. Example arrows point towards ovaries that did not initiate seed development. Ovules of heterozygous *ZmDSUL*-RNAi plants were analyzed after silk emergence. At this stage, wt ovule contained fully differentiated and mature embryo sacs. (**C** and **D**) Mutant ovules are arrested at stage FG 5/6. All eight nuclei are localized in the center of the FG (three of eight nuclei localized in the center of the FG are visible in the focus plane in C) or not completely positioned at the poles (D). Egg apparatus and antipodal regions are not specified. (**E** and **F**) FG from two focus planes of one specimen at the eight-nucleate stage (FG 6). Each FG pole contains four nuclei of a different size, but cellularization and thus cell fate determination did not take place. (**G**) Similar phenotype as in (E/F): a group of four nuclei at each pole attached to each other and varying in size especially at the micropylar pole (arrowhead). (**H**) Arrest of FG pole differentiation at stage FG 5/6. Nuclei (arrows) of a mutant female gametophyte have started to degenerate. (**J** and **K**) Progression of degeneration culminated in tiny empty female gametophytes lacking nuclei. Scale bars are 20 µm.

**Table 2. Developmental defects of maize female gametophytes (FGs) in *ZmDSUL*-RNAi lines.** Sporophytic tissues of the ovary were fully differentiated in WT and RNAi lines. FG: female gametophyte.

| | n[1] | Fully differentiated FGs (%) | Nuclei accumulation in the FG center (%) | Unequal nuclei size (%) | Collapsed FG (%) | Empty FG (%) |
|---|---|---|---|---|---|---|
| WT a/b | 63 | 96 | - | - | 4 | - |
| RNAi #1[a] | 67 | 77 | 6 | 7 | 10 | - |
| RNAi #2[a] | 78 | 79 | 4 | 8 | 9 | - |
| RNAi #2[b] | 52 | 62 | - | 4 | 12 | 22 |

**n[1]** = number of scanned embryo sacs
[a] = silk length 3-6 mm
[b] = silk length >6 mm

## DISCUSSION

### Cell specification and viability of the female gametophyte

Although the maturation of the angiosperm female gametophyte is an attractive system to study fundamental cellular and developmental processes such as asymmetric nuclei position and migration as well as position dependent cell fate determination, until recently little progress has been made due to the deep embedding of the embryo sac in the maternal tissues of the ovary. The establishment of powerful forward and reverse genetics methods combined with a toolkit of cellular markers now enables to study these processes in the model plant Arabidopsis (Pagnussat et al. 2005; Jones-Rhoades et al. 2007; Berger et al. 2008) and led researchers to the conclusion that the 'angiosperm female gametophyte is no longer the forgotten generation' (Brukhin et al. 2005). However, until now only few genes expressed in the female gametophyte have been studied at the functional level and we are just beginning to uncover the genes involved, for example, in cell specification during embryo sac maturation (Groß-Hardt et al. 2007). In other plants such as maize, which, due to the large size of its embryo sac, is especially suited for these studies, until now only one report described the molecular identity of a gene involved in position-based determination of female gametophyte cell identity. IG1 encoding a LOB domain protein restricts nuclei division before

cellularization (Huang and Sheridan, 1996; Evans 2007). In contrast to *dsul* mutant phenotypes described in this report, the *ig1* mutant is viable in most genetic backgrounds. A large scale genetic deficiency screen was conducted to characterize female gametogenesis in maize (Vollbrecht and Hake, 1995). Although this screen did not result in the identification of the genes involved, genetically separable female gametogenesis programs were identified and it was further demonstrated that embryo sac development requires postmeiotic gene expression. In conjunction with the *dsul* phenotypes it is noteworthy that many mutant embryo sacs described were degenerated and degeneration often began at the micropylar pole where *DSUL* is expressed. Moreover, some mutant embryo sacs defective in cellular patterning/cell specification contained nuclei of a different size and occasionally micronuclei similar to findings in *dsul* mutant ovaries. The cytological analysis of partly sterile *indica/japonica* hybrids in rice indicated that sterility was mainly caused by female gametophyte development defects (Zeng et al. 2009). The described phenotypes partly overlapped with those described for *dsul* mutant ovaries: the eight-nucleate stage was shown to be most severely affected by asynchronous nuclear migration and abnormal positioning of nuclei as well as egg apparatus or complete female gametophyte degeneration. Due to our observations using young and very mature ovaries, we suggest that the latter phenotypes are likely a consequence of abnormal nuclei positioning as well as a failure of cell specification.

**Does DSUL play a role for spindle elongation and asymmetry?**

A detailed investigation of *dsul* mutant ovaries showed that mitotic nuclei division cycles were completed, but the eight nuclei of the immature female gametophyte were localized either centrally in the FG or not properly distributed towards the micropylar and chalazal poles. Moreover, nuclei often were not separated from each other, a prerequisite for cell specification. A similar phenotype has been described for Arabidopsis embryo sacs of double heterozygous F1 mutants defective in both *γ-tubulin* genes. About 16% abnormal female gametophytes were observed at the eight-nucleate stage displaying abnormal number, position and appearance of nuclei. Spindle and phragmoplast structures associated with cytokinesis were aberrant (Pastuglia et al., 2006). Highly conserved γ-tubulin plays a major role for microtubule nucleation at MTOCs (microtubule organizing centers) and thus the establishment and organization of the mitotic spindle apparatus (Hendrickson et al., 2001).

SUMO has recently been reported to be a key of regulating miotic spindle-asymmetry in yeast (Leisner et al., 2008). It was shown that SUMOylation of the spindle-orientation protein Kar9 regulates its asymmetric localization and thus positioning of both the spindle poles and

the daughter nuclei. A number of reports showed an important role of SUMOylation for chromosome segregation in yeast (for review Watts 2007). In mammalian cells, it was shown that SUMO-2/3 localized to centromeres and condensed chromosomes, whereas SUMO-1 localizes to the mitotic spindle and spindle midzone (Zhang et al., 2008). In summary the various reports indicate that SUMOylation is essential for mitotic chromosome condensation, sister chromatid cohesion, kinetochore function, mitotic spindle elongation and asymmetry. Regarding that *dsul* mutant embryo sacs contained eight nuclei, although partly of a different size and attached to each other, we suggest that DSUL might be involved in the regulation of spindle elongation and asymmetry during megagametogenesis, but that it is not or less important for chromosome segregation itself.

**ZmDSUL localization to the nucleoplasm, cytoplasm and aggresome**

The subcellular localization of the unprocessed N-terminal ZmDSUL-GFP fusion protein displayed localization in both nucleoplasm and cytoplasm, with a stronger accumulation in the nucleus excluding the nucleolus of some cells. A similar pattern has been described for the diubiquitin-like protein FAT10 (Kalveram et al., 2008). SUMO and SUMOylation substrates are predominately nuclear, although a number of targets are also exclusively cytoplasmic (Herrmann et al., 2007; Seeler and Dejean, 2003; Vertegaal et al., 2006; Zhao, 2007). The subcellular localization pattern of GFP-ZmDSUL suggests that it might also be involved to modify target proteins both in the cytoplasm and nucleoplasm. A very interesting subcelluar localization pattern was observed when GFP was C-terminally fused to ZmDSUL. The fusion protein localized exclusively perinuclear at one site of the nuclear surface. Such a protein accumulation pattern has been reported previously to occur when cytosolic GFP-fusion proteins are either overexpressed, misfolded, inappropriately assembled, aberrant modified or induced by environmental stress and has thus been termed aggresome formation (Johnston et al., 1998; García-Mata et al., 1999; Kawaguchi et al., 2003). The aggresome represents a huge proteasome complex in immediate proximity to the centrosome in animal cells. In our studies we never observed aggresome formation when GFP was fused N-terminally to ZmDSUL. With the exception of a MATH/BTB domain protein probably involved in designating target proteins in the female gametophyte for ubiquitinylation (D. Leljak-Levanić, K. Srilunchang, M. Juranic, L. Soljic, T. Dresselhaus and S. Sprunck, unpublished data), we never observed this pattern when the same GFP protein was C-terminal fused to a number of other cytoplasmic proteins. Considering that ZmDSUL is cleaved at the C-terminus, it is possible that the aggregate formation observed either represents the subcellular ZmDSUL maturation site or GFP is recognized as a ZmDSUL target for

degradation via a perinuclear plant aggresome/proteasome complex that is deviating in structure from the previously reported animal aggresome of a ball-like shape. Provided that ZmDSUL utilizes the same or similar enzyme complexes, this hypothesis is supported by the finding that animal SUMO hydrolases and desumoylases occur in distinct domains in and around the nucleus (Zhao, 2007). Moreover, the cytoplasmic protein histone deacetylase 6 (HDAC6), which mediates the transport of polyubiquitylated cargo to the aggresome (Hubbert et al., 2002; Kawaguchi et al., 2003) was recently found to also interact with FAT10. Endogenous and ectopically expressed FAT10 as well FAT10-GFP localized to the aggresome under proteasome inhibiting conditions in a microtubule-dependent manner (Hipp et al., 2005; Kalveram et al., 2008). However, in contrast to our observations, N- and C-terminal fusion of GFP to FAT10 both displayed aggresome localization only under proteasome inhibiting conditions, suggesting that ZmDSUL might possess other or additional functions than labeling proteins for degradation.

**ZmDSUL structure and maturation**

Based on the data presented we conclude that both ZmSUMO1a/b and ZmDSUL preproteins are carboxy-terminally truncated to expose a diglycine (GG) motif for SUMOylation and DSULylation, respectively. In contrast to the diubiquitin-like proteins FAT10 and ISG15, diSUMO-like DSUL from maize and wheat contain the conserved GG motif also centrally and exposed between both SUMO-like domains. Biochemical studies in tobacco have revealed that DSUL is not cleaved at this position. Therefore, we conclude that DSUL is a third member of the family of dimeric ubiquitin-related proteins. Another open question is related to the occurrence of polyDSULylation: while SUMO-1 generally leads to monomodification, SUMO-2/3 can lead to chain formation via the N-terminally located and conserved SUMOylation motif ψKxE/D (where ψ is a large hydrophobic residue such as Val, Leu, Ile, Phe or Met and x is any kind of amino acid; Tatham et al., 2001; Matic et al., 2008). While ZmDSUL contains this motif only once in the middle of the C-terminal and not N-terminal SUMO-like domain, TaDSUL does not contain this motif indicating that polyDSULylation likely does not occur.

Although ZmDSUL is only about 13% homologous to HsISG at the amino acid level, we were able to predict a 3-D model based on the available X-ray diffraction data for ISG15 (Narasimhan et al., 2005), conserved core amino acid positions and a very similar predicted secondary structure. The predicted DSUL structure is amazingly similar to that of ISG15 and it will be interesting to find out whether similar enzymes used for ISGylation/deISGylation, which are different from those required for SUMOylation/deSUMOylation, are also involved in

conjugation/deconjugation of DSUL. ISG15 utilizes, for example, the E2 enzyme UBC8 while SUMO utilizes the single E2 enzyme UBC9 (Kim et al., 2004; Zhao 2007). UBC7 as well as UBC9, the latter of which is likely involved in ZmSUMO1a/b conjugation, are expressed in the maize embryo sac (de Vries et al., 1998; Yang et al. 2006), but a gene encoding UBC8 was not yet reported. Future work should thus include the detection of the enzymatic DSUL maturation, activation, conjugation as well as deconjugation machinery. However, due to very specific and restricted expression pattern of *DSUL* in the female gametophyte, these efforts are biochemically limited and a technical challenge.

**Outlook**

Loss-of-function and gain-of-function studies in various organisms have resulted in an emerging paradigm that SUMOylation regulates a number of developmental processes in both animals and plants (for review Zhao 2007; Miura et al., 2007.). Although most biological processes regulated by SUMOylation are not yet identified, T-DNA insertions in SUMO E2 enzymes or SUMO1/SUMO2 double mutants, for example, cause early embryo lethality in Arabidopsis (Saracco et al., 2007). In animals, mutations of the single SUMO E2 enzyme UBC9 have been shown to lead to meiotic defects in the fruit fly as well as to embryogenic lethality in *C. elegans* and mice (for review Zhao 2007). Moreover, in mammalians SUMO-1 has been reported to be required for development of lip and palate during later embryonic stages (Alkuraya et al., 2006). Although a large number of reports are already available about diubiquitin-like ISG15 and FAT10, surprisingly little is known about their role in development. Mice homozygous for the disruption of the *FAT10* gene were viable and fertile (Nakayama et al., 2006). Detailed studies revealed that lymphocytes were more prone to spontaneous apoptotic death and FAT10 was thus suggested as a survival factor (Canaan et al., 2006).

Even less is known about SUMOylation during gametogenesis. It was shown that SUMOylation is dynamic and likely involved in the modulation of gene expression during mammalian oocyte and spermatid growth and maturation, but functional data have not yet been provided (Ihara et al., 2008, La Salle et al., 2008). The role of SUMOylation for plant male and female gametogenesis has not been investigated before. Due to the overall expression pattern of *ZmSUMO1a/b* and the expectation to obtain numerous phenotypes and lethality of *ZmSUMO1a/b*-RNAi silencing, we have restricted our studies on *diSUMO-like* from maize, which is specifically expressed in the female gametophyte. However, due to the termination of embryo sac development at FG stage 5/6, it was not possible to study the role of ZmDSUL in mature eggs as well as during zygote and early embryo development. The

increased expression pattern after fertilization indicates that ZmDSUL likely also has post-zygotic functions. A mature egg/zygote-specific loss-of-function approach will be required to address this question. Moreover, in contrast to the stages of megagametogesis, mature and fertilized egg cells as well as early embryos are more easily accessible and may provide access to identify both, DSUL targets and the corresponding enzymatic machinery.

**ACKNOWLEDGEMENTS**

We are grateful to Stefanie Sprunck for helpful discussions and for providing wheat egg cell expressed *DSUL* cDNA clones. Ulrich Hammes is acknowledged for critical comments on the manuscript, Matthew M.S. Evans for helpful suggestions for the histological studies and Marco Bocola for the introduction into 3-D protein modeling. We thank Svenja Rademacher for providing ER-GFP protein. This work was supported by a post-graduate scholarship to K.S. in accordance with Hamburg's Young Academics Funding Law.

## REFERENCES

**Alkuraya, F. S., Saadi, I., Lund, J. J., Turbe-Doan, A., Morton, C. C. and Maas, R. L.** (2006). SUMO1 haploinsufficiency leads to cleft lip and palate. *Science* **313**, 1751.

**Anckar, J. and Sistonen, L.** (2007). SUMO: getting it on. *Biochem Soc Trans* **35**, 1409-13.

**Becker, D., Brettschneider, R. and Lörz, H.** (1994). Fertile transgenic wheat from microprojectile bombardment of scutellar tissue. *Plant J* **5**, 299-307.

**Berger, F., Hamamura, Y., Ingouff, M. and Higashiyama, T.** (2008). Double fertilization - caught in the act. *Trends Plant Sci* **13**, 437-43.

**Borges, F., Gomes, G., Gardner, R., Moreno, N., McCormick, S., Feijó, J.A. and Becker, J.D.** (2008) Comparative transcriptomics of Arabidopsis sperm cells. *Plant Physiol* **148**, 1168-81.

**Brettschneider, R., Becker, D. and Lörz, H.** (1997). Efficient transformation of scutellar tissue of immature maize embryos. *Theor Appl Genet* **94**, 737-48.

**Brukhin, V., Curtis, M.D. and Grossniklaus, U.** (2005). The angiosperm female gametophyte: no longer the hidden generation. *Curr Sci* **89**, 1844-52.

**Canaan, A., Yu, X., Booth, C. J., Lian, J., Lazar, I., Gamfi, S. L., Castille, K., Kohya, N., Nakayama, Y., Liu, Y.C., Eynon, E., Flavell, R., and Weissmann, S.M.** (2006) FAT10/diubiquitin-like protein-deficient mice exhibit minimal phenotypic differences. Mol Cell Biol *26*, 5180-9.

**Cordts, S., Bantin, J., Wittich, P. E., Kranz, E., Lörz, H. and Dresselhaus, T.** (2001). ZmES genes encode peptides with structural homology to defensins and are specifically expressed in the female gametophyte of maize. *Plant J* **25**, 103-14.

**Desterro, J. M., Rodriguez, M. S., Kemp, G. D. and Hay, R. T.** (1999). Identification of the enzyme required for activation of the small ubiquitin-like protein SUMO-1. *J Biol Chem* **274**, 10618-24.

**de Vries, A., Cordts, S., Dresselhaus, T.** (1998). Molecular characterization of a cDNA encoding an ubiquitin carrier protein (UBC7) isolated from egg cells of maize (Accession No. AJ002959) (PGR98-177). *Plant Physiol* **118**, 1011.

**D'Halluin, K., Bonne, E., Bossut, M., De Beuckeleer, M. and Leemans, J.** (1992). Transgenic maize plants by tissue electroporation. *Plant Cell* **4**, 1495-505.

**Dresselhaus, T., Lörz, H. and Kranz, E.** (1994). Representative cDNA libraries from few plant cells. *Plant J* **5**, 605-10.

**Drews, G. N. and Yadegari, R.** (2002). Development and function of the angiosperm female gametophyte. *Annu Rev Genet* **36**, 99-124.

**Evans, M. M.** (2007). The indeterminate gametophyte1 gene of maize encodes a LOB domain protein required for embryo Sac and leaf development. *Plant Cell* **19**, 46-62.

**García-Mata, R., Bebok, Z., Sorscher, E. J. and Sztul, E. S.** (1999). Characterization and dynamics of aggresome formation by a cytosolic GFP-chimera. *J Cell Biol* **146**, 1239-54.

**Gross-Hardt, R., Kagi, C., Baumann, N., Moore, J. M., Baskar, R., Gagliano, W. B., Jurgens, G. and Grossniklaus, U.** (2007). LACHESIS restricts gametic cell fate in the female gametophyte of Arabidopsis. *PLoS Biol* **5**, e47.

**Geiss-Friedlander, R. and Melchior, F.** (2007). Concepts in sumoylation: a decade on. *Nat Rev Mol Cell Biol* **8**, 947-56.

**Gill, G.** (2004). SUMO and ubiquitin in the nucleus: different functions, similar mechanisms? *Genes Dev* **18**, 2046-59.

**Green, C. E. and Phillips, R. L.** (1975). Plant regeneration from tissue cultures of maize. *Crop Sci* **15**, 417-421.

**Haglund, K. and Stenmark, H.** (2006). Working out coupled monoubiquitination. *Nat Cell Biol* **8**, 1218-9.

**Hatakeyama, S. and Nakayama, K. I.** (2003). Ubiquitylation as a quality control system for intracellular proteins. *J Biochem* **134**, 1-8.

**Hay, R. T.** (2005). SUMO: a history of modification. *Mol Cell* **18**, 1-12.

**Hendrickson, T. W., Yao, J., Bhadury, S., Corbett, A. H. and Joshi, H. C.** (2001). Conditional mutations in gamma-tubulin reveal its involvement in chromosome segregation and cytokinesis. *Mol Biol Cell* **12**, 2469-81.

**Herrmann, J., Lerman, L. O. and Lerman, A.** (2007). Ubiquitin and ubiquitin-like proteins in protein regulation. *Circ Res* **100**, 1276-91.

**Hipp, M. S., Kalveram, B., Raasi, S., Groettrup, M. and Schmidtke, G.** (2005). FAT10, a ubiquitin-independent signal for proteasomal degradation. *Mol Cell Biol* **25**, 3483-91.

**Holsters, M., Silva, B., Van Vliet, F., Genetello, C., De Block, M., Dhaese, P., Depicker, A., Inze, D., Engler, G., Villarroel, R. et al.** (1980). The functional organization of the nopaline A. tumefaciens plasmid pTiC58. *Plasmid* **3**, 212-30.

**Huang, B.-Q. and Sheridan, W. F.** (1994). Female gametophyte development in maize: microtubular organization and embryo sac polarity. *Plant Cell* **6**, 845-61.

**Hubbert, C., Guardiola, A., Shao, R., Kawaguchi, Y., Ito, A., Nixon, A., Yoshida, M., Wang, X. F. and Yao, T. P.** (2002). HDAC6 is a microtubule-associated deacetylase. *Nature* **417**, 455-8.

**Ihara, M., Stein, P. and Schultz, R. M.** (2008). UBE2I (UBC9), a SUMO-conjugating enzyme, localizes to nuclear speckles and stimulates transcription in mouse oocytes. *Biol Reprod* **79**, 906-13.

**Johnson, E. S.** (2004). Protein modification by SUMO. *Annu Rev Biochem* **73**, 355-82.

**Johnston, J. A., Ward, C. L. and Kopito, R. R.** (1998). Aggresomes: a cellular response to misfolded proteins. *J Cell Biol* **143**, 1883-98.

**Jones-Rhoades, M. W., Borevitz, J. O. and Preuss, D.** (2007). Genome-wide expression profiling of the Arabidopsis female gametophyte identifies families of small, secreted proteins. *PLoS Genet* **3**, 1848-61.

**Kalveram, B., Schmidtke, G. and Groettrup, M.** (2008). The ubiquitin-like modifier FAT10 interacts with HDAC6 and localizes to aggresomes under proteasome inhibition. *J Cell Sci* **121**, 4079-88.

**Karimi, M., Inze, D. and Depicker, A.** (2002). GATEWAY vectors for Agrobacterium-mediated plant transformation. *Trends Plant Sci* **7**, 193-5.

**Kawaguchi, Y., Kovacs, J. J., McLaurin, A., Vance, J. M., Ito, A. and Yao, T. P.** (2003). The deacetylase HDAC6 regulates aggresome formation and cell viability in response to misfolded protein stress. *Cell* **115**, 727-38.

**Kerscher, O.** (2007). SUMO junction-what's your function? New insights through SUMO-interacting motifs. *EMBO Rep* **8**, 550-5.

**Kim, K. I., Giannakopoulos, N. V., Virgin, H. W. and Zhang, D. E.** (2004). Interferon-inducible ubiquitin E2, Ubc8, is a conjugating enzyme for protein ISGylation. *Mol Cell Biol* **24**, 9592-600.

**Kim, H.J., Oh, S.A., Brownfield, L., Hong, S.H., Ryu, H., Hwang, I., Twell, D., Nam, H.G.** (2008). Control of plant germline proliferation by SCF (FBL17) degradation of cell cycle inhibitors. *Nature* **455**, 1134-7.

**Kirkin, V. and Dikic, I.** (2007). Role of ubiquitin- and Ubl-binding proteins in cell signaling. *Curr Opin Cell Biol* **19**, 199-205.

**Kranz, E., Bautor, J. and Lörz, H.** (1991). In vitro fertilization of single, isolated gametes of maize mediated by electrofusion. *Sex Plant Reprod* **4**, 12-6.

**La Salle, S., Sun, F., Zhang, X. D., Matunis, M. J. and Handel, M. A.** (2008). Developmental control of sumoylation pathway proteins in mouse male germ cells. *Dev Biol* **321**, 227-37.

**Leisner, C., Kammerer, D., Denoth, A., Britschi, M., Barral, Y. and Liakopoulos, D.** (2008). Regulation of mitotic spindle asymmetry by SUMO and the spindle-assembly checkpoint in yeast. *Curr Biol* **18**, 1249-55.

**Liu, J., Zhang, Y., Qin, G., Tsuge, T., Sakaguchi, N., Luo, G., Sun, K., Shi, D., Aki, S., Zheng, N., Aoyama, T., Oka, A., Yang, W., Umeda, M., Xie, Q., Gu, H., Qu, L.J.** (2008) Targeted degradation of the cyclin-dependent kinase inhibitor ICK4/KRP6 by RING-type E3 ligases is essential for mitotic cell cycle progression during Arabidopsis gametogenesis. *Plant Cell* **20**, 1538-54.

**Márton, M. L., Cordts, S., Broadhvest, J. and Dresselhaus, T.** (2005). Micropylar pollen tube guidance by egg apparatus 1 of maize. *Science* **307**, 573-6.

**Matic, I., van Hagen, M., Schimmel, J., Macek, B., Ogg, S. C., Tatham, M. H., Hay, R. T., Lamond, A. I., Mann, M. and Vertegaal, A. C.** (2008). In vivo identification of human small ubiquitin-like modifier polymerization sites by high accuracy mass spectrometry and an in vitro to in vivo strategy. *Mol Cell Proteomics* **7**, 132-44.

**Melchior, F.** (2000). SUMO--nonclassical ubiquitin. *Annu Rev Cell Dev Biol* **16**, 591-626.

**Miura, K., Jin, J.B. and Hasegawa, P.M.** (2007). Sumoylation, a post-transcriptional regulatory process in plants. *Curr Opin Plant Biol* **10**, 495-502.

**Müller, S., Hoege, C., Pyrowolakis, G. and Jentsch, S.** (2001). SUMO, ubiquitin's mysterious cousin. *Nat Rev Mol Cell Biol* **2**, 202-10.

**Murashige, T. and Skoog, F.** (1962) A revised medium for rapid growth and bioassays with tobacco tissue cultures. *Physiol Plant* **15**, 473-97.

**Nakayama, Y., Liu, Y. C. et al.** (2006). FAT10/diubiquitin-like protein-deficient mice exhibit minimal phenotypic differences. *Mol Cell Biol* **26**, 5180-9.

**Narasimhan, J., Wang, M., Fu, Z., Klein, J. M., Haas, A. L. and Kim, J. J.** (2005). Crystal structure of the interferon-induced ubiquitin-like protein ISG15. *J Biol Chem* **280**, 27356-65.

**Nicholas, K. B., Nicholas, H. B. Jr. and Deerfield, D. W. II.** (1997). GeneDoc: analysis and visualization of genetic variation. *Embnew News*, **4**, 14.

**Page, R. D.** (1996). TreeView: an application to display phylogenetic trees on personal computers. *Comput Appl Biosci* **12**, 357-8.

**Pagnussat, G. C., Yu, H. J., Ngo, Q. A., Rajani, S., Mayalagu, S., Johnson, C. S., Capron, A., Xie, L. F., Ye, D. and Sundaresan, V.** (2005). Genetic and molecular identification of genes required for female gametophyte development and function in Arabidopsis. *Development* **132**, 603-14.

**Pallotta, M. A., Graham, R.D., Langridge, P., Sparrow, D.H.B. and Barker, S.J.** (2000). RFLP mapping of manganese efficiency in barley. *Theor Appl Genet* **101**, 1100-8.

**Pastuglia, M., Azimzadeh, J., Goussot, M., Camilleri, C., Belcram, K., Evrard, J. L., Schmit, A. C., Guerche, P. and Bouchez, D.** (2006). Gamma-tubulin is essential for microtubule organization and development in Arabidopsis. *Plant Cell* **18**, 1412-25.

**Saracco, S. A., Miller, M. J., Kurepa, J. and Vierstra, R. D.** (2007). Genetic analysis of SUMOylation in Arabidopsis: conjugation of SUMO1 and SUMO2 to nuclear proteins is essential. *Plant Physiol* **145**, 119-34.

**Schwartz, D. C. and Hochstrasser, M.** (2003). A superfamily of protein tags: ubiquitin, SUMO and related modifiers. *Trends Biochem Sci* **28**, 321-8.

**Seeler, J. S. and Dejean, A.** (2003). Nuclear and unclear functions of SUMO. *Nat Rev Mol Cell Biol* **4**, 690-9.

**Sprunck, S., Baumann, U., Edwards, K., Langridge, P. and Dresselhaus, T.** (2005). The transcript composition of egg cells changes significantly following fertilization in wheat (Triticum aestivum L.). *Plant J* **41**, 660-72.

**Tatham, M. H., Jaffray, E., Vaughan, O. A., Desterro, J. M., Botting, C. H., Naismith, J. H. and Hay, R. T.** (2001). Polymeric chains of SUMO-2 and SUMO-3 are conjugated to protein substrates by SAE1/SAE2 and Ubc9. *J Biol Chem* **276**, 35368-74.

**Thompson, J. D., Higgins, D. G. and Gibson, T. J.** (1994). CLUSTAL W: improving the sensitivity of progressive multiple sequence alignment through sequence weighting, position-specific gap penalties and weight matrix choice. *Nucleic Acids Res* **22**, 4673-80.

**Ulrich, H. D.** (2008). The fast-growing business of SUMO chains. *Mol Cell* **32**, 301-5.

**Vertegaal, A. C., Andersen, J. S., Ogg, S. C., Hay, R. T., Mann, M. and Lamond, A. I.** (2006). Distinct and overlapping sets of SUMO-1 and SUMO-2 target proteins revealed by quantitative proteomics. *Mol Cell Proteomics* **5**, 2298-310.

**Voinnet, O., Lederer, C. and Baulcombe, D. C.** (2000). A viral movement protein prevents spread of the gene silencing signal in *Nicotiana benthamiana*. *Cell* **103**, 157-67.

**Voinnet, O., Rivas, S., Mestre, P. and Baulcombe, D.** (2003). An enhanced transient expression system in plants based on suppression of gene silencing by the p19 protein of tomato bushy stunt virus. *Plant J* **33**, 949-56.

**Vollbrecht, E. and Hake, S.** (1995). Deficiency analysis of female gametogenesis in maize. *Dev Genet* **16**, 44-63.

**Watts, F. Z.** (2007). The role of SUMO in chromosome segregation. *Chromosoma* **116**, 15-20.

**Welchman, R. L., Gordon, C. and Mayer, R. J.** (2005). Ubiquitin and ubiquitin-like proteins as multifunctional signals. *Nat Rev Mol Cell Biol* **6**, 599-609.

**Yang, H., Kaur, N., Kiriakopolos, S. and McCormick, S.** (2006). EST generation and analyses towards identifying female gametophyte-specific genes in Zea mays L. *Planta* **224**, 1004-14.

**Young, B., Sherwood, R. T. and Bashaw, E. C.** (1979). Cleared-pistil and thick-sectioning techniques for detecting aposporous apomixis in grasses. *Can J Bot* **57**, 1668-72.

**Zeng, Y. X., Hu, C. Y., Lu, Y. G., Li, J. Q. and Liu, X. D.** (2009). Abnormalities occurring during female gametophyte development result in the diversity of abnormal embryo sacs and leads to abnormal fertilization in indica/japonica hybrids in rice. *J Integr Plant Biol* **51**, 3-12.

**Zhang, F. P., Mikkonen, L., Toppari, J., Palvimo, J. J., Thesleff, I. and Janne, O. A.** (2008). Sumo-1 function is dispensable in normal mouse development. *Mol Cell Biol* **28**, 5381-90.

**Zhao, J.** (2007). Sumoylation regulates diverse biological processes. *Cell Mol Life Sci* **64**, 3017-33.

# CHAPTER 6

## Summary

Megagametophyte development involves many fundamental phenomena, such as nuclear migration and fusion, polarity, cell death, asymmetric cell division, and cell fate specification. So far, very little is known about genes or gene products that regulate these cellular processes during female gametophyte (FG) development (Drews et al., 1998; Grossniklaus and Schneitz, 1998). To identify genes expressed in the FG, several advanced molecular approaches have been used. One of these is the ability of isolate gametophyte cells and generate cDNA libraries from single embryo sac cell types (Dresselhaus et al., 1994; Le et al., 2005; Márton et al., 2005; Sprunck et al., 2005). Several studies on the transmission of chromosomal deletions have been performed in maize (Vollbrecht and Hake, 1995) and *Arabidopsis* (Vizir et al., 1994) which suggest that a large number of genes are required for FG development as most chromosomal deletion are defective in embryo sac development. Moreover, mutations in genes required in the megagametophyte result in reduced fertility and seed set (Evans and Grossniklaus, 2009). Considering the FG development studies, most mutants have been isolated from *Arabidopsis* (Berger et al., 2008; Jones-Rhoades et al., 2007), but only a few genes have been described in maize (Evans and Grossniklaus, 2009) and their functions elucidated such as IG1 (Evans, 2007). However, the establishment of powerful forward and genetic methods combined with several molecular markers toolkit now allows to study the processes that control FG development also in more detail in maize. By using several molecular techniques, such as RNA interference (RNAi) I could correlate defective phenotypes of maize FG development with various gene activities. Moreover, I have established a histological method to monitor embryo sac development defects occurring at early and late FG stages of transgenic RNAi plants. Subcellular protein localization studies complemented these experiments to visualize the various pattern during development and during the cell cycle.

Following FG development in maize which produces an eight-nucleate embryo sac, the functional megaspore first has to undergo three nuclear divisions. This suggests that the basic cell cycle machinery is required, and any mutation in these cell cycle genes would likely disrupt nuclear division. **Chapter 4** and **Chapter 5** describe the different stages of maize FG development comparing wild-type with mutant phenotypes. In one study, I could

show that knock-down of the MATH-BTB domain containing *ZmMAB1* gene (**Chapter 4**) is required for the first nuclear divisions since embryo sac are arrested at the two-nucleate stage in *mab1* mutants. Besides, the two nuclei were not properly segregated to each pole. This suggests that *ZmMAB1* is essential for the second nuclear division and proper nuclei positioning. The knock-down of the diSUMO-like *ZmDSUL* gene (**Chapter 5**) causes the embryo sac to arrest at the eight-nucleate stage (FG5) and the immature embryo sac degenerated afterwards, indicating that *ZmDSUL* is an essential gene for progression of FG development. More interesting, some *dsul* mutant embryo sacs show unequally nuclei size and a fault of nuclei segregation towards the two poles. This indicates that *ZmDSUL* plays important roles in nuclear division and segregation/position, a prerequisite for cell fate specification. Similar to my studies, mutants of FG mitotic division that occur during megagametognesis (from FG1 to early FG5) were characterized in Arabidopsis by an unusual number of nuclei, or an aberrant distribution of nuclei in the developing embryo sac (Christensen et al., 1998; 2002; Moore et al., 1997; Pagnussat et al., 2005). Therefore, *MAB1* and *DSUL* may control multiple steps to make sure that different development events are spatially and temporally coordinated during embryo sac formation.

A member of the Mini-Chromosome-Maintenance protein family (PROLIFERA/MCM7) has been shown to be essential for FG development in Arabidopsis (Springer et al., 1995). I have therefore studied the role of maize *ZmMCM6* (**Chapter 2**) whose transcripts where first detected in egg cells (Dresselhaus et al., 1999) and strongly induced shortly after fertilization (our data, chapter 2). Besides, the expression of *ZmMCM6* is also detected only in tissues containing proliferating cells, similarly to *AtMCM7* in Arabidopsis (Springer et al., 1995). The mutant *mcm6* phenotype was however pleiotropic due to the broad expression pattern of the gene. A phenotype during FG development could not be studied in detail, as ovules often did not develop properly and the transgene was not transmitted towards progeny generations. However, we could show that knock-down of *ZmMCM6* affects both male and female flower organ and FG development. The effects on female site are mutants with small ears and sterile anthers on the male side. These suggested that *ZmMCM6* is essential for plant growth and development.

Gametophytic FG mutants can however also affect post-fertilization development. A mutant phenotype of this kind that depends on the genotype of the FG, but is independent of the paternal contribution, is referred to as a gametophytic maternal effect mutation. The mechanistic basis of such maternal effects varies and can be caused by mutations in genes that are expressed during FG development, but whose products are required after fertilization for embryo and/or endosperm development (Brukhin et al., 2005) and which are generally imprinted. The instance of such a maternal effect gene in plants is the maternally

imprinted *medea* (*mea*) gene. Embryo and endosperm derived from a *mea* mutant embryo sac show abnormal cell proliferation without fertilization leading to the formation of diploid endosperm tissue (Grossniklaus et al., 1998). I was involved in the molecular analysis of the imprintied polycomb group *Fie* genes in maize (**Chapter 3)**. *Fie* genes were supposed to be involved in gene imprinting being differentially expressed from maternal and paternal alleles. We showed that *Fie1* and *Fie2* seemed to have distinct expression pattern and distinct function in FG development before and after fertilization. The *Fie1* transcript was not detected in the individual gametes, while *Fie2* transcript was detected in individual female gametes but not in the male gametes. However, since mutants of *Fie1* and *Fie2* are not available in maize, a detailed phenotypic study was not feasible.

**Outlook**

**Role of *MCM* genes for FG development**

The cell cycle regulators CDKs and MCM have been reported to regulate the cell cycle of eukaryotes including plants (reviewed in Masai et al., 2005; Masuda et al., 2003; Shultz et al., 2009). MCM proteins such as MCM6 have been reported to play an important role in plant growth (**Chapter 2**). MCM proteins interact genetically and physically with one another and that this association is essential for their function (reviewed in Masai et al., 2005). Many general questions about MCM function remain unanswered such as, how many complexes are present at each origin, and are there additional complexes flanking the pre-replicative complex (pre- RC)? MCM proteins are encoded by multigene families and knockouts of individual cell cycle regulators rarely resulted in lethality. However, from our study, lacking activity of individual *MCM* genes such as *MCM6* caused lethality indicating that they do not complement another member of the hexamer. This suggests that each member might be required to form a functional hexamer and might have specific functions for the hexamer. One possibility of future analyses of *MCM* genes and proteins in plants, using their own or inducible promoters should be to avoid lethality. Using specific antibodies the whole MCM complex should be accessible in maize. Yeast two-hybrid screens or co-immunoprecipitation might be useful to identify interacting partners and demonstrate of the existence of MCM proteins in maize, respectively. Moreover, the fixing/clearing method described above would be another alternative experiment to follow *ZmMCM6* silencing phenotypes in maize FG development at earlier stages.

**MATH-BTB proteins are required for early FG development**

Selective ubiquitination of proteins is directed by diverse families of ubiquitin-protein ligases (or E3s) in eukaryotic cells (Gingerich et al., 2007). One type of ubiquitination systems uses Cullin-3 as a scaffold to assemble multi-subunit E3 complexes containing MATH proteins that function as substrate recognition (**Chapter 4**). At present, the substrates of the core plant MATH-BTB proteins are unknown. The MATH-BTB domain configuration is also present in animal genomes (Aravind and Koonin, 1999; Geyer et al., 2003; Huang et al., 2004; Stogios et al., 2005) and various substrates were identified including the katanin AAA-type ATPase protein MEI-1 (Furukawa et al., 2003; Pintard et al., 2003; Xu et al., 2003), (Ci/Gli2/Gli3 transcription factors (Zhang et al., 2006), the polycomb protein BMI1, and the MacroH2A histone (Hernandez-Munoz et al., 2005). Unfortunately, the animal MATH domain sequences have sufficiently diverged from those in plants to preclude target predictions based solely on sequence similarity. The main task of the future work will be the description of ZmMAB1-CUL3 activity in maize and the identification of possible substrate proteins. Approximately, a dozen substrates have been identified so far for plant CULLIN-based E3 complexes, whereas several hundreds are expected. Another challenge will be to understand how these substrates are recognized by the MATH-BTB-E3 complex. Are these substrates modified at the post-translational level? And if yes, which enzymes are involved? How are the CULLIN-based E3s enzymes regulated? It is also presently unknown how these enzymes are interconnected, whereas in yeast and metazoan it has already been found that certain substrates are degraded by two or even three different E3s, and that some E3 components are themselves targets of other classes of E3s (reviewed in Thomann et al., 2005). Moreover, further work is also necessary to investigate the possible link between BTB proteins and ubiquitin-dependent degradation. Therefore, yeast two-hybrid screen should be further study to identify the protein partner(s) of ZmMAB1. Considering to our *mab1* mutant phenotype, one question might point out to the spindle assemble during FG development. Previous studied in *C. elegans* during meiosis-to-mitosis transition show that microtubule-severing protein MEI1 need to be degraded via ubiquitination (Pintard et al., 2003; Xu et al., 2003). Therefore, immunolabeling might be achieved to visualize the microtubules organization in maize FG development as well.

**DSUL function in maize FG development**

Since the discovery of SUMO a decade ago, a wealth of information has been gathered about the properties and functions of this small modifier protein (reviewed in Gill, 2003;

Johnson, 2004; Melchior et al., 2003; Müller et al., 2001; Seeler and Dejean, 2003). Advances in mass spectrometry technology have allowed the identification of hundreds of SUMO targets, and many more will undoubtedly emerge in the future (Ulrich, 2009). Our study in **Chapter 5** of the DSUL in maize adds more questions to the molecular role of SUMOylation/DSYLylation in plants. The main question is, if the mechanism of DSUL conjugation is similar to SUMO conjugation and whether the same conjugating enzymes SCE1, Ubc9 or hus5 (for review Bachmair et al., 2001; Novatchkova et al., 2004; Smalle and Vierstra, 2004) are involved. Moreover, deconjugation has to be studied in detail with a number of representative model substrates, and especially the important question concerning substrate recognition and selectivity has to be addressed. Due to the limitation of FG material the necessary experiments are challenging and standard biochemical methods cannot be applied. *In vivo* analysis should be combined with biochemical approaches in order to gain insight into the dynamic regulation of the DSUL system by cellular and extracellular signals. Importantly, much more is to be learned about the ways in which DSUL, and in particular if poly-DSUL chains occur, affect the properties of the modified targets. The identification of additional DSUL interacting proteins and motifs is expected to reveal important downstream effectors of the DSUL pathway, and may help to provide the missing links between individual DSUL substrates and cellular phenotypes associated with defects in DSUL conjugation. As new areas of DSUL function are expected to be revealed for early embryo development, where strong gene expression was observed, it is certain that the DSUL pathway will eventually be recognized as an important and flexible regulatory system in more aspects of cellular metabolism and development.

### *Fie* mutations affect the induction of seed development

Kernel development can be affected by parent-of-origin effects that stem from events occurring during megagametogenesis (Evans and Grossniklaus, 2009). Various gametophyte maternal effect mutants belonging to the polycomb group (PcG) complex have been reported in *Arabidopsis* such as *FIS2*, *MEA* (*FIS1*) and *FIE* (*FIS3*) (Chaudhury et al., 1997; Grossniklaus et al., 1998; Luo et al., 2000; Ohad et al., 1996). Mutations affecting any of the complex components lead to over proliferation of the endosperm and embryo cells in fertilized FGs, and to autonomous endosperm formation in the absence of fertilization (Chaudhury et al., 1997; Grossniklaus et al., 1998; Kiyosue et al., 1999; Köhler et al., 2003; Luo et al., 1999; Ohad et al., 1996). As an example, the loss-of-functions Arabidopsis *fie* mutant produce pleiotropic phenotypes including initiation of endosperm development without fertilization, embryo abortion at early stages, premature flowering by seedling shoots,

and formation of flower-like structures along the roots and hypocotyls (Kinoshita et al., 2001; Ohad et al., 1996; 1999). There are several genes that are imprinted in maize, but in our study we have investigated only maize *FIE1* and *FIE2* (**Chapter 3**). Of the two maize *FIE* genes, only *FIE2* is a plausible candidate for a repressor of endosperm development before fertilization, and the function performed by the single *Arabidopsis* FIE protein (Danilevskaya et al., 2003). A loss-of-function mutant of maize *FIE2* is now required to address this question. Another unanswered question is the interaction partner(s) or complexes of the maize FIE proteins with other proteins such as MEA. In *Arabidopsis* it was shown that the MEA-FIE complex acts on *PHE1* in embryo development starting at the globular stage and in the central domain of the endosperm (Köhler et al., 2003). Yeast-two-hybrid experiments would be useful to find interaction partner(s) of the *FIE* genes in the maize FG. Moreover, in contrast to other model plant systems such as *Arabidopsis*, relatively large protein amounts can be isolated from early seed development stages of maize allowing the isolation of these complexes using biochemical methods.

In conclusion, the study of FG development in maize is limited compared to *Arabidopsis*. The ease of transforming *Arabidopsis* has facilitated the establishment of lines carrying GUS or GFP reporters specially expressed in the embryo sac or individual cell types of the embryo sac (Gross-Hardt et al., 2007; Huanca-Mamani et al., 2005; Ngo et al., 2007; Punwani et al., 2007; Yang et al., 2005). With these marker lines, therefore *Arabidopsis* plant have much more advantage of permitting in mutant screens than in maize. Moreover, the histology study to follow FG development in *Arabidopsis* is much easier than in maize due to the thickness of the ovules. However, maize offers advantages in the biochemical analysis of the identified proteins and protein complexes, which cannot be isolated from *Arabidopsis* in sufficient quantities. Thus many of the questions addressed above are more likely to be answered using maize as a model system, especially taking into consideration that the complete genome sequence will be soon available, and a large set of cellular markers has been developed over the past few years.

## References

**Aravind, L. and Koonin, E. V.** (1999). Fold prediction and evolutionary analysis of the POZ domain: structural and evolutionary relationship with the potassium channel tetramerization domain. *J Mol Biol* **285**, 1353-61.

**Bachmair, A., Novatchkova, M., Potuschak, T. and Eisenhaber, F.** (2001). Ubiquitylation in plants: a post-genomic look at a post-translational modification. *Trends Plant Sci* **6**, 463-70.

**Bell, S. P. and Stillman, B.** (1992). ATP-dependent recognition of eukaryotic origins of DNA replication by a multiprotein complex. *Nature* **357**, 128-34.

**Berger, F., Hamamura, Y., Ingouff, M. and Higashiyama, T.** (2008). Double fertilization - caught in the act. *Trends Plant Sci* **13**, 437-43.

**Bowerman, B. and Kurz, T.** (2006). Degrade to create: developmental requirements for ubiquitin-mediated proteolysis during early *C. elegans* embryogenesis. *Development* **133**, 773-84.

**Bradley, J. R. and Pober, J. S.** (2001). Tumor necrosis factor receptor-associated factors (TRAFs). *Oncogene* **20**, 6482-91.

**Brukhin, V., Gheyselinck, J., Gagliardini, V., Genschik, P. and Grossniklaus, U.** (2005). The RPN1 subunit of the 26S proteasome in Arabidopsis is essential for embryogenesis. *Plant Cell* **17**, 2723-37.

**Chaudhury, A. M., Ming, L., Miller, C., Craig, S., Dennis, E. S. and Peacock, W. J.** (1997). Fertilization-independent seed development in Arabidopsis thaliana. *Proc Natl Acad Sci U S A* **94**, 4223-8.

**Christensen, C. A., Gorsich, S. W., Brown, R. H., Jones, L. G., Brown, J., Shaw, J. M. and Drews, G. N.** (2002). Mitochondrial GFA2 is required for synergid cell death in Arabidopsis. *Plant Cell* **14**, 2215-32.

**Christensen, C. A., Subramanian, S. and Drews, G. N.** (1998). Identification of gametophytic mutations affecting female gametophyte development in Arabidopsis. *Dev Biol* **202**, 136-51.

**Conti, L., Price, G., O'Donnell, E., Schwessinger, B., Dominy, P. and Sadanandom, A.** (2008). Small ubiquitin-like modifier proteases OVERLY TOLERANT TO SALT1 and -2 regulate salt stress responses in Arabidopsis. *Plant Cell* **20**, 2894-908.

**Danilevskaya, O. N., Hermon, P., Hantke, S., Muszynski, M. G., Kollipara, K. and Ananiev, E. V.** (2003). Duplicated fie genes in maize: expression pattern and imprinting suggest distinct functions. *Plant Cell* **15**, 425-38.

**Dreher, K. and Callis, J.** (2007). Ubiquitin, hormones and biotic stress in plants. *Ann Bot (Lond)* **99**, 787-822.

**Dresselhaus, T., Cordts, S. and Lorz, H.** (1999). A transcript encoding translation initiation factor eIF-5A is stored in unfertilized egg cells of maize. *Plant Mol Biol* **39**, 1063-71.

**Dresselhaus, T., Lorz, H. and Kranz, E.** (1994). Representative cDNA libraries from few plant cells. *Plant J* **5**, 605-10.

**Dresselhaus, T., Srilunchang, K. O., Leljak-Levanic, D., Schreiber, D. N. and Garg, P.** (2006). The fertilization-induced DNA replication factor MCM6 of maize shuttles between cytoplasm and nucleus, and is essential for plant growth and development. *Plant Physiol* **140**, 512-27.

**Drews, G. N., Lee, D. and Christensen, C. A.** (1998). Genetic analysis of female gametophyte development and function. *Plant Cell* **10**, 5-17.

**Edward, C. J. H.** (2001). The origins of maize genetics. *Nat Rev Genet* **2**, 898-905.

**Ellis, C., Turner, J. G. and Devoto, A.** (2002). Protein complexes mediate signalling in plant responses to hormones, light, sucrose and pathogens. *Plant Mol Biol* **50**, 971-80.

**Evans, M. M.** (2007). The indeterminate gametophyte1 gene of maize encodes a LOB domain protein required for embryo Sac and leaf development. *Plant Cell* **19**, 46-62.

**Evans, M. M. and Grossniklaus, U.** (2009). Handbook of Miaze: Its Biology. The maize megagametophyte. Springer. New York. 79-104.

**Figueroa, P., Gusmaroli, G., Serino, G., Habashi, J., Ma, L., Shen, Y., Feng, S., Bostick, M., Callis, J., Hellmann, H. et al.** (2005). Arabidopsis has two redundant Cullin3 proteins that are essential for embryo development and that interact with RBX1 and BTB proteins to form multisubunit E3 ubiquitin ligase complexes in vivo. *Plant Cell* **17**, 1180-95.

**Furukawa, M., He, Y. J., Borchers, C. and Xiong, Y.** (2003). Targeting of protein ubiquitination by BTB-Cullin 3-Roc1 ubiquitin ligases. *Nat Cell Biol* **5**, 1001-7.

**Geyer, R., Wee, S., Anderson, S., Yates, J. and Wolf, D. A.** (2003). BTB/POZ domain proteins are putative substrate adaptors for cullin 3 ubiquitin ligases. *Mol Cell* **12**, 783-90.

**Gill, G.** (2003). Post-translational modification by the small ubiquitin-related modifier SUMO has big effects on transcription factor activity. *Curr Opin Genet Dev* **13**, 108-13.

**Gill, G.** (2004). SUMO and ubiquitin in the nucleus: different functions, similar mechanisms? *Genes Dev* **18**, 2046-59.

**Gingerich, D. J., Hanada, K., Shiu, S. H. and Vierstra, R. D.** (2007). Large-scale, lineage-specific expansion of a bric-a-brac/tramtrack/broad complex ubiquitin-ligase gene family in rice. *Plant Cell* **19**, 2329-48.

**Glotzer, M., Murray, A. W. and Kirschner, M. W.** (1991). Cyclin is degraded by the ubiquitin pathway. *Nature* **349**, 132-8.

**Gross-Hardt, R., Kagi, C., Baumann, N., Moore, J. M., Baskar, R., Gagliano, W. B., Jurgens, G. and Grossniklaus, U.** (2007). LACHESIS restricts gametic cell fate in the female gametophyte of Arabidopsis. *PLoS Biol* **5**, e47.

**Grossniklaus, U. and Schneitz, K.** (1998). The molecular and genetic basis of ovule and megagametophyte development. *Semin Cell Dev Biol* **9**, 227-38.

**Grossniklaus, U., Vielle-Calzada, J. P., Hoeppner, M. A. and Gagliano, W. B.** (1998). Maternal control of embryogenesis by MEDEA, a polycomb group gene in Arabidopsis. *Science* **280**, 446-50.

**Gutierrez-Marcos, J. F., Costa, L. M. and Evans, M. M.** (2006). Maternal gametophytic baseless1 is required for development of the central cell and early endosperm patterning in maize (Zea mays). *Genetics* **174**, 317-29.

**Gutierrez-Marcos, J. F., Pennington, P. D., Costa, L. M. and Dickinson, H. G.** (2003). Imprinting in the endosperm: a possible role in preventing wide hybridization. *Philos Trans R Soc Lond B Biol Sci* **358**, 1105-11.

**Hernandez-Munoz, I., Taghavi, P., Kuijl, C., Neefjes, J. and van Lohuizen, M.** (2005). Association of BMI1 with polycomb bodies is dynamic and requires PRC2/EZH2 and the maintenance DNA methyltransferase DNMT1. *Mol Cell Biol* **25**, 11047-58.

**Herrmann, J., Lerman, L. O. and Lerman, A.** (2007). Ubiquitin and ubiquitin-like proteins in protein regulation. *Circ Res* **100**, 1276-91.

**Hershko, A. and Ciechanover, A.** (1998). The ubiquitin system. *Annu Rev Biochem* **67**, 425-79.

**Hershko, A., Ganoth, D., Pehrson, J., Palazzo, R. E. and Cohen, L. H.** (1991). Methylated ubiquitin inhibits cyclin degradation in clam embryo extracts. *J Biol Chem* **266**, 16376-9.

**Hicke, L. and Dunn, R.** (2003). Regulation of membrane protein transport by ubiquitin and ubiquitin-binding proteins. *Annu Rev Cell Dev Biol* **19**, 141-72.

**Huh, J. H., Bauer, M. J., Hsieh, T. F. and Fischer, R. L.** (2008). Cellular programming of plant gene imprinting. *Cell* **132**, 735-44.

**Huanca-Mamani, W., Garcia-Aguilar, M., Leon-Martinez, G., Grossniklaus, U. and Vielle-Calzada, J. P.** (2005). CHR11, a chromatin-remodeling factor essential for nuclear proliferation during female gametogenesis in Arabidopsis thaliana. *Proc Natl Acad Sci U S A* **102**, 17231-6.

**Huang, C. J., Chen, C. Y., Chen, H. H., Tsai, S. F. and Choo, K. B.** (2004). TDPOZ, a family of bipartite animal and plant proteins that contain the TRAF (TD) and POZ/BTB domains. *Gene* **324**, 117-27.

**Huh, J. H., Bauer, M. J., Hsieh, T. F. and Fischer, R. L.** (2008). Cellular programming of plant gene imprinting. *Cell* **132**, 735-44.

**Jentsch, S. and Pyrowolakis, G.** (2000). Ubiquitin and its kin: how close are the family ties? *Trends Cell Biol* **10**, 335-42.

**Johnson, E. S.** (2004). Protein modification by SUMO. *Annu Rev Biochem* **73**, 355-82.

**Jones-Rhoades, M. W., Borevitz, J. O. and Preuss, D.** (2007). Genome-wide expression profiling of the Arabidopsis female gametophyte identifies families of small, secreted proteins. *PLoS Genet* **3**, 1848-61.

**Kearsey, S. E. and Labib, K.** (1998). MCM proteins: evolution, properties, and role in DNA replication. *Biochim Biophys Acta* **1398**, 113-36.

**Kerscher, O.** (2007). SUMO junction-what's your function? New insights through SUMO-interacting motifs. *EMBO Rep* **8**, 550-5.

**Kiesselbach, T. A.** (1999). The structure and reproduction of corn: 50th Anniversary edition, Cold Spring Harbor Laboratory Press, Cold Spring Harbor, New York.

**Kinoshita, T., Yadegari, R., Harada, J. J., Goldberg, R. B. and Fischer, R. L.** (1999). Imprinting of the MEDEA polycomb gene in the Arabidopsis endosperm. *Plant Cell* **11**, 1945-52.

**Kirkin, V. and Dikic, I.** (2007). Role of ubiquitin- and Ubl-binding proteins in cell signaling. *Curr Opin Cell Biol* **19**, 199-205.

**Kiyosue, T., Ohad, N., Yadegari, R., Hannon, M., Dinneny, J., Wells, D., Katz, A., Margossian, L., Harada, J. J., Goldberg, R. B. et al.** (1999). Control of fertilization-independent endosperm

development by the MEDEA polycomb gene in Arabidopsis. *Proc Natl Acad Sci U S A* **96**, 4186-91.

**Köhler, C. and Grossniklaus, U.** (2002). Epigenetic inheritance of expression states in plant development: the role of Polycomb group proteins. *Curr Opin Cell Biol* **14**, 773-9.

**Köhler, C. and Grossniklaus, U.** (2005). Seed development and genomic imprinting in plants. *Prog Mol Subcell Biol* **38**, 237-62.

**Köhler, C., Hennig, L., Spillane, C., Pien, S., Gruissem, W. and Grossniklaus, U.** (2003). The Polycomb-group protein MEDEA regulates seed development by controlling expression of the MADS-box gene PHERES1. *Genes Dev* **17**, 1540-53.

**Kranz, E., Hoshino, Y. and Okamoto, T.** (2008). In vitro fertilization with isolated higher plant gametes. *Methods Mol Biol* **427**, 51-69.

**Kranz, E. and Lörz, H.** (1993). In Vitro Fertilization with Isolated, Single Gametes Results in Zygotic Embryogenesis and Fertile Maize Plants. *Plant Cell* **5**, 739-746.

**Kranz, E. and Lörz, H.** (1994). In vitro fertilisation of maize by single egg and sperm cell protoplast fusion mediated by high calcium and high pH. *Zygote* **2**, 125-8.

**Krek, W.** (2003). BTB proteins as henchmen of Cul3-based ubiquitin ligases. *Nat Cell Biol* **5**, 950-1.

**Kurepa, J., Walker, J. M., Smalle, J., Gosink, M. M., Davis, S. J., Durham, T. L., Sung, D. Y. and Vierstra, R. D.** (2003). The small ubiquitin-like modifier (SUMO) protein modification system in Arabidopsis. Accumulation of SUMO1 and -2 conjugates is increased by stress. *J Biol Chem* **278**, 6862-72.

**Le, Q., Gutierrez-Marcos, J. F., Costa, L. M., Meyer, S., Dickinson, H. G., Lorz, H., Kranz, E. and Scholten, S.** (2005). Construction and screening of subtracted cDNA libraries from limited populations of plant cells: a comparative analysis of gene expression between maize egg cells and central cells. *Plant J* **44**, 167-78.**Hemerly, A., Ferreira, P., Van Montagu, M. and Inze, D.** (1999). Cell cycle control and plant morphogenesis: is there an essential link? *Bioessays* **21**, 29-37.

**Leduc, N., Matthys-Rochon, E., Rougier, M., Mogensen, L., Holm, P., Magnard, J. L. and Dumas, C.** (1996). Isolated maize zygotes mimic in vivo embryonic development and express microinjected genes when cultured in vitro. *Dev Biol* **177**, 190-203.

**Lisch, D., Carey, C. C., Dorweiler, J. E. and Chandler, V. L.** (2002). A mutation that prevents paramutation in maize also reverses Mutator transposon methylation and silencing. *Proc Natl Acad Sci U S A* **99**, 6130-5.

**Lois, L. M., Lima, C. D. and Chua, N. H.** (2003). Small ubiquitin-like modifier modulates abscisic acid signaling in Arabidopsis. *Plant Cell* **15**, 1347-59.

**Luke-Glaser, S., Pintard, L., Tyers, M. and Peter, M.** (2007). The AAA-ATPase FIGL-1 controls mitotic progression, and its levels are regulated by the CUL-3MEL-26 E3 ligase in the C. elegans germ line. *J Cell Sci* **120**, 3179-87.

**Luo, M., Bilodeau, P., Dennis, E. S., Peacock, W. J. and Chaudhury, A.** (2000). Expression and parent-of-origin effects for FIS2, MEA, and FIE in the endosperm and embryo of developing Arabidopsis seeds. *Proc Natl Acad Sci U S A* **97**, 10637-42.

**Luo, M., Bilodeau, P., Koltunow, A., Dennis, E. S., Peacock, W. J. and Chaudhury, A. M.** (1999). Genes controlling fertilization-independent seed development in Arabidopsis thaliana. *Proc Natl Acad Sci U S A* **96**, 296-301.

**Márton, M. L., Cordts, S., Broadhvest, J. and Dresselhaus, T.** (2005). Micropylar pollen tube guidance by egg apparatus 1 of maize. *Science* **307**, 573-6.

**Masai, H., You, Z. and Arai, K.** (2005). Control of DNA replication: regulation and activation of eukaryotic replicative helicase, MCM. *IUBMB Life* **57**, 323-35.

**Masuda, T., Mimura, S. and Takisawa, H.** (2003). CDK- and Cdc45-dependent priming of the MCM complex on chromatin during S-phase in Xenopus egg extracts: possible activation of MCM helicase by association with Cdc45. *Genes Cells* **8**, 145-61.

**McCormick, S.** (2004). Control of male gametophyte development. *Plant Cell* **16 Suppl**, S142-53.

**Melchior, F.** (2000). SUMO--nonclassical ubiquitin. *Annu Rev Cell Dev Biol* **16**, 591-626.

**Melchior, F., Schergaut, M. and Pichler, A.** (2003). SUMO: ligases, isopeptidases and nuclear pores. *Trends Biochem Sci* **28**, 612-8.

**Meulmeester, E. and Melchior, F.** (2008). Cell biology: SUMO. *Nature* **452**, 709-11.

**Miura, K., Jin, J. B., Lee, J., Yoo, C. Y., Stirm, V., Miura, T., Ashworth, E. N., Bressan, R. A., Yun, D. J. and Hasegawa, P. M.** (2007). SIZ1-mediated sumoylation of ICE1 controls CBF3/DREB1A expression and freezing tolerance in Arabidopsis. *Plant Cell* **19**, 1403-14.

**Miura, K., Rus, A., Sharkhuu, A., Yokoi, S., Karthikeyan, A. S., Raghothama, K. G., Baek, D., Koo, Y. D., Jin, J. B., Bressan, R. A. et al.** (2005). The Arabidopsis SUMO E3 ligase SIZ1 controls phosphate deficiency responses. *Proc Natl Acad Sci U S A* **102**, 7760-5.

**Moore, J. M., Calzada, J. P., Gagliano, W. and Grossniklaus, U.** (1997). Genetic characterization of hadad, a mutant disrupting female gametogenesis in Arabidopsis thaliana. *Cold Spring Harb Symp Quant Biol* **62**, 35-47.

**Muratani, M. and Tansey, W. P.** (2003). How the ubiquitin-proteasome system controls transcription. *Nat Rev Mol Cell Biol* **4**, 192-201.

**Murtas, G., Reeves, P. H., Fu, Y. F., Bancroft, I., Dean, C. and Coupland, G.** (2003). A nuclear protease required for flowering-time regulation in Arabidopsis reduces the abundance of SMALL UBIQUITIN-RELATED MODIFIER conjugates. *Plant Cell* **15**, 2308-19.

**Müller, S., Hoege, C., Pyrowolakis, G. and Jentsch, S.** (2001). SUMO, ubiquitin's mysterious cousin. *Nat Rev Mol Cell Biol* **2**, 202-10.

**Müller, S., Ledl, A. and Schmidt, D.** (2004). SUMO: a regulator of gene expression and genome integrity. *Oncogene* **23**, 1998-2008.

**Ngo, Q. A., Moore, J. M., Baskar, R., Grossniklaus, U. and Sundaresan, V.** (2007). Arabidopsis GLAUCE promotes fertilization-independent endosperm development and expression of paternally inherited alleles. *Development* **134**, 4107-17.

**Novatchkova, M., Budhiraja, R., Coupland, G., Eisenhaber, F. and Bachmair, A.** (2004). SUMO conjugation in plants. *Planta* **220**, 1-8.

**Ohad, N., Margossian, L., Hsu, Y. C., Williams, C., Repetti, P. and Fischer, R. L.** (1996). A mutation that allows endosperm development without fertilization. *Proc Natl Acad Sci U S A* **93**, 5319-24.

**Ohad, N., Yadegari, R., Margossian, L., Hannon, M., Michaeli, D., Harada, J. J., Goldberg, R. B. and Fischer, R. L.** (1999). Mutations in FIE, a WD polycomb group gene, allow endosperm development without fertilization. *Plant Cell* **11**, 407-16.

**Pagnussat, G. C., Yu, H. J., Ngo, Q. A., Rajani, S., Mayalagu, S., Johnson, C. S., Capron, A., Xie, L. F., Ye, D. and Sundaresan, V.** (2005). Genetic and molecular identification of genes required for female gametophyte development and function in Arabidopsis. *Development* **132**, 603-14.

**Perez-Torrado, R., Yamada, D. and Defossez, P. A.** (2006). Born to bind: the BTB protein-protein interaction domain. *Bioessays* **28**, 1194-202.

**Petroski, M. D. and Deshaies, R. J.** (2005). Function and regulation of cullin-RING ubiquitin ligases. *Nat Rev Mol Cell Biol* **6**, 9-20.

**Pintard, L., Willems, A. and Peter, M.** (2004). Cullin-based ubiquitin ligases: Cul3-BTB complexes join the family. *Embo J* **23**, 1681-7.

**Pintard, L., Willis, J. H., Willems, A., Johnson, J. L., Srayko, M., Kurz, T., Glaser, S., Mains, P. E., Tyers, M., Bowerman, B. et al.** (2003). The BTB protein MEL-26 is a substrate-specific adaptor of the CUL-3 ubiquitin-ligase. *Nature* **425**, 311-6.

**Punwani, J. A. and Drews, G. N.** (2008). Development and function of the synergid cell. *Sex Plant Reprod* **21**, 7-15.

**Punwani, J. A., Rabiger, D. S. and Drews, G. N.** (2007). MYB98 positively regulates a battery of synergid-expressed genes encoding filiform apparatus localized proteins. *Plant Cell* **19**, 2557-68.

**Ranganath, R. M.** (2003). Female Gametophyte Development in Higher Plant-Meiosis and Mitosis Break the Cellular Barrier. *Plant biol.* **5**, 42-49.

**Ray, S. M., Park, S. S. and Ray, A.** (1997). Pollen tube guidance by the female gametophyte. *Development* **124**, 2489-98.

**Russell, S. D.** (1992). Double fertilization *Int. Rev. Cytol.* **140**, 357-388.

**Saracco, S. A., Miller, M. J., Kurepa, J. and Vierstra, R. D.** (2007). Genetic analysis of SUMOylation in Arabidopsis: conjugation of SUMO1 and SUMO2 to nuclear proteins is essential. *Plant Physiol* **145**, 119-34.

**Schwartz, D. C. and Hochstrasser, M.** (2003). A superfamily of protein tags: ubiquitin, SUMO and related modifiers. *Trends Biochem Sci* **28**, 321-8.

**Schwed, G., May, N., Pechersky, Y. and Calvi, B. R.** (2002). Drosophila minichromosome maintenance 6 is required for chorion gene amplification and genomic replication. *Mol Biol Cell* **13**, 607-20.

**Seeler, J. S. and Dejean, A.** (2003). Nuclear and unclear functions of SUMO. *Nat Rev Mol Cell Biol* **4**, 690-9.

**Shultz, R. W., Lee, T. J., Allen, G. C., Thompson, W. F. and Hanley-Bowdoin, L.** (2009). Dynamic Localization of the DNA Replication Proteins MCM5 and MCM7 in Plants. *Plant Physiol* **150**, 658-69.

**Smalle, J. and Vierstra, R. D.** (2004). The ubiquitin 26S proteasome proteolytic pathway. *Annu Rev Plant Biol* **55**, 555-90.

**Springer, N. M., Danilevskaya, O. N., Hermon, P., Helentjaris, T. G., Phillips, R. L., Kaeppler, H. F. and Kaeppler, S. M.** (2002). Sequence relationships, conserved domains, and expression patterns for maize homologs of the polycomb group genes E(z), esc, and E(Pc). *Plant Physiol* **128**, 1332-45.

**Springer, P. S., Holding, D. R., Groover, A., Yordan, C. and Martienssen, R. A.** (2000). The essential Mcm7 protein PROLIFERA is localized to the nucleus of dividing cells during the G(1) phase and is required maternally for early Arabidopsis development. *Development* **127**, 1815-22.

**Springer, P. S., McCombie, W. R., Sundaresan, V. and Martienssen, R. A.** (1995). Gene trap tagging of PROLIFERA, an essential MCM2-3-5-like gene in Arabidopsis. *Science* **268**, 877-80.

**Sprunck, S., Baumann, U., Edwards, K., Langridge, P. and Dresselhaus, T.** (2005). The transcript composition of egg cells changes significantly following fertilization in wheat (Triticum aestivum L.). *Plant J* **41**, 660-72.

**Stogios, P. J., Downs, G. S., Jauhal, J. J., Nandra, S. K. and Prive, G. G.** (2005). Sequence and structural analysis of BTB domain proteins. *Genome Biol* **6**, R82.

**Su, T. T., Feger, G. and O'Farrell, P. H.** (1996). Drosophila MCM protein complexes. *Mol Biol Cell* **7**, 319-29.

**Sumara, I. and Peter, M.** (2007). A Cul3-based E3 ligase regulates mitosis and is required to maintain the spindle assembly checkpoint in human cells. *Cell Cycle* **6**, 3004-10.

**Sun, L. and Chen, Z. J.** (2004). The novel functions of ubiquitination in signaling. *Curr Opin Cell Biol* **16**, 119-26.

**Tian, H. Q., Yuan, T. and and Russell, S. D.** (2005). Relationship between double fertilization and the cell cycle in male and female gametes of tobacco. *Sex Plant Reprod* **17**, 243-252.

**Thomann, A., Dieterle, M. and Genschik, P.** (2005). Plant CULLIN-based E3s: phytohormones come first. *FEBS Lett* **579**, 3239-45.

**Ulrich, H. D.** (2009). The SUMO system: an overview. *Methods Mol Biol* **497**, 3-16.

**Vizir, I. Y., Anderson, M. L., Wilson, Z. A. and Mulligan, B. J.** (1994). Isolation of deficiencies in the Arabidopsis genome by gamma-irradiation of pollen. *Genetics* **137**, 1111-9.

**Vollbrecht, E. and Hake, S.** (1995). Deficiency analysis of female gametogenesis in maize. *Dev Genet* **16**, 44-63.

**Walbot, V. and Evans, M. M.** (2003). Unique features of the plant life cycle and their consequences. *Nat Rev Genet* **4**, 369-79.

**Watts, F. Z.** (2007). The role of SUMO in chromosome segregation. *Chromosoma* **116**, 15-20.

**Xu, L., Menard, R., Berr, A., Fuchs, J., Cognat, V., Meyer, D. and Shen, W. H.** (2009). The E2 ubiquitin-conjugating enzymes, AtUBC1 and AtUBC2, play redundant roles and are involved in activation of FLC expression and repression of flowering in Arabidopsis thaliana. *Plant J* **57**, 279-88.

**Xu, L., Wei, Y., Reboul, J., Vaglio, P., Shin, T. H., Vidal, M., Elledge, S. J. and Harper, J. W.** (2003). BTB proteins are substrate-specific adaptors in an SCF-like modular ubiquitin ligase containing CUL-3. *Nature* **425**, 316-21.

**Yadegari, R. and Drews, G. N.** (2004). Female gametophyte development. *Plant Cell* **16 Suppl**, S133-41.

**Yang, W., Jefferson, R. A., Huttner, E., Moore, J. M., Gagliano, W. B. and Grossniklaus, U.** (2005). An egg apparatus-specific enhancer of Arabidopsis, identified by enhancer detection. *Plant Physiol* **139**, 1421-32.

**Yoo, C. Y., Miura, K., Jin, J. B., Lee, J., Park, H. C., Salt, D. E., Yun, D. J., Bressan, R. A. and Hasegawa, P. M.** (2006). SIZ1 small ubiquitin-like modifier E3 ligase facilitates basal thermotolerance in Arabidopsis independent of salicylic acid. *Plant Physiol* **142**, 1548-58.

**Zhao, J.** (2007). Sumoylation regulates diverse biological processes. *Cell Mol Life Sci* **64**, 3017-33.

**Zhang, Q., Zhang, L., Wang, B., Ou, C. Y., Chien, C. T. and Jiang, J.** (2006). A hedgehog-induced BTB protein modulates hedgehog signaling by degrading Ci/Gli transcription factor. *Dev Cell* **10**, 719-29.

**Contribution to the various papers and manuscripts**

**P1** Dresselhaus, T., **Srilunchang, K.-o,** Leljak-Levanic, D., Schreiber, D.N., Garg, P**.** (2006). The fertilization-induced DNA replication factor MCM6 of maize shuttles between cytoplasm and nucleus, and is essential for plant growth and development. *Plant Physiol.*, **140**, 512-527.

I manually isolated gametic cells from male and female gametophytes (sperm cell, egg cell, central cell and zygote) and carried out all SC RT-PCR and qRT-PCR experiments to determine the *ZmMCM6* expression pattern. Moreover, I performed immunocytochemical experiments to measure ZmMCM6 levels during the cell cycle in BMS suspension cells.

**P2** Hermon, P., **Srilunchang, K.-o,** Zou, J., Dresselhaus, T., Danilevskaya, O.N. (2007). Activation of the imprinted Polycomb Group Fie1 gene in maize endosperm requires demethylation of the maternal allele. *Plant Mol. Biol.*, **64**, 387-395.

I manually isolated gametic cells from male and female gametophytes (sperm cell, egg cell, central cell and zygote) and carried out all SC RT-PCR experiments to determine the *ZmFie1/2* expression pattern. Additionally, I conducted MSRE (methylation sensitive restriction enzyme digestion) PCR and biosulfite treatment of single cells.

**P3** Leljak-Levanic, D., **Srilunchang, K.-o.**, Juranic, M., Soljic, L., Mocibob, M., Dresselhaus, T., Sprunck, S. Asymmetrically inherited maize MATH-BTB proteins are involved in nuclei positioning and mitotic progression during megagametogenesis. *Plant Cell*, in revision.

I isolated single cells as described above as well as RNAs from various maize tissues to determine *ZmMAB1* expression patter. I also generate all transgenic maize plants by using the RNAi technique and analyzed the transgenics at the molecular and phenotypical level using the methods described including confocal laser scanning microscopy.

**P4** **Srilunchang, K.-o**., Dresselhaus, T. (2009). DiSUMO-like DSUL is required for nuclei positioning and cell specification during female gametophyte maturation in maize. *Development*, in revision.

I have generated all experimental data described in the manuscript. Moreover, I wrote the first draft of the manuscript.

Herewith I confirm the accuracy of the statements.

Prof. Dr. Thomas Dresselhaus

## ABBREVIATIONS

| | |
|---|---|
| ACD | asymmetric cell division |
| BMS | black maxican sweet |
| BTB | Brick-a-brac/tramtrack broad complex |
| cc | central cell |
| CLSM | confocal laser scanning microscopy |
| CUL | cullin |
| DAP | day after pollination |
| DSUL | DiSUMO-like |
| ea | egg apparatus |
| ec | egg cell |
| FG | female gametophyte |
| Fie | Fertilization-independent endosperm |
| GFP | green fluorescent protein |
| HAP | hour after pollination |
| MAB | MATH-BTB |
| MATH | Meprin and TRAF homology |
| MCM | minichromosome maintenance |
| MEA | MEDEA |
| MTOC | microtubular organizing centre |
| MTs | microtubules |
| ORC | origin recognition complex |
| PcG | polycomb group |
| PTGS | post-transcriptional gene silencing |
| RT-PCR | reverse transcription- polymerase chain reaction |
| SC | single cell |
| sp | sperm |
| SUMO | small ubiquitin-related modifier |
| sy | synergid |
| Ub | Ubiquitin |
| UBLs | ubiquitin-like proteins |
| Zm | *Zea mays* |

## Acknowledgments

I am deeply indebted to my advisor Prof. Dr. Thomas Dresselhaus for supporting me during the Ph.D. program. He was always there to listen, to stimulate suggestions and give me many advices. Besides, I would also like to thank Dr. Stefanie Sprunck and Dr. Ulrich Hammes for critical reading.

I would like to thank my colleagues from both the University of Hamburg and the Universitiy of Regensburg. First of all from the old time in Hamburg, I thank Dr. Jörg Bantin (Baak Bantin) who first taught me how to manually isolate single cell from maize. Jörg was not only a good trainer but also a good fighter. We keep fighting sometime in the lab just for relaxing and being a bit out of science. Thanks also to a good friend, Dunja, who gave me good advices on lab work and we exchanged ideas of life. Secondly, special thanks for colleagues from the 'blue lab' in Regensburg. Thanks to my best friend Birgit, who not only gave me support in the lab but also taught me to behave properly in Germany. Thanks for all support and friendship from Nadia (who I first imagine of her differently in term of being a 'Brazilian'), Svenja (who we always share a birthday party together), Andi (the only lucky man in the lab), Lucija (who keeps practicing people to speak correct English), Irina (who is always helping on German papers) and all of you of whom I did not mention the names.

I am so grateful to my former supervisor from Thailand, Assist. Prof. Dr. Mariena Ketudat-Cairns, who first let me have a chance to see the different world and support me with advice, also for getting me interested in plant molecular biology and supporting my coming to Germany. Thanks also to my good friend Dr. Panlada Tittabutr (OF) for helping correcting English and spending time reading some parts of my thesis.

Apart of work, I would like to thank my fiancé Gunnar. Thank you for understanding, being with me and supporting me when I am down. Thanks for your love, hands and patience (most important one). You prove that the distance does not make us apart.

The deepest thanks to my family from home, my dad and my brothers for their lasting love, encouragement, support and helping me through difficult times. Most of all, I would like to thank my beloved Mum. Although you are not here anymore to listen but you will be always in my heart. Without you, there is no either crazy Jeab or

Dr. Jeab. Life without you is so difficult. But I hope you will see me and are proud of me. Therefore, I would like to give this song for you mum….

**เพลง อิ่มอุ่น**
**ศุ บุญเลี้ยง**

**อุ่นใดๆ โลกนี้ไม่มีเทียบเทียม**
**อุ่นอกอ้อมแขน อ้อมกอดแม่ตระกอง**
**รักเจ้าจึงปลูก รักลูกแม่ย่อมห่วงใย**
**ไม่อยากห่างไปไกล แม้เพียงครึ่งวัน**

**ให้กายเราใกล้กัน ให้ดวงตาใกล้ตา**
**ให้ดวงใจเราสอง เชื่อมโยงผูกพัน**

**อิ่มใดๆ โลกนี้ไม่มีเทียบเทียม**
**อิ่มอก อิ่มใจ อิ่มรักลูก หลับนอน**
**น้ำนมจากอก อาหารของความอาทร**
**แม่คร่ำครวญ พร่ำสอน สอนสั่ง**

**ให้เจ้าเป็นเด็กดี ให้เจ้ามีพลัง**
**ให้เจ้าเป็นความหวัง ของแม่ต่อไป**

**ใช่เพียงอิ่มท้อง**
**ที่ลูกร่ำร้องเพราะต้องการไออุ่น**
**อุ่นไอรัก อุ่นละมุน**
**ขอน้ำนมอุ่น จากอกให้ลูกดื่มกิน**

I Love you mum…

Regensburg, im Juli 2009

# Bibliography

Kanok-orn Srilunchang was born on October 12, 1976 in Udonthani, Thailand. In 1998 she obtained her bachelor degree from the School of Animal Production Technology, Institute of Agricultural Technology, Suranaree University of Technology (SUT). Four years later she started a Master degree in the Biotechnology School at the same university in the topic of 'The study of genetic relationship and molecular markers identification of SUT *Dendrocalamus asper* (Pai Tong Kaew)'. During her master enrollment, she had a great opportunity to go train more molecular techniques under a French-Thai Cooperation program in the Laboratory of Molecular Biology and Physiology of Fruit Ripening, Toulouse, France during May-September 2002. Her experience in France has opened her eye and her mind to seek for a Ph.D. position abroad. She has a further chance to work at Prof. Dr. Thomas Dresselhaus's lab starting in September 23, 2003. She first came as a training student and succeeded to start a Ph.D. in February 2004 at the Faculty of Biology, University of Hamburg with a Post-graduate scholarship with Hamburg's Young Academics Funding Law (2004-2006). In October 2006, the whole lab moved from Hamburg to the University of Regensburg and she continued her work on 'Molecular characterization and identification of genes involved in maize female gametophyte development'.

# Curriculum Vitae: Kanok-orn Srilunchang

## PESONAL DATA


| | |
|---|---|
| Name | Kanok-orn Srilunchang |
| Current Address | Universitätstr. 100a, 93053, Regensburg, Germany |
| Date of Birth | 12 October 1976 |
| Birth Place | Udonthani, Thailand |
| Nationality | Thai |
| Family Status | Single |
| Email | ksrilunchang@hotmail.com |
| Tel | +49 1762 4518379 |


## EDUCATIONS

| | |
|---|---|
| Oct2006-present | **Ph.D**. study in the topic of<br>` Molecular characterization and identification of genes involve in maize female gametophyte development'<br>Cell Biology & Plant Physiology, **University of Regensburg**, Germany. |
| Mar2004-Oct2006 | **Ph.D**. study in the topic of<br>` Molecular characterization and identification of genes involve in maize female gametophyte development', **University of Hamburg**, Germany. |
| 1999-2002 | **Suranaree University of Technology, Nakhon Ratchasima, Thailand.**<br>Degree: **Master of Science** in **Biotechnology**<br>GPA: 3.31/4.00 (Very good)<br>Thesis study of Master degree:<br>'The Study of genetic relationship and molecular markers identification of D. asper by RAPD and AFLP techniques'. |
| 1995-1999 | **Suranaree University of Technology, Nakhon Ratchasima, Thailand.**<br>Degree: **Bachelor of Science** in **Animal Production Technology**<br>GPA: 2.56/4.00 (good) |
| 1992-1995 | **Kumpawapi School, Udonthani, Thailand**<br>High School (Science)<br>Note: GPA 3.2/4.00 (Very good) |

## TRAINING AND WORKING EXPERIENCES

| | |
|---|---|
| May2002-Sept2002 | **Training molecular techniques** in the topic 'The role of the ethylene phytohormone on tomato ripening mechanisms'. Laboratory of Molecular Biology and Physiology of Fruit Ripening, Toulouse. France. |
| Dec2002-Aug2003 | **Research assistant** in the topic 'Cloning chitinase class I and III genes from grape'. Suranaree University of Technology. Thailand. |
| Aug2003-Feb2004 | **Research training** in the topic 'Transcript profiles during parthenogenesis in the apomict Tripsacum dactyloides'. Developmental Biology and Biotechnology, University of Hamburg. Germany. |

## POSTER PRESENTATIONS

**K. Srilunchang and Mariena Ketudat-Cairns**
'The Study of Genetic relationship and molecular markers identification of D. asper by RAPD and AFLP techniques'. (Queen Sirikit National Convention Center Bangkok, Thailand, 7-10 November 2001).

**K. Srilunchang and Thomas Dresselhaus**
`Molecular analysis of the ubiquitin system in the maize egg cell`. (47$^{th}$ Annual maize genetics conference, Lake Geneva, Wisconsin, USA, 10-13 March 2005).

**K. Srilunchang and Thomas Dresselhaus**
`Molecular analysis of the ubiquitin system in the maize egg cell`. (8$^{th}$ International congress plant molecular biology, Adelaide, Australia, 20-25 August 2006)

**K. Srilunchang and Thomas Dresselhaus**
`Functional analysis of a SUMO-like gene in the maize egg cell`. (1$^{st}$ International Ph.D. School Plant Development, Retzbach-Würzburg, Germany, 17-19 September 2008)

## ORAL PRESENTATIONS

**K. Srilunchang and Mariena Ketudat-Cairns**
The Study of genetic relationship and molecular markers identification of D. asper in SUT farm by RAPD and AFLP techniques. (Khon Kaen, Thailand 12-15 November 2002).

**K. Srilunchang and Thomas Dresselhaus**
Functional analysis of SUMO-like genes in the maize egg cell. (RZBB Ph.D. symposium, Kostenz, Germany, 17-18 September 2007).

## FELLOWSHIPS/GRANTS

- Thai-French exchange student program grant (May-September 2002).
- Post-graduate scholarship with Hamburg's Young Academics Funding Law (2004-2006).

# LIST OF PUBLICATIONS

**Srilunchang, K-o** and Dresselhaus, T. (2009). `DiSUMO-like DSUL is required for nuclei positioning and cell specification during female gametophyte maturation in maize' **Submitted.**

Leljak-Levanić, D., **Srilunchang, K-o.,** Solijic, L., Juranić, M., Dresselhaus, T., and Sprunck, S. (2009)**. '**Asymmetrically inherited maize MATH-BTB proteins are involved in nuclei positioning and mitotic progression during megagametogenesis'. **Submitted.**

Lausser, A., Kliwer, I., **Srilunchang, K-o**., and Dresselhaus, T. (2009). 'Sporophytic control of pollen tube growth and guidance in maize' **In preparation**.

Hermon, P., **Srilunchang, K-o**., Zou, J., Dresselhaus, T., and Danilevskaya, O N. (2007) `Activation of the imprinted Polycomb Group *Fie1* gene in maize endosperm requires demethylation of the maternal allele´. **Plant Mol. Bio**., **64,** 387-395.

Dresselhaus, T., **Srilunchang, K-o.,** Leljak-Levanić, D., Schreiber, D N., and Garg, P. (2006) `The Fertilization Induced DNA Replication Factor MCM6 of Maize Shuttles between Cytoplasm and Nucleus, and is Essential for Plant Growth and Development´ **Plant Phys**., **140**, 512-527.

**Eidesstattliche Erklärung**

Ich erkläre hiermit an Eides statt, dass ich die vorliegende Arbeit ohne unzulässige Hilfe Dritter und ohne Benutzung anderer als der angegebenen Hilfsmittel angefertigt habe; die aus anderen Quellen direkt oder indirekt übernommenen Daten und Konzepte sind unter Angabe des Literaturzitats gekennzeichnet.

Kanok-orn Srilunchang Regensburg, den 14 Juli 2009